2019

Endogenous Antioxidant Overexpression as an Adjuvant to Diet or Exercise Intervention as Therapy to Counteract Obesity and Beneficially Shift the Gut Microbiome

Deborah Lynn Amos

ENDOGENOUS ANTIOXIDANT OVEREXPRESSION AS AN ADJUVANT TO DIET OR EXERCISE INTERVENTION AS THERAPY TO COUNTERACT OBESITY AND BENEFICIALLY SHIFT THE GUT MICROBIOME

A Dissertation submitted to
the Graduate College of
Marshall University
In partial fulfillment of
the requirements for the degree of
Doctor of Philosophy
In
Biomedical Research
by
Deborah Lynn Amos
Approved by
Dr. Nalini Santanam, Committee Chairperson
Dr. Elsa Mangiarua
Dr. Jung Han Kim
Dr. Shekher Mohan
Dr. Regina Lamendella

Marshall University
May 2019

APPROVAL OF DISSERTATION

We, the faculty supervising the work of Deborah L. Amos, affirm that the dissertation, *Endogenous Antioxidant Overexpression as an Adjuvant to Diet or Exercise Intervention as Therapy to Counteract Obesity and Beneficially Shift the Gut Microbiome*, meets the high academic standards for original scholarship and creative work established by the Biomedical Research program and the Graduate College of Marshall University This work also conforms to the editorial standards of our discipline and the Graduate College of Marshall University. With our signatures, we approve the manuscript for publication.

Dr. Nalini Sankaram	Chairperson	3/25/19 Date
Dr. Elsa Kanagama	Committee Member	3/22/2019 Date
Dr. Jung Han Kim	Committee Member	3/21/2019 Date
Dr. Shekhar Mohan	Committee Member	3/21/19 Date
Dr. Regina Lamendella	Committee Member	3/25/19 Date

DEDICATION

This work is dedicated to my Father in Heaven. He has blessed me with so many wonderful people that have helped me come thus far in addition to unique talents to use for His good works. I pray that my work in this program has pleased Him.

ACKNOWLEDGEMENTS

First and foremost, I must acknowledge my advisor and prime investigator, Dr. Nalini Santanam. As I completed my lab rotations in the beginning of my PhD work, I knew her laboratory would be where I conducted my research. My years as a graduate student have been tough, but Dr. Santanam kept pushing me to the finish. Dr. Santanam, or "Dr. S" for short, has a work ethic and passion for research I have seen in no other individual, and it is often discussed among the numerous students she has advised over the years. She has greatly aided me in the process of attaining my degree, and for that I am truly grateful.

I would also like to extend a special word of thanks to the administration in the Biomedical Research (previously Biomedical Science-BMS) program (special emphasis to Dr. Green and Diana Maue). From recruitment, to my tears and struggles through the journey, and all the way up to my defense, to you I am grateful. May God bless you!

To the rest of my committee members, Dr. Mangiarua, Dr. Kim, Dr. Mohan, and Dr. Lamendella, I thank you for both your guidance in my research project and my life's endeavors. Having you on my committee and in my life has definitely improved my critical thinking skills and made me a better researcher as a result.

Lastly, but NOT least, thank you to my family and friends who have been so encouraging on this journey. To my Dad, Mama "Bear," and my favorite sibling (Stephen- aka "Brother") who have sacrificed so much to allow me to come to this point in my life, I am eternally thankful.

I pray to always be a blessing in your life and the life of others as a child of our Heavenly Father and you.

TABLE OF CONTENTS

LIST OF TABLES

LIST OF FIGURES

ABSTRACT

Oxidative stress plays a key role in metabolic syndrome which includes obesity and cardiometabolic diseases. It is implicated that oxygen-derived free radicals generated during the mitochondrial electron transport chain alter the function of specific biological components, thus activating obesogenic pathways such as glucose and lipid signaling. Research on this topic is of vital importance as obesity is a high-risk factor in the development and progression of severe, debilitating, life-threatening maladies such as cardiometabolic diseases, chronic inflammatory pathologies, and cancer. Furthermore, there is no universal effective therapy to combat the rising rates of obesity with over 1.9 billion (39%) adults classified as obese worldwide. Catalase is an antioxidant enzyme that helps to catabolize hydrogen peroxide and has been shown in vivo and/or in vitro to decrease oxidative stress in vascular cells, skeletal muscle tissue, and adipose tissue which results in mitigating free radical damage in the heart, aging-effects in muscle tissue, insulin resistance as well as dysfunctional glucose signaling, and cancer progression. With redox stress being one of the major hallmarks of obesity, we hypothesized that overexpression of antioxidant catalase would suppress redox stress-mediated obesogenic pathways. In our studies, we first generated and investigated the effect of excess endogenous antioxidant by using a novel mouse model termed “Bob-Cat.” These mice are a cross between heterozygous, leptin-deficient mice (Ob/+) and [Tg(CAT)$^{\pm}$] mice that ubiquitously express human catalase in addition to mouse catalase. We first showed sex specific changes in redox stress, phenotype, metabolic parameters, and adipose tissue function. These findings indicated this ‘stress-less’ model (overexpressing antioxidant) would be optimal to study in combination with frequently prescribed diet and exercise intervention strategies to alter key biomarkers related to obesogenic pathways. In an 8 week feeding study, we showed ad libitum feeding of an enriched omega 3 diet, in contrast to a

high saturated fatty acid/ polyunsaturated fatty acid diet, promoted maintenance of body weight and fat mass, increased energy metabolism, normal circadian rhythm, and insulin sensitivity within the novel mice. These findings were evidenced to be a result of up-regulation of GPR120-Nrf2 cross-talk (>30 fold, $p<0.05$), which to our knowledge, had not been previously evidenced in any other studies. We also showed the role of sexual dimorphism in response to OM3 rich diet. In relation to exercise, we showed evidence that antioxidant overexpression in addition to moderate treadmill exercise 30 min. a day, 5 days/week for 8 weeks resulted in maintenance or lowered body weight and fat mass, balanced energy metabolism, a normal feeding circadian rhythm, and improvement in the lipid profile. Most interestingly, we saw significant differences in skeletal muscle Type 1 / Type 2 fiber ratio and mRNA expression of key myokines which may have induced a change in adipose tissue-brain cross-talk. Additionally, this study provided evidence of an exercise and redox-induced shift in the taxa and predicted function of the gut microbiome which beneficially impacted energy metabolism in the mice overexpressing antioxidant catalase. Taken together, our studies suggest antioxidant overexpression is an efficient adjuvant to diet and exercise intervention to combat metabolic dysfunction. Therefore, the newly generated Bob-Cat mouse is an effective model to investigate redox stress in the context of energy metabolism, metabolic tissue dysfunction, and the gut microbiome to discover new preventative treatments and therapies to reduce the rising levels of obesity, cardiometabolic diseases, chronic inflammatory – related illnesses, and cancer.

CHAPTER I: INTRODUCTION

1.1 OBESITY DEFINED AND PREVALENCE

Obesity, now considered a world-wide epidemic (Sharma, Lee, Youssef, Salifu, & McFarlane, 2017), is a serious health concern as it increases the risk of morbidity of several pathologies including insulin resistance (IR), hypertension, dyslipidemia, type 2 diabetes (T2D), coronary heart disease, stroke, non-alcoholic fatty liver disease (NAFLD), osteoarthritis, sleep apnea, and numerous cancers (Savini, Catani, Evangelista, Gasperi, & Avigliano, 2013). Since 1975, global obesity rates have tripled. As of 2016, more than 1.9 billion adults (39%) are overweight and more than 650 million are considered obese (13%) (Organization, 2018). Of even greater concern, childhood obesity is also on the rise with more than 41 million children less than 5 years old and 340 million children and adolescents between the ages of 5-19 years old categorized as overweight or obese (Organization, 2018). Specifically, at the conclusion of 2018 in the United States, adult obesity rates exceeded 35% in 7 states, 30% in 29 states, and 25% in 48 states. West Virginia currently has the highest obesity rate at 38.1%. Seven states have increased the number of obese residents in the past year, and all other states have maintained or increased the number of obese individuals (Foundation, 2018).

Obesity is the result of a number of genetic, behavioral, and environmental factors that contribute to disequilibrium between energy intake and expenditure (Gonzalez-Muniesa et al., 2017; Manna & Jain, 2015). This results in accumulation of visceral adipose tissue to the extent that both physical and psychosocial health and well-being are impaired (James, 2004). In the clinical setting, overweight is defined as a Body Mass Index (BMI: weight (kg) / height (m^2)) of 25.0 to 29.9 kg/m^2 and obesity as a BMI of $\geq$ 30.0 kg/m^2 (Manna & Jain, 2015; Paniagua, 2016). BMI is a robust yet indirect measure of body fat that provides more reliable information than

"ideal weight" or other ratios involving weight and/or height. Nonetheless, exceptions to the accuracy of BMI include athletes (higher percentages of muscle mass), the elderly, and individuals who are extremely tall or short because it does not distinguish between lean or fat mass (James, 2004). Additionally, although BMI is easy to measure, it indicates an overall measure of "fat," and does not identify the distribution of adipose tissue which directly correlates with metabolic health (C. H. Jung, Lee, & Song, 2017). Increased visceral (central) fat contributes to higher levels of pro-oxidant and pro-inflammatory states in addition to alterations in both glucose and lipid metabolism in comparison to subcutaneous fat (directly under the skin). Numerous studies have shown increased visceral fat is a high risk factor in T2D, dyslipidemia, and cardiovascular diseases (CVD) (Figueroa et al., 2016; James, 2004; Luna-Luna et al., 2015). For this reason, some clinicians prefer to look at the waist to height ratio in addition to the BMI to measure the distribution of body fat. In general, higher levels of visceral adipose tissue (abdominal, omental, and mesenteric) is more prevalent in males than females (Karastergiou, Smith, Greenberg, & Fried, 2012). Females have higher levels of subcutaneous fat, and thus are at lower risk for cardiometabolic diseases (Karastergiou et al., 2012). Mechanisms have not been fully elucidated; however, higher levels of fat mass, especially within the visceral compartment, contribute to adipose tissue dysfunction- defined as impaired adipose tissue expandability, adipocyte hypertrophy, altered lipid metabolism, local inflammation, and dysregulation of adipokine production and secretion (Fietta & Delsante, 2013; Goossens, 2017).

1.2 ADIPOSE TISSUE FUNCTION

Adipose tissue is currently characterized as an important endocrine organ having autocrine, paracrine, and endocrine effects. Increases in adipose tissue deposition alter the production and secretion of a number of cytokines- bioactive signaling molecules known as

adipokines (Fietta & Delsante, 2013; Scherer, 2006). These alterations regulate signaling mechanisms that control food intake, energy expenditure, inflammation, and fat storage (Kershaw & Flier, 2004). (**Figure 1**) For example, leptin, a 42 kD protein, has been shown to have a direct influence on food intake through regulating hypothalamic appetite regulating genes (Ex. proopiomelanocortin - POMC and neuropeptide Y - NPY) (Frago & Chowen, 2015; Wilson & Enriori, 2015).

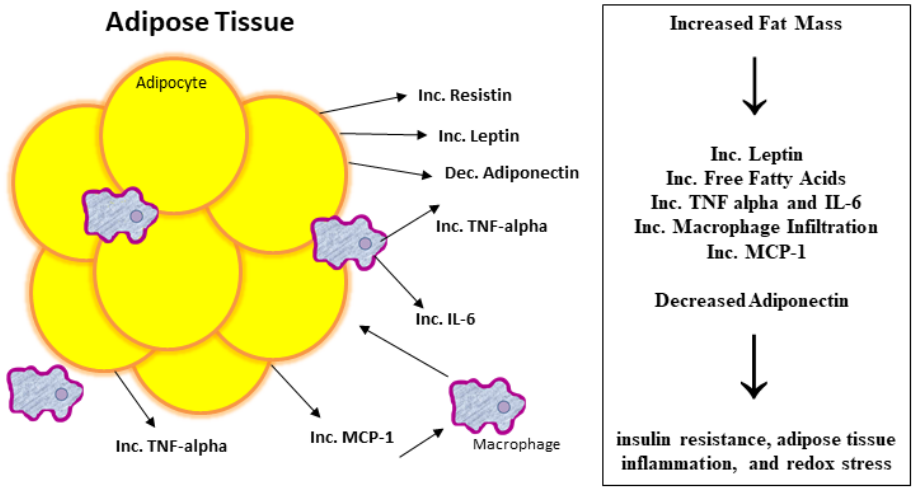

Figure 1. Increased deposition of adipose tissue. Increases in fat mass cause alterations in adipocytokine levels secreted by adipocytes and macrophages within adipose tissue. These changes can result in insulin resistance, adipose tissue inflammation and redox stress.

Histology has allowed characterization of adipose tissue according to its morphology. Adipose tissue is classified as a type of connective tissue with specific properties (M. T. Sheehan & Jensen, 2000) and is composed of multiple types of cells including preadipocytes, adipocytes, immune cells (e.g. macrophages), fibroblasts, endothelial cells, and stem cells (Rosen & Spiegelman, 2014). Preadipocytes are committed, immature forms of adipocytes and when activated by specific transcription factors, will form mature adipocytes. Adipocytes primarily regulate the storage and release of lipids, but they also use specific lipids for intracellular signaling and numerous proteins (i.e. adipokines such as leptin and adiponectin) for intracellular

signaling and communication with nearly every system of the organism (Scherer, 2006). Immune cells play a key role in the inflammatory response and help maintain adipose tissue integrity. Fibroblasts play a role in the integrity of the adipose tissue by secreting precursors of the extracellular matrix. They have also been shown to modulate the behavior and function of epithelial cells and stem cells, but mechanisms have yet to be elucidated (R. Zhang et al., 2018). The endothelial cells play a major role in growth and function of adipose tissue by interaction with leukocytes, nutrients, and oxygen between circulation and adipose tissue (Villaret et al., 2010). Finally, stem cells are mesenchymal cells with the capability of self-renewal and multipotentiality allowing them to become adipocytes, chondrocytes, myocytes, osteoblasts, or neurocytes dependent upon environmental factors (i.e. transcription factors). (Miana & González, 2018)

Classically, there are two main types of adipose tissue with different origins and functions relating to energy homeostasis. These are known as white adipose tissue (WAT) and brown adipose tissue (BAT) (Choe, Huh, Hwang, Kim, & Kim, 2016; A. Rodriguez, Ezquerro, Mendez-Gimenez, Becerril, & Fruhbeck, 2015; Tsoli et al., 2012). WAT is found in various regions of the body and is primarily responsible for storing excess energy inside of its cells as triacylglycerol which can be used during a caloric deficit (Kajimura, Spiegelman, & Seale, 2015). As previously described, the location of WAT determines its influence on metabolic homeostasis with increased fat in the visceral region correlating with metabolic dysfunction (Kusminski, Bickel, & Scherer, 2016). On the other hand, BAT is found in very few depots compared to WAT. In rodents, it is found in the interscapular, axillary, and cervical regions. In humans, the largest depot is concentrated in the interscapular region (Cypess et al., 2009; Kajimura et al., 2015; Sacks & Symonds, 2013). The cellular structure of BAT also differs from

WAT in that it is highly vascularized and has a high density of mitochondria promoting non-shivering thermogenesis through the induction of uncoupling protein 1 (UCP-1) (Kajimura et al., 2015; A. Rodriguez et al., 2015; Sacks & Symonds, 2013). Additionally, research has shown within WAT, increased cold exposure, exercise, and/or adrenergic signaling promotes a browning effect resulting in the formation of beige ("brite") adipose tissue (S. H. Kim & Plutzky, 2016; J. Wu, Cohen, & Spiegelman, 2013; L. Ye et al., 2013). Beige tissue has characteristics of both WAT and BAT. However, in relevance to obesity, like BAT, beige fat cells display higher levels of mitochondria and increased energy-dissipating capacity by promoting triacylglycerol clearance, glucose disposal, and thermogenic properties (i.e. induction of UCP-1) that release energy as heat (A. Rodriguez et al., 2015).

With differences in morphology and function, research has also discovered the type and production of cytokines differ within the various types of adipose tissue (Balistreri, Caruso, & Candore, 2010). Key adipokines and secreted factors that have been the concentration of numerous studies are discussed in the proceeding paragraphs: (leptin, adiponectin, tumor necrosis factor - alpha (TNF-α), interleukin – 6 (IL-6), resistin, monocyte chemotactic protein 1 (MCP-1/JE), and UCP-1 (Abella et al., 2017; Bluher & Mantzoros, 2015).

a) Leptin

Leptin is an adipokine (hormone) that functions in a negative feedback loop to maintain energy homeostasis through regulating adipose tissue storage (J. Friedman, 2016). When functioning properly, it decreases appetite and simultaneously increases energy expenditure by binding to the long form of the leptin receptor (LepR) located on the hypothalamic neurons of the brain. LepR is located on both neuropeptide Y (NPY) and proopiomelanocortin (POMC) neurons on the arcuate nucleus (ARC) of the hypothalamus. When leptin binds to its receptor,

NPY is inhibited while POMC is activated thus creating a satiety effect and increasing energy expenditure (Flak, 2017; Funahashi et al., 2003). Due to this function, leptin is referred to as the "satiety" hormone (Chowen & Argente, 2011). Mutations in leptin and/or its receptor promotes obesity in both rodent models and humans (Clement et al., 1998), but leptin administration can effectively counteract obesity (Chong, Lupsa, Cochran, & Gorden, 2010). Leptin acts on hypothalamic neurons (in addition to other locations), and mutations affecting this neuronal circuit elicit "Mendelian" forms of obesity (J. Friedman, 2016). When leptin levels fall, many physiological systems are affected causing a reduction in energy expenditure. This includes, but is not limited to, reduction or termination of menstrual cycles in females, decrease in insulin sensitivity, and compromised immune and neuroendocrine systems (Chong et al., 2010). These effects are all common in patients with lipodystrophy. Lipodystrophy is a condition associated with severe metabolic disease, but leptin administration is an approved treatment for the generalized form of this condition (Bluher & Mantzoros, 2015). Many patients characterized as obese have high endogenous levels of leptin, and some cases are related to mutations in the normal signaling pathway by which leptin acts. However, in the majority of patients, improper leptin signaling is characterized as a state of leptin resistance (Kuryszko, Slawuta, & Sapikowski, 2016). Nonetheless, more research will be necessary to understand the function of this adipokine in the context of obesity and energy metabolism.

b) Adiponectin

In addition to leptin, adiponectin is another fat-derived hormone that accounts for 0.01% of total serum protein, making it the most abundant adipokine in circulation (Achari & Jain, 2017; Villarreal-Molina & Antuna-Puente, 2012). Adiponectin serves as a critical signaling molecule in the cross-talk between adipose tissue and other metabolic organs including liver,

heart, kidney, and skeletal muscle (Z. V. Wang & Scherer, 2016). Through binding to one of its two targeted receptors, AdipoR1 or AdipoR2, it promotes insulin sensitization, and therefore, improvement in whole body energy homeostasis (Balistreri et al., 2010; Fang & Judd, 2018). In skeletal muscle, adiponectin enhances fatty acid oxidation and nutrient utilization (Fang & Judd, 2018; Yamauchi et al., 2001) and in liver, gluconeogenesis is significantly suppressed by the inhibition of genes involved in glucose production (Combs & Marliss, 2014). Most importantly, adiponectin serves as an anti-inflammatory factor by inhibiting pro-inflammatory cytokine signaling pathways such as tumor necrosis factor - alpha (TNF-α) – induced endothelial adhesion molecules, and macrophage-to-foam cell transformation (Villarreal-Molina & Antuna-Puente, 2012). In addition, adiponectin also has both anti-apoptotic and anti-oxidant effects (Ebrahimi-Mamaeghani, Mohammadi, Arefhosseini, Fallah, & Bazi, 2015; Ren et al., 2017). It is now well established that plasma levels of adiponectin are decreased in individuals characterized as obese, having T2D, or with a history of coronary artery disease (Villarreal-Molina & Antuna-Puente, 2012). With these known roles, adiponectin serves as a means of preventing numerous pathological events, including but not limited to, obesity, T2D, atherosclerosis, and cardiometabolic diseases (Achari & Jain, 2017; Z. V. Wang & Scherer, 2016).

III. TNF-alpha

Contrary to the beneficial anti-inflammatory effects of the adipokine adiponectin, TNF-alpha is a pro-inflammatory cytokine secreted by adipose tissue (Engin, 2017b). Within adipose tissue, TNF-α is produced by macrophages, adipocytes and stromal cells and is responsible for inducing IR by blocking receptors for adiponectin (J. Liu et al., 1998). Additionally, it also inhibits the adipose tissue's ability to esterify fatty acids, prevents glucose transport to liver cells,

and blocks fatty acid oxidation (Kuryszko et al., 2016). TNF-alpha can also compromise insulin production in pancreatic beta cells thus inhibiting insulin secretion (Kuryszko et al., 2016).

c) IL-6

Interleukin-6 (IL-6) is an adipokine, but is also expressed in other metabolic tissues such as skeletal muscle causing it to also be considered a myokine as well as an adipomyokine (Raschke & Eckel, 2013). In adipose tissue, it is a pro-inflammatory hormone. Approximately 30% of circulating IL-6 is derived from adipose tissue with much higher concentrations secreted from visceral vs. subcutaneous adipose tissue depots (Kuryszko et al., 2016). Like TNF-alpha, excessive production of IL-6 causes IR. IL-6 decreases insulin receptor expression, adipogenesis, secretion of adiponectin, and induces liver gluconeogenesis (Kern, Ranganathan, Li, Wood, & Ranganathan, 2001).

d) Resistin

Like TNF-alpha, Resistin, a 12 kD peptide produced by both macrophages and adipocytes, also exerts opposite effects compared to adiponectin (Banerjee & Lazar, 2003). Contrary to what is desired in promoting metabolic homeostasis in individuals characterized as obese or having one of its co-morbidities, resistin's primary role is to maintain fasting glycaemia by forming an excess accumulation of WAT (Kuryszko et al., 2016). Resistin induces gluconeogenesis, increases glycogenolysis, and promotes IR. Additionally, as a pro-inflammatory factor, it increases the production of TNF-α, Interleukin (IL) IL-1β, IL-6, and IL-12 (Kuryszko et al., 2016).

e) MCP-1

MCP-1, monocyte- chemotactic protein-1, has now been characterized as an adipokine due to its high abundance in adipose tissue although it is primarily expressed and secreted by

macrophages and endothelial cells (Kanda et al., 2006; Sartipy & Loskutoff, 2003). It functions as a potent chemotactic factor for monocytes. Increased levels of MCP-1 contribute to chronic low-grade inflammation in adipose tissue and IR by recruitment of macrophages that infiltrate and exacerbate the inflammatory state (Kanda et al., 2006). Another result of increased MCP-1 and infiltration of macrophages is overproduction of reactive oxygen species (ROS) and other inflammatory cytokines (Surmi & Hasty, 2010).

f) UCP-1

Adipose-derived UCP-1 is expressed primarily in BAT, but also in the beige cells of WAT (Leal, Lopes, & Batista, 2018). UCP-1 dissipates the proton gradient in the form of heat by uncoupling cellular respiration from mitochondrial ATP synthesis thus playing a key role in non-shivering thermogenesis. (Kajimura et al., 2015). With the uncoupling protein's ability to increase energy expenditure (S. H. Kim & Plutzky, 2016), it has been investigated as a potential candidate to treat obesity and its related co-morbidities.

Depending on the type and level of adipokine produced, chronic low-grade inflammation may result thus impacting other metabolic tissues that contribute to overall energy homeostasis (skeletal muscle, brain, liver, gut-microbiome). Although the precise mechanisms are still unclear, dysregulated production or secretion of these adipokines caused by excess adipose tissue and/or adipose tissue dysfunction can contribute to the development of obesity-related metabolic diseases.

1.3 THE REDOX STATE

Redox stress is an imbalanced oxidative or reductive environment which leads to detrimental effects such as increased production of oxidative free radicals and ROS (Rani, Deep, Singh, Palle, & Yadav, 2016), alterations in metabolic signaling pathways, increased

inflammation, and eventually cell death. ROS are a normal product of cellular metabolism and at low or moderate concentrations, they function to control physiological cell processes (Birben, Sahiner, Sackesen, Erzurum, & Kalayci, 2012). However, excessive ROS (high levels of oxidants) can attack cellular proteins, lipids, and nucleic acids resulting in dysregulation of energy metabolism, altered cell signaling and cell cycle control, gene mutations, dysfunctional cellular transport, a hampered immune system, and increased inflammation (Rani et al., 2016). This shift in redox balance is termed "oxidative stress." Nonetheless, a balance is required between oxidants and antioxidants. Therefore, not only are excessive levels of oxidants detrimental, significantly lower oxidants compared to reducing factors result in disorder when the body naturally attempts to compensate to resume redox homeostasis (Korge, Calmettes, & Weiss, 2015; Lloret, Fuchsberger, Giraldo, & Vina, 2016; Mentor & Fisher, 2017; L. J. Yan, 2014). The excessive levels of reducing reagents/oxidants has been coined "reductive stress" (Lipinski, 2002).

The major oxidants involved in normal cellular metabolism include the superoxide anion, hydroxyl radical, and hydrogen peroxide (H_2O_2). Xanthine oxidase, nicotinamide adenine dinucleotide phosphate (NADPH), and electron leakage in the electron transport chain all stimulate the formation of the superoxide anion as well as hydrogen peroxide through specific redox reactions. Additionally, when dismutated by superoxide dismutase (an endogenous antioxidant), H_2O_2 is generated as one of the products (Birben et al., 2012). H_2O_2 can then be broken down further into water and oxygen by endogenous antioxidants: catalase or glutathione peroxidase.

In order to maintain redox homeostasis, such as when there are excessive levels of oxidants (as occurs in oxidative stress), the antioxidant response system is activated. Numerous

studies have investigated this system in the context of obesity, chronic pathologies, and metabolic dysfunction (Brewer, Mustafi, Murray, Rajasekaran, & Benjamin, 2013; J. Chen, Zhang, & Cai, 2014; Gao et al., 2007; Tarantini et al., 2018). The transcription factor, nuclear factor erythroid 2-related factor 2 (Nrf2), plays a key role in the antioxidant response system. In a quiescent environment, the transcription factor interacts with kelch like ECH associated protein 1 (Keap1) in the cytoplasm, thus maintaining a low expression of Nrf2 target genes. Nevertheless, when stimulated by oxidative and electrophilic stress factors, Nrf2 disassociates from Keap1, translocates to the nucleus and induces the expression of several antioxidant genes (i.e. catalase) which are able to aid in regaining redox homeostasis (Kensler, Wakabayashi, & Biswal, 2007).

Redox balance is commonly assessed by evaluating markers of antioxidant defense or oxidative stress. The most widely used biomarkers of the antioxidant environment are tissue levels or plasma concentrations of antioxidant enzymatic activity (Superoxide dismutase (SOD), glutathione peroxidase (GPX), and catalase), non-enzymatic antioxidants (vitamin E, vitamin C, glutathione, and retinol), and minerals (selenium, zinc, and manganese) (Savini et al., 2013). Other studies have also used the total antioxidant capacity (TAC) to study the integrated action of all plasma antioxidants (Pinchuk, Shoval, Dotan, & Lichtenberg, 2012). High levels of oxidants can be measured either directly or indirectly. Electron spin resonance (ESR) and immune spin trapping are two methods to directly measure oxidative stress (O.S.) (M. C. Lee, 2013). Indirect methods such as oxidized protein carbonyl groups, 3-nitrotyrosine, advanced glycosylation end products, and advanced oxidation protein products, F2-isoprostanes, malondialdeyde, oxidized low-density lipoproteins (LDLs), thiobarbituric acid reactive

molecules, and 4-hydroxynonenal assays focus on measurement of the end-products of oxidative damage (Savini et al., 2013).

1.4 ASSOCIATION OF THE REDOX STATE AND OBESITY

Excessive fat accumulation, resulting from higher energy intake vs. expenditure, can occur due to a high calorie/low nutrient rich diet, low physical activity (sedentary lifestyle), nutritional/early- life hormonal status, as well as genetic, cultural, and economic factors (Gonzalez-Muniesa et al., 2017; Savini et al., 2013; Sies, Stahl, & Sevanian, 2005; Silventoinen et al., 2016). Numerous epidemiological, clinical, and animal studies have provided evidence that obesity is coupled with redox stress and increased risk for cardiometabolic diseases in both sexes and is independent of age (Carrier, 2017; Codoner-Franch et al., 2012; Hermsdorff et al., 2014; Karaouzene et al., 2011; Krzystek-Korpacka et al., 2008; Rani et al., 2016; Tran, Oliver, Rosa, & Galassetti, 2012). Numerous studies conducted throughout the past decade have shown juvenile aged individuals who were obese or overweight have high levels of oxidative stress compared to lean individuals (Tran et al., 2012). Additionally, adult obese subjects show higher levels of oxidized lipids including oxidatively modified low density lipoproteins (oxLDLs), arachidonic acid oxidation products (AAOPs), and thiobarbituric acid reactive substances (TBARS) in comparison to control subjects (D'Archivio et al., 2012). Additionally, other studies have shown BMI, total body fat, and waist circumference were positively correlated with urinary F2-isoprostane levels (Keaney et al., 2003). Oxidative stress levels have also been evaluated in highly metabolic tissues and body systems. In DIO models, cerebrocortical O.S. was shown to be increased (Freeman et al., 2013), a positive correlation was observed between O.S. and mitochondrial dysfunction in both skeletal muscle and liver (Yuzefovych, Musiyenko, Wilson, & Rachek, 2013), and in a third study there were increased levels of lipid and protein oxidation as

well as markers indicative of apoptosis (S. Wang & Kaufman, 2012). Additionally, excess fat mass can increase the inflammatory state. This is important with the accumulating evidence of an association between oxidative stress and inflammatory markers, hyperlipidemia, and hyperglycemia in overweight and obese subjects (Codoner-Franch et al., 2012; Pou et al., 2007). Combined, these studies implicate the interaction between O.S. and obesity/fat mass in addition to the negative consequences on tissue function and energy metabolism.

In contrast to assessing levels of oxidative stress by determining if there are increased levels of oxidants, there is also evidence showing that circulating antioxidant levels are lower and/or antioxidant defense mechanisms are compromised in obese individuals (Gutierrez-Lopez et al., 2012; Nikolaidis, Kerksick, Lamprecht, & McAnulty, 2012). Specific relationships between the BMI, body fat, and antioxidant defense signaling mechanisms are still being investigated due to variability in results. Differing outcomes in past research is likely a result of differences in availability of antioxidants and functionality of antioxidant defense systems in each individual (Savini et al., 2013). It is well-documented that antioxidant expression and enzymatic activity is progressively depleted as obesity worsens. Therefore, depending on the characteristics of the obese individual analyzed including the progression of obesity, inflammatory state, and dietary intake/ physical activity levels, antioxidant levels could dramatically differ. Nonetheless, despite variability between individuals in the aforementioned research, there are some consistencies in the data. In Attica, Greece an inverse relationship between visceral fat and TAC was shown independent of sex, age, physical activity level, and dietary habits. It was interesting that the correlation between the two variables was stronger for waist circumference than BMI (Chrysohoou et al., 2007). Then, another study showed the TAC, vitamin C, and vitamin E were lower while hydroperoxides and carbonylated proteins were

higher in obese patients compared to their lean controls (Karaouzene et al., 2011). Endogenous enzymatic antioxidants SOD, catalase, and GPx activity was also found to be inversely related to BMI regardless of age (Amirkhizi, Siassi, Djalali, & Shahraki, 2014; Mittal & Kant, 2009; Viroonudomphol et al., 2000). Additionally, specifically in obese women, serum GPx activity levels were significantly increased after a reduction in body weight (Bougoulia, Triantos, & Koliakos, 2006). Some studies have indicated a dietary effect on antioxidant content as well. In mice, when fed a high fat diet, there were increases in antioxidant activity within heart tissue, and specifically, a rapid induction of catalase. This is expected to have occurred to protect the mitochondria from being damaged due to high oxidants being produced (Rindler, Plafker, Szweda, & Kinter, 2013).

Individuals who are overweight or obese tend to have diets low in minerals and vitamins that contribute to inadequate antioxidant defenses that aid in protection from oxidative stress (Strauss, 1999; Via, 2012). In obese children, it was reported that there were lower levels of selenium, especially when the individuals had higher levels of central adiposity (Ortega et al., 2012). Furthermore, in morbidly obese patients, low levels of magnesium, selenium, iron, and zinc were observed (Kaidar-Person, Person, Szomstein, & Rosenthal, 2008b). In addition to metals, low levels of carotenoids have been inversely related to BMI and central fat distribution in a number of different studies in obese patients (Andersen et al., 2006; Canoy et al., 2005; Harnroongroj et al., 2002; Kaidar-Person et al., 2008b; Reitman, Friedrich, Ben-Amotz, & Levy, 2002; Schleicher, Carroll, Ford, & Lacher, 2009; Strauss, 1999).

1.5 CONDITIONS THAT GENERATE REDOX STRESS

Free radicals, including reactive oxygen species (ROS) and reactive nitrogen species (RNS), are produced by several mechanisms in individuals with high levels of adiposity

including dyslipidemia (Furukawa et al., 2004), hyperglycemia (Grattagliano, Palmieri, Portincasa, Moschetta, & Palasciano, 2008), increased inflammation (Bondia-Pons, Ryan, & Martinez, 2012), dysfunction of metabolic tissues (Serra, Mera, Malandrino, Mir, & Herrero, 2013), hyperleptinemia (Beltowski, 2012), and post ingestion of a high fat and/or high carbohydrate meal (Sies et al., 2005). When adipose tissue depots become full and adipocytes can no longer store triglycerides (TG), lipotoxicity occurs and ectopic fat accumulates in tissues including the heart, skeletal muscle, liver, and pancreas. As fat accumulates, organ dysfunction results and free radicals are formed. One mechanism by which this occurs is inhibition of the adenosine nucleotide translocator which results in adenosine triphosphate (ATP) accumulation in mitochondria, reducing the speed of oxidative phosphorylation, leading to mitochondrial uncoupling and free radical production. This was shown to occur in the skeletal muscle and liver of rodents provided a high fat diet (Serra et al., 2013; Yuzefovych et al., 2013). Ectopic fat accumulation also blocks glucose and insulin signaling pathways (Coen & Goodpaster, 2012; Olivares-Corichi, Viquez, Gutierrez-Lopez, Ceballos-Reyes, & Garcia-Sanchez, 2011), and hyperglycemia enhances the glycolytic pathway/ tricarboxylic acid (TCA) cycle promoting nicotinamide adenine dinucleotide (NADH) and flavin adenine dinucleotide (FADH) overproduction (J. Wu, Jin, Zheng, & Yan, 2016). This leads to electron leakage and thus superoxide (ROS/free radical) production. Superoxide is then able to inhibit glyceraldehyde-3-phosphate dehydrogenase which redirects metabolites of the normal TCA cycle to alternative pathways which induce further oxidative stress as well as nitrosative stress (J. Wu et al., 2016). Free radical production then progresses even further since hyperglycemia/oxidative stress/inflammation is an ongoing, vicious cycle. Many inflammatory mediators disrupt insulin signaling and exacerbate both ROS and glucose levels (Bondia-Pons et al., 2012). Another

mechanism by which free radicals are produced from increased adiposity is Endoplasmic Reticulum (ER) stress. In a homeostatic environment, the ER favors disulfide bond formation and proper protein folding. However, during ER stress, the unfolded protein response is activated. If prolonged, chronic oxidative protein folding machinery promotes ROS production in addition to release of free fatty acids and inflammatory mediators (S. Wang & Kaufman, 2012).

Metabolic tissue dysfunction increases oxidative stress as well as inflammation by exacerbating insulin resistance, hyperglycemia, and hypertriglyceridemia. In adipose tissue an increased expression of MCP-1, 2, and 4 recruits macrophages and leads to overproduction of ROS and additional inflammatory cytokines (Surmi & Hasty, 2010). Additionally, adipose dysfunction leads to deletion of redox sensitive, Nrf2, which weakens antioxidant defenses (Xue et al., 2013).

As previously mentioned, leptin is an adipokine that regulates appetite and prevents lipotoxicity in non-adipose tissue (Paz-Filho, Mastronardi, Wong, & Licinio, 2012). Hyperlipidemia induces O.S. primarily by increased mitochondrial fatty acid oxidation (Ceci et al., 2007). It also promotes inflammation by recruitment of macrophages and induction of TNF-alpha and IL-6 (Tilg & Moschen, 2006).

Overweight and obese individuals generally consume diets higher in fat and carbohydrates which is another contributor to O.S. in obesity. In fact, obese subjects show evidence of having an exacerbated and prolonged oxidative and inflammatory response to a large high fat/high carbohydrate meal than lean individuals (C. Patel et al., 2007). Therefore, chronic intake of high fat and carbohydrate diet in obese individuals has an increased adverse effect in comparison to a normal weight individual consuming the same diet.

1.6 REDOX STRESS IS ASSOCIATED WITH OBESITY AND ITS COMORBIDITIES

Current research provides evidence that oxidative stress may be the mechanistic link between obesity and its co-morbidities including metabolic syndrome, T2D, CVD, and cancer (Manna & Jain, 2015; Rani et al., 2016; Savini et al., 2013). A flow chart of this process is depicted in **Figure 2**.

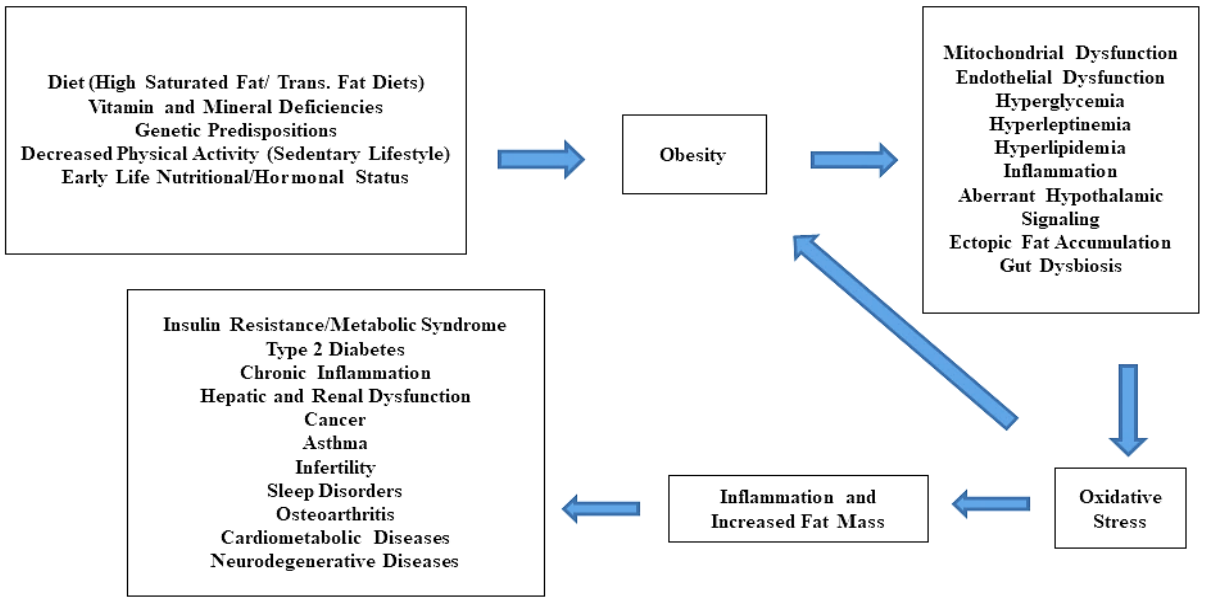

Figure 2. Associations among obesity, oxidative stress, and other metabolic and chronic diseases. Current research provides evidence that redox stress may be the mechanistic link between obesity, its comorbidities, and other chronic diseases. Relationships linking the three are shown in the flow chart above.

I. Metabolic Syndrome

Metabolic syndrome (MetS) is characterized as a cluster of cardiometabolic risk factors associated with central adiposity and IR including hypertriglyceridemia, high levels of low-density lipoproteins (LDL), low levels of high-density lipoproteins (HDL), IR, hyperglycemia, and hypertension (Bonomini, Rodella, & Rezzani, 2015). An individual with central adiposity and two or more of these conditions is characterized as having the metabolic syndrome (Carrier, 2017; Savini et al., 2013). Location of adipose depots is a strong determinant in levels of O.S.

and inflammation. Increased levels of visceral fat, having high levels of resident macrophages and cytokines in comparison to subcutaneous adipose tissue (Harman-Boehm et al., 2007), promotes higher levels of oxidative stress and inflammation, making it a high risk factor for MetS (Bonomini et al., 2015). A study investigating the relationship between visceral fat mass and MetS in patients with high central adiposity demonstrated visceral fat area was strongly correlated with O.S. and MetS when high levels of oxidants were observed in the urine (Fujita, Nishizawa, Funahashi, Shimomura, & Shimabukuro, 2006). Numerous additional studies have used in vivo and ex vivo models that have also demonstrated the role of oxidative stress in the development of MetS (Bryan, Baregzay, Spicer, Singal, & Khaper, 2013; Furukawa et al., 2004). High ROS also contributes to IR, a common disease of MetS, through several mechanisms involving activation of signaling kinases (Dokken, Saengsirisuwan, Kim, Teachey, & Henriksen, 2008), chronic inflammation by induction of pro-inflammatory cytokines such as TNF-alpha and IL-6 (Styskal, Van Remmen, Richardson, & Salmon, 2012), as well as damage to insulin-stimulated signals in its downstream signaling pathways (Bryan et al., 2013).

Increased levels of ROS also induce hypertension in obese subjects. One key mechanism is through deregulation of insulin signaling by modifying the phosphatidylinositol 3-kinase (PI3K)/ protein kinase B (Akt) pathway in endothelial cells. This decreases Nitric Oxide (NO/NOX) synthesis and vasodilation while increasing blood pressure. Additionally, the renin-angiotensin system is activated which further promotes hypertension (Whaley-Connell & Sowers, 2012).

Liver dysfunction, promoted by redox stress and inflammation in obesity, contributes to other aspects of MetS such as dyslipidemia, hypertriglyceridemia, high cholesterolemia, and low HDL levels (Bryan et al., 2013). Additionally, low HDL levels can exacerbate O.S. by an

inability to bind to transition metals used to eradicate oxidative species when there are already high levels of oxidants (Bjelakovic, Nikolova, Gluud, Simonetti, & Gluud, 2012). This has the propensity to perpetuate a negative continuous cycle of increasing O.S. and complications of the MetS.

II. Type 2 Diabetes

T2D, non-insulin-dependent diabetes mellitus, develops as a result of hyperinsulinemia in individuals with excess adiposity levels. When insulin-resistance develops, the pancreatic β-cells undergo hyperplasia to compensate for low insulin sensitivity which can lead to exhaustion and β-cell death (Cerf, 2013). Additionally, over time, hyperglycemia ensues due to lack of insulin and β-cells which can promote ROS and RNS formation. At this point, β-cells begin to die due to a low scavenging capacity when in an environment of chronic oxidative stress and adipokine secretion (Chetboun et al., 2012; Dandona, Aljada, Chaudhuri, Mohanty, & Garg, 2005).

III. Cardiovascular Disease

In obesity, high levels of visceral fat, in addition to IR, oxidative stress, mitochondrial dysfunction, endothelial dysfunction, and altered NO release are key factors in the development of CVD (Figueroa et al., 2016; Luna-Luna et al., 2015; Parthasarathy & Santanam, 1994; Standl, 2012). One manner O.S. promotes the development of atherosclerosis and thrombosis is by inhibiting the protective effects of NO in endothelial cells. Progression of vascular disease is then exacerbated by obesity and hypertension which cause an induction of NOX-derived ROS and release of cytokines which begins a continuous and vicious cycle (Carnevale et al., 2014; Furukawa et al., 2004; Savini et al., 2013). ROS also triggers oxidation of LDL and macrophage activation which promotes the formation of foam cells and atherosclerotic lesions (Ferretti, Bacchetti, Masciangelo, & Bicchiega, 2010; Santanam, Auge, Zhou, Keshava, & Parthasarathy,

1999; Shimasaki, Maeba, Tachibana, & Ueta, 1995; N. Wang et al., 1996). With regard to adipose tissue, altered adipokine levels (leptin, resistin, chemerin, vaspin, visfatin, and omentin) are correlated with cardiometabolic diseases (DeClercq, Enns, Yeganeh, Taylor, & Zahradka, 2013; Guzik, Mangalat, & Korbut, 2006). Elevated levels of leptin directly damage endothelial and vascular smooth muscle cells which induce the secretion of lipoprotein lipase, retention of lipoproteins, and formation of foam cells (Beltowski, 2012). Evidence has also been shown for an age effect in obesity-associated vascular complications where elderly individuals are more vulnerable to obesity-associated vascular diseases in comparison to the younger population. This has been postulated to occur due to increased obesity-induced inflammation in perivascular adipose tissue which elevates O.S. and inflammation (Bailey-Downs et al., 2013).

IV. Cancer

Cancer can also be stimulated as a result of redox imbalances in obesity. Evidence has been provided from epidemiological studies that there is a positive correlation between BMI, fat distribution, obesity, and cancer oncogenesis (Calle, Rodriguez, Walker-Thurmond, & Thun, 2003; Engin, 2017a; Martinez-Useros & Garcia-Foncillas, 2016). In fact, obesity was responsible for approximately 14% and 20% of cancer deaths in men and women respectively in the past two decades with obesity-associated mortality for primarily prostate and stomach cancer in men and breast, endometrium, cervical, uterine, and ovarian cancer in women (Calle et al., 2003). Even intermediate levels of O.S. cause DNA damage resulting in genomic instability and induction of oncogenes/ inhibition of genes involved in suppressing tumor growth (Crujeiras, Diaz-Lagares, Carreira, Amil, & Casanueva, 2013). For example, it was shown that oxidative metabolites of estrogens in breast cancer stimulated ROS generation causing DNA oxidative damage and promotion of cancer progression (Crujeiras et al., 2013). Evidence for O.S. with inflammation

promoting oncogenesis was shown when IR patients were at higher risk for several types of cancer through the activation of PI3K/Akt and rapamycin (mTOR) pathways (Vucenik & Stains, 2012).

1.7 THERAPIES TO COUNTERACT OBESITY AND ITS COMORBIDITIES BY MODIFYING THE REDOX STATE

I. Vitamins and Phytochemicals

With the significant amount of evidence showing O.S. plays a key role in metabolic syndrome and its related pathologies, research has investigated the use of vitamins/dietary supplements effective in counteracting free radicals. A plethora of studies have established there is a strong correlation between redox balance/metabolic stability and diets rich in phytochemicals/antioxidants (Crujeiras, Parra, Rodriguez, Martinez de Morentin, & Martinez, 2006; Gonzalez-Castejon & Rodriguez-Casado, 2011). Their mechanism of action primarily stems from scavenging or neutralization of free radicals, induced antioxidant enzymatic activity, and anti-inflammatory effects (Del Rio et al., 2011; O'Neil, Nicklas, Rampersaud, & Fulgoni, 2012). A beneficial role of citrus fruits in obesity and its co-morbidities has been shown in numerous studies. The positive effects of citrus juices in relation to obesity have been shown in neutralizing O.S. and inflammation in individuals consuming high fat/high carbohydrate meals and obese children (Codoner-Franch et al., 2010; Ghanim et al., 2010). Additionally, broccoli and carrots, known to have high concentrations of phytochemicals, improve oxidative stress levels and increase serum antioxidant levels (Bahadoran et al., 2011; Potter, Foroudi, Stamatikos, Patil, & Deyhim, 2011). Direct antioxidant supplementation by intake of Vitamin E and C has been thought to be beneficial to obese individuals since there is a high rate of deficiency of these vitamins in individuals with high levels of adiposity and/or IR (Aasheim & Bohmer, 2008;

Kaidar-Person, Person, Szomstein, & Rosenthal, 2008a; Schleicher et al., 2009; Via, 2012). Additionally, most observational studies have shown these vitamins are inversely associated with cardiometabolic diseases and cancer. Nonetheless, results are controversial in supplementation with Vitamin E. Some short-term studies show lowering of oxidative stress and improved lipid profile while others show no effect, increased risk for CVD, or higher incidences of cancer (Bjelakovic et al., 2012; Chae, Albert, Moorthy, Lee, & Buring, 2012; Garelnabi et al., 2012). Vitamin C is non-toxic and has been shown to be beneficial in individuals with hypertension and lowering the risk of CVD and cancer (Boekholdt et al., 2006; Juraschek, Guallar, Appel, & Miller, 2012; Pfister, Sharp, Luben, Wareham, & Khaw, 2011). Therefore, it is recommended if individuals are deficient since there are little side effects (Savini et al., 2013). Incorporating polyphenols into the diet is another method of increasing antioxidant activity. Like Vitamin C and E, it has been reported that obese individuals have lower serum levels of some polyphenols (Suzuki et al., 2006). Therefore, dietary incorporation of foods high in polyphenols may prove to be beneficial. Furthermore, some short-term clinical trials have studied the impact of polyphenols on obesity and its comorbidities and observed a beneficial role in almost every study evaluating oxidative stress/inflammatory markers, glucose homeostasis, and risk factors of cardiometabolic diseases (Hokayem et al., 2013; Leiherer, Mundlein, & Drexel, 2013).

II. Dietary Intervention

Dietary fatty acid composition has a profound effect on measures of oxidative stress and energy homeostasis (Calder et al., 2011; Sies et al., 2005). Therefore, incorporating dietary compounds evidenced to be effective in improving the redox state and energy metabolism may be beneficial to obese individuals and those at high risk for its comorbidities. Diets rich in saturated fatty acids (SFA) have been shown to increase fat deposition and body weight (Calder

et al., 2011; Yuzefovych et al., 2013). Diet Induced Obesity (DIO) rodent models (i.e. C57Bl6 mice) are routinely used to investigate metabolic changes as a result of increased fat deposition among the various fat pads. Generally, diets comprised of > 40% high-fat lard, milk, and butter (primarily composed of SFA) fosters excess lipid storage in adipose tissue leading to adipocyte hyperplasia and hypertrophy, abnormal adipokine secretion, hypoxia, elevated circulating free fatty acids (FFA), endothelial dysfunction, and ectopic fat deposition in less than 8 weeks of SFA diet intervention (Choe et al., 2016; Heydemann, 2016; Snel et al., 2012). Additionally, adipose tissue inflammation is increased consequently to high levels of fat mass which induces a pro-inflammatory state further inducing IR and inflammation in other metabolic tissues (liver, skeletal muscle, and pancreas) (Z. Chen, Yu, Xiong, Du, & Zhu, 2017; Snel et al., 2012). The fatty acid composition, length, and degree of saturation determine the severity of consequences to a high-fat diet (HFD) (McArdle, Finucane, Connaughton, McMorrow, & Roche, 2013; Yeop Han et al., 2010). Opposing the negative effects of diets high in saturated fat, diets primarily comprised of unsaturated fatty acids have shown evidence toward being beneficial to metabolic function (Albracht-Schulte et al., 2018; Luo et al., 2016; Saini & Keum, 2018; Shahidi & Ambigaipalan, 2018). In humans, Mediterranean Diets (rich in fruits, vegetables, legumes, nuts, oily fish, low-fat dairy products, and olive oil as the primary source of fat) exert preventive effects in incidence or mortality from obesity, CVD, stroke, cancer, as well as neurodegenerative diseases (Agnoli et al., 2013; Buckland et al., 2013; Demarin, Lisak, & Morovic, 2011; Hadziabdic, Bozikov, Pavic, & Romic, 2012; Samieri, Okereke, E, & Grodstein, 2013; Sofi, Abbate, Gensini, & Casini, 2010; Visioli, Grande, Bogani, & Galli, 2004). This effect was shown in a study on abdominally overweight men and women where the Mediterranean Diet reduced O.S. and inflammation after eight weeks of diet intervention (van Dijk et al., 2012). Omega 6

polyunsaturated fatty acids (OM6 PUFA) include conjugated linoleic acids (CLA), which are prevalent in meat and dairy products. These fatty acids have been investigated for their anti-obesity and anti-diabetic effects in specific animal models showing results of decreased energy intake, lipogenesis, increased energy expenditure, and increased lipid catabolism. Nonetheless, numerous other studies have shown no effect on loss of fat mass (Dilzer & Park, 2012). Additionally, no evidence has been provided on antioxidant defense systems after supplementation of CLA in human trials (J. Kim, Paik, Shin, & Park, 2012). Monounsaturated fatty acids (MUFA - major component of olive oil) and Omega 3 polyunsaturated fatty acids (OM3 PUFA - major component in oily fish) have shown evidence of a protective role against obesity, oxidative stress, and cardiometabolic diseases by in vitro and in vivo studies. In one study, when SFA was replaced by MUFA for eight weeks, metabolic stress was reduced through decreases in oxidative phosphorylation and apoB concentrations in men and women with high levels of central adiposity (van Dijk et al., 2012). Specifically, diets with high concentrations of fish oil (high OM3) have been mechanistically shown to lower systemic IR (Oliveira et al., 2015), decrease fasting TG levels (Bargut, Silva-e-Silva, Souza-Mello, Mandarim-de-Lacerda, & Aguila, 2016) and cholesterol levels (Ide & Koshizaka, 2018; Tani, Matsuo, & Matsumoto, 2018), and reduce inflammation (Oliveira et al., 2015). This directly opposes the effects that have been evidenced in diets comprised of high levels of SFA (lard based HFD) (Bargut et al., 2016; Yeop Han et al., 2010). Mechanisms behind the effects of OM3 supplementation were better understood by Olefsky's group when G-protein coupled receptor 120/Free fatty acid receptor 4 (GPR120/FFAR4) was discovered (D. Y. Oh et al., 2010). GPR120 is a receptor for long chain OM3 free fatty acids that is highly expressed in adipose tissue. Since its discovery, researchers have shown its proposed mechanistic role in improving adipose tissue function and

energy metabolism by its insulin sensitizing and anti-inflammatory effects (D. Y. Oh & Olefsky, 2012; D. Y. Oh et al., 2010; D. Y. Oh et al., 2014). OM3 fatty acids alter the balance of reductive and oxidative species, and are additionally critical in glucose and lipid metabolism (McDonald, O'Kane, McConville, Devine, & McVeigh, 2013; D. Y. Oh et al., 2010). Furthermore, alterations in redox homeostasis through increased intake of OM3 fatty acids have been linked to activation of the Nrf2 pathway (Cipollina, 2015; Kusunoki et al., 2013). Nrf2 is a transcription factor, key in regulating redox homeostasis (Seo & Lee, 2013) by inducing the transcription of endogenous antioxidants including catalase, glutathione transferase, heme oxygenase (HO-1), and NAD(P)H: Quinone Oxidoreductase 1 (S. E. Lee et al., 2015; Yamamoto, Kensler, & Motohashi, 2018; Zhu et al., 2008). Therefore, overall, these studies have pointed to plausible mechanisms by which varying dietary fat composition (with particular emphasis on OM3 enriched diet) can influence metabolic homeostasis by regulating the redox state.

III. Exercise Intervention

Physical activity is a highly effective, non-pharmacological approach to preventing dyslipidemia, hyperglycemia, hypertension, IR/T2D, atherosclerosis, CVD, osteoporosis, and even some cancers (Golbidi & Laher, 2014; Leal et al., 2018; Nunan, Mahtani, Roberts, & Heneghan, 2013; Savini et al., 2013). The mechanisms involved stem from an overall increase in energy expenditure that results in a reduction of fat mass and body weight (Fiuza-Luces, Garatachea, Berger, & Lucia, 2013; Golbidi, Mesdaghinia, & Laher, 2012; Leal et al., 2018). Additionally, physical activity improves the lipoprotein profile through decreasing TG and LDL and increasing HDL levels (Fiuza-Luces et al., 2013; Sanchis-Gomar, Fiuza-Luces, & Lucia, 2015; Warburton, Nicol, & Bredin, 2006). Exercise has also been shown to enhance glucose and insulin signaling (Garelnabi et al., 2012; Tan, Du, Zhao, Pang, & Wang, 2018), lower systemic

inflammation (Pedersen & Febbraio, 2012; Pil-Byung et al., 2011), improve cardiac function (Barauna et al., 2005; Laterza et al., 2007; Phillips, Mahmoud, Brown, & Haus, 2015), boost physical performance (Vina, Sanchis-Gomar, Martinez-Bello, & Gomez-Cabrera, 2012), and augment neurological function (Radak, Marton, Nagy, Koltai, & Goto, 2013). Many of these beneficial effects may be linked to the evidence that physical activity paradoxically increases redox stress and in turn signals antioxidant production which aids in facilitation of redox homeostasis (Done & Traustadottir, 2016; Mach & Fuster-Botella, 2017; Meilhac, Ramachandran, Chiang, Santanam, & Parthasarathy, 2001; Savini et al., 2013; Vina et al., 2012). The physical stress involved in physical activity modulates the structure and function of a number of metabolic tissues including liver, adipose tissue, and skeletal muscle (Guo, Liong, So, Fung, & Tipoe, 2015; Leal et al., 2018). During physical activity, skeletal muscle, the largest human endocrine organ, generates the energy necessary for movement primarily by carbohydrate and lipid oxidation, thus constituting it as a key player in energy metabolism (Iizuka, Machida, & Hirafuji, 2014; Pedersen, 2013). Skeletal muscle is composed of numerous types of cells including motor neurons, stem cells, fibroblasts, adipocytes, pericytes, connective tissue, and muscle fibers (Ex. Type 1 and 2). Not only are genes upregulated to maintain energy homeostasis by regulating glucose levels (i.e. glucose transporter 4 – GLUT 4) and producing adequate levels of ATP (Fryer et al., 2002; Holmes, Kurth-Kraczek, & Winder, 1999) upon increased skeletal muscle contraction in aerobic exercise, there are also shifts in the muscle fiber type ratio toward higher levels of Type 1 / Type 2 muscle fibers (Fry et al., 2017; Y. X. Wang et al., 2004). Additionally, there are alterations in the expression and secretion of bioactive secretory factors termed myokines (e.g. GLUT 4, PGC1-alpha, FGF-21) (Iizuka et al., 2014). Specifically, Fibroblast Growth Factors (FGFs) and Interleukins (Ex. IL-6 and IL-15) play an

important metabolic or immunological role with autocrine and paracrine functions (S. M. Sheehan, Tatsumi, Temm-Grove, & Allen, 2000). Research to date concentrating on the autocrine, paracrine, and endocrine effects of myokines have contributed to our knowledge of the beneficial effects of exercise on the nervous, endocrine, and immune systems in addition to systemic energy homeostasis (Hoffmann & Weigert, 2017; Huh, 2018).

Adding to the beneficial effects of decreasing adipose tissue mass, physical activity also plays a role in modulating adipose tissue function and contributing to systemic metabolic homeostasis (Leal et al., 2018). Recent studies have shown evidence that one of the key mechanisms is through the induction and secretion of "exercise-induced" myokines (Leal et al., 2018; B. So, Kim, Kim, & Song, 2014). Furthermore, skeletal muscle cross-talk with adipose tissue has been a current topic of interest. As previously discussed, adipose tissue is more than a storage unit, it also is an important endocrine organ (Trayhurn, Bing, & Wood, 2006) allowing for an adipokine effect on skeletal muscle function and vice versa. Key myokines postulated to be involved in the "talk" between skeletal muscle and adipose tissues include, but are not limited to, IL-6, FGF-21, and Irisin (Leal et al., 2018; Raschke & Eckel, 2013).

a) IL-6

There are numerous isoforms of interleukins, but IL-6, in addition to being an adipokine as previously mentioned, is an exercise induced myokine that plays a key role in inflammatory signaling (Pratesi, Tarantini, & Di Bari, 2013). Higher levels of IL-6 have been reported after exercise intervention (Leal et al., 2018). With their upregulation, they have also been shown to directly contribute to increased expression of IL-1 receptor agonist and IL-10 thus constituting a role in the anti-inflammatory effects of exercise. Plasma concentrations of IL-6 have been shown to increase > 100 fold post-exercise. However, this effect does not occur in a linear pattern over

time (MacDonald, Wojtaszewski, Pedersen, Kiens, & Richter, 2003). In addition to inducing anti-inflammatory signaling pathways, it has also shown that IL-6 can inhibit inflammatory cytokines such as TNF-alpha (Petersen & Pedersen, 2005). Furthermore, various studies have shown a cross-talk between skeletal muscle interleukins and adipose tissue, which has shown to increase adiponectin expression in exercised conditions (Macpherson, Huber, Frendo-Cumbo, Simpson, & Wright, 2015; Quinn, Strait-Bodey, Anderson, Argiles, & Havel, 2005).

b) FGF-21

Fibroblast growth factor 21 (FGF-21) is an exercised-induced myokine with pleotropic effects (Cuevas-Ramos et al., 2012; K. H. Kim et al., 2013). Studies show it plays an important role in energy metabolism by decreasing glucose levels and increasing lipolysis (Hojman et al., 2009; Izumiya et al., 2008; Kharitonenkov et al., 2005; B. So et al., 2014; X. Zhang et al., 2008). Not only is it expressed in skeletal muscle, it is also expressed in liver, adipose tissue, and pancreas (Canto & Auwerx, 2012) where expression levels are dependent on factors such as nutritional status, dietary fat intake, hormone levels, transcription factors, oxidative stress, and physical activity (Gomez-Samano et al., 2017; Kharitonenkov et al., 2005). FGF-21 acts as an endocrine factor. Evidence has shown that it cross-talks with adipose tissue and that it can increase thermogenesis and WAT browning through induction of UCP-1 (Fisher et al., 2012). Additionally, there is evidence of an interaction with adiponectin in adipose tissue. A recent study showed that in adipocytes, both transcription and secretion of adiponectin are induced by FGF-21 which has now been termed the "FGF-21-adiponectin axis." Furthermore, in adiponectin – null mice, the glucose-lowering, lipid clearance, and the anti-atherosclerotic benefits of FGF-21 were diminished (Hui, Feng, Liu, Gao, & Xu, 2016). With these evidences, it is plausible that

FGF-21 is another muscle-derived bioactive molecule involved in skeletal muscle – adipose tissue cross-talk.

c) PGC1-alpha/FNDC5/Irisin

Irisin has been considered one of the most promising myokines for metabolic maintenance (Leal et al., 2018) and thus a potential therapeutic method in diseases relating to metabolic dysfunction. When stimulated by exercise, peroxisome proliferator-activated receptor-γ coactivator-1α (PGC1-alpha) stimulates the expression of fibronectin type III domain-containing protein 5 (FNDC5) which encodes irisin, a type I membrane protein secreted into circulation. Since its discovery, by Bostrom et al. in 2012 (Bostrom et al., 2012), further research has shown irisin is secreted in an exercise-dependent manner by skeletal muscle and mediates WAT metabolism (Aydin et al., 2014). Reports have discussed its ability to convert WAT to BAT (browning of adipose tissue), resulting in increasing energy expenditure by inducing UCP-1 expression (Bostrom et al., 2012; Mahgoub, D'Souza, Al Darmaki, Baniyas, & Adeghate, 2018). Additionally, a study conducted in obese humans on 8 weeks of aerobic exercise and resistance exercise showed a positive correlation between irisin and changes of muscle mass, and a negative correlation between the circulating irisin level and changes of fat mass and body fat percentage (Huh et al., 2012). Mechanisms behind the effects of Irisin have been intensely investigated in a number of studies (Aydin et al., 2014; Daskalopoulou et al., 2014; Hecksteden et al., 2013; Huh, 2018; Huh et al., 2014; Huh et al., 2012; Huh, Siopi, Mougios, Park, & Mantzoros, 2015; H. J. Kim, So, Choi, Kang, & Song, 2015; Pekkala et al., 2013; Roca-Rivada et al., 2013; Tsuchiya et al., 2014). However, until a study was conducted by Huh et al., most irisin investigations concentrated on plasma levels of its precursor, FNDC5, and the cleaved protein -irisin (Leal et al., 2018). Huh et al. investigated the effect of physical activity

specifically on skeletal muscle irisin levels and found that there was an age dependent effect with higher serum levels in younger exercisers and that secretion rates were dependent on exercise intensity. In addition, Huh et al. also showed increased irisin levels directly regulates muscle metabolism through adenosine monophosphate-activated protein kinase (AMPK- activated protein kinase) activation (Huh et al., 2014).

1.8 THE GUT MICROBIOME

I. Composition and Development

The human gastrointestinal tract is occupied by more than 10^{13}-10^{14} microorganisms, termed the "gut microbiome." Although only located within the intestinal tract, their genome consists of a gene set approximately 150 times larger than the human genome (J. Chen, Guo, Gui, & Xu, 2018; Gill et al., 2006; J. Qin et al., 2010). This microbiome is comprised of about 1,000–1,150 bacterial species, primarily consisting of two phyla: the Bacteroidetes and Firmicutes (approximately 80-90%), followed by Actinobacteria and Proteobacteria (J. Chen et al., 2018; Kallus & Brandt, 2012; Monda et al., 2017), and Verrucomicrobia, Fusobacteria, and Euryarchaeota to a much lesser extent (Backhed et al., 2015). Among the phyla, Firmicutes chiefly include the Ruminococcus, Clostridium, Lactobacillus, Eubacterium, Faecalibacterium, and Roseburia. The Bacteroides phyla primarily consists of Prevotella and Xylanibacter (J. Chen et al., 2018). The number, type, and function of microorganisms found within the gut varies from the upper to lower ends of the intestine, but the majority are located in the large bowel where nondigestible food is fermented providing the host with essential nutrients (Backhed, Ley, Sonnenburg, Peterson, & Gordon, 2005; Conlon & Bird, 2014; Denou, Marcinko, Surette, Steinberg, & Schertzer, 2016). The development of the microbiome begins during fetal development when the intestine is sterile within the uterus of the mother (Mackie, Sghir, &

Gaskins, 1999). Post conception, the gut is surrounded by the maternal microflora which begin to colonize the intestine (Mackie et al., 1999; Mandar & Mikelsaar, 1996). However, numerous factors influence the bacterial development in the infant stage promoting colonization of different microorganisms. By the time the infant turns one year old, the microbiome presents an "adult" signature with a dense population of microbes (C. Palmer, Bik, DiGiulio, Relman, & Brown, 2007; Tannock, 2007). From this time point, numerous genetic, epigenetic, and environmental factors shift the microbial population and its activity promoting high inter-individual variability (Adlerberth & Wold, 2009; Ley, Peterson, & Gordon, 2006; Nicholson et al., 2012). One key environmental factor is physical activity (type, duration, intensity, etc.), which plays a key role in the diversity and function of the microbiome (C. C. Evans et al., 2014; Matsumoto et al., 2008). Nonetheless, the gut microbiome continues to change throughout the lifespan as the body ages. For example, the elderly show significant decreases in Bacteroidetes and an increase in Firmicutes, but the cause has yet to be determined.

II. Functions of the Gut Microbiome

The gut microbiota play many important roles including maturation of the host's immune system, regulation of intestinal barrier function, preventing colonization of pathogenic microbes (Heiss & Olofsson, 2018), release of gut hormones, and regulation of oxidative stress and inflammation (Savini et al., 2013). Microbiota also modulate host energy homeostasis through harvesting energy from the diet as well as secreting various factors that affect its host's metabolic tissues responsible for energy metabolism (Monda et al., 2017). Thus, the role of the commensal microbes is vital to the health status of the host due to their potential commensal or symbiotic relationship.

III. Association of Microbiome and Pathological Conditions

With more studies concentrating on the gut microbiome, evidence is surmounting showing the gut microbiota is essential to maintaining host gut and systemic homeostasis (G. Clarke et al., 2014; Grenham, Clarke, Cryan, & Dinan, 2011). Several pathologies/diseases have been associated with an altered composition of the gut microbiome, termed dysbiosis, which has independently been shown to increase fat mass and elevate body weight (Monda et al., 2017). Diseases associated with dysbiosis include (but are not limited to) obesity, cardiometabolic diseases, IR/T2D, cancer, and inflammatory bowel disease (IBD) (J. Chen et al., 2018; Heiss & Olofsson, 2018; Monda et al., 2017; Savini et al., 2013). Although all these pathologies have a well-known multifactorial origin, part of which has previously been discussed (genetic, epigenetic, diet, redox state, physical activity level, and environment), more recently, the contribution of the microbiota has been considered a highly influential environmental factor (Backhed et al., 2004; Bleau, Karelis, St-Pierre, & Lamontagne, 2015). This presents the gut microbiome as a potential way to work as an intervention to counteract obesity, cardiometabolic diseases, cancer, and other chronic inflammatory diseases (Small & Bloom, 2004). In 2005, Ley et al. showed the leptin deficient, obese Ob/Ob mice exhibit a significant reduction of Bacteroidetes and increase in Firmicutes (Ley et al., 2005; Savini et al., 2013) which was also shown in obese humans when compared with lean controls (Turnbaugh et al., 2009; Turnbaugh et al., 2006). Most interesting, this ratio has been shown to be reversed with an alteration in dietary intake (Ley et al., 2006) or exercise intervention (S. F. Clarke et al., 2014). Additionally, not only the composition, but the number of different bacterial taxa present (diversity) also impacts host physiology. For example, decreased diversity has been shown in organisms consuming HFD (Garcia-Mantrana, Selma-Royo, Alcantara, & Collado, 2018), those with obesity-associated inflammatory characteristics (Ley et al., 2005), and/or sedentary individuals

(Monda et al., 2017). Numerous studies have shown that a reduction in the phylogenetic diversity is characteristic of obese vs. lean subjects and correlates with key metabolic parameters including high serum insulin levels, Homeostasis Model Assessment for Insulin Resistance (HOMA-IR), and plasma TG levels (Le Chatelier et al., 2013). Recovery from decreased phylogenetic diversity has been observed in studies investigating the effect of exercise (Monda et al., 2017) on microbial function as well as dietary intervention studies where a diet is lowered in fat (lard) content (Garcia-Mantrana et al., 2018).

IV. Microbial – Host Interaction

The gut microbiome plays a key role in the metabolic signaling of its host by regulating tissue cross-talk with the brain, liver, adipose, and skeletal muscle (Grosicki, Fielding, & Lustgarten, 2018; Mach & Fuster-Botella, 2017; Monda et al., 2017). The microbiome releases a variety of factors dependent on the host diet as well as the permeability of the gut.

a) Bile Acids

Primary bile acids are synthesized from cholesterol, secreted in bile, and bio-transformed into secondary bile acids upon contact with the resident colonic microbiota. It is estimated that approximately 50% of secondary bile acids are reabsorbed in the intestine and return to the liver by the portal vein (Di Ciaula et al., 2017). Bile acids aid in the digestion and absorption of fat, cholesterol, and fat-soluble vitamins in addition to acting as signaling molecules with anti-inflammatory functions (Di Ciaula et al., 2017). It is expected that physical activity may improve gastrointestinal motility and peristalsis, thus regulating the concentration of circulating bile acids and their pleiotropic functions. Previous animal studies found that moderate physical activity increased bile acid excretion (Bouchard et al., 1994; Watkins, Crawford, & Sanders, 1994; Yiamouyiannis, Martin, & Watkins, 1993). Bile acids also interact with a variety of receptors in

the adipose tissue, skeletal muscle, intestine, and liver (ie. G protein-coupled Bile Acid Receptor 1 (GPBAR-1) and Farnesoid X Receptor (FXR)) (Brighton et al., 2015; Di Ciaula et al., 2017). This results in the modification of metabolically relevant hormonal pathways (ie, release of peptide YY (PYY) and glucagon-like peptides) thus modulating appetite as well as glucose and insulin metabolism (Molina-Molina et al., 2018).

b) Short Chain Fatty Acids

One of the most significant contributions made by the gut microbiota to host function is the supply of short chain fatty acids (SCFAs) (J. M. Evans, Morris, & Marchesi, 2013). Upon fermentation (anaerobic) of a variety of carbon sources from the host diet, specific classes of the microbiota produce SCFAs. The three most predominant are butyrate, acetate, and propionate (Cummings & Macfarlane, 1997; J. M. Evans et al., 2013) which provide a significant source of energy for the host (J. M. Evans et al., 2013). However, this is not the only function served by SCFAs. It has also been shown that SCFAs act as signaling molecules and play a key role in metabolic function by exerting effects on a variety of metabolic organs (Nicholson et al., 2012). For example, within the gut, they bind to free fatty acid receptors and stimulate the release of PYY and 5-hydroxytryptamine (5-HT) (Cherbut et al., 1998; Fukumoto et al., 2003) which contributes to decreased intestinal transit rate as well as downstream signaling that controls appetite regulation within the hypothalamic region of the brain (Heiss & Olofsson, 2018). Another important function of which all the SCFAs play is the stimulation of leptin production in adipose tissue (Xiong et al., 2004; Yonekura et al., 2003). This is of considerable relevance to host metabolism with leptin being involved in a wide range of physiological processes including appetite regulation, reproduction, and metabolic rate (J. M. Evans et al., 2013). The number of SCFAs produced is determined by the host diet, microbial composition, and interaction between

the microbes (Jumpertz et al., 2011). The production of acetate, propionate, and butyrate are all upregulated by physical activity, but butyrate has become a particular interest in many exercise studies. (J. Chen et al., 2018; J. M. Evans et al., 2013; Matsumoto et al., 2008; Monda et al., 2017). The main microbes known to produce butyrate are *Clostridia, Eubacteria, and Roseburia*. Butyrate regulates neutrophil function and migration, increases expression of tight junction proteins (prevents "leaky gut"), lowers redox stress, and exhibits anti-inflammatory effects (Nicholson et al., 2012). Its anti-inflammatory effects include increasing IL-10 and IL-8, lowering IL-6, TNF-alpha, and IL-1B (S. F. Clarke et al., 2014; Molina-Molina et al., 2018), and inhibiting Nuclear factor kappa-light-chain-enhancer of activated B cells (NF-κB) (Lai et al., 2018). Propionate and acetate are substrates for gluconeogenesis and lipogenesis in the liver, adipose tissue, and skeletal muscle (Samuel et al., 2008; Wong, de Souza, Kendall, Emam, & Jenkins, 2006). Furthermore, specifically in skeletal muscle, SCFA activates the AMPK pathway which controls cholesterol and glucose metabolism providing evidence of cross-talk between the gut and skeletal muscle (Monda et al., 2017).

c) Other Microbial Products

Along with bile acids and SCFAs, the gut microbiome impacts the host by producing microbial products that play a significant role in metabolic processes such as the production of lipopolysaccharides (LPS) /endotoxins, Caseinolytic Protease B (ClpB), and other endocrine molecules. Obesity and its comorbidities are characterized by low-grade inflammation and increased levels of circulating LPS (Cani et al., 2007). Chronically elevated LPS, as those observed after consistent intake of a HFD (lard), can result in weight gain, insulin resistance, higher expression of inflammatory mediators, and macrophage infiltration in WAT (Caesar, Tremaroli, Kovatcheva-Datchary, Cani, & Backhed, 2015; Cani et al., 2007). Evidence suggests

that the increased circulating LPS levels after HFD intervention could be the result of a more permeable intestinal barrier (leaky gut). Contrary to a HFD, interventions such as an OM3 diet or increased physical activity can cause a decrease in LPS production from the gut microbiome (Heiss & Olofsson, 2018; Lai et al., 2018). In addition to the previously mentioned indirect cross-talk between the microbiome and appetite regulation (Ex. through leptin), evidence has been shown the microbiome also modulates the neuronal function of POMC by the bacterial product ClpB (Breton et al., 2016). ClpB acts as a mimetic of α-melanocyte-stimulating hormone, thus inducing satiety (Breton et al., 2016). Recent evidence has also confirmed that in addition to the production of endocrine molecules produced by the host, there is a significant level of dopamine and norepinephrine production in the human gut due to the expression of β-glucuronidases by commensal gut bacteria (Asano et al., 2012; Eisenhofer et al., 1997). Gut microbes can also produce non-noradrenergic, non-cholinergic transmitters such as NO, which play a pivotal role in the regulation of gastric emptying (Orihata, Sarna, Orihata, & Sarna, 1994) by the anaerobic reduction of nitrate to nitrogen (Cutruzzolà & Cutruzzolà, 2012; Sobko et al., 2005) thus modulating the redox environment. This is evidence that specific microbes have the potential to directly regulate host appetite, energy metabolism, the redox environment, and even mood/behavior by directly signaling to the central nervous system (CNS).

d) Bacterial Transfer

In an inflammatory or disease environment, the gut may increase permeability due to modification of tight junctions (leaky gut). When this occurs, fragments of bacteria can leak from the gut and activate immune responses in other tissues by activating receptors stimulated by foreign particles (Burcelin, 2016). It is also of significant interest that whole bacteria from the gut may be transferred from a leaky gut (inflammatory responses) and modulate what is now

known as the “tissue microbiome.” This is of particular interest in the transfer of pathogenic bacteria from the intestines that could cause havoc in other metabolic tissues by inducing tissue dysfunction, inflammation, and possibly cell death (Burcelin, 2016).

With the metabolic function of the gut microbiome and its role as an endocrine organ impacting key metabolic tissues through cross-talk, it has become evident that modifying the species present and ensuring proper function could play a role in the incidence of obesity, its comorbidities, and other chronic diseases (Brown, DeCoffe, Molcan, & Gibson, 2012; Small & Bloom, 2004).

1.9 THE POTENTIAL OF ANTIOXIDANT CATALASE

As a natural response to alleviate oxidative stress, the body activates antioxidant defense systems to upregulate endogenous antioxidant production and reduce the negative consequences that result from oxidant insult. Antioxidants catabolize oxidative species and form products that are less reactive/harmful to the cellular environment. Numerous investigations have been undertaken to determine the impact of antioxidants inhibiting disease pathways facilitated by increased levels of free radicals (Haidara et al., 2011; Spychalowicz, Wilk, Sliwa, Ludew, & Guzik, 2012). A major antioxidant involved in detoxifying H_2O_2 (a ROS) to the neutral products water and oxygen is catalase (X. Chen, Liang, Van Remmen, Vijg, & Richardson, 2004). Catalase exists as a tetramer composed of four identical monomers, each of which contain a heme moiety at the active site with a molecular weight of 62kD (Birben et al., 2012; Glorieux & Calderon, 2017). It is able to catabolize H_2O_2 in a two-step process. First, catalase is oxidized to a hypervalent iron intermediate which is subsequently reduced back to a balanced redox state by a second H_2O_2 molecule forming water and oxygen (Glorieux & Calderon, 2017). Although the mechanisms involved in the production of catalase have yet to be fully elucidated, evidence has

been shown it is induced by oxidative insult (Glorieux & Calderon, 2017). When the level of oxidant species rises within a cell, the endogenous antioxidant response system (i.e. Keap1/Nrf2) is activated thus upregulating the transcription of second phase antioxidants including catalase (Dreger et al., 2009; Pall & Levine, 2015; Xue et al., 2013; Yamamoto et al., 2018). Antioxidant catalase's beneficial effects have been shown by investigating its overexpression using both in vivo and in vitro analysis. Previous studies in our own laboratory showed evidence for prevention of oxidative damage to vascular cells (Meilhac, Zhou, Santanam, & Parthasarathy, 2000; Santanam et al., 1999) and in vivo in diet induced atherosclerosis and exercise intervention in a LDL r−/− mouse model (Meilhac et al., 2001). We specifically observed that increased redox stress/inflammation, as a result of a controlled insult, led to increased antioxidant expression. In a majority of our analysis, the antioxidant upregulated was catalase (Meilhac et al., 2001; Meilhac et al., 2000). In skeletal muscle tissue, function in aged rodents was improved by overexpression of human catalase targeted to the mitochondria (Umanskaya et al., 2014). Cancer progression was delayed where catalase was targeted to the mitochondria and attenuated mitochondrial H_2O_2 signaling (Ge et al., 2015). A cardiac-targeted overexpression of catalase prevented O.S. and decelerated aging effects in mice (Yao et al., 2015). Directly relevant to obesity and increases in fat mass, overexpression of catalase specific to the mitochondria attenuated mitochondrial ROS emission, preserved insulin signaling, and prevented inflammation when mice were provided HFD (high saturated fat) (Paglialunga, Ludzki, Root-McCaig, & Holloway, 2015). It is hypothesized this effect may have been the result of catalase's ability to regulate the polarization of macrophages within adipose tissue which would result in decreased inflammation and insulin resistance. Contrary to overexpression, in a mouse model

devoid of catalase, an obese, prediabetic phenotype was displayed that was exacerbated with age (Heit et al., 2017).

Although our knowledge is limited in the field of redox stress in the context of the microbiome, we are aware that oxidants are required for normal function of the microbiome, but as with the host, too high of levels is also damaging (Imlay, 2018). This was made clear by Yoon et al. when their laboratory showed the level of ROS inside the host intestine must be carefully regulated, yet, most interestingly, it can be controlled by a single-microbe gene product: catalase (M. Y. Yoon et al., 2016). Additionally, research has shown specific organisms such as *Escherichia coli (E. coli), Salmonella, typhimurium, Bacillus subtilis,* and *Saccharomyces cerevisiae* are sensitive and damaged by excessive oxidant levels in their environment (Imlay, 2018). For example, *E. coli*. mutants that lack either SOD or catalase and peroxidase exhibit distinctive inhibition of growth showing the specific injuries that O_2 and H_2O_2 can produce (Carlioz & Touati, 1986; Seaver & Imlay, 2001). Additionally, the *Bacteroides thetaiotaomicron* is an oxygen-sensitive bacterium. When fully aerated, growth ceases, and it resumes only when anoxia is restored. Within the gut, scavenging enzymes including catalase and NADH peroxidase are induced when the environment becomes too highly oxidized. They largely suppress damage of oxidants in air-tolerant bacteria, but sometimes the antioxidants are unable to counter the higher rate of ROS production in obligate anaerobes (Zheng et al., 2001). Recently, it was also shown that catalase-positive bacteria are vital to the establishment of certain *Bifidobacteria* in non-anaerobic human niches of the infant gastrointestinal tract. When absent, health of the gut and its host deteriorates (E. Rodriguez, Peiroten, Landete, Medina, & Arques, 2015). These investigations provide evidence from human and animal models that catalase is an ideal

antioxidant to study redox regulation in metabolic diseases (e.g. Obesity, cardiometabolic disease, IR/T2D) and other chronic diseases for which there is no current universal therapy.

1.10 THESIS PROJECT

With redox stress being a major hallmark of obesity and its co-morbidities (McMurray, Patten, & Harper, 2016), **it was hypothesized that excess catalase (antioxidant) expression would suppress redox stress mediated obesogenic pathways**. Based on the current literature, our laboratory generated the "Bob-Cat" stress-less mice model, a hybrid between catalase transgenic mice [Tg(CAT)$^{\pm}$] (X. Chen et al., 2003) and the leptin-deficient, obese mice (heterozygous JAX 000632, B6.Cg-Lep^{ob}/J). Upon its generation, we developed three specific hypotheses. First, we predicted that modulating redox stress by altering endogenous antioxidant content (overexpression of catalase) alone would enhance adipose tissue function, glucose and lipid signaling, and overall energy metabolism. The second hypothesis we developed was that by modulating redox stress by antioxidant overexpression or dietary intervention with an enriched OM3 diet (45%) vs. a HFD (45% lard) would positively modulate fatty acid signaling, glucose and lipid homeostasis, energy metabolism, and overall metabolic function. Third, we hypothesized antioxidant overexpression in addition to exercise would both enhance skeletal muscle and adipose tissue function, alter appetite signaling, and shift the composition and function of the gut microbiome thus improving overall energy metabolism in the 'stress-less' mice.

To better understand the interplay between redox regulation and dietary or exercise intervention in metabolic pathways, we addressed our first hypothesis and characterized male and female Bob-Cat mice where we showed the ubiquitous expression of human catalase in addition to mouse catalase altered body composition measurements, overall energy metabolism,

and adipose tissue function compared to WT controls. Details of the collected phenotyping data is discussed in **Chapter II**. After realizing the insight that could be gained from further analyzing this unique mouse model, we then tested our second hypothesis and compared the redox effects of a high-fat omega 3-enriched diet (OM3) and high-fat lard diet (HFD) in both male and female catalase-overexpressing 'stress-less' mice which can be found in **Chapter III**. Our study showed that an OM3 enriched diet, in contrast to a HFD intervention, activated cross-talk between the free fatty acid receptor, GPR120, and redox-sensitive transcription factor, Nrf2, to maintain balanced energy metabolism, normal circadian rhythm, and insulin sensitivity in mice overexpressing catalase compared to their WT controls. Another prevention strategy and therapy to counteract obesity and its co-morbidities is regular, moderately intense physical activity. Therefore, with our novel mouse model, we tested our third hypothesis where we sought to determine the synergistic effect of antioxidant overexpression and exercise on metabolic signaling pathways and the "forgotten endocrine organ" - the gut microbiome. As with our diet study, the overexpression of antioxidant catalase and exercise moved the field forward. We showed evidence of crosstalk between key metabolic organs and that the microbiome is significantly altered by overexpression of catalase and/or exercise intervention which will be further discussed in **Chapter IV**. A timeline of the experiments involved in the investigation of the newly generated mouse model is depicted in **Figure 3**. The conclusions derived from the aforementioned investigations solidify our claim that overexpression of antioxidant catalase is a beneficial adjuvant to an enriched OM3 diet/exercise intervention to suppress redox stress-mediated obesogenic pathways by altering metabolic tissue function, maintaining glucose and lipid homeostasis, and improving energy metabolism. Finally, we showed that antioxidant overexpression and/or exercise intervention causes significant shifts in the gut microbiome in a

manner that may be contributing to the observed improvement in obesogenic markers. Therefore, it is evident the Bob-Cat mouse is an excellent model to study the effect of an altered redox environment on pathways regulating energy metabolism. Future studies using this novel mouse model with an altered redox status have the potential to direct the pathway to discovering promising therapeutics involving alterations of diet, physical activity, and manipulation of the gut microbiome to decrease risk of obesity, its comorbidities, and other chronic/debilitating illnesses.

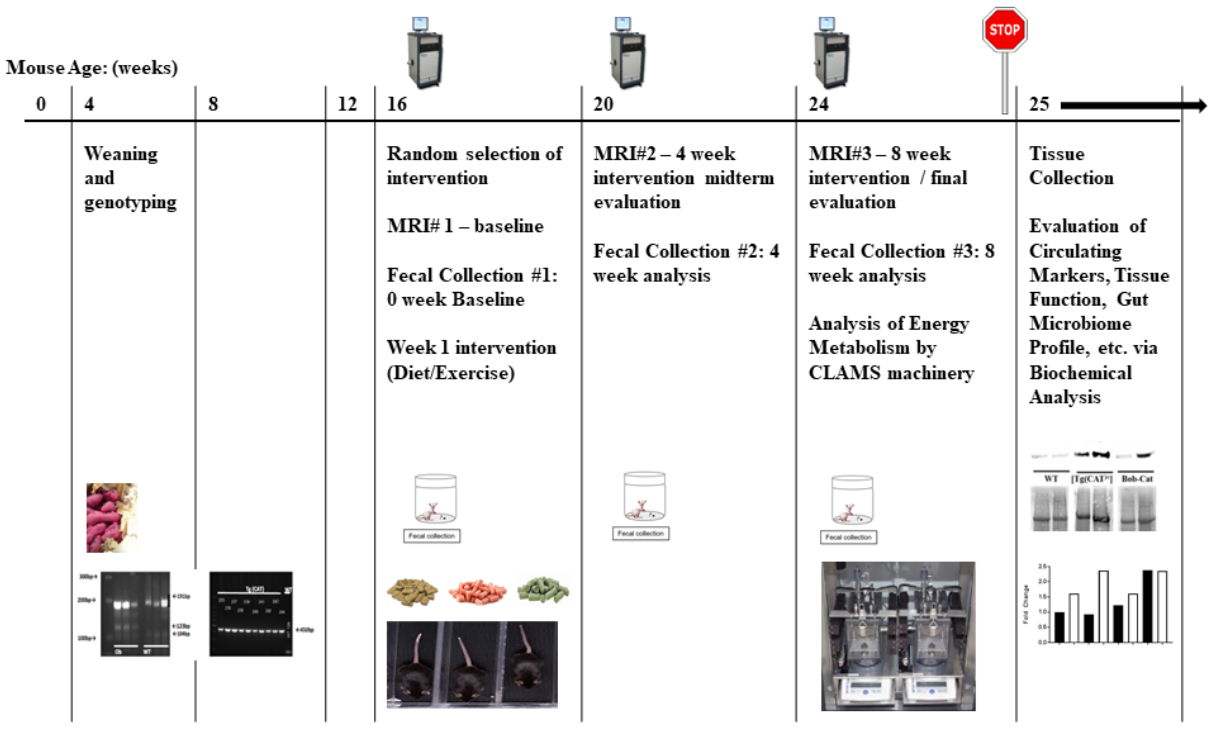

Figure 3. Timeline of proposed investigations of the novel 'stress-less' mouse. In order to phenotype and investigate the effects of dietary and exercise interventions using the newly generated mouse model overexpressing endogenous antioxidant catalase, an array of experiments was conducted at specific timepoints. An outline of these investigations based on the age of the mouse is shown in the figure above.

CHAPTER II: CATALASE OVEREXPRESSION MODULATES METABOLIC PARAMETERS IN A NEW 'STRESSLESS' LEPTIN-DEFICIENT MOUSE MODEL

A manuscript published in *Biochim Biophys Acta: Molecular Basis of Disease*

Amos, D. L., Robinson, T., Massie, M. B., Cook, C., Hoffsted, A., Crain, C., & Santanam, N. (2017). Catalase overexpression modulates metabolic parameters in a new 'stress-less' leptin-deficient mouse model. *Biochim Biophys Acta*, 1863(9), 2293-2306. doi:10.1016/j.bbadis.2017.06.016

Deborah L. Amos, Tanner Robinson, Melissa B. Massie, Carla Cook, Alexis Hoffsted, Courtney Crain, Nalini Santanam∗

Department of Biomedical Sciences, Joan C. Edwards School of Medicine, Marshall University, 1700 3rd Ave., Huntington, WV 25755-0001, United States

∗ Corresponding author: Department of Biomedical Sciences, Joan C. Edwards School of Medicine, Marshall University, 1700 3rd Ave, 435S BBSC, Huntington, WV 25755, U.S.

E-mail addresses: amos23@marshall.edu (D.L. Amos), robinson329@live.marshall.edu (T. Robinson), massie30@live.marshall.edu (M.B. Massie), schneide@marshall.edu (C. Cook), hoffsted@live.marshall.edu (A. Hoffsted), crain1@marshall.edu (C. Crain), santanam@marshall.edu (N. Santanam).

Received 8 March 2017; Received in revised form 1 June 2017; Accepted 19 June 2017

Available online 20 June 2017 0925-4439/

ABSTRACT

Oxidative stress plays a key role in obesity by modifying the function of important biological molecules, thus altering obesogenic pathways such as glucose and lipid signaling. Catalase is an important endogenous antioxidant enzyme that catabolizes hydrogen peroxide produced by the dismutation of superoxide. Recent studies have shown knockdown of catalase exacerbates insulin resistance and leads to obesity. We hypothesized that overexpressing catalase in an obese mouse will modulate obesogenic pathways and protect against obesity. Therefore, we bred catalase transgenic [Tg(CAT)$^{\pm}$] mice with Ob/Ob mice to generate the hybrid "Bob-Cat" mice. This newly generated "stress-less" mouse model had decreased oxidative stress (oxidized carbonylated proteins). ECHO-MRI showed lower fat mass but higher lean mass in "Bob-Cat" mice. Comprehensive Lab Animal Monitoring System (CLAMS) showed light and dark cycle increase in energy expenditure in Bob-Cat mice compared to wild type controls. Circulating levels of leptin and resistin showed no change. Catalase mRNA expression was increased in key metabolic tissues (adipose, liver, intestinal mucosa, and brain) of the Bob-Cat mice. Catalase activity, mRNA and protein expression was increased in adipose tissue. Expression of the major adipokines leptin and adiponectin was increased while pro-inflammatory genes, MCP-1/JE and IL-1β were lowered. Interestingly, sexual dimorphism was seen in body composition, energy expenditure, and metabolic parameters in the Bob-Cat mice. Overall, the characteristics of the newly generated "Bob-Cat" mice make it an ideal model for studying the effect of redox modulators (diet/exercise) in obesity.

2.1 INTRODUCTION

Rates of cardiometabolic diseases including obesity and Type 2 diabetes (T2D), are rising in developed and developing nations (Arroyo-Johnson & Mincey, 2016; Smith & Smith, 2016). In the United States of America (U.S.A), obese individuals make up approximately 35% of the population and the levels will continue to rise without appropriate interventions (Arroyo-Johnson & Mincey, 2016; Lewis, Edwards-Hampton, & Ard, 2016). The obese phenotype is a consequence of a number of factors including genetics (Arroyo-Johnson & Mincey, 2016; Pigeyre, Yazdi, Kaur, & Meyre, 2016) as well as environmental influences (Silventoinen et al., 2016; Smith & Smith, 2016). Both of these factors impact physiological processes and the function of biological molecules within an individual. When homeostasis is disrupted, body function is compromised. Redox stress is an imbalance between antioxidants and oxidants, leading to detrimental effects, such as increased production of oxidative species, alterations in signaling pathways, increased inflammation, and eventually cell death. Redox stress is known to play a role in various metabolic diseases including obesity (Santilli, Guagnano, Vazzana, La Barba, & Davi, 2015; Spahis, Borys, & Levy, 2017).

Increased free radical generation (redox stress) leads to a progressive accumulation of oxidative damage leading to increased adiposity stemming from an imbalance between pro-oxidants and antioxidants (Manna & Jain, 2015; McMurray et al., 2016; Santilli et al., 2015; Savini et al., 2013). Increases in fat mass, manifested as an increase in white adipose tissue (WAT), increases oxidative stress/oxidant production and results in an obese phenotype (Paglialunga et al., 2015) characterized by a BMI (Body Mass Index) $\geq 30 kg/m^2$ (Krueger, Coleman-Minahan, & Rooks, 2014). The obese phenotype is accompanied by mitochondrial dysfunction and increased lipid peroxidation, further leading to the dysfunction of other

metabolic tissues such as liver, muscle, (Paglialunga et al., 2015; Shill et al., 2016) gut, and brain (Ma, Yuan, Yu, Xi, & Xiao, 2014).

Strong evidence of the redox theory in obesity stems from research concentrated in models with high levels of adiposity and altered appetite regulation as a result of increased oxidative stress (Drougard, Fournel, Valet, & Knauf, 2015; Haas & Staels, 2016). Rodent body weight changes were shown to alter appetite regulation with alterations in oxidative stress markers (Diane et al., 2015). Redox stress has also been implicated in the process of adipogenesis (X. Wang & Hai, 2015). Adipose dysfunction results in abnormal levels of adipokines and cytokines secreted into circulation, such as leptin, adiponectin, resistin, monocyte chemotactic protein-1 (MCP-1/JE), and interleukin 1 beta (IL1β). These molecules play key roles in appetite and metabolic function, as well as inflammatory processes (Abella et al., 2017; Bluher & Mantzoros, 2015). In turn, this can further impact superoxide release and promote oxidative stress (Camargos et al., 2016; Fernandez-Sanchez et al., 2011). These molecules also mediate their effects by acting on immune cells leading to local and generalized inflammation thus impacting obesity related disorders (hypertension, diabetes, atherosclerosis, and insulin resistance) (Trostchansky, Quijano, Yadav, Kelley, & Cassina, 2016).

The body activates defense systems such as the endogenous antioxidants in order to counteract and prevent the negative consequences of increased redox stress. Antioxidants are able to catabolize reactive oxidants and yield products that are less reactive/toxic. Numerous studies have focused on the role of antioxidants in inhibiting disease pathways caused by increased levels of free radical production (Haidara et al., 2011; Spychalowicz et al., 2012). Catalase is one of the major endogenous antioxidant enzymes that detoxify the reactive oxygen species (ROS) hydrogen peroxide (H_2O_2) to water and oxygen. Overexpression of catalase was

shown to be beneficial in numerous studies. Our earlier studies have shown a role for catalase overexpression in the prevention of oxidative damage in vascular cells (Meilhac et al., 2000; Santanam et al., 1999) and in vivo in diet-induced atherosclerosis and exercise intervention in LDL r-/- mice (Meilhac et al., 2001). Other evidence includes studies where mitochondria targeted catalase showed a delay of cancer progression by attenuation of mitochondria-generated H_2O_2 signaling (Ge et al., 2015). A cardiac-specific overexpression of catalase protected from oxidative stress and displayed evidence of delayed cardiac aging in mice (Yao et al., 2015). In regard to obesity, a mouse model expressing mitochondria specific catalase on a high fat diet displayed attenuated mitochondrial ROS emission, preserved insulin signaling, and no inflammatory response compared to wild type controls (Paglialunga et al., 2015). This may be because overexpression of endogenous catalase was shown to regulate the polarization of macrophages within adipose tissue and thereby inhibit inflammation and insulin resistance (Park et al., 2016). On the other hand, mice devoid of antioxidant catalase developed an obese, prediabetic phenotype that was exacerbated with age (Heit et al., 2017). All these evidences suggest catalase as an ideal candidate for modulating redox stress in obesity.

Since high redox stress is one of the major hallmarks of obesity (McMurray et al., 2016), we hypothesized that excess catalase (antioxidant) expression would suppress redox stress mediated obesogenic pathways. In this study, catalase transgenic [Tg(CAT)$^{\pm}$] mice (X. Chen et al., 2004; X. Chen et al., 2003) expressing 3-4 fold higher levels of catalase were bred with the heterozygous, leptin deficient, Ob/Ob mice to create a hybrid that expresses high levels of catalase in an obese background (**"Bob-Cat"** mice). This newly generated mouse model showed sex specific changes in redox stress and metabolic parameters. Our results suggest that this

"stress-less" mouse model can be used as a good model to study the effect of modulators of redox stress (diet or exercise) on obesogenic pathways.

2.2 MATERIALS AND METHODS

2.2.1 Generation of "Bob-Cat" Mice

A successful breeding colony of the catalase transgenic [Tg(CAT)$^{\pm}$] mice has been established in our laboratory (a generous gift of a breeding pair from Drs. Arlan Richardson and Holly Van Remmen at the University of Texas Health Sciences Center in San Antonio, TX). The transgenic model that overexpresses Catalase was originally generated in C57Bl6 mice using a 33kb human CAT (*hCAT*) gene as well as the 41kb of 5' and the 6 kb of 3' flanking regions. This mouse model was the first transgenic model with increased catalase expression in all tissues (X. Chen et al., 2003).

Using the well-established colony at our facility, [Tg(CAT)$^{\pm}$] mice and the heterozygous Ob/+ mice (homozygous Ob/Ob are a leptin deficient, sterile model which spontaneously develops obesity – Jackson Labs, B6.V-Lep/^{ob}/J) were bred to engineer a novel mouse model with the goal of further understanding the mechanistic effect of lowering redox stress (by increasing catalase) on obesogenic pathways. Through cross-breeding the two genotypes, we developed a mouse model expressing the *hCAT* gene with a genetically obese background called "**Bob-Cat**" mice. The "Bob-Cat" mouse model was generated by following the breeding plan as described in **Figure 4A**. Four breeding pairs of the catalase transgenic mice [Tg(CAT) $^{\pm}$] were crossbred with Ob/+ mice (purchased from Jackson Labs) (2-male [Tg(CAT)$^{\pm}$] mice x 2-female Ob/+ mice or 2-male Ob/+ mice x 2-female [Tg(CAT)$^{\pm}$] mice) allowing the generation of the novel hybrid "Bob-Cat" mice. Once the first generation was established, four breeding pairs were used to sufficiently generate hybrid F2 pups for creating the F3 generation. Both F2 and F3 generation mice were used for further study purposes.

2.2.2 Characterization of "Bob-Cat" Mice

The newly generated hybrid "Bob-Cat" mice were compared to: i) Catalase transgenic [Tg(CAT) $^{\pm}$] mice that over-express the *hCAT* gene by approximately 3-4 fold in comparison to

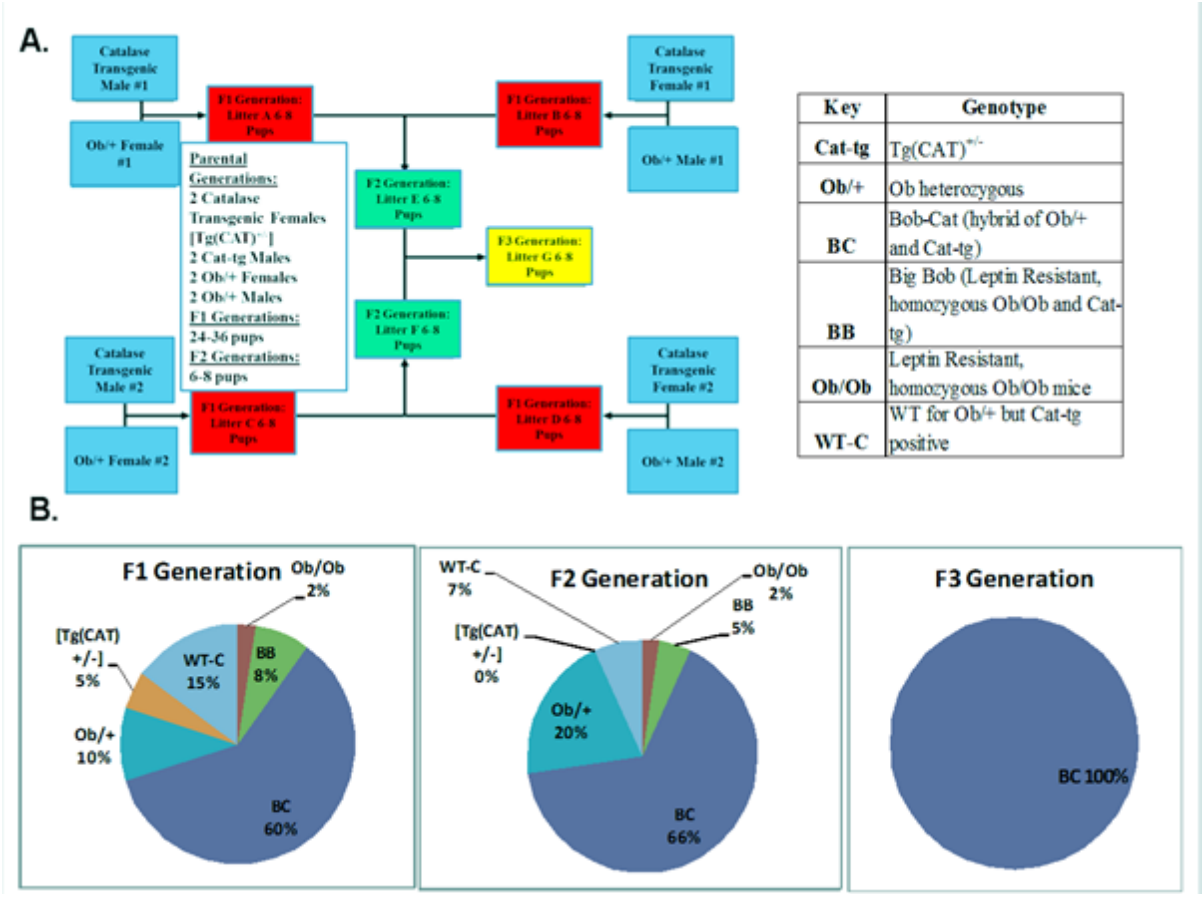

Figure 4. Generation of the Bob-Cat mouse. Four breeding pairs were mated (2-male [Tg(CAT)$^{\pm}$] mice x 2-female ob/+ mice) or (2-male ob/+ x 2-female [Tg(CAT)$^{\pm}$] mice) to create the F1 generation. F1 generation offspring were then bred to generate the F2 generation. F3 generations were produced by mating breeding pairs of the F2 generation. F2 and F3 generations were used in characterizing the novel "Bob-Cat" mouse. Pie charts represent the percent of the males and females generated in the (B) F1 generation, F2 generation, and F3 generation of each genotype. The key denotes each genotype generated from the breeding pairs. The figure provided displays each genotype generated from two breeding pairs. However, multiple breeding pairs were used in the generation of the Bob-Cat mice.

C57Bl6 (X. Chen et al., 2004), ii) wild type/C57Bl/6J mice (Jackson Lab stock number 000664) and iii) Ob/Ob (Jackson Lab stock number 000632), leptin deficient obese mice purchased from Jackson Laboratories (Bar Harbor, MA). Ob/Ob mice are homozygous for the mutant ob gene.

They increase in weight rapidly after 4 weeks of age, and can become up to three times the size of their parent strain C57Bl6 (Ioffe, Moon, Connolly, & Friedman, 1998). Along with accumulation of fat, Ob/Ob mice express hyperphagia, hyperglycemia, glucose intolerance, elevated plasma insulin (Ioffe et al., 1998), and increased hormone production from both pituitary and adrenal glands. The mice are hypometabolic, hypothermic, (Jackson Laboratory) and immunosuppressed (Lord et al., 1998). Due to the subfertility of Ob/Ob mice (Ingalls, Dickie, & Snell, 1950), the heterozygous Ob/+ mice are generally used for breeding. All mice were maintained on "standard chow" (Lab Diet Rodent Chow 5001) consisting of 30% protein, 13% fat, and 57% carbohydrate ad libitum. In the present study, the care and use of animals was conducted according to protocols approved by Marshall University IACUC.

2.2.3 Genotyping

Four weeks post-birth, animals were ear marked for identification and genotyped by collecting approximately 3-4 mm of the tail and isolating DNA. Tails were lysed in 300 µL of tail lysis buffer and 15 µL of proteinase K then placed overnight in a 55˚C water bath followed by centrifugation for 10 min. at 12,000g at room temperature. The supernatant was placed in another eppendorf tube with 300 µL of 100% isopropanol. The tube was centrifuged again at 12,000g for 5 min at room temperature to pellet the DNA. Pellets were dried and subsequently washed with 500 µL of 95% ethanol (EtOH) and centrifuged 5 min. at 12,000g. EtOH was discarded and the DNA pellets were air dried. 10 µL of Tris-EDTA (TE) Buffer was added to each tube and then all samples were placed into a 37˚C water bath 5-10 min. until the DNA was completely suspended. DNA was quantified by NanoDrop (Nanodrop Technologies Inc., Thermo Scientific, Wilmington, DE, USA). For genotyping, 0.25 µg (1 µL) of each DNA sample was added to a reaction mix of 18.125 µL RNase free H_2O, 2.5 µL of 10X i Taq Buffer, 0.75 µL

of $MgCl_2$ 50 mM, 0.5 µL dNTP mix 10 mM, 1 µL forward primer, 1 µL reverse primer, 0.125 µL i Taq DNA polymerase to prepare for amplification of DNA in the BioRad MyiQ (BioRad, Hercules, CA). PCR protocol was conducted as described in previous publications (X. Chen et al., 2003; Ellett, Evans, Zhang, Chavin, & Spyropoulos, 2009). Catalase primers: E12F: 5'-GAGGTCCACCCTGACTACGGG-3' and E13R: 5'-GCCTCCTCCCTTGCCGCCAAG-3' (X. Chen et al., 2003). Primers for Ob gene characterization: RFLP-F: 5'-TGAGTTTGTCCAAGATGGACC-3'; RFLP-R: 5'-GCCATCCAGGCTCTCTGG-3'; WtLep-F: 5'-AATGACCTGGAGAATCTCC-3'; and Lepob-R: 5'-GCAGATGGAGGAGGTCTCA-3' (Ellett et al., 2009). After amplification by PCR, agarose gel electrophoresis was used to determine the presence of the *hCAT* gene (450bp), and the Lep Ob genes (heterozygous Ob with WT-specific primer bands at 191 and 104bp and bands at 191 and 123bp for ob-specific primers; homozygous Ob if band at 191bp for Wt-specific primer and bands at 191 and 123bp for the Ob-specific primer). Catalase bands were detected on a 1.2% agarose gel and Ob related bands were detected by use of a 3% agarose gel that also contained Ethidium Bromide (EtBr) that had been electrophoresed at 100V for approximately one hour. Bands were detected using the ChemiDoc and Image Lab Software (BioRad, Hercules, CA) (**Figure 5**).

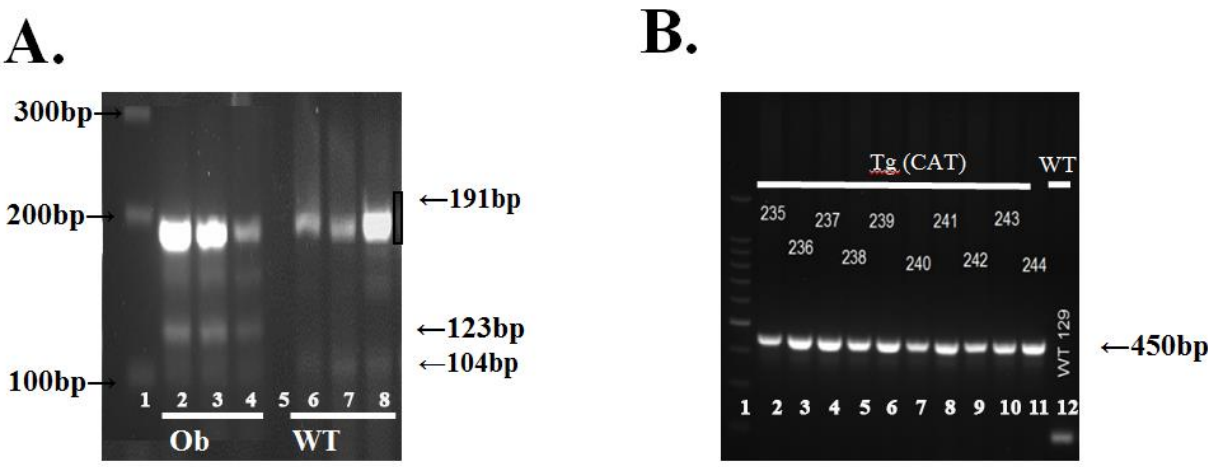

Figure 5. Genotyping [Tg(CAT)$^{\pm}$] and Bob-Cat mice. Images show the ethidium bromide-stained agarose gels of the PCR product during genotyping of: (A) Ob, WT, and (B) human catalase (hCAT) genes. Molecular weight markers are shown in lane 1 (100bp ladder Invitrogen) of images A and B. The sizes of the PCR markers are indicated on the side of each panel. Image A displays the three-primer PCR products representing control and Wt Lep-F primers which produce the control 191 bp product in all tail samples, but only produce the wild-type-specific 104 bp product when a wild-type allele is present (+/+ and ob/+) indicated in lanes 2-4. Lane 5 is no sample control. Three-primer PCR involving control and Lepob-R primers produce the control 191 bp fragment in all tail samples, but only produce the Lepob-specific 123 bp product when a Lepob allele is present (Ob/+ and Ob/Ob) as seen in lanes 2-4. Image B represents samples in lanes 2-11 that have the hCAT gene, while lane 12 is a wild type (WT).

2.2.4 Body Weight and Body Composition (fat and lean mass)

[Tg(CAT)$^{\pm}$] and Bob-Cat mice were weighed weekly from weaning until 20 weeks of age to determine differences in growth rate prior to full development. Growth rates of C57Bl6 and Ob/Ob mice were derived from studies conducted at Jackson Laboratory (where animals were purchased). Body composition (fat and lean mass) was determined using magnetic resonance imaging, ECHO-MRI (Magnetic Resonance Imaging) (Houston, TX). Mice were singly entered in the MRI machine and five measurements were performed on each mouse. The median values of fat and lean mass were computed per mouse, averaged per genotype, and subsequently compared to one another by one-way ANOVA.

2.2.5 Metabolic Parameters Using Comprehensive Lab Animal Monitoring System (CLAMS)

Metabolic parameters were measured indirectly by determining Volume O_2 consumption (VO_2) and Volume CO_2 production (VCO_2), respiratory exchange ratio (RER) as well as X-Ambulatory counts (XAMB) using the CLAMS system (Columbus Instruments, Columbus, OH, USA). Mice were supplied with a sufficient amount of ground standard chow (Lab Diet Rodent Chow 5001) for the duration of the analysis (three days). Computations were made on the middle 48 hours of the three day CLAMS procedure that the mice were subjected to, from approximately 0600 hours of the first day to 0600 hours of the third day. Heat production/energy expenditure (EE), RER average, average food intake (FI) per day, as well as X-Ambulatory locomotor activity per day (counts of movement made across the cage) were determined for each mouse in all groups. Group averages were compared by using a one-way ANOVA.

2.2.6 Tissue Collection

Animals were anesthetized using isoflurane after overnight fasting. Blood was taken by cardiac puncture, centrifuged, separated into red blood cells (RBCs) and plasma. Tissues (kidney, lung, skeletal muscle, heart, adipose, liver, intestinal mucosa (IM), and brain) were removed, weighed, and flash frozen in liquid nitrogen, followed by storage at -80˚C.

2.2.7 Blood Analysis

Whole blood was used to measure fasting glucose levels by a Precision Xtra Glucometer. Blood was then centrifuged for 10 min. to separate the plasma and RBCs. 35 µL of plasma was placed on a Cholestech cassette and read on a LDX Cholestech Machine (Cholestech Corporation, Hayward, CA) to determine Glucose, HDL, LDL, Total Cholesterol (TC), and TG levels. The remaining plasma was frozen at -80˚C.

Circulating levels of IL-6, TNF α, MCP-1/JE, Insulin, Leptin, and Resistin were measured in the plasma of C57Bl6, [Tg(CAT)$^{\pm}$], and Bob-Cat mice by the use of a Milliplex Mouse Adipokine Array (Millipore) by a Luminex 200 system (Millipore, Austin, TX).

2.2.8 Catalase RNA Expression

Catalase gene expression in various tissues (kidney, lung, muscle, heart, adipose, liver, intestinal mucosa (IM), and brain) of C57Bl6 (C), [Tg(CAT)$^{\pm}$] (T), and Bob-Cat (B) mice (male and female) was evaluated by PCR and gel electrophoresis. Total RNA was isolated using Tri-Reagent (Sigma). RNA concentration was measured by the use of the NanoDrop 1000 (NanoDrop Technologies Inc., Thermo Scientific, Wilmington, DE, USA) followed by RT-PCR for amplification (BioRad, Hercules, CA). Samples were evaluated for both Human (*hCAT*) and Mouse (*mCAT*) Catalase using gel electrophoresis in comparison to the housekeeping gene β-Actin. Primers used were as follows: Human Catalase (*hCAT*) (Accession Number: NM-001752) Forward: 5'- acatggtctgggacttctgg -3' and Reverse: 5'- tttgcaataaactgcctccc -3'; Mouse Catalase (*mCAT*) (Accession Number: NM-009804) Forward: 5'- agtcttcgtcccgagtctctc -3' and Reverse: 5'- ctggtcggtcttgtaatggaa -3.' β-Actin (Accession Number NM-007393) Forward: 5'- ctacctcatgaagatcctcaccga -3' and Reverse: 5'- ttctccttaatgtcacgcacgatt -3.' Bands were detected using the ChemiDoc and Image Lab Software (BioRad, Hercules, CA).

2.2.9 Abdominal Adipose Tissue mRNA Expression

RNA was isolated from 100 mg of abdominal adipose tissue using TRI Reagent according to the manufacturer's recommended protocol (Sigma). Concentrations of RNA were measured by use of the NanoDrop 1000 (NanoDrop Technologies Inc., Thermo Scientific, Wilmington, DE, USA). Reverse transcription of total RNA (1 µg) was performed using iScript™ cDNA Synthesis Kit (Bio-Rad Hercules, CA, USA). RT-qPCR was conducted using iQ

SYBR™ Green Supermix (Bio-Rad). The mouse primers for catalase, leptin, adiponectin, MCP-1/JE, IL1β, and β-Actin include: Catalase (Accession Number: NM-009804) Forward: 5'-agtcttcgtcccgagtctctc -3' and Reverse: 5'- ctggtcggtcttgtaatggaa -3.' Leptin (Accession Number: NM-008493) Forward: 5'- ctcatgccagcactcaaaaa -3' and Reverse: 5'- agcaccacaaaacctgatcc -3.' Adiponectin (Accession Number NM-009605) Forward: 5'- gcagagatggcactcctgga -3' and Reverse 5'- cccttcagctcctgtcattcc -3.' MCP-1JE (Accession Number: NM-011333.3) Forward: 5'- ttccttcttggggtcagcacagac -3' and Reverse 5'- actgaagccagctctctcttcctc -3.' IL1β (Accession Number: NM-008361.3) Forward: 5'- aggagaaccaagcaacgaca -3 and Reverse 5'-tgggtgtgccgtctttcatt -3.' β-Actin (Accession Number NM-007393) Forward: 5'-ctacctcatgaagatcctcaccga -3' and Reverse: 5'- ttctccttaatgtcacgcacgatt -3.' RT-qPCR was performed in the Bio-Rad MyiQ or Bio-Rad CFX Connect™ instrument. All samples were run in duplicates or triplicates. Results were calculated using the Pfaffl Equation (2^{-ddCt}) (Pfaffl, 2001), and expressed as fold change compared to the control wild type/C57Bl6 mice.

2.2.10 Western Blot

Approximately 50 mg of abdominal adipose tissue was homogenized in 100 µL Radioimmunoprecipitation assay buffer (RIPA buffer) supplemented with protease inhibitor cocktail. Protein concentrations were determined by the Lowry Method (Lowry, Rosebrough, Farr, & Randall, 1951). Based on these concentrations, predetermined amounts of protein (40-50 µg) per sample were prepared in loading buffer (90% Laemmli and 10% 2-mercaptoethanol) and boiled for 5 min. Samples were run on a SDS-PAGE and separated on 12% or 12.5% EZ Run Protein Gel Solution (Fisher), at 120V for 60-90 minutes. Electrophoretic transfer of the proteins onto a nitrocellulose membrane was performed at 100V for 60 min. on ice. Thermo Scientific Memcode Stain: Pierce MemCode™ Reversible Protein Stain Kit was then used as a loading

control. Membranes were blocked with 1X Tris Buffered Saline (1X TBST), 0.05% Tween 20, pH 7.6, and 5% dry milk for one hour at room temperature. Blots were then incubated overnight at 4˚C with rabbit anti-bovine catalase antibody (1:3000 in 1X TBST and 5% dry milk) (VWR Rockland) which cross-reacts with both mouse and human catalase. After washing with 1X TBST, membranes were incubated with secondary anti-rabbit IgG (1:1000) in 1X TBST and 5% dry milk for 60 min. at room temperature. The immunocomplex was detected with Luminata™ Forte Western HRP (Millipore, Billerica MA). Densitometry of the bands was quantified using BioRad Image Lab Software (BioRad, Hercules, CA) and normalized to MemCode Stain of total protein in each lane.

2.2.11 Catalase Enzymatic Activity

Catalase enzymatic activity was measured according to the method of Aebi (Aebi, 1984). A standard curve was first generated using 1-5 units of bovine catalase (Sigma, 9001-9502). Approximately 50 mg of abdominal adipose tissue from each mouse was homogenized in 100 µL of 50 mM KH_2PO_4, 5 ug/µL Aprotinin, and 2 µL of 0.1 M PMSF. Appropriate dilutions were made and 8 µL of each homogenate was added to 1 mL of 25 mM Hydrogen Peroxide (H_2O_2) solution (Sigma) and analyzed on a Shimadzu Spectrophotometer for one minute. Initial rate of disappearance of H_2O_2 was recorded at a wavelength of 240 nm during the 1 minute (ΔA240 nm/min). Each sample was analyzed in duplicate or triplicate. Change in absorbance was recorded for each tissue sample and specific activity was calculated based on protein estimation of the homogenate by the Lowry Method.

2.2.12 Protein Carbonylation Using OxyBlot

Approximately 50 mg of abdominal adipose tissue per sample was prepared by denaturing and derivatizing the proteins with a solution of 12% Sodium Dodecyl Sulfate (SDS) and Dinitrophenylhydrazine (DNPH) according to OxyBlot (Millipore) protocol. Neutralization solution was used to terminate the derivatization reaction after 15 min. The separation of proteins was achieved using a 12.5% EZ Run Protein Gel Solution (Fisher) or 12% mini PROTEAN TGX 12% (BioRad) at 100V for 50-60 minutes followed by transfer to a nitrocellulose membrane at 100V for 90 minutes. To determine equal loading and transfer efficiency, Pierce MemCode™ Reversible Protein Stain was used to visualize proteins in a BioRad ChemiDoc and analyzed using BioRad Image Lab (BioRad, Hercules, CA). Non-specific binding sites were blocked with 1X Phosphate Buffered Saline and Tween 20 (1X PBST) and 10% Bovine Serum Albumin (BSA) rocking for one hour. A 1:500 dilution of primary antibody, Rabbit-Anti-DNP (Millipore OxyBlot Kit) was added and rocked overnight at 4˚C, followed by washes with 1X PBST. Blots were conjugated with a 1:300 dilution of goat anti-rabbit IgG (Horseradish Peroxidase conjugated) for one hour at room temperature with rocking. Bands were visualized with Luminata™ Forte Western HRP (Millipore, Millerica, MA) using BioRad Chemidoc and Image Lab (BioRad, Hercules, CA). OxyBlot data of oxidized proteins were expressed as the densitometric ratio of the dinitrophenylhydrazone (DNP) bands to total protein in each lane obtained by the Memcode stain.

2.2.13 Statistical Analysis

Results for body composition and enzymatic activity are presented as mean ± standard error of the mean (S.E.M.) and plotted using GraphPad Prism. One-way ANOVA and Multiple Comparisons were used to evaluate the differences between the genotypes with Bonferonni post

hoc analysis. $p<0.05$ was considered statistically significant. For RT-qPCR analysis, expression was determined by use of the Pfaffl equation 2^⁻ddCT (Pfaffl, 2001) and represented as fold change with significance denoted as differences in delta CT/genotype.

2.3 RESULTS

2.3.1 Breeding Outcomes for the Bob-Cat Mouse Model

The breeding scheme depicted in **Figure 4A** was used to generate Bob-Cat mice for three generations. Ratios of genotype of each generation of breeding pairs is depicted in **Figure 4B**. Approximately 50:50 ratios of males to females were observed in each of the F1-F3 generations. The first and second generations of pups were approximately 60% Bob-Cat while the third generation, F3, consisted of 100% Bob-Cat. In addition to "Bob-Cat" which is heterozygous for the *ob* gene, there was also the generation of mice that were homozygous for the *ob* gene that overexpressed catalase (**Big-Bob**). However, this genotype was rare in occurrence and was more skewed towards females than males (7% F1 and 2% F2 generations). In an effort to elucidate high antioxidant (catalase) effect in a leptin-resistant model, we are continuing to cross-breed, to generate more homozygous *ob* mutant mice overexpressing catalase.

3.2 Mouse and Human Catalase Gene Expression in Various Tissues

Bob-Cat (B) male and female mice were evaluated for the expression levels of human and mouse *catalase* in various tissues and compared to C57Bl6 (C) and [Tg(CAT)$^{\pm}$] (T) mice. Mouse catalase (*mCAT*) as well as human catalase (*hCAT*) mRNA levels were analyzed and compared by densitometry ratios to *β-Actin* using BioRad Image Lab (BioRad, Hercules, CA). Male Bob-Cat mice generally had higher levels of *hCAT* in comparison to the other genotypes of mice. However, levels of *mCAT* trended to be lower in comparison to the other two genotypes (**Figure 6A-F**). In general, female Bob-Cat mice showed no statistical difference in *hCAT* across most tissues, but there was a trend for increase in the brain, significant increase in the liver, and a decrease in muscle compared to C57Bl6. Additionally, there was a decrease in intestinal mucosa (IM) compared to [Tg(CAT)$^{\pm}$] (**Figure 6 G-L**). With regard to *mCAT* in female Bob-Cat mice,

levels trended to be lower except in the IM and brain where there was a significant increase in comparison to both the other genotypes analyzed.

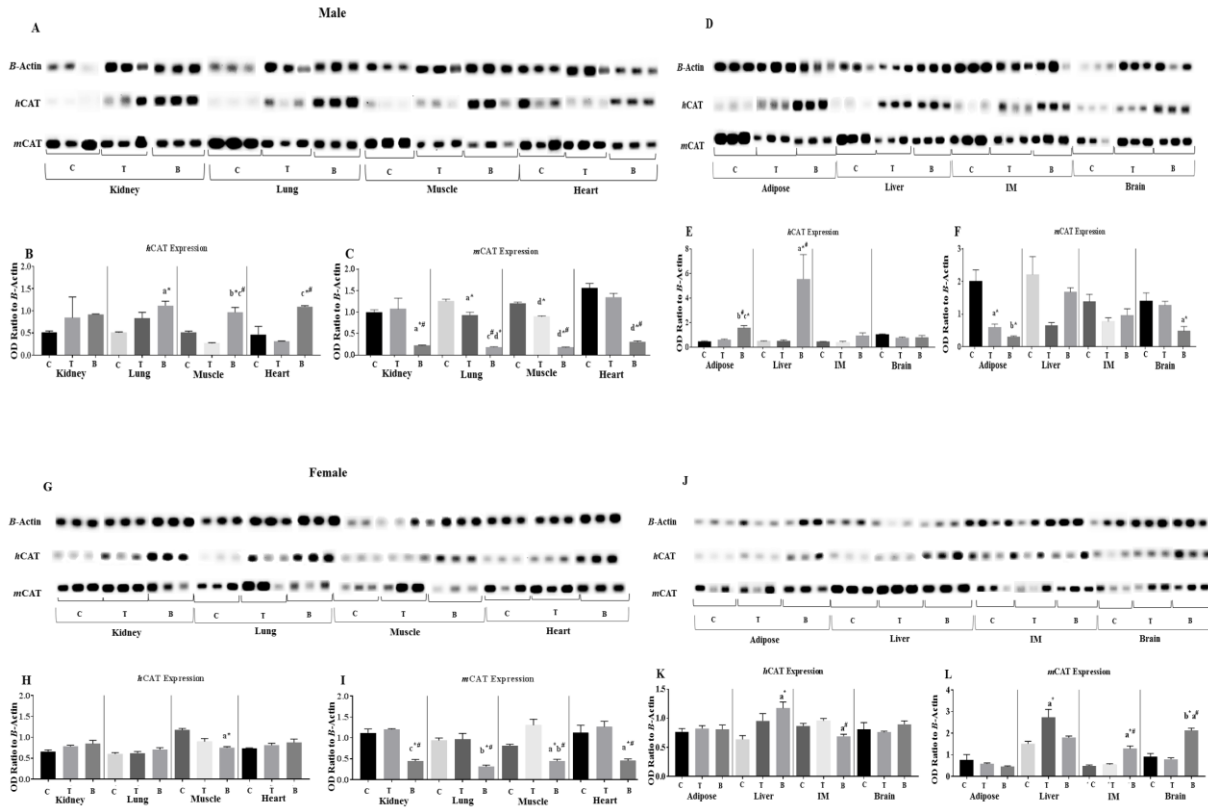

Figure 6. Mouse and human catalase gene expression in various tissues. (A) Densitometric images of β-Actin, Human Catalase (hCAT) and Mouse Catalase (mCAT) PCR products of kidney, lung, muscle, and heart. (B) and (C) show densitometry ratios of hCAT and mCAT to β-Actin respectively from male mice. (D) Densitometric images of β-Actin, hCAT and mCAT PCR products of adipose, liver, intestinal mucosa (IM), and brain. (E-F) show densitometry ratios of hCAT and mCAT to β-Actin respectively from female mice. (G-L) The representative images from female mice are displayed. The genotype of the mice groups are depicted as C for C57Bl6, T for [Tg(CAT)$^{\pm}$], and B for Bob-Cat mice. Densitometric ratios of catalase to β-Actin were determined using BioRad Image Lab. Data are expressed as mean densitometric ratio of each group +/- SEM from n≥3 mice. Data were analyzed by One-way ANOVA and differences between genotypes were significant at $p<0.05$a*, $p<0.01$b*, $p<0.001$c*, $p<0.0001$d* to C57Bl6; $p<0.05$a#, $p<0.01$b#, $p<0.001$c#, $p<0.0001$d# to [Tg(CAT)$^{\pm}$].

2.3.2 Body Composition and Tissue Weight

As seen in **Table 1A and 1B**, both male and female mice that overexpress antioxidant catalase have significantly lower body weight in comparison to the Ob/Ob mice (background of Bob-Cat mice) as do the control C57Bl6 mice. However, body weights of the novel Bob-Cat mouse were not significantly different from the C57Bl6 or [Tg(CAT)$^{\pm}$] mouse. The male [Tg(CAT)$^{\pm}$] mice on the other hand are slightly heavier than the C57Bl6 mice at adulthood as seen in **Table 1A**. No significant differences were seen between Bob-Cat mice and C57Bl6 or [Tg(CAT)$^{\pm}$] with regard to liver and adipose weight, but as expected, Ob/Ob adipose and liver weights were significantly heavier than all other groups ($p<0.0001$). This effect was the same in both genders (**Table 1A and 1B**).

A.

Male	Body Weight (g)	Abdominal Adipose (g)	Liver Weight (g)
C57Bl6/WT	27.09 ± 0.79	0.77 ± 0.02	1.04 ± 0.07
[Tg(CAT)$^{\pm}$]	33.32 ± 0.46^{a*}	1.28 ± 0.11	1.55 ± 0.06
Bob-Cat	31.00 ± 1.02	1.73 ± 0.17	1.43 ± 0.05
Ob/Ob	54.45 ± 2.21$^{d*\#\$}$	8.13 ± 0.71$^{d*\#\$}$	4.35 ± 0.24$^{d*\#\$}$

B.

Female	Body Weight (g)	Abdominal Adipose (g)	Liver Weight (g)
C57Bl6/WT	22.74 ± 0.37	0.91 ± 0.12	1.05 ± 0.05
[Tg(CAT) $^{\pm}$]	21.18 ± 0.74	0.53 ± 0.06	1.05 ± 0.06
Bob-Cat	24.21 ± 0.24	1.12 ± 0.13	1.18 ± 0.06
Ob/Ob	51.71 ± 1.50$^{d*\#\$}$	7.76 ± 0.21$^{d*\#\$}$	2.61 ± 0.07$^{d*\#\$}$

Table 1: Body weight and tissue weights. (A) Adult male (n≥4) body weight, adipose and liver weights of C57Bl6, [Tg(CAT)$^{\pm}$], Bob-Cat, and Ob/Ob (n≥4) mice. (B) Adult female (n≥6) body weight, adipose weight, and liver weight of C57Bl6, [Tg(CAT)$^{\pm}$], Bob-Cat, and Ob/Ob (n≥6) mice. One-way ANOVA was performed on GraphPad Prism 7. Data reported as mean ± S.E.M. and significant differences are displayed with letters indicating p values: a=$p<0.05$, b= $p<0.01$, c=$p<0.001$, d=$p<0.0001$; symbols represent significant differences between genotypes, *= to C57Bl6, #= to [Tg(CAT)$^{\pm}$], $= to Bob-Cat.

From 4 to 20 weeks of age, mice considerably gained weight. However, statistical significance within the four genotypes of males is noted at 5 weeks of age between the Ob/Ob mice and the other three genotypes ($p<0.05$) (**Figure 7A**). Female mice, shown in **Figure 7B**, on the other hand, showed a significant difference in body weight beginning at 4 weeks between the Ob/Ob mice and every other genotype ($p<0.0001$). C57Bl6 and Ob/Ob body weights were obtained from Jackson Labs: (C57BL/6J https://www.jax.org/jax-mice-and-services/straindata-sheet-pages/body-weight-chart-000664; B6 Cg-Lepob/J https://www.jax.org/jax-mice-and-serviceccs/strain-data-sheet-pages/body-weight-chart-000632).

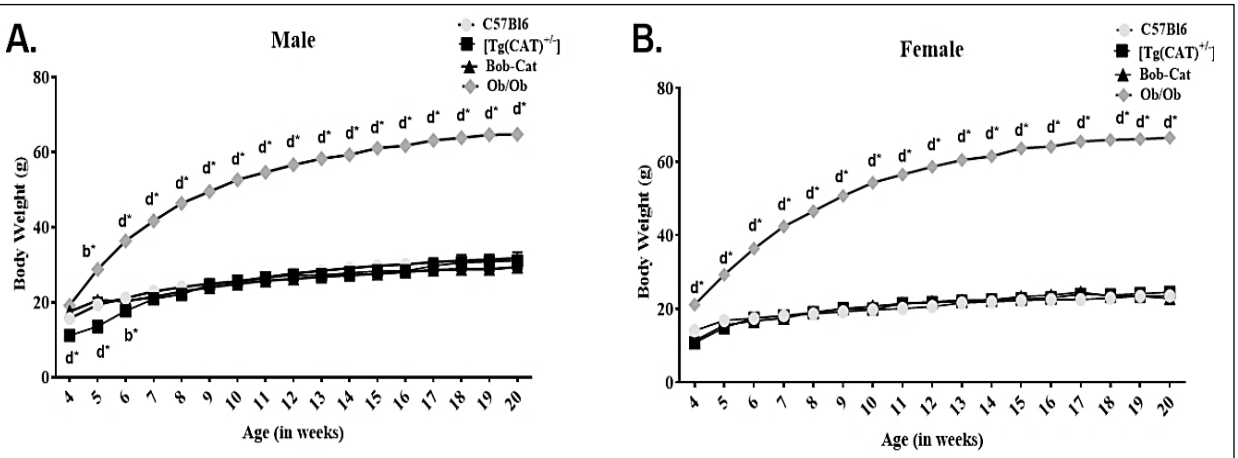

Figure 7. Weekly body weights. (A) Male and (B) Female weekly body weight of ($n\geq7$/group) C57Bl6, [Tg(CAT)$^{\pm}$], Bob-Cat, and Ob/Ob mice. C57Bl6 and Ob/Ob measured by Jackson Laboratories. One-way ANOVA was performed on GraphPad Prism 7. Data represented as mean ± S.EM. and considered significant at $p<0.01$a*, $p<0.0001$d* to C57Bl6.

2.3.3 Body Composition (ECHO-MRI)

ECHO-MRI was used to determine the lean and fat mass of all genotypes. A significant difference was observed in the fat mass of the Ob/Ob mouse group compared to both genders of the other genotypes. The lean mass was observed to be greater ($p<0.04$) for each male genotype that overexpresses antioxidant catalase in comparison to both C57Bl6 and Ob/Ob mice (**Figure 8A1 and A2**), revealing a difference in body composition that should be further investigated. In

the female groups, Bob-Cat mice have a significantly higher fat mass compared to [Tg(CAT)$^{\pm}$], and lean mass compared to C57Bl6 and [Tg(CAT)$^{\pm}$] genotypes ($p<0.02$) (**Figure 8B1 and B2**). The sex differences in body composition are intriguing and worth investigating in the future.

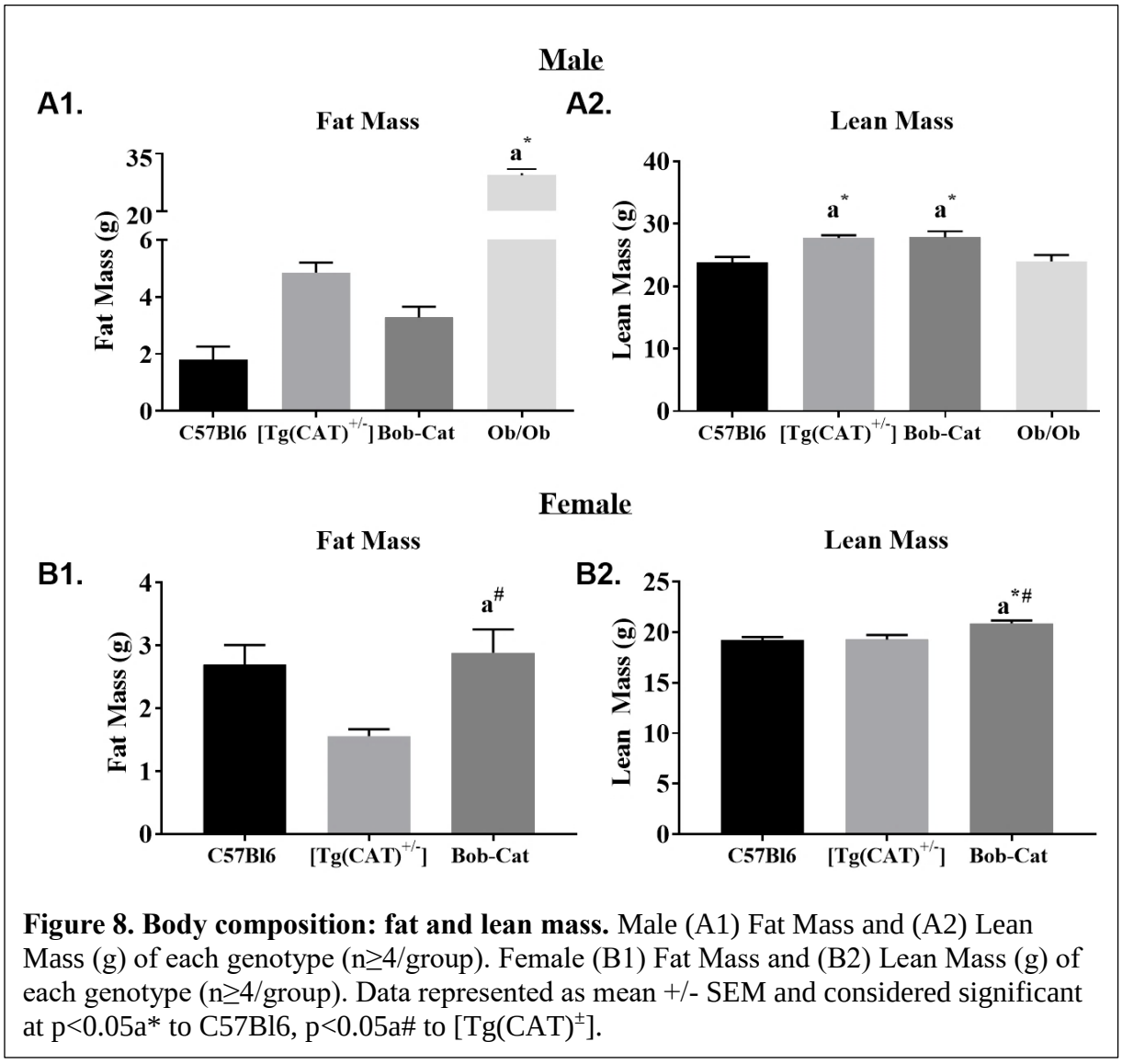

Figure 8. Body composition: fat and lean mass. Male (A1) Fat Mass and (A2) Lean Mass (g) of each genotype (n≥4/group). Female (B1) Fat Mass and (B2) Lean Mass (g) of each genotype (n≥4/group). Data represented as mean +/- SEM and considered significant at $p<0.05$a* to C57Bl6, $p<0.05$a# to [Tg(CAT)$^{\pm}$].

2.3.4 Metabolic Parameters Analyzed by CLAMS

Although body weight and fat mass did not significantly differ between C57Bl6 and mice overexpressing antioxidant catalase, significant changes were seen in metabolic parameters as determined by CLAMS within the adult genotypes (**Figure 9**). Overall (combination of both light/dark cycles) analysis of CLAMS data showed that neither male nor female mice

significantly differed with regard to FI per day. Significant differences were observed in the energy expenditure levels and XAMB counts in male Ob/Ob mice compared to the other genotypes. RER was not significantly different in either gender.

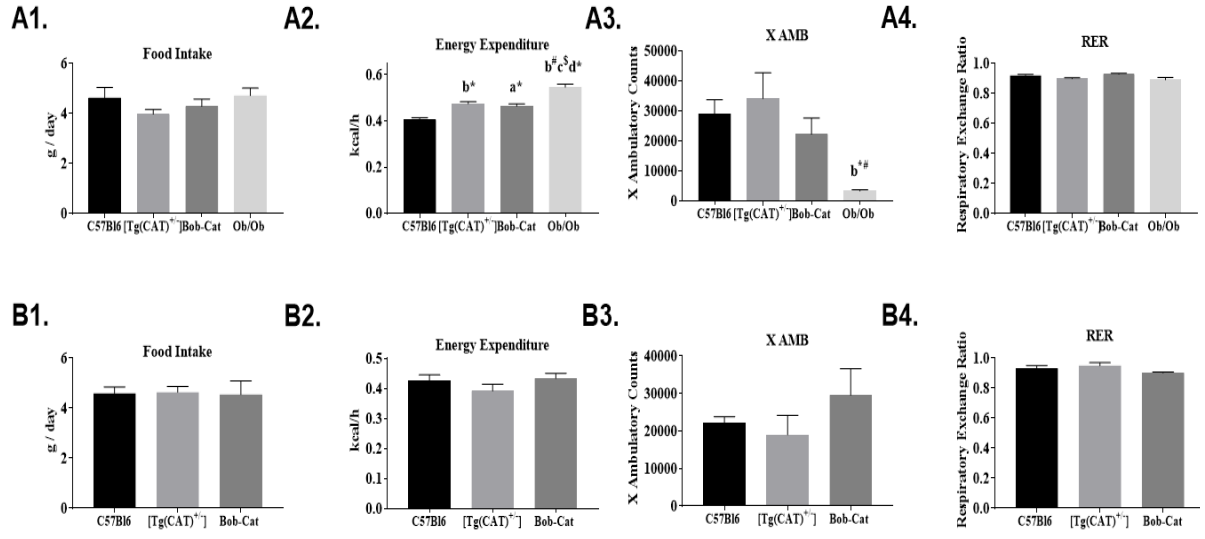

Figure 9. Metabolic parameters. Male- (A1) Food Intake of C57Bl6, [Tg(CAT)$^{\pm}$], Bob-Cat, and Ob/Ob averaged per day; (A2) Metabolic Energy Expenditure of each genotype averaged kcal/h over the middle 48h; (A3) XAMB Counts of each genotype over 48h; (A4) Respiratory Exchange Ratio (RER) average over 48h; Female- (B1) Food Intake of each genotype averaged grams (g) per day; (B2) Metabolic Energy Expenditure of each genotype averaged kcal/h over the middle 48h; (B3) X-AMB Counts of each genotype over 48h; (B4) RER average over 48h. Data represented as mean ± S.E.M. $p<0.05$a*, $p<0.01$b*, $p<0.0001$d* to C57Bl6; $p<0.01$b# to [Tg(CAT)$^{\pm}$]; $p<0.001$c$ to Bob-Cat.

Independent analysis of CLAMS data collected during the light and dark cycle **(Table 2 and Figure 10)**, showed that the FI and RER did not significantly differ among genotypes of either gender. However, significant differences in EE were seen among the male groups in both light and dark cycles. Bob-Cats showed a trend towards higher levels and [Tg(CAT)$^{\pm}$] showed significantly higher levels of EE ($p<0.008$) compared to C57Bl6 males. The same effect was noted for the dark cycle where, Bob-Cats and [Tg(CAT)$^{\pm}$] did have statistically higher levels of energy expenditure in comparison to C57Bl6 mice ($p=0.021$). In assessment of physical activity,

Group	LIGHT				DARK			
Male	**FI (g)**	**EE (kcal/h)**	**XAMB**	**RER (VCO_2/ VO_2)**	**FI (g)**	**EE (kcal/h)**	**XAMB**	**RER (VCO_2/ VO_2)**
C57Bl6/WT	1.43 ± 0.196	0.366 ± 0.010	7398 ± 963	0.886 ± 0.005	3.07 ± 0.271	0.445 ± 0.009	24858 ± 3432	0.942 ± 0.009
[Tg(CAT)$^{\pm}$]	1.34 ± 0.042	0.442 ± 0.008 b#	9581 ± 2770	0.871 ± 0.006	2.64 ± 0.208	0.509 ± 0.009 a*	24392 ± 4911	0.920 ± 0.009
Bob-Cat	1.35 ± 0.042	0.422 ± 0.010	5088 ± 1209	0.899 ± 0.010	2.98 ± 0.247	0.508 ± 0.008 a*	17000 ± 3340	0.952 ± 0.009
Ob/Ob	1.04 ± 0.146	0.503 ± 0.013 b$ d*#	874.4 ± 112.4 a*#	0.867 ± 0.014	3.10 ± 0.444	0.589 ± 0.015 a*b#$	2421 ± 243.7 a$b#c*	0.913 ± 0.016
Female								
C57Bl6/WT	1.78 ± 0.137	0.398 ± 0.019	4791 ± 405	0.924 ± 0.015	2.82 ± 0.109	0.453 ± 0.017	17357 ± 1136	0.939 ± 0.024
[Tg(CAT)$^{\pm}$]	1.67 ± 0.140	0.362 ± 0.020	4502 ± 910	0.932 ± 0.022	2.97 ± 0.137	0.421 ± 0.022	14556 ± 3845	0.973 ± 0.017
Bob-Cat	1.74 ± 0.218	0.387 ± 0.017	11206 ± 2440	0.891 ± 0.010	2.80 ± 0.323	0.477 ± 0.021	40300 ± 8352 a*#	0.910 ± 0.008

Table 2. Light and dark cycles of metabolic parameters. Male and female averaged light and dark cycles of food intake (FI) as average grams (g) of chow consumed per cycle, metabolic energy expenditure kcal/h of each mouse group, counts of physical movement as XAMB / cycle, and average Respiratory Exchange Ratio (RER) as VCO_2/VO_2 per cycle. One-way ANOVA was performed using Graph-Pad Prism 7. Data are represented as mean ± S.E.M. and significant differences are displayed with letters indicating p values: a=$p<0.05$, b= $p<0.01$, c=$p<0.001$, d=$p<0.0001$; symbols represent significant differences between genotypes, *= to C57Bl6/WT, #= to [Tg(CAT)$^{\pm}$], $= to Bob-Cat.

there was also a trend for higher levels of activity (XAMB) in Bob-Cat males in comparison to the Ob/Ob mouse group; most notably in the light cycle (**Figure 10A1-A4**). Ob/Ob male mice also had significantly lower activity levels (XAMB) in both the light and dark cycles compared to [Tg(CAT)$^{\pm}$] and C57Bl6 mice ($p<0.01$) yet higher levels of energy expenditure compared to all other groups ($p<0.01$). Within females, all measured parameters with the CLAMS did not significantly differ between the groups except that XAMB counts were much higher in the Bob-

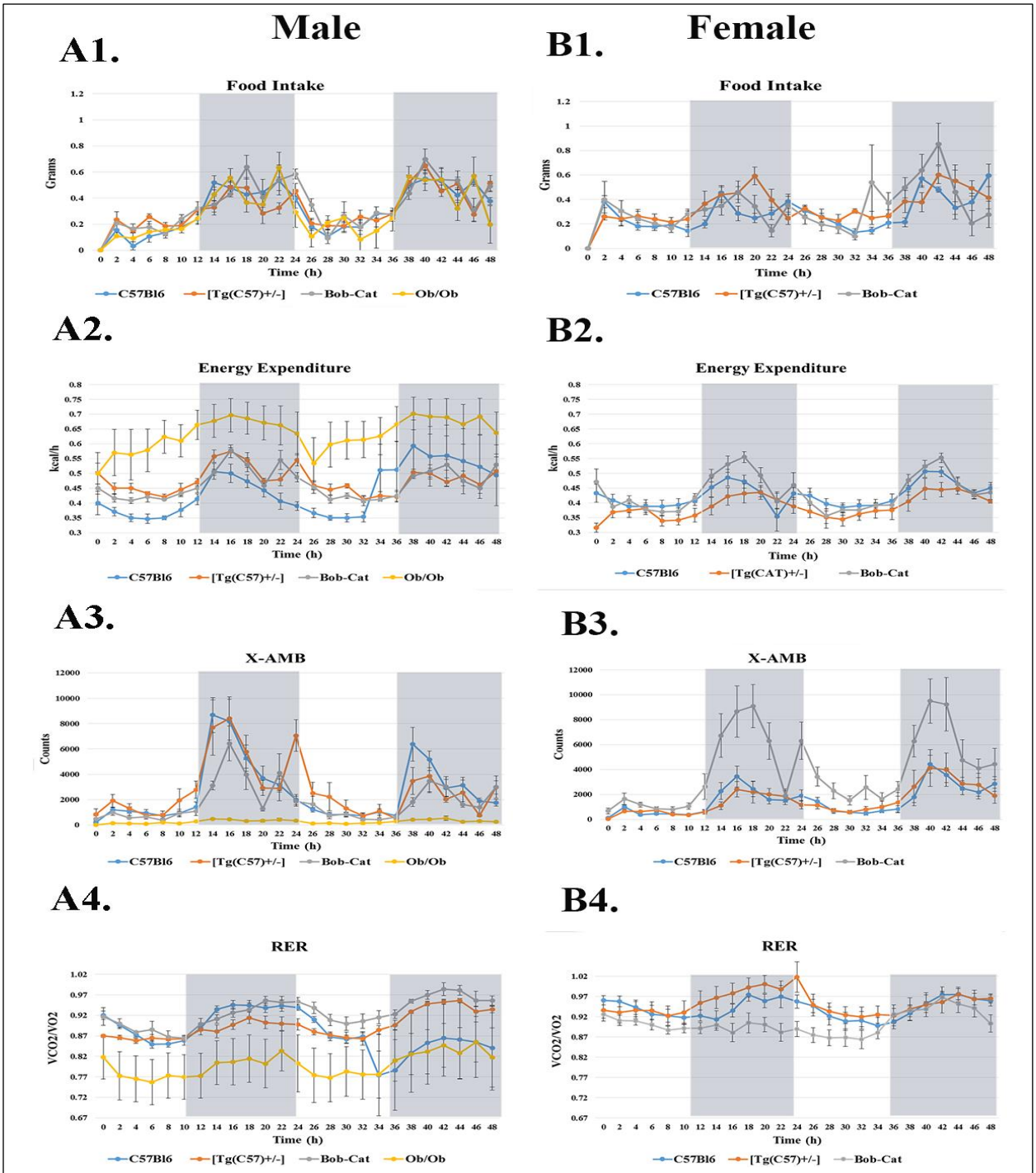

Figure 10. Two hour time interval analysis of metabolic parameters. (A1) Food Intake grams/day (A2) Metabolic Energy Expenditure averaged kcal/h over the middle 48h (A3) X-AMB Counts over 48h (A4) Respiratory Exchange Ratio (RER) average over 48h of male C57Bl6, [Tg(CAT)$^{\pm}$], Bob-Cat, and Ob/Ob. (B1) Food Intake averaged g/day (B2) Metabolic Energy Expenditure averaged kcal/h over the middle 48h (B3) X-AMB Counts of each genotype over 48h (B4) RER average over 48h of female mice of each genotype. Data represented as mean ± S.E.M.

Cat female group ($p<0.04$) compared to both female C57Bl6 and [Tg(CAT)$^{\pm}$] in both light and

dark cycles (**Figure 10B1-B4**).

Data comparing the Bob-Cat (het Ob/+) to Big Bob (homozygous Ob/Ob) genotypes mice overexpressing catalase is displayed in **Table 3**. Big Bob mice have significantly higher body weight and fat mass. CLAMS data showed a trend toward an overall increase in FI and decrease in XAMB (combined light and dark cycles) as well as significantly higher levels of EE compared to the Bob-Cat mice.

Genotype	Bob-Cat (n≥4)	Big Bob (n≥3)
Adult Images	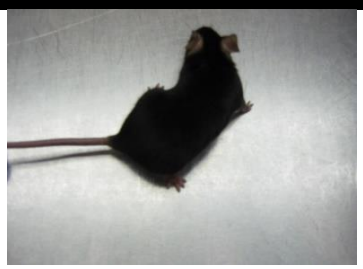	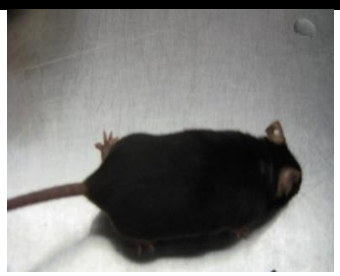
Body Weight (g)	31.0 ± 1.02	49.7 ± 2.4$^{d\$}$
Fat Mass (g)	3.28 ± 0.33	22.6 ± 1.11$^{d\$}$
Lean Mass (g)	27.8 ± 0.86	24.5 ± 1.69
24h RER VCO_2/VO_2	0.927 ± 0.01	0.934 ± 0.01
24h EE (Kcal/h)	0.46 ± 0.01	0.55 ± 0.03$^{a\$}$
24h FI (g/24h)	4.28 ± 0.26	4.953 ± 0.60
24h XAMB (counts/24h)	22238 ± 4686	12408 ± 9760

Table 3. Characteristics of Bob-Cat and Big Bob mouse models. Data are reported as average ± S.E.M. An unpaired t test was performed for each parameter on GraphPad Prism 7. Data reported as mean ± S.E.M. and significant differences are displayed with letters indicating p values: a=p<0.05 and d=p<0.0001; symbols represent significant differences between genotypes: $= to Bob-Cat.

2.3.5 Circulating Metabolic Profile

Blood glucose levels did not significantly differ between the Bob-Cat mice of either sex compared to C57Bl6 or [Tg(CAT)$^{\pm}$] (**Table 4A-4B)**. However, the Ob/Ob mouse group had

significantly higher levels of plasma glucose compared to all other genotypes. HDL and TC levels were significantly elevated in both sexes of the Ob/Ob mouse strain compared to all other genotypes. Interestingly, male [Tg(CAT)$^{\pm}$] mice had significantly higher levels of plasma TG (**Table 4A**) compared to the other male groups, while Bob-Cat mice were highly similar to the C57Bl6 control mice.

A.

Male	Total Cholesterol (mg/dL)	HDL (mg/dL)	TG (mg/dL)	Glucose (mg/dL)
C57Bl6/WT	<100	61.8 ± 9.68	46.3 ± 1.08	188.4 ± 9.1
[Tg(CAT) $^{\pm}$]	<100	64.8 ± 2.38	95.3 ± 15.9 ^{a*}	220.1 ± 14.1
Bob-Cat	<100	65.8 ± 4.56	47.5 ± 0.9 $^{b\#}$	203.4 ± 7.3
Ob/Ob	150 ± 7.49 $^{d*\#\$}$	≥ 98.8 ± 1.08 **a#$b***	67.5 ± 8.5	319.8 ± 27.1 **a#b*$**

B.

Female	Total Cholesterol (mg/dL)	HDL (mg/dL)	TG (mg/dL)	Glucose (mg/dL)
C57Bl6/WT	<100	48.63 ± 3.45	47.4 ± 2.22	192.9 ± 13.0
[Tg(CAT) $^{\pm}$]	<100	51.42 ± 3.2	50.2 ± 2.72	225 ± 9.0
Bob-Cat	<100	47.45 ± 2.93	54.8 ± 3.27	176.3 ± 12.4
Ob/Ob	119.4 ± 3.8 $^{d*\#\$}$	≥93.43 ± 3.87 **d*#$**	80.3 ± 9.23 $^{c*\#}$	367.8 ± 44.6 **d*#$**

Table 4. Blood lipid profile and glucose level. A) Total Cholesterol, High Density Lipoprotein (HDL), Triglyceride (TG), and Glucose levels in C57Bl6/WT, [Tg(CAT)$^{\pm}$], Bob-Cat, and Ob/Ob mice (n≥4/group) (B) Total Cholesterol, High Density Lipoprotein (HDL), Triglyceride (TG), and Glucose levels in C57Bl6/WT, [Tg(CAT)$^{\pm}$], Bob-Cat, and Ob/Ob female mice (n≥6/group). Data reported as mean ± S.E.M. and significant differences are displayed with letters indicating p values: a=p<0.05, b= p<0.01, c=p<0.001, d=p<0.0001; symbols represent significant differences between genotypes, *= to C57Bl6/WT, #= to [Tg(CAT)$^{\pm}$], $= to Bob-Cat.

Milliplex Mouse Adipokine Array was used to measure circulating levels of IL-6, TNF α, MCP-1/JE, insulin, leptin, and resistin in blood plasma. Results shown in **Figure 11A** revealed that [Tg(CAT)$^{\pm}$] and Bob-Cat mice trended to have similar levels of insulin. There were no statistically significant differences for plasma levels of leptin or resistin which are two major

adipokines released from adipose tissue, between the control C57Bl6 parent group and mouse groups that over express catalase. The trend was similar in females (**Figure 11B**); however, it is intriguing to note, the levels were higher compared to male groups. Ob/Ob had significantly higher levels of insulin and resistin and very minimal leptin compared to all other groups. IL-6, TNF α, and MCP-1/JE were undetected or no trends were seen between mouse groups.

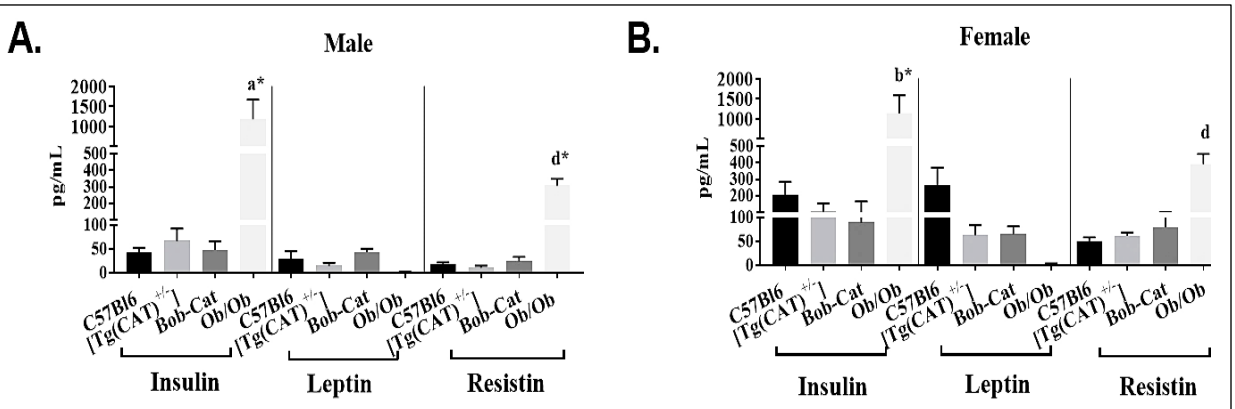

Figure 11. Circulating levels of metabolic parameters. Circulating levels of insulin, leptin, and resistin were measured using an adipokine array on a Luminex system: (A) C57Bl6, Bob-Cat, [Tg(CAT)$^{\pm}$], and Ob/Ob male mice; (B) C57Bl6, Bob-Cat, [Tg(CAT)$^{\pm}$], and Ob/Ob female mice. Data displayed as mean ± S.E.M. $p<0.05$a*, $p<0.01$b*, $p<0.0001$d* to C57Bl6, Bob-Cat, and [Tg(CAT)$^{\pm}$].

2.3.6 Catalase mRNA, Protein Expression, and Enzyme Activity in Adipose Tissue

Being a key metabolic tissue that plays a role in obesity, catalase mRNA expression was determined in visceral adipose tissue (WAT) obtained from both male and female mice of all genotypes using RT-qPCR on a Bio-Rad MyiQ. In male mice, *catalase* mRNA expression was upregulated by about 35 fold in Bob-Cat mice and was about 5 fold higher in the Ob/Ob mice compared to C57Bl6 (**Figure 12A1**). Western blot showed increase in catalase protein in [Tg(CAT)$^{\pm}$] and Bob-cat mice but lower levels in the Ob/Ob mice (**Figure 12B)**. Catalase

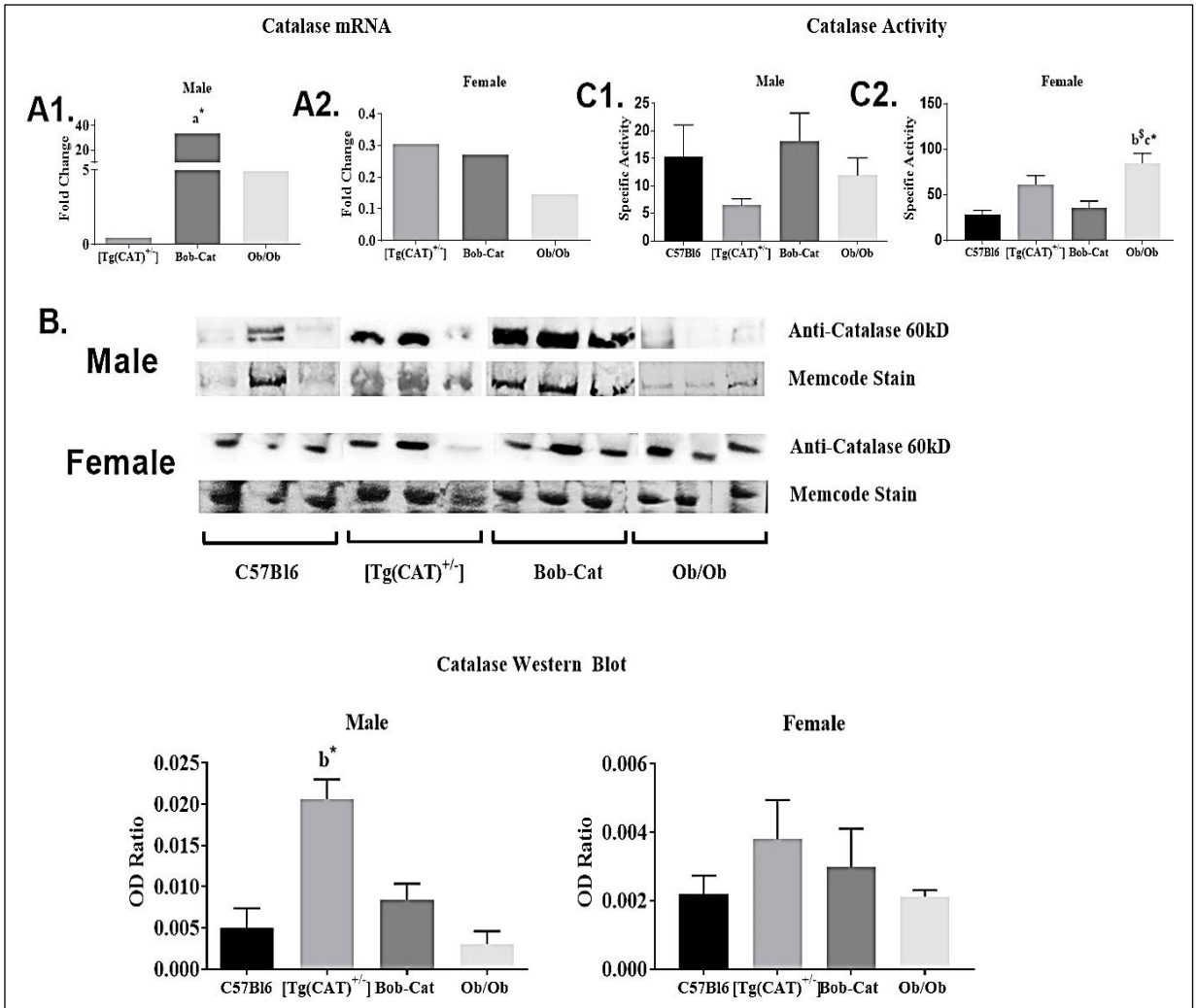

Figure 12. Catalase mRNA expression, protein, and enzyme activity in adipose tissue. (A1) Male and (A2) Female Catalase mRNA expression measured by RT-qPCR of the adipose tissue in [Tg(CAT)+/-], Bob-Cat, and Ob/Ob mice and depicted as fold change compared to C57Bl6 mice (n≥4/genotype) by ddCT Method. (B) Western Blot of catalase protein as shown by densitometric ratio of anti-Catalase and memcode stain of each genotype (n=3/group). Catalase enzyme activity as measured by Aebi method (C1) Male and (C2) Female specific activity of catalase (n≥7/group). Data reported as mean +/- SEM. p<0.05a* p<0.01b*, p<0.001c* considered significant to C57Bl6; p<0.01b$ to Bob-Cat.

enzyme activity, as determined by measuring the decomposition of H_2O_2, showed varying activities in the adipose tissue **(Figure 12C1)**. No significant differences were detected, but Bob-Cat mice trended to have higher activity levels compared to C57Bl6 mice. In contrast, females displayed no significant difference in catalase mRNA and protein expression in adipose tissue (**Figure 12A2 and B)**. However, mice overexpressing catalase trended to have higher levels

within adipose tissue in comparison to C57Bl6 and Ob/Ob mice. With regard to enzyme activity, catalase activity in females was highest in the Ob/Ob mice, but all genotypes trended to have higher levels than the C57Bl6 mice (**Figure 12C2**).

2.3.7 Oxyblot Detection of Oxidized Proteins in Adipose Tissue

Oxidized carbonyl groups are a commonly used marker of oxidative stress. Carbonylation of proteins in the adipose tissue was detected using oxyblot and evaluated based on densitometry ratios for each genotype. Male [Tg(CAT)$^{\pm}$] had significantly lower ($p<0.05$) and Bob-Cat mice trended to have lower levels of carbonylated proteins within adipose tissue compared to the C57Bl6 control group (**Figure 13A1-3**). However, Ob/Ob mice had significantly higher levels of oxidized carbonyl groups than the Bob-Cat mice as well as the other two genotypes within the males ($p<0.001$). Female Bob-Cat mice showed no significant differences in oxidized proteins **(Figure 13B1-3)**.

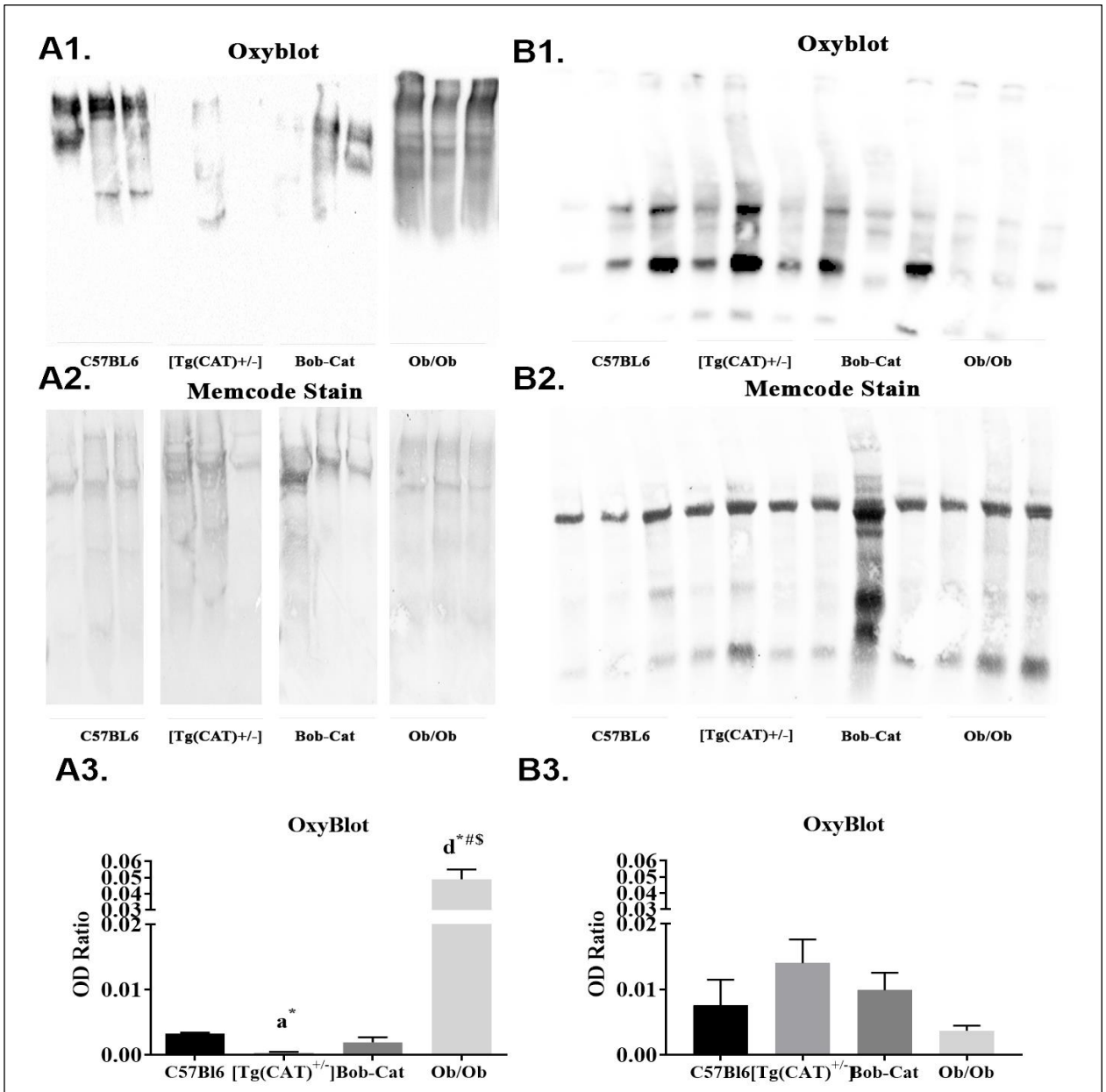

Figure 13. Oxyblot of oxidized proteins. (A1) Oxyblot of oxidized carbonyl groups; (A2) Memcode stain of total proteins; (A3) Densitometric ratios of oxidized proteins to total proteins (memcode) in adipose tissue of C57Bl6, [Tg(CAT)+/-], Bob-Cat, and Ob/Ob male mice; (B1) Female memcode stain of each genotype followed by (B2) blot of oxidized carbonyl groups and the (B3) Respective densitometric ratios per group. Error reported as mean +/- SEM. $p<0.05$ a* considered significant to C57Bl6; $p<0.0001$ d# to [Tg(CAT)+/-].

2.3.8 mRNA Expression of Metabolic Genes in Adipose Tissue

The mRNA expression of genes involved in adipose function: *leptin*, *adiponectin*, *MCP-1/JE*, and *IL1β* was evaluated by RT-qPCR. In males, leptin, a key regulator of fat mass, was increased by about 4 fold in [Tg(CAT)$^{\pm}$], approximately 188-fold in the Bob-Cat mice, and 88 fold in the Ob/Ob genotype compared to the C57Bl6 controls (**Figure 14A1**). In female mice, there was a significant increase in leptin in both the Bob-Cat and Ob/Ob mice; approximately 69 and 169-fold respectively **(Figure 14B1)**.

Adiponectin, an anti-inflammatory adipokine which plays a key role in glucose and lipid signaling was also increased in the male Bob-Cat mice compared to C57Bl6 and [Tg(CAT)$^{\pm}$] mice **(Figure 14A2)**. A similar trend was also noted in female mice ($p<0.05$). Female Bob-Cat mice had significantly higher adiponectin levels than C57Bl6 mice ($p<0.01$) followed by the Ob/Ob female mice ($p<0.01$) (**Figure 14B2**). Both IL1β and MCP-1/JE, key pro-inflammatory adipokines, showed no significant differences between any of the lean genotypes in either sex; however, increased levels were seen in Ob/Ob mice (**Figure 14A3-4, B3-4**).

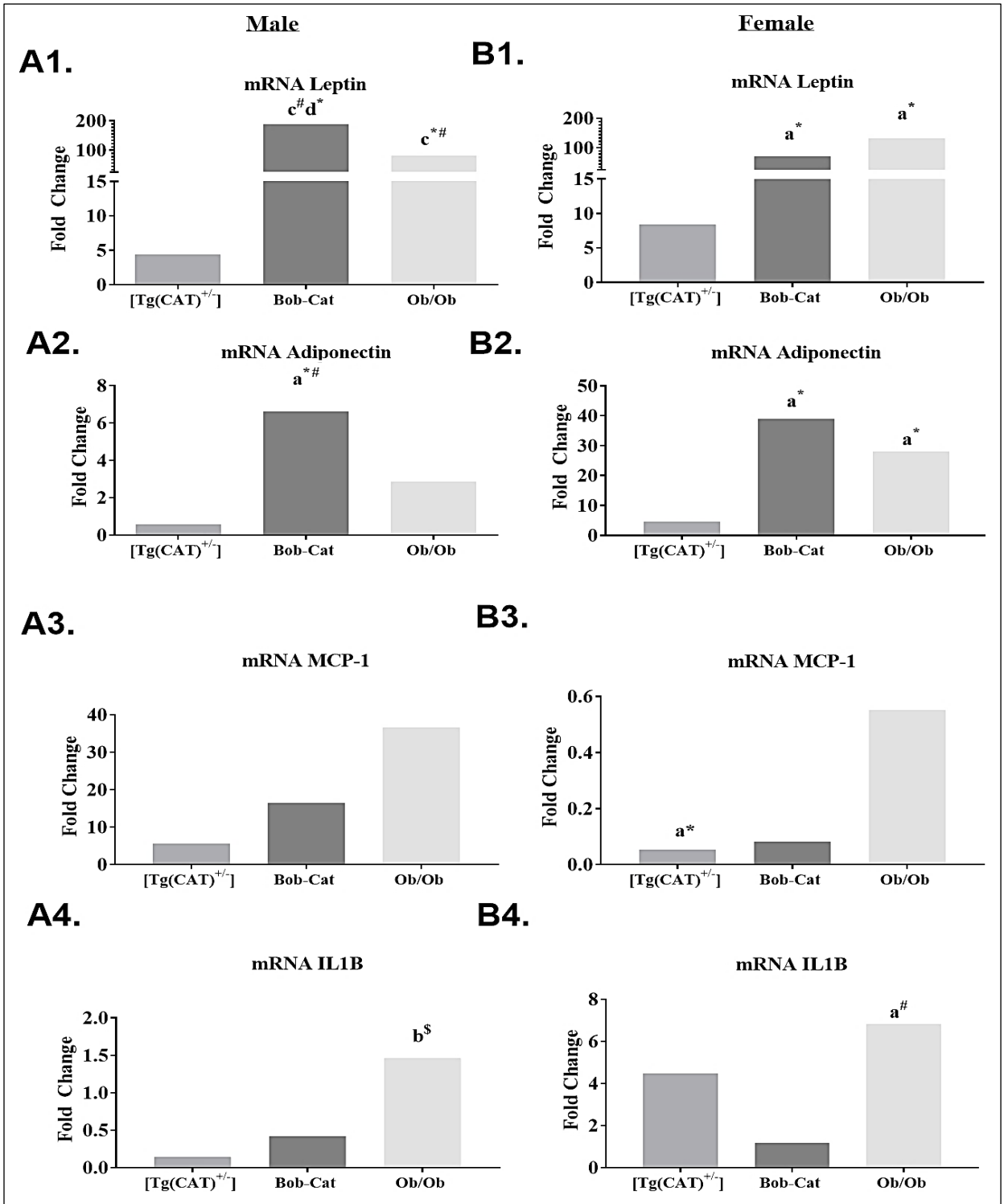

Figure 14. Adipocytokine mRNA expression levels in adipose tissue. Gene expression levels of (A1 and B1) leptin, (A2 and B2) adiponectin, (A3 and B3) IL1B, and (A4 and B4) MCP-1 levels in C57Bl6, [Tg(CAT)+/-], Bob-Cat, and Ob/Ob male (A) and female (B) mice, n≥3 /genotype and gender. Data reported as mean +/- SEM. Results considered significant at p<0.05a*, p<0.001c*, p<0.0001d* to C57Bl6, p<0.01b#, p<0.001c# to [Tg(CAT)+/-], p<0.05$ to Bob-Cat.

2.4 DISCUSSION

Obesity, which is at its all-time peak worldwide, increases the risk to other metabolic diseases such as T2D, dyslipidemia, hypertension and atherosclerosis (Lewis et al., 2016; Manna & Jain, 2015). Adipose tissue expansion and dysfunction is a hallmark of obesity. Over the years, researchers have attempted to understand the pathophysiology of obesity and how it leads to increased cardiometabolic diseases with the hope of finding preventive or treatment strategies (Lewis et al., 2016; R. L. Martin, Perez, He, Dawson, & Millard, 2000; Santilli et al., 2015). Redox stress is one such common phenomenon that has been associated with obesity and its co-morbidities and is attributed to excess adipose mass and meta-inflammation (Fernandez-Sanchez et al., 2011).

Mitochondrial generation of superoxide or hydrogen peroxide is a major intermediate between intracellular metabolism and insulin signaling (Hoehn et al., 2009). Modulating mitochondrial energetics by using mito-targeted antioxidants or excess catalase lowered metabolic and energy imbalance and improved insulin sensitivity (Anderson et al., 2009). Overexpression of Superoxide Dismutase (SOD) in mice prevented insulin resistance but had very little impact on mitochondrial function (Y. Liu, Qi, et al., 2013). Except for studies that showed that overexpression of catalase in a leptin resistant diabetic mouse model (db/db mice) prevented diabetic nephropathy (Brezniceanu et al., 2008; Godin et al., 2010; Lau et al., 2012) and that a catalase knockout mice developed obesity and prediabetic phenotype (Heit et al., 2017), the effects of increased endogenous catalase expression in obesity models are understudied.

In this study, we successfully generated a new mouse model with an obese parent (Ob/Ob) background that expresses the *hCAT* gene, named Bob-Cat. Due to its increased

catalase activity, it has lower "redox stress," hence remains "stress-less." As depicted in **Figure 4** and the representative pie charts, Bob-Cat mice (heterozygous to Ob and expressing *hCat*) dominated the F2 and F3 generations. It was interesting to note that extremely low numbers of mice homozygous for the Ob gene and carrying the catalase gene were obtained during breeding. It is presumptive to assume that this skewness towards heterozygous mice might be due to higher catalase expression.

Confirmation of increased catalase expression in key metabolic tissues (liver, IM, adipose, and brain) of Bob-Cat mice makes this an excellent model to study obesogenic pathways. Phenotyping showed no obvious differences in body weights between the genotypes at weaning ages but ECHO-MRI showed obvious differences in body composition. There were sex differences in overall fat and lean mass. Male Bob-Cat mice had a similar fat mass compared to C57Bl6 mice but lower compared to the Ob/Ob mice. In contrast, female Bob-Cats had a higher fat mass compared to [Tg(CAT)$^{\pm}$]. The higher lean mass in male Bob-Cat compared to C57Bl6 mice and in female mice compared to both C57Bl6 and [Tg(CAT)$^{\pm}$] was intriguing. As expected, only Ob/Ob mice had a significantly higher body weight and fat mass beginning at 4 weeks of age in comparison to C57Bl6.

It has been shown that even though body weights may not be different, the metabolic parameters may be functioning more efficiently in an individual with increased BMI. In contrast, individuals whose BMI falls within a "normal range" may still be metabolically unhealthy (Denis & Hamilton, 2013). Therefore, we measured the metabolic parameters using CLAMS technology, and determined the VO_2 intake, CO_2 output, RER (VCO_2/VO_2), EE (kcal/h), average FI per day, and the XAMB (physical activity) within each genotype. Catalase overexpression, by virtue of lowering redox stress levels, altering adipocyte secretion of key adipokines, and

modulating appetite regulation, was expected to increase EE and lower levels of FI. FI did not differ significantly between any genotypes, however, the antioxidant overexpressing mice trended towards decreased FI. Both groups of male mice that overexpressed catalase, [Tg(CAT)$^{\pm}$] and Bob-Cat, significantly used more energy in heat production. The [Tg(CAT)$^{\pm}$] genotype trended to have a higher activity level (though not statistically significant) in comparison to the other two genotypes. This may be due to the body's response to the trend in higher body weight observed in adult [Tg(CAT)$^{\pm}$] mice. The same could be noted for the Ob/Ob genotype. Heterozygosity of *Lep^{ob}* mice has been shown to display increased FI and altered glucose homeostasis, although mice did not differ in body weights compared to wild type (Flatt & Bailey, 1981). The adult Ob/+ mice had increased fat mass compared to wild types which might be attributed to lower leptin protein production in these mice (Chung et al., 1998). Bob-Cat mice, in spite of its heterozygous Ob/+ genotype, did not significantly differ from the control mouse in respect to RER. Less differences in RER and EE were seen in female Bob-Cats. Cumulatively, CLAMS showed that catalase overexpression has a positive influence on energy metabolism.

Bob-Cat mice also did not significantly differ in blood glucose, HDL cholesterol, or TC levels in comparison to C57Bl6 mice or [Tg(CAT)$^{\pm}$]. However, Ob/Ob mice had higher levels indicative of a healthier phenotype, the overall ratio of HDL cholesterol and TC is more important, explaining why the Ob/Ob mice do not have a healthier lipid profile in comparison to antioxidant-excess or control mice. It was interesting to note that [Tg(CAT)$^{\pm}$] mice had significantly higher levels of TG in comparison to C57Bl6, Bob-Cat, and even Ob/Ob mice. Insulin, leptin, and resistin levels did not differ significantly between mice overexpressing

catalase (Bob-Cat and [Tg(CAT)$^{\pm}$]) compared to C57Bl6. However, females seemed to have a trend towards slightly lower levels of circulating insulin and leptin.

Catalase expression and activity in the adipose tissue, which is one of the key metabolic tissues in obesity, showed differences between the genotypes. The mice overexpressing catalase had higher catalase expression compared to the parent strains. Males had increased expression compared to female mice. Catalase expression was almost 35 fold higher in the adipose tissue of Bob-Cat compared to C57Bl6 mice. The 5 fold increased expression observed in Ob/Ob mice may be the result of a compensatory response to higher levels of oxidative stress in these mice due to increased fat mass and production of pro-inflammatory cytokines (Espinosa-Diez et al., 2015). Catalase activity was increased in Bob-Cat mice compared to C57Bl6 mice in male and females. This increase in activity validated the genetic overexpression of endogenous catalase. The increases in catalase activity and lowered oxidative stress, as shown by decreased oxidatively modified proteins in the Bob-Cat mice (**Figure 13**), make this a novel "stress-less" mouse model.

Leptin and adiponectin are two adipokines that play a key role in adipose function. Leptin is a fundamental regulatory hormone that is primarily produced by adipocytes within WAT of both humans and rodents (Birsoy et al., 2011). The concentration of circulating leptin is directly proportional to total body fat (J. M. Friedman & Mantzoros, 2015). The hormone's main function is demonstrated within the arcuate nucleus of the hypothalamic region of the brain where it is able to decrease appetite and increase energy expenditure (Spiegelman & Flier, 2001) through signaling systems involved in the orexigenic and anorexigenic pathways (Frago & Chowen, 2015). Oxidative stress modulates leptin's action leading to changes in fat mass, metabolic parameters, and inflammatory status (Drougard et al., 2015). Like leptin, adiponectin

is most abundantly expressed in WAT, yet is downregulated during obesity (Nigro et al., 2014). Adiponectin protects against diseases such as diabetes and atherosclerosis (Z. V. Wang & Scherer, 2016). Specifically, administration of adiponectin has been shown to both elicit glucose lowering effects and ameliorate insulin resistance (Y. Liu, Turdi, et al., 2013). In other studies, suppression of adiponectin signaling pathway resulted in decreased oxidative stress detoxifying enzymes such as catalase (Iwabu et al., 2010). Leptin and adiponectin expression in the WAT were elevated in both sexes of Bob-Cat mice ($p<0.0001$) in comparison to the control C57Bl6 mice. There was a significant increase in adiponectin in the Bob-Cat genotype in comparison to C57Bl6 mice ($p<0.05$). Due to elevated leptin and adiponectin expression in Bob-Cat adipose tissue and an increase in catalase expression in other metabolic tissues such as brain, this mouse model can be used to study appetite regulation through the adipose-brain axis. With lower levels of the pro-inflammatory genes, IL1β and MCP-1/JE levels, the Bob-Cat mouse is also ideal for studying metabolic changes resulting from dietary interventions or exercise. **Table 5** provides a summary of the metabolic characteristics of the novel "stress-less" mouse model. The

differences in phenotype observed between the two sexes are intriguing and require further explanation.

Male Characteristics	Bob-Cat	Female Characteristics
- **Lean mass +** - **Metabolic energy expenditure +** - **Catalase mRNA in adipose tissue +** - **Catalase enzymatic activity trend +** - **Oxidative stress in adipose tissue trend -** - **Leptin mRNA in adipose tissue ++++** - **Adiponectin mRNA in adipose tissue +**		- **Adipose weight +** - **Lean mass +** - **Physical activity trend +** - **Catalase protein expression trend +** - **Enzymatic activity in adipose tissue trend +** - **Leptin mRNA in adipose tissue +** - **Adiponectin mRNA in adipose tissue +**

Table 5. Key characteristics of the novel 'stress-less' Bob-Cat mouse. Bob-Cat genotype compared to C57Bl6 mice increase depicted as (+). Significance represented as $p<0.05$ +, $p<0.0001$ ++++.

Caution should be placed on the knowledge that excess oxidative stress induces antioxidant defense which in turn tilts the balance towards excess reductive stress (Margaritelis et al., 2014). Reductive stress in turn then leads to increased oxidative stress and has been implicated in various diseases (Korge et al., 2015). This vicious cycle might have been at play in some of the previous studies using antioxidant overexpressing mouse models such as the study where excess glutathione peroxidase-1 showed increased body weight and insulin resistance (McClung et al., 2004). Increased quenching of ROS in these mouse models interfered with insulin signaling pathways (Lei & Cheng, 2005). Therefore, the Bob-Cat mouse model can also be used as a good model to study the role of reductive stress in metabolic diseases.

2.5 CONCLUSION

Overall, based on the phenotypic results obtained in the Bob-Cat mice, it is apparent that the overexpression of catalase in an obese genotype modulated body composition while retaining a similar body weight in relation to the C57Bl6 and [Tg(CAT)$^{\pm}$] mice. Significant changes in energy expenditure and activity levels of Bob-Cat mice compared to other genotypes suggest catalase is playing a role in appetite regulation of this novel "stress-less" mouse model. Significant differences in metabolic profile and oxidative stress make it a good model to study dietary and exercise interventions.

2.6 FUNDING

This study was partially supported by NIH Grant 5R01HL-074239 (NS) and 5P20RR016477 (NS) and WV-NASA Grant Consortium NNX15A101H (DA).

2.7 ACKNOWLEDGEMENTS

The authors acknowledge Dr. Jung Han Kim for her assistance with ECHO-MRI and CLAMS studies. This study was partially supported by NIH Grant 5R01HL-074239 (NS) and 5P20RR016477 (NS) and WV-NASA Grant Consortium (DA).

CHAPTER III: OMEGA 3 RICH DIET MODULATES ENERGY METABOLISM VIA GPR120-NRF2 CROSSTALK IN A NOVEL ANTIOXIDANT MOUSE MODEL

A manuscript published in *Biochim Biophys Acta: Molecular and Cell Biology of Lipids.*

Amos, D., Cook, C., & Santanam, N. (2019). Omega 3 rich diet modulates energy metabolism via GPR120-Nrf2 crosstalk in a novel antioxidant mouse model. *Biochim Biophys Acta Mol Cell Biol Lipids*. doi:10.1016/j.bbalip.2019.01.002

Deborah Amos, Carla Cook, Nalini Santanam∗

Department of Biomedical Sciences, Joan C. Edwards School of Medicine, Marshall University, 1700 3rd Ave, Huntington, WV 25755-0001, United States

∗Corresponding author at: Department of Biomedical Sciences, Joan C. Edwards School of Medicine, Marshall University, 1700 3rd Ave, 435S BBSC, Huntington, WV 25755, United States. E-mail address: santanam@marshall.edu (N. Santanam).

E-mail addresses: amos23@marshall.edu (D.L. Amos), schneide@marshall.edu (C. Cook), santanam@marshall.edu (N. Santanam).

Received 6 October 2018; Received in revised form 12 December 2018; Accepted 7 January 2019

Available online 16 January 2019 1388-1981/

ABSTRACT

With obesity rates reaching epidemic proportions, more studies concentrated on reducing the risk and treating this epidemic are vital. Redox stress is an important metabolic regulator involved in the pathophysiology of cardiovascular disease, Type 2 diabetes, and obesity. Oxygen and nitrogen-derived free radicals alter glucose and lipid homeostasis in key metabolic tissues, leading to increases in risk of developing metabolic syndrome. Oxidants derived from dietary fat differ in their metabolic regulation, with numerous studies showing benefits from a high omega 3 rich diet compared to the frequently consumed "western diet" rich in saturated fat. Omega 3 (OM3) fatty acids improve lipid profile, lower inflammation, and ameliorate insulin resistance, possibly through maintaining redox homeostasis. This study is based on the hypothesis that altering endogenous antioxidant production and/or increasing OM3 rich diet consumption will improve energy metabolism and maintain insulin sensitivity. We tested the comparative metabolic effects of a diet rich in saturated fat (HFD) and an omega 3-enriched diet (OM3) in the newly developed 'stress-less' mouse model that overexpresses the endogenous antioxidant catalase. Eight weeks of dietary intervention showed that mice overexpressing endogenous catalase compared to their wild-type controls when fed an OM3 enriched diet, in contrast to HFD, activated GPR120-Nrf2 cross-talk to maintain balanced energy metabolism, normal circadian rhythm, and insulin sensitivity. These findings suggest that redox regulation of GPR120/FFAR4 might be an important target in reducing risk of metabolic syndrome and associated diseases.

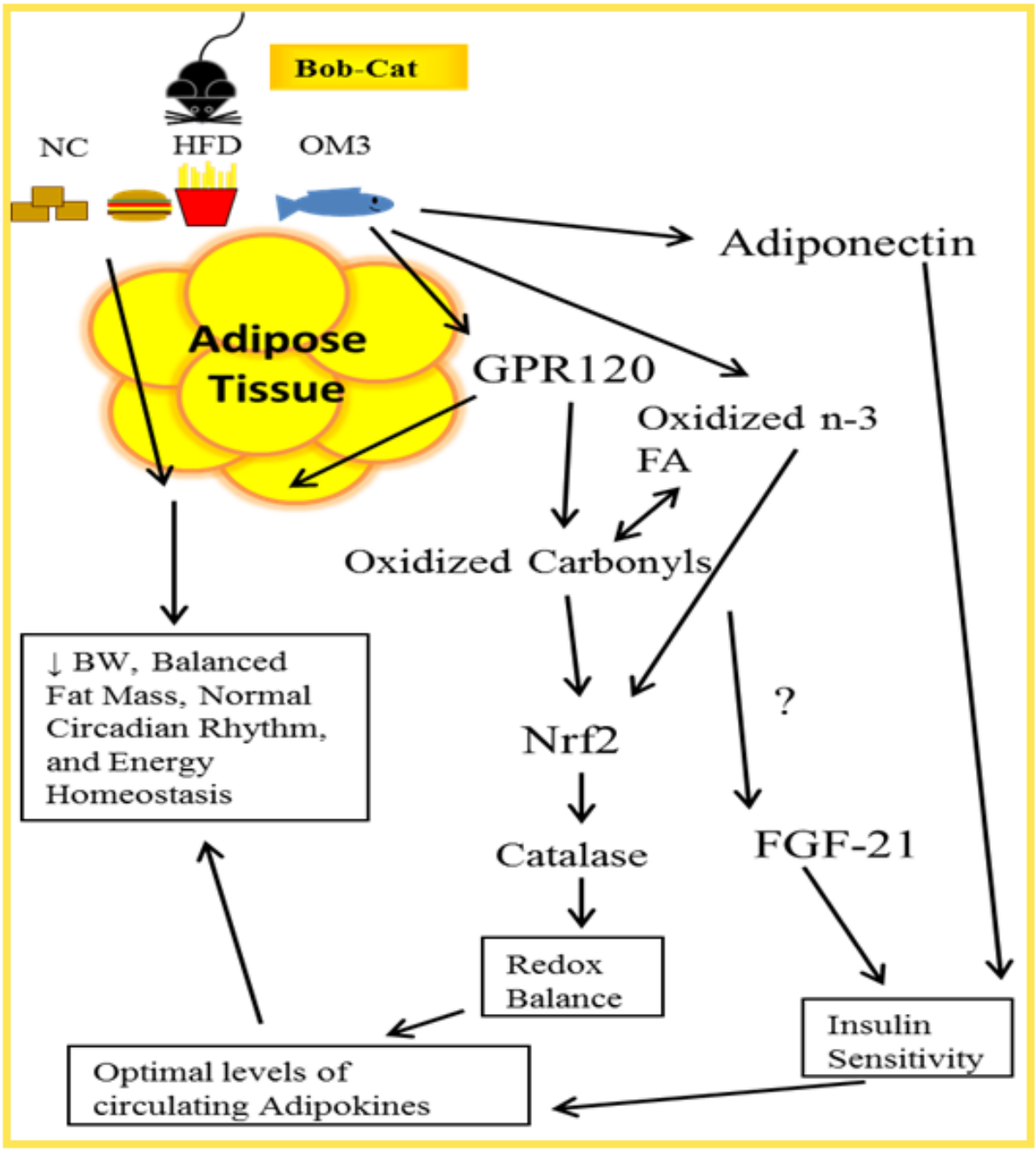

Figure 15. Redox regulation of GPR120-Nrf2 cross-talk in an OM3 fed catalase overexpressing mice. Overexpression of catalase in the Bob-Cat mouse model coupled with an enriched diet of OM3 fatty acids was shown to be metabolically beneficial. Energy homeostasis seen in this model was the result of induction of the GPR120/FFAR4, which by interacting with Nrf2 pathway (redox-sensitive) in adipose tissue resulted in redox balance, improved insulin sensitivity, anti-inflammation, enhanced circadian rhythm, decreased body weight and healthy fat mass.

3.1 INTRODUCTION

The overwhelming prevalence of diet-induced obesity (DIO) and insulin resistance (IR) is strongly associated with the increased morbidity and mortality related to metabolic syndrome (Smith & Smith, 2016). This is of great concern in the United States of America where the obesity rates are rising and is currently approximately 39.8%, with over 93.3 million adults affected, and there is still a lack of understanding of its etiology (Division of Nutrition, 2018). Redox regulation is key for systemic metabolic homeostasis. Furthermore, redox stress is an important mediator of metabolic changes seen in obesity and its comorbidities which comprise the metabolic syndrome (Carrier, 2017). Oxygen and nitrogen-derived free radicals alter glucose and lipid homeostasis in key metabolic tissues such as adipose, liver, brain, and skeletal muscle. During conditions of high redox stress, the body naturally attempts to compensate by increasing the production of endogenous antioxidants (including superoxide dismutase-SOD, catalase etc.) to counteract the excess free radicals that could damage signaling pathways necessary for energy production. It is believed that an increased level of reactive oxygen species (ROS) plays a key role in IR, since human and rodent models of IR are typically characterized by an imbalance in ROS compared to antioxidants/reducing agents (Rochette, Zeller, Cottin, & Vergely, 2014; Teodoro, Rolo, & Palmeira, 2013). However, recent studies have also shown the importance of maintaining adequate ROS production for intracellular signaling (McMurray et al., 2016). Furthermore, the concept of reductive stress, an imbalance in the oxidative state where the ratio of oxidized to reduced molecules is too low (Brewer et al., 2013; Korge et al., 2015; Lipinski, 2002), is also shown to be associated with an altered metabolic state such as hyperglycemia (L. J. Yan, 2014) or IR (Williamson, Kilo, & Ido, 1999). Therefore, a balance between free radicals and antioxidants is key in maintenance of tissue function and systemic metabolic homeostasis.

In addition to redox stress, nutritional intake plays a key role in modulating energy metabolism. DIO animal models are commonly used to study altered metabolic changes consequential to fat storage within various fat pads. In general, diets containing > 40% high-fat lard, milk, and butter promote excess lipid accumulation in adipose tissue leading to adipocyte hyperplasia and hypertrophy, alterations in adipokine secretion, hypoxia, and elevated circulating free fatty acids (FFA) in less than 8 weeks of ad libitum diet intervention (Choe et al., 2016; Heydemann, 2016). Furthermore, inflammatory pathways within the adipose tissue are activated as a consequence of excess lipid accumulation, which in turn drives a pro-inflammatory state provoking IR and inflammation in other metabolic tissues including liver, skeletal muscle, and pancreatic β-cells (Z. Chen et al., 2017; Snel et al., 2012). The severity of the consequences to a high-fat diet is dependent on the composition, length, and degree of fatty acid saturation (McArdle et al., 2013; Yeop Han et al., 2010). Contrary to the negative effects seen in diets with high levels of saturated fat (lard, milk fat, and butter), high-fat diets predominately composed of omega 3 (OM3) polyunsaturated fatty acids (PUFA) have been shown to have beneficial effects on metabolic function (Albracht-Schulte et al., 2018; Luo et al., 2016; Saini & Keum, 2018; Shahidi & Ambigaipalan, 2018). In general, diets comprised of fish oil, which is high in OM3, lower systemic IR (Oliveira et al., 2015), decrease fasting TG (Bargut et al., 2016) and cholesterol levels (Ide & Koshizaka, 2018; Tani et al., 2018), and reduce inflammation (Oliveira et al., 2015). These beneficial outcomes are in contrast to diets with high levels of saturated fats (Bargut et al., 2016; Yeop Han et al., 2010). Further understanding of the possible mechanisms by which OM3 fatty acids promote metabolic health came when Olefsky's group discovered that GPR120/FFAR4, a free fatty acid receptor (highly expressed in adipose tissue) for which long chain omega 3 fatty acids are ligands, improved adipose tissue function and energy metabolism

by its insulin sensitizing and anti-inflammatory effects (D. Y. Oh & Olefsky, 2012; D. Y. Oh et al., 2010; D. Y. Oh et al., 2014). OM3 fatty acids also alter the balance of reductive and oxidative species, and are additionally critical in glucose and lipid metabolism (D. Y. Oh et al., 2010). Furthermore, alterations in redox homeostasis through increased intake of OM3 fatty acids have been linked to activation of the nuclear factor E2-related factor 2 (Nrf2) pathway (Cipollina, 2015). Nrf2 is a transcription factor, key in regulating redox homeostasis (Seo & Lee, 2013) by inducing the transcription of endogenous antioxidants including catalase, glutathione transferase, HO-1, and NAD(P)H: Quinone Oxidoreductase 1 (S. E. Lee et al., 2015; Yamamoto et al., 2018; Zhu et al., 2008). These studies pointed to the plausible mechanisms by which varying dietary fat composition can influence metabolic homeostasis by modulating redox stress.

In our previous studies investigating dietary or exercise interventions in atherosclerotic mice models, we observed that increased redox stress or inflammation led to an increased antioxidant response by the tissues affected by the insult (for example vasculature). Our results showed that in most instances, the major endogenous antioxidant upregulated in response to the insults was catalase (Meilhac et al., 2001; Meilhac et al., 2000). Catalase is a major antioxidant, endogenously produced by various tissues, to neutralize excess H_2O_2 produced by dismutation of superoxide, yielding water and oxygen (X. Chen et al., 2004). In addition to our studies, numerous other studies have shown that catalase (mouse) overexpression for example, targeted to mitochondria (mCAT) in mice provided evidence of being an anti-cancer agent by delaying the progression of transgenic oncogene and syngeneic tumors (Ge et al., 2015), while overexpression of catalase (human) in mitochondria showed improvements in skeletal muscle function in aged rodents vs their WT littermates (Umanskaya et al., 2014). In the context of cardiovascular disease, restoration of catalase activity in the vascular aortic wall profoundly

reduced inflammatory markers and prevented abdominal aortic aneurisms through modulation of matrix metalloproteinase activity (Parastatidis, Weiss, Joseph, & Taylor, 2013). On the other hand, negative metabolic consequences occur in systems devoid of catalase. Within the context of DIO, a catalase knockout rodent model had exacerbated IR, amplified oxidative stress, and accelerated macrophage infiltration in epididymal white adipose tissue (Park et al., 2016) indicating catalase is a key antioxidant vital for glucose homeostasis and adipose tissue function. More recently, Heit et al. showed mice devoid of catalase developed an obese, pre-diabetic phenotype, further showing the importance of antioxidant catalase in metabolic regulation (Heit et al., 2017). These evidences support catalase as an ideal antioxidant for investigating the effects of redox balance in obesity and its associated comorbidities due to its vital role in metabolic homeostasis in both humans and rodent models. The findings discussed in these studies led us to generate a mouse overexpressing catalase which will serve as a good model to study redox regulation of metabolic diseases. We hence generated the "Bob-Cat" 'stress-less' mouse model: a hybrid between catalase transgenic mice [Tg(CAT)$^{\pm}$] (X. Chen et al., 2003) and leptin-deficient, Ob/+ mice (heterozygous JAX 000632, B6.Cg-Lepob/J). We have earlier shown that this novel mouse model had lower redox stress and improved adipose function compared to the Ob/Ob phenotype (JAX 000632, B6.Cg-Lepob/J) and expressed both human and mouse catalase (D. L. Amos et al., 2017).

We hypothesized that modulating redox stress by altering endogenous antioxidant content (overexpression of catalase) and/or via dietary intervention will improve energy metabolism, adipose tissue function, and overall glucose and lipid homeostasis. To better understand the interplay between redox regulation and dietary intervention in improving energy balance and maintaining insulin sensitivity, we compared the redox effects of a high-fat lard diet (HFD) and a

high-fat omega 3-enriched diet (OM3) in a catalase-overexpressing ‘stress-less’ mouse model (D. L. Amos et al., 2017). In this model, we previously showed the ubiquitous overexpression of catalase altered body composition parameters, overall energy metabolism, as well as adipose tissue function in both male and female mice compared to WT controls (D. L. Amos et al., 2017). These characteristics make this mouse model an excellent method for studying dietary effects of high fat lard and fish oil diets on metabolic homeostasis of both male and females, now critical for all clinical trials. Our study showed that OM3 enriched diet, in contrast to the HFD intervention, activated the GPR120-Nrf2 cross-talk to maintain balanced energy metabolism, normal circadian rhythm and insulin sensitivity in mice overexpressing catalase compared to the WT controls. Therefore, increasing endogenous antioxidant production in combination with an OM3 rich diet will maintain energy balance, improve adipose tissue function, and lower risk of obesity and its comorbidities.

3.2 MATERIALS AND METHODS

3.2.1 Mouse Model and Diets

A successful breeding colony of both catalase transgenic [Tg(CAT)$^{\pm}$] and the 'stress-less' Bob-Cat mice, which ubiquitously express both human and mouse catalase, has been established in our facility (D. L. Amos et al., 2017). The care and use of animals was performed according to protocols approved by Marshall University IACUC. To ensure relevance to human clinical studies conducted on obese adults, it was necessary to use fully developed mice (thus being between 12-24 weeks of age which correlates with a 20-30 year old human (Jackson et al., 2017)) and a 45% high fat diet. According to the Center for Disease Control (CDC database derived from NHANES studies), obese individuals typically consume a 45% fat diet (the "Western Diet") (Eicher-Miller & Boushey, 2017). Therefore, sixteen week old [Tg(CAT)$^{\pm}$], Bob-Cat, and their control C57Bl6/WT mice ($n \geq 8$/group/sex) were maintained on a 12h light/dark cycle and fed ad libitum either normal chow-NC (Lab Diet-5001, St. Louis, MO), High-Fat Lard-HFD diet (Envigo TD06415, Somerset, NJ) containing 45 kcal% Lard, or Omega-3 rich-OM3 diet (Envigo TD130700, Somerset, NJ) containing 45 kcal% of Menhaden Fish Oil, for 8 weeks (**Table 6**). Both male and females were used due to the differences in overall regulation of energy homeostasis and metabolism of essential fatty acids (such as OM3) between the two sexes (B. F. Palmer & Clegg, 2015; M. Yoon et al., 2002). In order to investigate chronic effect of the dietary intervention, we conducted an 8 week feeding study. Animal body weights and food consumption were recorded weekly. Energy consumed per diet group was determined by dividing the grams of chow consumed by kcal per grams (g) of chow.

Calories Provided By:	NC (5001)	HFD (TD:06415)	OM3 (TD:130700)
	kcal%	kcal%	kcal%
Protein	29.8	19.0	19.0
Carbohydrate	56.74	36.2	36.2
Fat	13.4	44.8	44.8
Total Kcal/gm	4.09	4.6	4.6

Diet Formulas	HFD (TD:06415)- g/Kg	OM3 (TD: 130700)- g/Kg
Casein	245	245
L-Cystein	3.5	3.5
Corn Starch	85	85
Maltodextrin	115	115
Sucrose	200	200
Lard	195	0
Fish Oil	0	195
Soybean Oil	30	30
Cellulose	58	58
Mineral Mix, AIN-93G-MX (94046)	43	43
Calcium Phosphate, dibasic	3.4	3.4
Vitamin Mix, AIN-93-VX (94047)	19	19
Choline Bitartrate	3	3
Red Food Color	0.1	0
Green Food Color	0	0.1

Cholesterol, ppm	234	1064.9
SFA, g/Kg	80	59.2
MUFA, g/Kg	103.5	51.2
PUFA, g/Kg	40.8	100.0
n-3, g/Kg	4.35	65.7
n-6, g/Kg	36.2	23.9
Linoleic Acid, g/kg	35.4	19.4
Linolenic Acid, g/kg	4.3	5.9
Arachidonic Acid, g/kg	0.78	4.4
Eicosapentaeoic Acid, g/kg	0	31.2
Docosahexaenoic Acid, g/kg	0	21.06
*HFD and OM3 diets obtained from Harlan Laboratories and NC diet obtained from LabDiet		

Table 6. Diet composition. High-fat lard diet (Envigo TD06415-HFD), high-fat Omega-3 rich diet (Envigo TD130700 -OM3), and standard chow diet (LabDiet 5001-NC).

3.2.2 Fat and Lean Body Mass-ECHO-MRI

Body composition (fat and lean mass) was determined using magnetic resonance imaging, ECHO-MRI (Houston, TX) according to manufacturers' recommendations. Each mouse was individually placed within the MRI machine and three or more measurements were taken. Median values of fat and lean mass readings were calculated per mouse and subsequently averaged per genotype and diet. Comparisons between groups were made by one or two-way ANOVA.

3.2.3 Metabolic Parameters (Comprehensive Laboratory Animal Monitoring System-CLAMS)

Changes in metabolic parameters in response to the dietary interventions were determined during the final week of the study using indirect calorimetry by measuring O_2 consumption (VO_2) and CO_2 production (VCO_2), respiratory exchange rate (RER), Food Intake (FI), Energy Expenditure (EE), as well as X-Ambulatory counts (XAMB, physical activity) using the CLAMS system (Columbus Instruments, Columbus, OH, USA). As recommended in the instruction manual, each mouse was placed individually in the metabolic cages and was supplied with a sufficient amount of their respective diet for the duration of the data collection (three consecutive days). Analyses were made using the data collected during the middle 48 hours of the 72-hour procedure, which is from approximately 0600 hours of the first day to 0600 hours of the third day. These time points allowed for both adequate time to acclimate to the CLAMS environment and provide accurate data for assessment of all measured parameters. Food intake (FI) was measured by CLAMS and energy intake was calculated by dividing the grams of food consumed by the kcal of energy per gram of each laboratory diet. RER is calculated as the ratio of carbon dioxide production and oxygen consumption. Carbohydrate (CHO) oxidation was

calculated using the formula $((4.585*VCO_2) - (3.226*VO_2))*4$, and similarly, fat oxidation was calculated using the formula $((1.695*VO_2) - (1.701*VCO_2))*9$ as described by Peronnet & Massicotte (Peronnet & Massicotte, 1991). EE (heat production) was calculated as the Cal/h/lean mass (g) to account for the lean body weight. Average values of EE, RER, FI per day, as well as XAMB locomotor activity per day (counts movement made across the cage measured with infrared sensors) were determined for each mouse in all groups. Results were further broken down into light and dark cycles at 2 h time intervals for a total of 48 hours per mouse. One and two-way ANOVA was used to determine comparative changes between the various genotypes fed NC, HFD or OM3 diets.

3.2.4 Blood and Tissue Collection

At the end of 8 weeks, animals were fasted overnight and anesthetized using isoflurane immediately prior to cardiac puncture. Blood was collected in heparinized tubes, centrifuged, plasma separated, and stored. Tissues including adipose and liver were removed, weighed, and flash frozen in liquid nitrogen, followed by long-term storage at -80˚C.

3.2.5 Circulating Metabolic Parameters

Whole blood was used to measure fasting glucose and ketone levels (Precision Xtra Glucometer) then centrifuged for 10 min. to separate the plasma and red blood cells. Thirty-five µL of plasma was placed on a Cholestech cassette and read on a LDX Cholestech system (Cholestech Corporation Hayward, CA) to determine Glucose, High Density Lipoprotein (HDL), Low Density Lipoprotein (LDL), and Total Cholesterol (TC) levels. If data collected fell outside the range (sensitivity of the assay), the less than ("<") or (">") was used to best represent the results. The remaining plasma was frozen at -80˚C for further analysis of circulating markers.

Triglyceride (TG) levels were assessed in plasma using a Triglyceride Colorimetric Assay Kit (Cayman Chemicals, Ann Arbor, MI). Plasma insulin was analyzed using an ultrasensitive mouse Insulin ELISA kit (Crystal Chem, Downers Grove, IL). The end point colorimetric assays were performed using a BioRad Benchmark Plus microplate reader according to manufacturer's instructions.

HOMA-IR is a surrogate measure of insulin resistance routinely used in research studies (Antunes, Elkfury, Jornada, Foletto, & Bertoluci, 2016; Cacho, Sevillano, de Castro, Herrera, & Ramos, 2008; M. Y. Lee et al., 2008). HOMA-IR was calculated using the formula: fasting insulin [μlU/ml] x fasting glucose [mmol/L])/22.5.

Circulating FGF-21 was assessed using Mouse and Rat FGF-21 ELISA (Biovendor, Modrice, Czech Republic) according to manufacturer's protocol. Absorbance was read using a BioRad Benchmark Plus microplate reader. Calculations were conducted in accordance with the best-fit line created from the standard curve of plotted absorbance values against the known concentrations of standards.

3.2.6 Adipose mRNA Expression

RNA was isolated from 100 mg of perigonadal adipose tissue using TRI Reagent according to the manufacturer's recommended protocol (Sigma, Saint Louis, MO). RNA concentration was determined using the NanoDrop 1000 (NanoDrop Technologies Inc., Thermo Scientific, Wilmington, DE, USA). Reverse transcription of total RNA (1 μg) was performed using iScript™ cDNA Synthesis Kit (Bio-Rad, Hercules, CA). RT-qPCR was conducted using iQ SYBR™ Green Supermix (Bio-Rad, Hercules, CA). The mouse primers used in this study are provided in **Table 7**. 18S and β-Actin primers were used as the housekeeping reference genes. All samples were analyzed in duplicate or triplicate in the Bio-Rad MyiQ or Bio-Rad CFX

Connect™ (Bio-Rad, Hercules, CA) instrument and a transcript was considered non-detectable when the CT value was ≥ 40. The mRNA level of the gene of interest for each group was normalized to that of the referenced control using the comparative Pfaffl Equation (2^-ddCT) (Pfaffl, 2001) and expressed as fold change compared to the control C57Bl6/WT mice fed normal chow (WT NC) or C57Bl6/WT within each dietary group.

Primer Name	Accession Number	Forward	Reverse
Mu-Adiponectin	NM-009605	5'- gcagagatggcactcctgga -3	5'- cccttcagctcctgtcattcc -3'
Mu-GPR120	NC_001195755.1	5'- tgtgtgctctagtgctggtg -3'	5'- gcgctggtgaagagcaaatc -3'
Mu-NrF2	NM_010902	5'- ccagaagccacactgacaga -3'	5'- ggagaggatgctgctgaaag -3'
Mu-HO-1	NC_000022.11	5'- cacgcatatacccgctacct -3'	5'- ccagagtgttcattcgagcac -3'
Mu-FGF-21	NC_000019.10	5'- cgtctgcctcagaaggactc -3'	5'- aatcctgcttggtcttgggg -3'
Mu-B-Actin	NM-007393	5'- ctacctcatgaagatcctcaccga -3'	5'- ttctccttaatgtcacgcacgatt -3'
Hu-18S	NR_003286.2	5'- gcaattattccccatgaacg -3'	5'- ggcctcactaaaccatccaa -3'

Table 7. Primer sequences for quantitative RT-PCR.

3.2.7 Western Blot

Approximately 50 mg of perigonadal adipose tissue was homogenized in 100 µL of Radio-immunoprecipitation assay buffer (RIPA buffer) supplemented with protease inhibitor cocktail. Protein concentrations were determined by the Lowry Method (Lowry et al., 1951). For each sample, 50-60 µg protein, were prepared in loading buffer (90% Laemmli and 10% 2-mercaptoethanol) and boiled for 5 min. at 100˚ C. Samples were run using SDS-PAGE and separated on 12% Precast Gel (BioRad, Hercules, CA), at 100 V for 60-70 min. Electrophoretic transfer of the proteins onto a nitrocellulose membrane was performed at 100V for 60 min. on

ice. Thermo Scientific Memcode Stain: Pierce MemCode™ Reversible Protein Stain Kit (Thermo Fisher Scientific, Rockford, IL) was used as a loading control. Membranes were blocked with 1X Tris Buffered Saline (1X TBST), 0.05% Tween 20, pH 7.6, and 5% dry milk for one hour at room temperature. Blots were incubated overnight with mouse GPR120 antibody (1:250 in 1X TBST and 5% dry milk) (Santa Cruz, Dallas, TX). After washing with 1X TBST, membranes were incubated with secondary anti-mouse IgG (1:3000 in 1X TBST and 5% dry milk) for 60 min. at room temperature. Membranes were washed and the immunocomplex was detected with Luminata™ Forte Western HRP (Millipore, Billerica MA). Densitometry of the bands was quantified using BioRad Image Lab Software (BioRad, Hercules, CA) and normalized to MemCode Stain of total protein.

3.2.8 Catalase Enzymatic Activity

Catalase activity was measured in perigonadal adipose tissue protein lysates using the method of Aebi (Aebi, 1984). Approximately 50 mg of adipose tissue was homogenized in 100 µL of 50 mM KH_2PO_4, 5 ug/µL Aprotinin, and 2 µL of 0.1 M PMSF. Eight microliters of each homogenate was added to 1 mL of 25 mM of Hydrogen Peroxide (H_2O_2) and analyzed on a Shimadzu Spectrophotometer for one minute. The initial rate of disappearance of H_2O_2 was recorded for 1 min. at a wavelength of 240 nM. Each sample was measured in duplicate or triplicate. A standard curve was generated using 1-5 units of bovine catalase (Sigma, Saint Louis, MO). Specific activity of catalase was calculated based on the standard curve and total protein used based on the Lowry's Method (Lowry et al., 1951).

3.2.9 Quantification of Oxidized Proteins

Carbonylated proteins are a hallmark of redox stress (Fedorova, Bollineni, & Hoffmann, 2014). Oxidized proteins were measured in lysates of perigonadal adipose tissue by determining

the presence of carbonylated proteins using the Protein Oxidation Detection OxyBlot kit (Millipore, Billerica, MA) in accordance with the manufacturer's instructions. The method is based on the principle that proteins modified by oxidative stress result in an addition of carbonyl groups to their side-chains. The carbonyl groups are detected after derivatization to 2,4-dinitrophenylhydrazone (DNP) by treating with 2,4-dinitrophenylhydrazine (DNPH). An antibody specific to DNP is then used to determine carbonylated proteins (relative oxidative stress levels) in each sample. Briefly, each lane was loaded with 20 µg of the derivatized protein and ran on a 12% BioRad Precast Gel. After gel electrophoresis, proteins were transferred to a nitrocellulose membrane at 100 V for 60 min. Equal loading and transfer efficiency was evaluated by use of the Pierce MemCode^{TM} Reversible Protein Stain Kit (Thermo Fisher Scientific, Rockford, IL). Non-specific binding sites were then blocked for one hour with 1X Phosphate Buffered Saline (1X PBST) and Tween 20 and 10% Bovine Serum Albumin (BSA). A 1:500 dilution of primary antibody, Rabbit-Anti-DNP (Millipore OxyBlot Kit, Billerica, MA) was added and rocked overnight at 4˚C, followed by washes with 1X PBST. Blots were conjugated with a 1:300 dilution of goat anti-rabbit IgG (Horseradish Peroxidase conjugated) for 1 h rocking at room temperature. Membranes were washed and the immunocomplex was detected with Luminata^{TM} Forte Western HRP (Millipore, Burlington, MA). All images were acquired and analyzed by a BioRad ChemiDoc and Image Lab Software (BioRad, Hercules, CA). Oxidized proteins were expressed as the ratio of the optical density of dinitrophenylhydrazone (DNP) to total protein as determined by the Memcode stain.

3.2.10 Statistical Analysis

Data were statistically analyzed using one and two-way ANOVA followed by Bonferroni's multiple comparison tests using Version 7 of GraphPad Prism among all mouse

groups. Data are presented as mean ± standard error of the mean (S.E.M.) unless fold change or percent of WT was provided. $p<0.05$ was considered statistically significant. RT-qPCR gene expression was determined by use of the Pfaffl equation (Pfaffl, 2001) and represented as fold change with significance denoted as differences in delta CT/genotype and diet. GPR120 protein and oxidized carbonyl protein analysis was represented as percentage of the WT control mouse group normalized by total protein quantified by memcode stain.

3.3 RESULTS

3.3.1 Body Weight and Body Composition

Sixteen week old male mice overexpressing (human and mouse) antioxidant catalase ([Tg(CAT)$^{\pm}$] and Bob-Cat) (D. L. Amos et al., 2017) were fed either normal chow (NC), high-fat lard (45% kcal, HFD), or high-fat omega 3 enriched (45% kcal, OM3) diet, ad libitum for a period of 8 weeks. Changes in body weight and body composition (fat and lean mass ratio) in the catalase overexpressing mice were compared to the control wild type (WT) mice fed similar diets over the 8 week intervention. Body weight was recorded each week and averaged per intervention group. As shown in **Figure 16**, all three genotypes maintained their body weights when fed NC over the 8 week period. However, WT and [Tg(CAT)$^{\pm}$] mice consuming a high-fat lard diet (HFD) gained significantly more weight (8 and 10 fold, $p<0.0001$) compared to their NC fed littermates (**Figure 16A and 16B**), but interestingly, Bob-Cat mice on HFD only gained approximately 5 fold increase in body weight (not significant) compared to their NC fed littermates. In contrast, when mice were fed OM3 (45% kcal menhaden fish oil), an increase in body weight was only observed in the WT mice group. In fact, there was a loss in body weight in both [Tg(CAT)$^{\pm}$] (5 fold lower) and Bob-Cat (>1 fold lower) mice fed OM3 diet compared to their NC fed littermates. Even more interesting was the significant decrease in body weight observed in the [Tg(CAT)$^{\pm}$] (>5 fold, $p<0.0001$) and Bob-Cat (>2 fold, $p<0.01$) mice fed OM3 diet compared to the WT mice fed the same diet. These dietary influences were observed in both the overall change in body weights (**Figure 16A**) as well as the average weekly changes in body weight measured throughout the study (**Figure 16B**), showing a general trend of increased body weight per week in the HFD and steady or decreased body weight in the OM3 fed groups among the mice overexpressing catalase. Two-way ANOVA showed a significant difference in body

weight between genotype ($p<0.05$) and diet ($p<0.0001$) groups in addition to the observed interaction between the two ($p<0.0001$) factors.

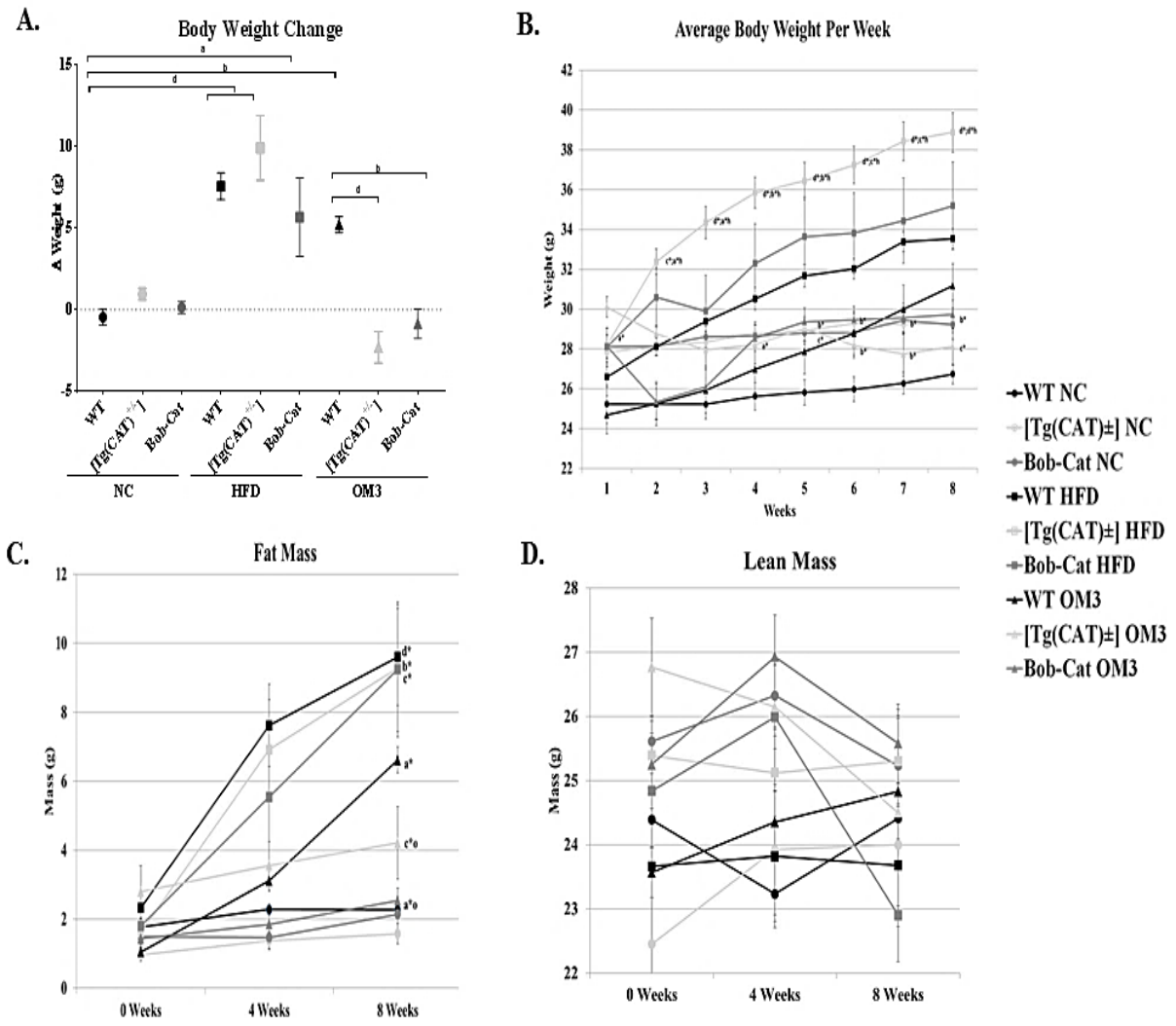

Figure 16. Body weight and body composition (fat/lean mass) in male mice overexpressing catalase. Body weight change (initial and final body weight) and body composition (fat/lean mass) determined by ECHO-MRI: A. Changes in whole body weight over 8 weeks; B. Overall weekly body weight measurements; C. Fat Mass (g) and; D. Lean Mass (g) of WT, [Tg(CAT)±], and Bob-Cat male mice fed NC, HFD, and OM3 diets ($n\geq6$/group). Mice overexpressing catalase on an OM3 diet in contrast to the HFD fed animals either had no change or lost body weight and fat mass compared to NC fed mouse groups. One-way and two-way ANOVA was performed on GraphPad Prism 7. Data is represented as mean ± S.E.M. Letters indicate significant p values, a=$p<0.05$, b=$p<0.01$, c=$p<0.001$, d=$p<0.0001$; symbols represent significant differences between genotypes * = compared to WT; an additional 'h' represents comparison to HFD fed WT.

Body composition (total fat and lean mass) were determined for each mouse group by ECHO-MRI at baseline, 4 week, and 8 week time points (**Figure 16C and 16D**). Within the male mouse groups, there was a significant difference among the diet groups in fat mass by the 8 week time point ($p<0.0001$). When provided a HFD, mice gained a significant amount of fat mass compared to the same genotypes provided NC ($p< 0.05$), but overall there was a trend for the WT mice to accumulate more fat mass at a faster rate than mice overexpressing catalase (**Figure 16C**). However, when provided an OM3 rich diet, the WT group gained only a 3 fold increase in fat mass ($p<0.05$) compared to the 8-10 fold increase when fed HFD. This gain in fat mass was even lower and not significantly different in [Tg(CAT)$^{\pm}$] and Bob-Cat mice compared to NC fed littermates (1-2 g) when fed OM3 rich diet. Lean mass measurements revealed NC fed WT mice trended to gain the largest amount of lean mass. HFD did not significantly alter the lean mass of any genotype, however, all male mice provided an OM3 diet gained lean mass from baseline to the 8 week time point (≥ 0.5 g) with the exception of the [Tg(CAT)$^{\pm}$] group (**Figure 16D**) which lost 2.2 g of lean mass. This loss in lean mass in the [Tg(CAT)$^{\pm}$] was reflective of their loss in total body weight when fed OM3 diet. Bob-Cat mice on OM3 rich diet gained 1.67 g of lean mass at 4 weeks and then decreased almost back to baseline by the 8 week time point.

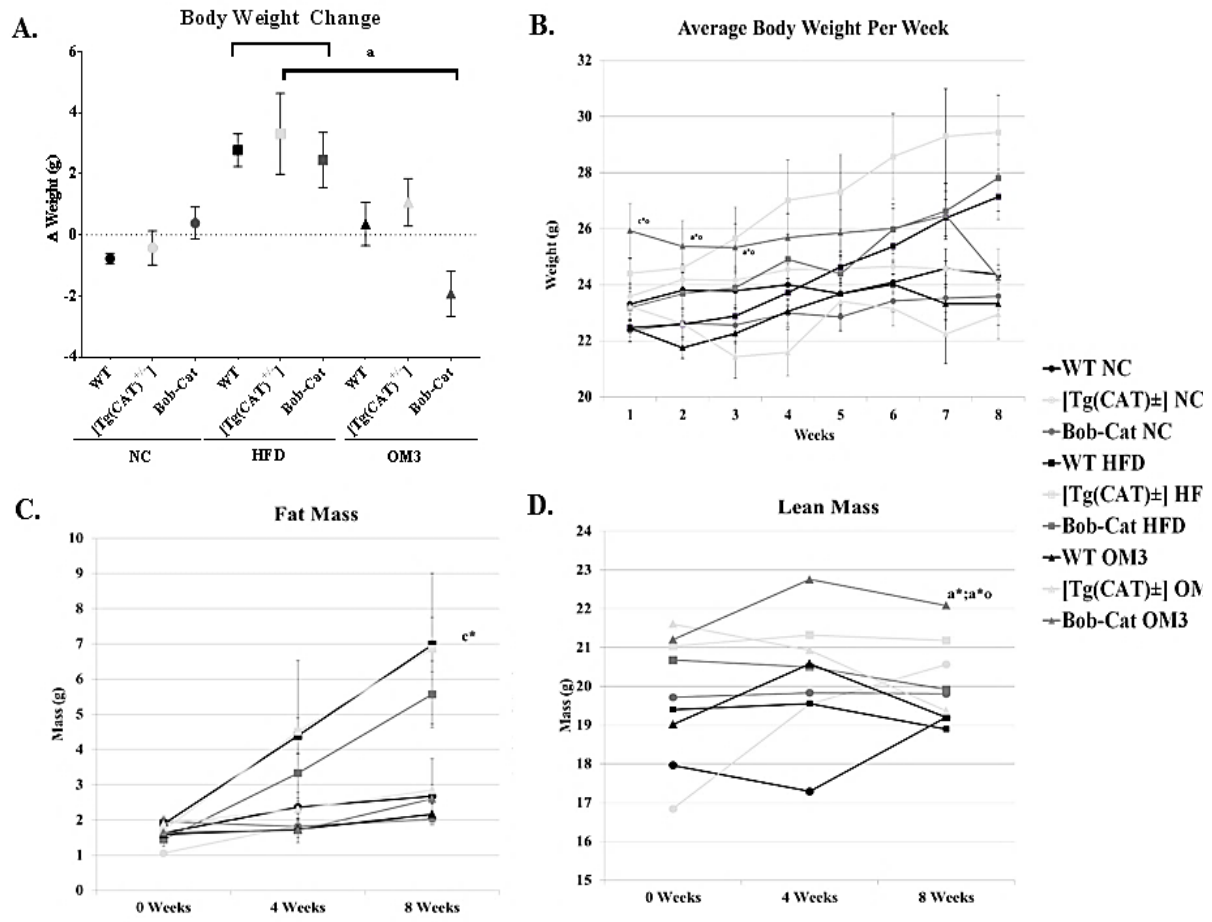

Figure 17. Body weight and body composition (fat/lean mass) in female mice overexpressing catalase. A. Changes in whole body weight over 8 weeks; B. Overall weekly body weight measurements; C. Fat Mass (g) and; D. Lean Mass (g) of WT, [Tg(CAT)$^{\pm}$], and Bob-Cat female mice fed NC, HFD, and OM3 diets (n≥4/group). Mice overexpressing catalase on an OM3 diet in contrast to the HFD fed animals either had no change or lost body weight and fat mass compared to NC fed mice groups. One-way and two-way ANOVA was performed on GraphPad Prism 7. Data is represented as mean ± S.E.M. Letters indicate significant p values, a=p<0.05, c=p<0.001; symbols represent significant differences between genotypes * = compared to WT; an additional 'o' represents comparison to OM3 fed WT.

Similar to what was seen in males, the female WT, [Tg(CAT)$^{\pm}$], and Bob-Cat mice of each diet group also showed an overall significant difference in body mass with regard to diet (p<0.0001) (**Figure 17**). The NC fed mice had minimal changes in body weight over the 8 week period, while all genotypes provided HFD gained between 2.5 - 3.5 g of body weight (not significant). Additionally, similar to males, female Bob-Cat mice provided an OM3 diet lost a

significant amount of weight compared to every other genotype provided HFD (**Figure 17A**). Weekly body weight changes (**Figure 17B**) showed that all mice fed an OM3 diet did not gain more than one gram of weight over the entire 8 week period.

Similar to males, ECHO-MRI showed that females on HFD, regardless of genotype, increased fat mass at a much faster rate and doubled the amount of fat gained in comparison to both their NC and OM3 fed littermates (**Figure 17C**). Mice provided an OM3 diet did not gain significant amounts of fat mass in comparison to the NC or OM3 fed WT groups. Interestingly, Bob-Cat females on OM3 diet had a >9% increase in lean mass in comparison to NC fed Bob-Cats and WT controls ($p<0.05$; **Figure 17D**) in spite of them losing the most body weight (**Figure 17A**).

3.3.2 Liver and Adipose Tissue Weights

In addition to a gain in visceral adiposity, another hallmark of the metabolic syndrome is the redistribution of ectopic fat in other metabolic tissues such as the liver. Therefore, visceral adipose tissue and liver weights were measured during tissue collection from all groups. In males, analysis by two-way ANOVA revealed a significant difference in visceral adipose tissue weight among diet groups ($p<0.0001$). A threefold increase in visceral adipose tissue was observed in all groups fed HFD in comparison to the NC fed WT group as displayed in **Table 8**. In contrast, mice provided OM3 diet did not have significantly larger visceral fat depots than NC fed mice groups. However, the [$Tg(CAT)^{\pm}$] and Bob-Cat mice fed OM3 diet had much lower levels of visceral fat in comparison to their respective HFD fed groups in addition to a twofold

Male									
	NC			HFD			OM3		
Tissue	**WT**	**[Tg (CAT)$^{\pm}$]**	**Bob-Cat**	**WT**	**[Tg (CAT)$^{\pm}$]**	**Bob-Cat**	**WT**	**[Tg (CAT)$^{\pm}$]**	**Bob-Cat**
Visceral Adipose Tissue (g)	0.93 ± 0.06	1.28 ± 0.02	0.83 ± 0.14	2.91 ± 0.47 **d***	3.78 ± 0.37 **d***	2.8 ± 0.58 **b***	2.03 ± 0.21	1.22 ± 0.20	1.11 ± 0.19
Liver (g)	1.18 ± 0.06	1.41 ± 0.11 **c***	1.21 ± 0.04	1.11 ± 0.07	1.56 ± 0.14 **b*;c*h**	1.25 ± 0.08	1.32 ± 0.07	1.39 ± 0.08	1.34 ± 0.05
Female									
Visceral Adipose Tissue (g)	0.72 ± 0.06	0.70 ± 0.04	0.60 ± 0.06	1.69 ± 0.16	2.12 ± 0.39	1.36 ± 0.22	0.79 ± 0.08	0.76 ± 0.07	0.90 ± 0.11
Liver (g)	1.20 ± 0.08	1.21 ± 0.05	1.23 ± 0.16	0.98 ± 0.04	1.13 ± 0.07	1.00 ± 0.04	1.36 ± 0.08	1.38 ± 0.05	1.38 ± 0.04

Table 8. Adipose tissue and liver weights of each mouse group. Visceral adipose tissue and liver weights (g) were measured during tissue collection, at the end of 8 weeks of dietary intervention, from all male (n≥6/group) and female (n≥4/group) mouse groups. Data are represented as mean ± S.E.M. Letters indicate significant p values, a=p<0.05, b=p<0.01, c=p<0.001, d=p<0.0001; symbols represent significant differences between genotypes * = compared to WT; an additional 'h' represents comparison to HFD fed WT.

lesser weight compared to the OM3 fed WT group. This data correlated with the observed body weight and fat mass (ECHO-MRI analysis) changes seen in these mouse groups. In regard to the liver weight, analysis by two-way ANOVA showed a significant effect among the genotypes of male mice ($p<0.0001$). It was intriguing that the NC and HFD fed [Tg(CAT)$^{\pm}$] groups had much larger livers (>17% increase, $p< 0.001$) compared to NC WT group. However, Bob-Cats and all mouse groups provided OM3 diet did not show significant differences in liver weight.

Female mice showed similar trends with the highest visceral adiposity seen among the HFD fed mice (**Table 8**). Significant increases in visceral adipose tissue was observed between [Tg(CAT)$^{\pm}$] on HFD and WT mice on NC diet ($p<0.0001$). OM3 fed female groups also did not

significantly differ in adipose tissue weight compared to their NC fed littermates. Interestingly, and contrary to male mice, females provided HFD had lower liver weights (no significance) and mice provided an OM3 diet showed a trend towards higher liver weight compared to all other diet groups.

3.3.3 Weekly Food and Energy Consumption

Weekly food and energy consumption for each mouse group were measured to determine if caloric intake was responsible for the observed differences seen in body weight or fat/lean mass. Two-way ANOVA showed an overall significant association between diet and genotype ($p<0.0001$) in addition to a significant difference observed within the genotypes ($p<0.0001$) and the various dietary interventions ($p<0.0001$). As depicted in **Figure 18A**, a significant increase in average food intake was seen for NC fed [Tg(CAT)$^{\pm}$] and Bob-Cat mice ($p<0.0001$ and $p<0.01$ respectively) compared to the NC fed WT group. Additionally, when provided a HFD or OM3 diet, all groups ate significantly less ($p<0.01$) grams (g) of food in comparison to NC fed [Tg(CAT)$^{\pm}$] and Bob-Cat mice. **Figure 18B** showed that as the study progressed, mice provided HFD or OM3 diet ate less chow per week. Due to differences in the total calories between the three diets (NC = 4.09 kcal/g compared to 4.6 kcal/g (HFD and OM3) shown in **Table 6**), the average kcal/g consumed was also calculated for each mouse group to determine total energy intake. Two-way ANOVA showed a significant difference with regard to male mouse genotype ($p<0.0001$) and diet group ($p<0.0001$). As shown in **Figure 18C**, there was a general trend of lower energy intake when mice were fed HFD or OM3 diet in comparison to NC. A significant trend was observed when mice overexpressing catalase fed NC consumed more energy than all groups fed HFD or OM3 diet.

Weekly food intake among the female mouse groups (**Figure 18 D-F**) showed similar eating patterns to those observed in the male mouse groups. There was a significant interaction between diet and genotype ($p=0.0013$), genotype alone ($p<0.001$), and diet alone ($p<0.0001$). The largest quantity of chow consumed was by the groups provided NC regardless of the genotype (**Figure 18 D**). A significant reduction in food intake was seen in all mice provided a

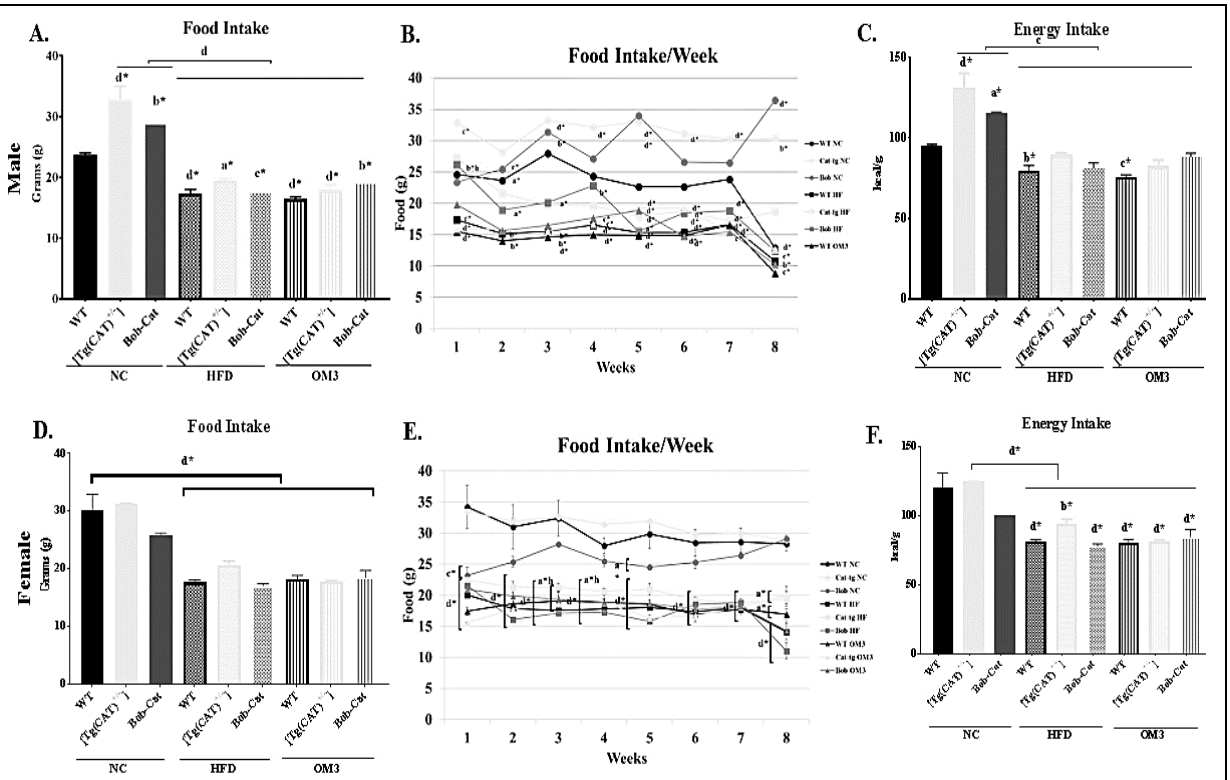

Figure 18: Weekly food and energy consumption in male and female mice overexpressing catalase. Weekly food and energy consumption measured in wildtype and catalase overexpressing mice for 8 weeks: Male, A. average weekly food consumption for 8 weeks; B. weekly food consumption for 8 weeks, and C. calculated average energy consumption per mouse ($n\geq6$/group). Female, D. average of overall food consumption for 8 weeks; E. weekly food consumption for 8 weeks, and; F. calculated average energy consumption per mouse ($n\geq4$/group). WT, [Tg(CAT)±], and Bob-Cat mice fed NC, HFD, and OM3 diet were analyzed for each gender. One-way and two-way ANOVA was performed on GraphPad Prism 7. Data is represented as mean ± S.E.M. Letters indicate significant p values: a=$p<0.05$, b=$p<0.01$, c=$p<0.001$, d=$p<0.0001$; symbols represent significant differences between genotypes * = compared to WT; an additional 'h' represents comparison to HFD fed WT.

HFD or OM3 diet ($p<0.0001$) in comparison to the NC fed WT group. This trend was similar between males and females. Regarding energy intake, there was a significant interaction between

the genotype and diet group ($p=0.0017$), as well as between genotype alone ($p<0.001$), and between diet groups ($p<0.0001$) (**Figure 18F**). Female mice provided HFD or OM3 diet

Male									
	NC			HFD			OM3		
Parameter	**WT**	**[Tg(CAT)$^{\pm}$]**	**Bob-Cat**	**WT**	**[Tg(CAT)$^{\pm}$]**	**Bob-Cat**	**WT**	**[Tg(CAT)$^{\pm}$]**	**Bob-Cat**
TC (mg/dL)	<100	<100	<100	134.6 ± 7.98	162.3 ± 9.16 **d*;d*h**	144 ± 10.8 **b***	<100	<100	<100
HDL (mg/dL)	55.3 ± 4.30	65.2 ± 1.62	55.83 ± 2.15	>82.9 ± 6.51**d***	>93.3 ± 6.36 **d***	>91.2 ± 3.61 **c***	66.6 ± 3.50	61.5 ± 3.35	>77.89 ± 4.78
TG (mg/dL)	60.7 ± 5.48	81.7 ± 5.68	225.7 ± 25.0 **d***	73.2 ± 4.87	79.5 ± 3.66	353.4 ± 24.87 **d*;d*h**	61.2 ± 2.85	41.5 ± 3.36	223.2 ± 9.40 **d*; d*o**
Ketone (mmol/L)	0.55 ± 0.28	0.38 ± 0.08	1.18 ± 0.07 **b***	1.25 ± 0.14	0.56 ± 0.08	0.35 ± 0.43 **a*h**	1.6 ± 0.23 **b***	1.01 ± 0.13	2.1 ± 0.11 **d*a*o**
Female									
TC (mg/dL)	<100	<100	<100	125 ± 0.38	<100	117.5 ± 4.79	<100	101	<100
HDL (mg/dL)	48.3 ± 5.48	55.83 ± 2.15	40.7 ± 3.98	>61.9 ± 5.67	>81.0 ± 5.41	>69.4 ± 7.84	>64.3 ± 4.29	62.1 ± 3.71	>75.2 ± 4.45
TG (mg/dL)	234.1 ± 34.3	197.7 ± 10.3	164.8 ± 10.9	220.6 ± 21.2	195.5 ± 7.8	254.4 ± 15.5	134.9 ± 9.29	190.4 ± 17.3	194.1 ± 3.0
Ketone (mmol/L)	1.35 ± 0.39	0.98 ± 0.12	1.48 ± 0.14	1.67 ± 0.30	1.0 ± 0.08	0.65 ± 0.56	0.9	1.2 ± 0.23	1.93 ± 0.10

Table 9. Circulating levels of metabolic parameters. Lipid Profile of Total Cholesterol (TC) and High Density Lipoprotein (HDL) determined using the Cholestech kit, Triglyceride levels (TG) using the Triglyceride Colorimetric Assay Kit in plasma of Male (n≥6/group) and Female (n≥4/group) mice. Ketone levels using a glucometer in plasma of Male (n≥4/group) and Female (n=2-9/group) mice. Measurements were performed in WT, [Tg(CAT)$^{\pm}$], and Bob-Cat mice fed NC, HFD, and OM3 diets for 8 weeks. One-way and two-way ANOVA was performed on GraphPad Prism 7. Data is represented as mean ± S.E.M. Letters indicate significant p values, a= $p<0.05$, b= $p<0.01$, c= $p<0.001$, d= $p<0.0001$; symbols represent significant differences between genotypes * = compared to WT; an additional 'h' or 'o' represents significant differences between HFD and OM3 fed WT mice respectively.

consumed less energy compared to NC fed littermates. However, the decrease in food and energy

intake did not correlate with the increase in body weight and adiposity seen in HFD fed animals compared to NC and OM3 diet fed littermates.

3.3.4 Blood Lipid Profile and Ketones

Post-surgery, the lipid profile was measured on plasma samples collected from each mouse fasted at least 12 h prior to the surgery using an LDX Cholestech kit. As shown in **Table 9**, all mouse groups fed HFD ($p<0.001$) had significantly higher Total Cholesterol (TC) levels in comparison to the NC fed WT mice and all mouse groups on OM3 rich diet. In the groups fed HFD or OM3, the Bob-Cat mice had the highest levels of HDL followed by the HFD fed [Tg(CAT)$^{\pm}$]. This is also true when comparing the OM3 Bob-Cat group to every group provided NC. Two-way ANOVA analysis of plasma triglyceride (TG) levels showed there was a significant genotype ($p<0.0001$) and diet ($p<0.01$) interaction among the groups. Interestingly, male Bob-Cat mice, regardless of diet, had the highest levels of plasma TG. In fact, within each diet group, Bob-Cat male mice had 3 fold higher TG levels compared to the other two genotypes.

As shown in **Table 9**, female TC level was < 100 mg/dL for all mouse groups except the HFD fed WT and Bob-Cat groups. The female HFD fed [Tg(CAT)$^{\pm}$] mice displayed much lower TC (<100 mg/dL) compared to the male mice (162.3 ± 9.16 mg/dL) fed the same diet. (It is to be noted, when individual mice readings fell outside the assay's range of sensitivity, the less than ("<") or (">") was used to best represent the average results from each mouse group.) Assessment of HDL revealed a significant diet interaction ($p<0.003$). Female mice trended to have a little lower HDL levels in comparison to males. However, consistent with males, highest levels of HDL was found in the [Tg(CAT)$^{\pm}$] HFD fed females. Another interesting trend observed was that within the OM3 diet fed groups, the Bob-Cat male and female groups had the highest levels of HDL. Data analysis of TG levels revealed a significant interaction between diet

and genotype ($p=0.01$) within the female mouse groups. There was an overall trend for HFD mice to have equal or increased levels of plasma TG in comparison to their respective genotypes on NC or OM3 diet. However, it was interesting that OM3 diet only showed a trend towards lower TG levels compared to NC and HFD in the WT group. There was also a gender effect where female WT and [Tg(CAT)$^{\pm}$] mice, regardless of diet, expressed higher levels of TG in comparison to the males. However, Bob-Cat females had lower levels of circulating TG in comparison to male Bob-Cats.

Ketone levels of NC fed [Tg(CAT)$^{\pm}$] mice were lower (not significant), but the Bob-cat group ($p<0.05$) were significantly higher than the NC fed WT male group. When mice were provided HFD, each genotype doubled its ketone level compared to their NC littermates with the exception of the HFD fed Bob-Cat mice, which showed the lowest levels within the HFD groups (3 fold decrease, $p<0.05$). OM3 diet feeding also increased plasma ketone levels (2 fold increase) in comparison to littermates provided NC. Specifically, the OM3 fed WT group ($p<0.01$) had significantly higher levels than the NC fed WT, and the OM3 Bob-Cat males having the highest levels of all groups [> 3 fold compared to the NC fed WT ($p<0.0001$) and ≈ 2 fold compared to the NC fed Bob-Cat group ($p<0.05$)].

A significant interaction between diet and genotype was seen in fasting ketone levels ($p<0.01$). Within females, the ketone levels showed a trend to be higher than males within each respective mouse group with the exception of mice provided the OM3 diet.

3.3.5 Metabolic Parameters Using CLAMS

Metabolic parameters were determined at the end of the 8 week study using indirect calorimetry by measuring O_2 consumption (VO_2) and CO_2 production (VCO_2), Respiratory Exchange Rate (RER), Food Intake (FI), Energy Expenditure (EE), as well as X-Ambulatory

counts (XAMB - physical activity) using the Comprehensive Laboratory Animal Monitoring System (CLAMS) (Columbus Instruments, Columbus, OH, USA).

3.3.5.1 Food Intake (CLAMS)

A three-day assessment of Food Intake (FI) (**Figure 19A-B**) was conducted using CLAMS, which allowed analysis of eating patterns and insight on circadian rhythm. All male mice on HFD in the WT and [Tg(CAT)$^{\pm}$] mouse groups ate at a more constant rate throughout the 48 hour time period compared to mice provided NC and mice overexpressing catalase (fed OM3 diet) which ate more frequently through the dark cycle and less during the light cycle. Most intriguing, was the evidence that male Bob-Cat mice followed a similar eating pattern to the NC fed group (decreased food intake during light cycle and increased during the dark cycle) indicating that diet (NC or OM3) had not altered their circadian rhythm to the degree that was observed in other two genotypes fed HFD and the WT mice fed OM3.

As shown in **Figure 19B**, CLAMS analysis on female mice provided NC showed a normal eating pattern (higher consumption in the dark vs light cycle). Similar to what was seen in the male mouse groups, the female Bob-Cats on HFD showed a normal eating pattern in

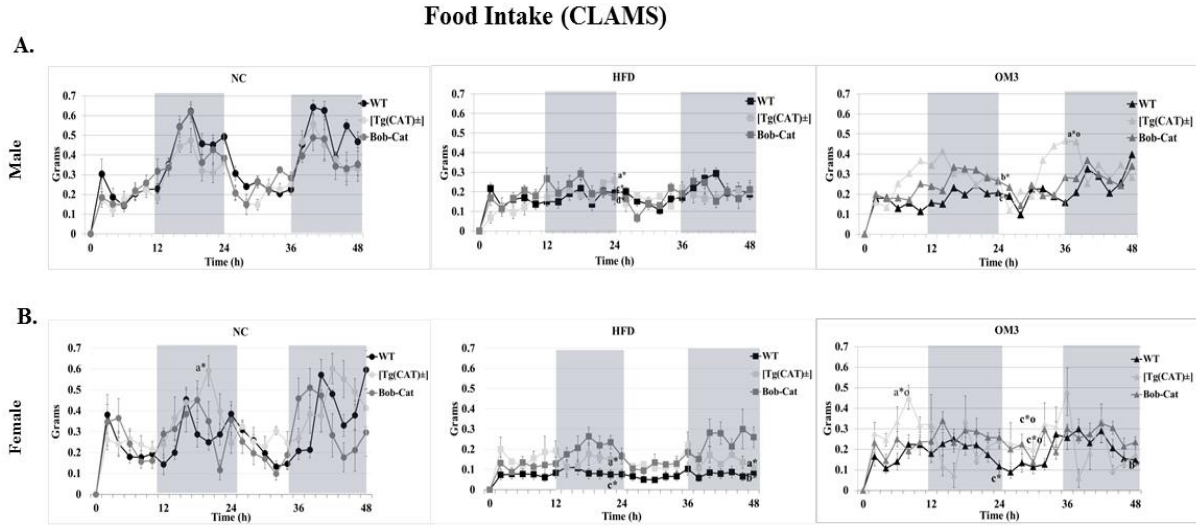

Figure 19: CLAMS analysis of food intake over a 48 hour period in male and female mice overexpressing catalase. Light and dark cycle analysis of CLAMS measurements for 48 hours are provided: Male, A. and Female, B. Food Intake as average grams/2h for 48 hours by WT, [Tg(CAT)±], and Bob-Cat mice fed NC, HFD, and OM3 diet (n≥3/group). One-way and two-way ANOVA was performed on GraphPad Prism 7. Data is represented as mean ± S.E.M. Letters indicate significant p values: a=p<0.05, b=p<0.01, c=p<0.001, d=p<0.0001; symbols represent significant differences between genotypes * = compared to WT; an additional 'o' represents comparison to OM3 fed WT.

contrast to the other two genotypes fed the same diet. However, when fed OM3 diet, the differences in the eating pattern were lost. In general, a more stable pattern of energy consumption occurred in mice with lower fat mass as shown previously in **Figure 16 and 17**.

3.3.5.2 Energy Expenditure and Physical Activity (CLAMS)

In addition to FI, Energy Expenditure (EE) and physical activity (XAMB) were also analyzed using the CLAMS technology. As seen in **Figure 20A**, EE, calculated indirectly as Cal/h/g of lean body mass in each male mouse group, did not significantly differ between genotypes when provided NC diet. The HFD fed groups had significantly higher levels of EE in

the dark cycle ($p<0.01$) compared to NC fed WT mice. However, during the light cycle, HFD [Tg(CAT)$^{\pm}$] mice had much lower levels than both groups overexpressing catalase provided HFD. EE in all groups provided OM3 diet remained at intermediate levels to that seen in the NC and HFD fed groups, yet levels were significantly higher than the NC WT group ($p<0.05$). Overall, differences between groups were much greater during the dark vs. light cycle. Analysis of the X-Ambulatory (XAMB) activity, depicted in **Figure 20B**, showed there was higher activity in the [Tg(CAT)$^{\pm}$] and Bob-Cat mice compared to NC WT mice ($p<0.05$). Interestingly, these were also the two groups where the greatest weekly food intake and energy intake (**Figure 18A & C**) was also observed. Likewise, when all genotypes were provided HFD or OM3 diet, the WT mice had the lowest activity levels, not reaching above 3000 counts per 2 hours,

suggesting that the overexpression of catalase might have some influence on the activity levels observed in the male groups.

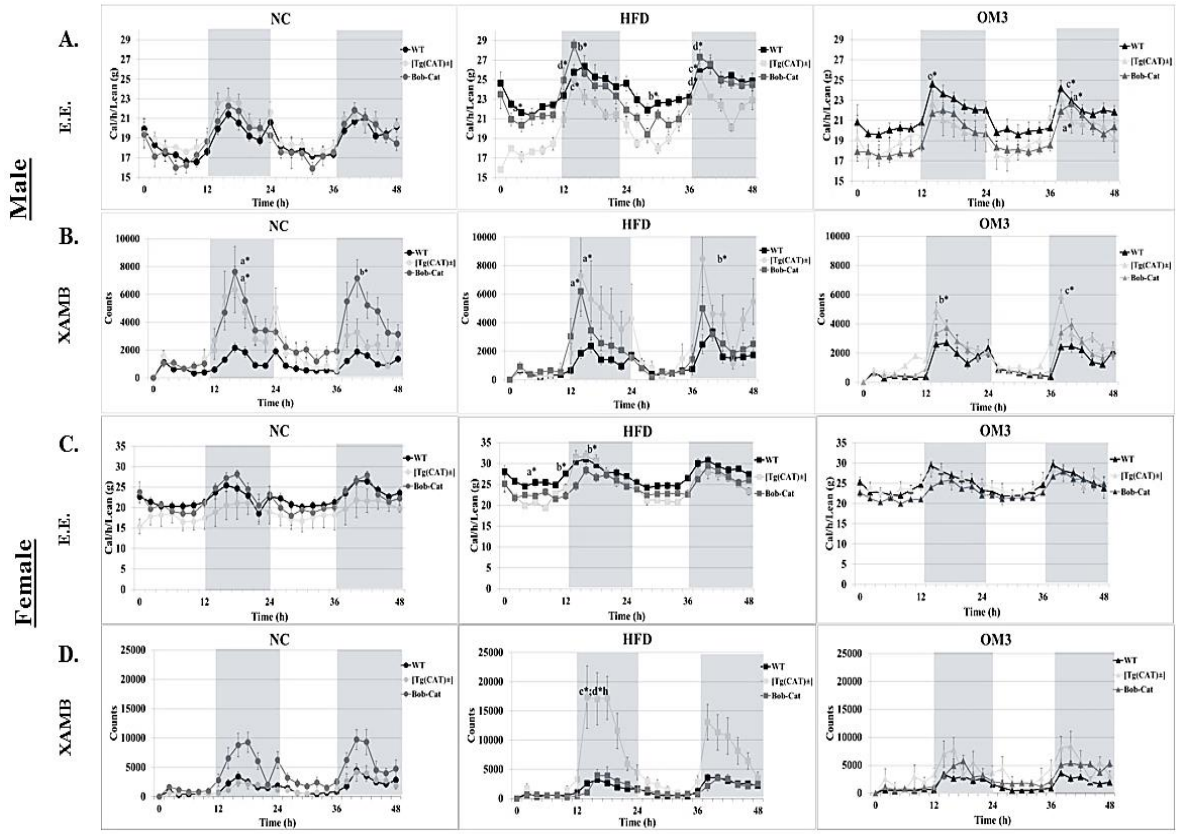

Figure 20: CLAMS analysis of energy expenditure and total activity over a 48 hour period in male and female mice overexpressing catalase. Light and dark cycle CLAMS analysis of Energy Expenditure (EE) and X-Ambulatory Movement (XAMB) per 2h over a 48 hour time period are provided: Male, A. Metabolic EE averaged as Cal/h/Lean(g) body mass and; B. XAMB Counts per 2h for 48 hours for WT, [Tg(CAT)±], and Bob-Cat mice fed NC, HFD, and OM3 diet (n≥4/group). C&D. represent data of female mice of each genotype and diet group (n≥3/group). One-way and two-way ANOVA were performed on GraphPad Prism 7. Data is represented as mean ± S.E.M. Letters indicate significant p values: a=p<0.05, b=p<0.01, c=p<0.001, d=p<0.0001; symbols represent significant differences between genotypes * = compared to WT; an additional 'h' represents comparison to HFD fed WT.

Overall, within female groups the analysis of EE showed less variation in circadian rhythm (**Figure 20C**) in comparison to that observed within male groups. Similar to males, females on HFD had higher levels of EE in comparison to the mice fed NC or OM3, with the WT mice fed HFD showing the highest levels during both the light and dark cycles ($p<0.05$) and

the [Tg(CAT)$^{\pm}$] mice mostly during the dark cycle ($p<0.01$). XAMB analysis among female groups on NC and OM3 diet showed a trend for Bob-Cat mice to have higher activity levels than WT or [Tg(CAT)$^{\pm}$] mice. This may have accounted for the observed lower body weight in the Bob-Cat mice shown earlier (**Figure 17**). Animals fed HFD had either similar or lower activity levels compared to NC fed WT mice with the exception of the female HFD fed [Tg(CAT)$^{\pm}$] mice which displayed significantly higher activity during the dark cycle (3 fold, $p<0.01$).

3.3.5.3 Respiratory Exchange Ratio (CLAMS)

Using CLAMS, we also determined the Respiratory Exchange Ratio (RER) for each mouse group at the end of the 8 week study. RER, an indication of which type of fuel (carbohydrate (CHO) or fat) is primarily being metabolized to supply energy demands, was lowest in the male NC fed WT mice group as well as in all HFD fed mice (**Figure 21A**). However, when groups overexpressing catalase were provided NC, the RER was significantly higher compared to the WT mice during both light ($p<0.01$) and dark cycles ($p<0.001$). When provided an OM3 enriched diet, the RER levels remained intermediate between the NC and HFD

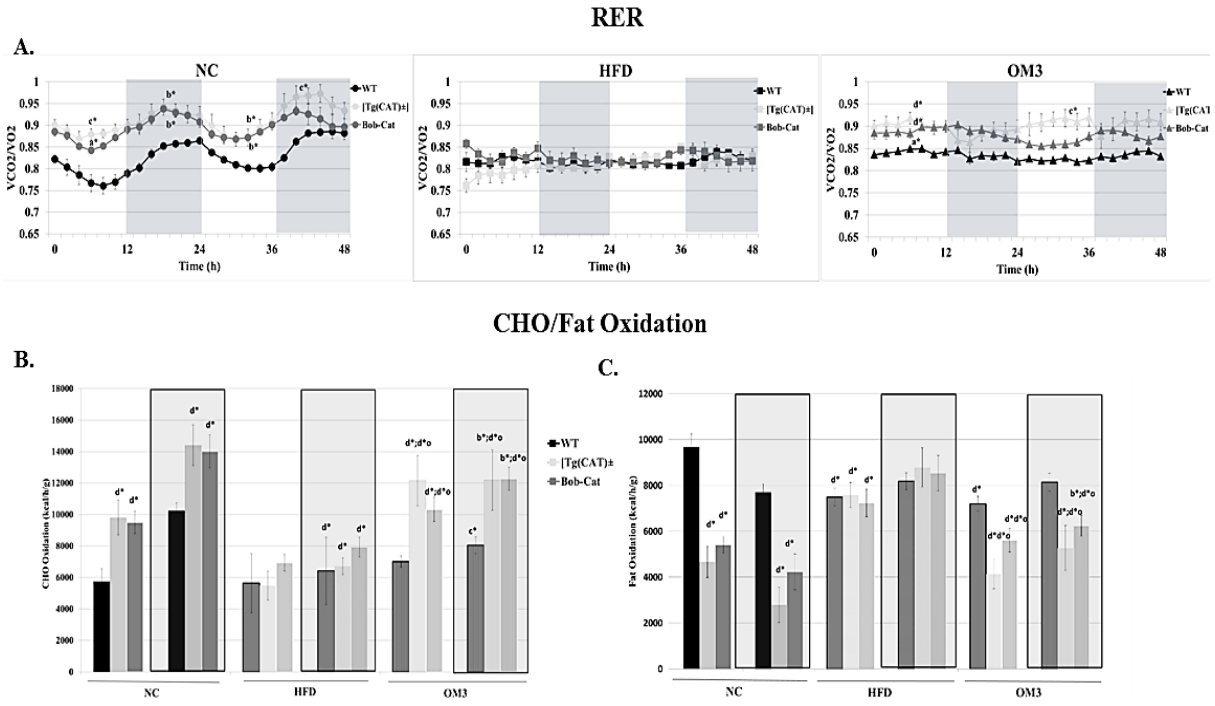

Figure 21. CLAMS analysis of RER and substrate oxidation over a 48 hour period in male mice overexpressing catalase. Light and dark cycle CLAMS analysis of average Respiratory Exchange Ratio (RER) and calculated CHO and Fat Oxidation per 2h over a 48 hour time interval: A. RER (CO_2 emission/O_2 consumption); B. CHO Oxidation, and; C. Fat Oxidation for WT, [Tg(CAT)±], and Bob-Cat mice fed NC, HFD, and OM3 diet ($n\geq4$/group). One-way and two-way ANOVA was performed on GraphPad Prism 7. Data is represented as mean ± S.E.M. Letters indicate significant p values: a=$p<0.05$, b=$p<0.01$, c=$p<0.001$, d=$p<0.0001$; symbols represent significant differences between genotypes * = compared to WT; an additional 'o' represents comparison to OM3 fed WT.

groups. As seen within the NC groups, the mice overexpressing catalase fed OM3 also had a higher RER in comparison to the OM3 fed WT groups. Since RER levels reflect the circadian patterns of food consumed, it also followed similar light and dark cycle patterns as seen with FI (**Figure 19**). The NC fed groups followed a normal circadian pattern, but the HFD fed groups did not. It was interesting to note that Bob-Cat mice fed NC or OM3 diet followed a normal pattern which was not evident when these mice were fed HFD.

We further delineated the levels of CHO and fat oxidation based on the VO_2 and VCO_2 data derived from the CLAMS analysis. As seen in **Figure 21B**, the most significant differences seen in CHO oxidation of male groups were observed during the dark cycle. However, in comparison to the WT groups, mice overexpressing catalase provided NC had significantly higher levels of CHO oxidation ($p<0.0001$) independent of the light or dark cycle. Conversely, when provided HFD, there were no differences between genotypes, but all mouse groups had significantly lower levels of CHO oxidation than the NC fed WT groups during the dark cycle. Similar to that seen with the NC groups, OM3 diet also showed that mice overexpressing catalase had significantly higher levels of CHO oxidation compared to both the NC fed WT mice and OM3 fed WT mice independent of the time of day. Contrary to CHO oxidation, NC fed WT mice had significantly higher levels of fat oxidation ($p<0.0001$) compared to every other group during the light cycle and significantly higher levels compared to mice overexpressing catalase ($p<0.0001$) on NC diet in addition to OM3 diet during the dark cycle. Mice provided HFD showed a trend for having the highest levels of fat oxidation regardless of the genotype during the dark cycle (not significant). When fed an OM3 diet, it was interesting that the mice overexpressing catalase had significantly lower levels of fat oxidation in comparison to the WT mice provided OM3 diet during both light and dark cycles. However, in comparison to

littermates provided NC, both groups overexpressing antioxidant catalase had significantly lower levels of fat oxidation ($p<0.01$) during the dark cycle.

When comparing the various diets, female mice followed similar trends in RER compared to what was seen in male mice (**Figures 21& 22**).

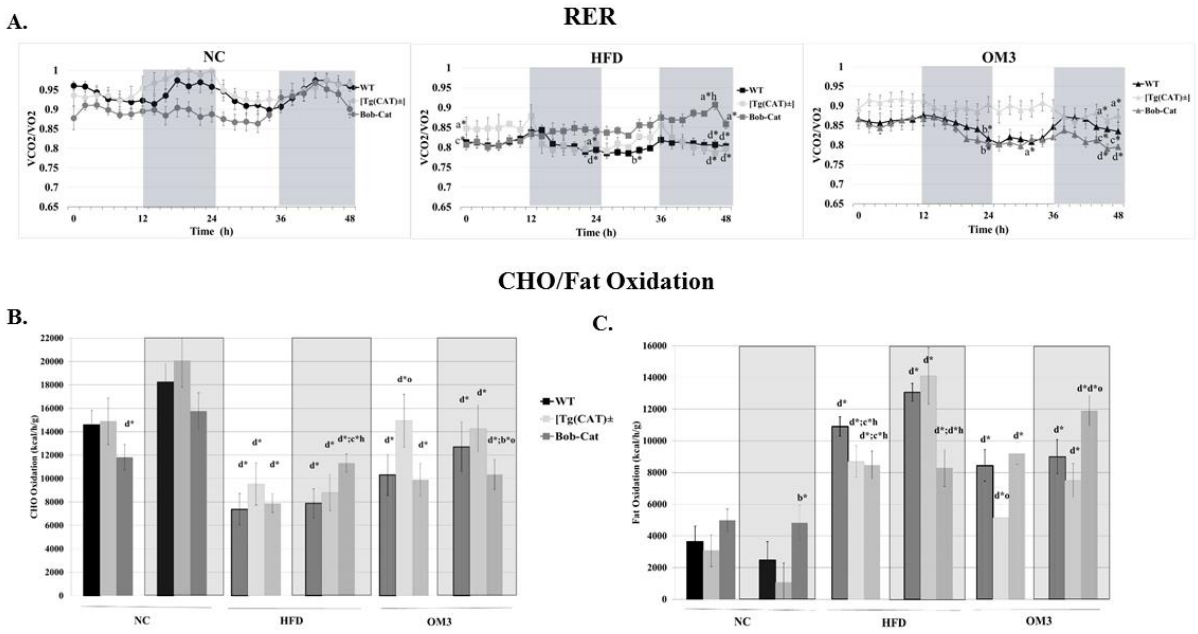

Figure 22. CLAMS analysis of RER and substrate oxidation over a 48 hour period in female mice overexpressing catalase. Light and dark cycle CLAMS analysis of average Respiratory Exchange Ratio (RER), and calculated CHO and Fat Oxidation for 48 hours: A. RER (CO_2 emission/O_2 consumption); B. CHO Oxidation, and; C. Fat Oxidation for WT, [Tg(CAT)±], and Bob-Cat mice fed NC, HFD, and OM3 diet (n≥3/group). One-way and two-way ANOVA was performed on GraphPad Prism 7. Data is represented as mean ± S.E.M. Letters indicate significant p values: a=p<0.05, b=p<0.01, c=p<0.001, d=p<0.0001; symbols represent significant differences between genotypes * = compared to WT; an additional 'h' represents comparison to HFD fed WT while an additional 'o' represents comparison to OM3 fed WT.

NC fed female diet groups had the typical circadian cycles. Although unlike male mice, female NC fed Bob-Cats showed a trend for having a lower RER than the NC fed WT females throughout the light and dark cycles. Within the female HFD groups, WT and [Tg(CAT)$^{\pm}$] had a significantly lower RER during both light and dark cycles ($p<0.01$), while Bob-Cats only showed a trend. However, it was interesting that the HFD fed Bob-Cats had a significantly higher RER

compared to the HFD fed WT group during the dark cycle ($p<0.05$). When provided an OM3 diet, Bob-Cat and WT groups had a significantly lower RER compared to NC fed WT mice ($p<0.01$), but [Tg(CAT)$^{\pm}$] mice only had significantly lower levels ($p<0.05$) during the dark cycle. This was not seen in the male mouse groups overexpressing catalase fed OM3 diet, where we observed higher levels of RER than the NC fed WT mice.

Calculations of CHO oxidation in females showed that in contrast to males, NC fed female mice overexpressing catalase had similar or significantly lower levels of CHO oxidation (NC fed Bob-Cat) compared to their WT littermates (**Figure 22B**). On the other hand, similar to males, when fed a HFD, the CHO oxidation in each mouse group was significantly decreased in the dark cycle compared to NC fed WT mice and no significant differences were seen among the female genotypes fed HFD. Also, as observed in males, OM3 fed female [Tg(CAT)$^{\pm}$] mice had significantly higher levels of CHO oxidation ($p<0.0001$) compared to both NC and OM3 fed WT mice, but levels did not significantly differ from NC fed WT mice. On the other hand, Bob-Cat females either had similar or significantly lower levels of CHO oxidation compared to their NC or OM3 fed WT control groups. With regard to fat oxidation, the same general trends occurred in both female and male diet groups with the exception that female fat oxidation trended to be much higher (kcal/h/g) than males on the same intervention. It is of special interest however, among the female groups, the NC and OM3 Bob-Cat mice groups trended to have the highest levels of fat oxidation regardless of the time of day. This may be an indication of why these groups trended to have one of the lowest body weight and fat mass averages compared to the other intervention groups (**Figure 17**).

3.3.6 Insulin Sensitivity

Both redox stress and dietary interventions (HFD and OM3) can modulate insulin sensitivity; hence we measured fasting levels of glucose and insulin and subsequently calculated

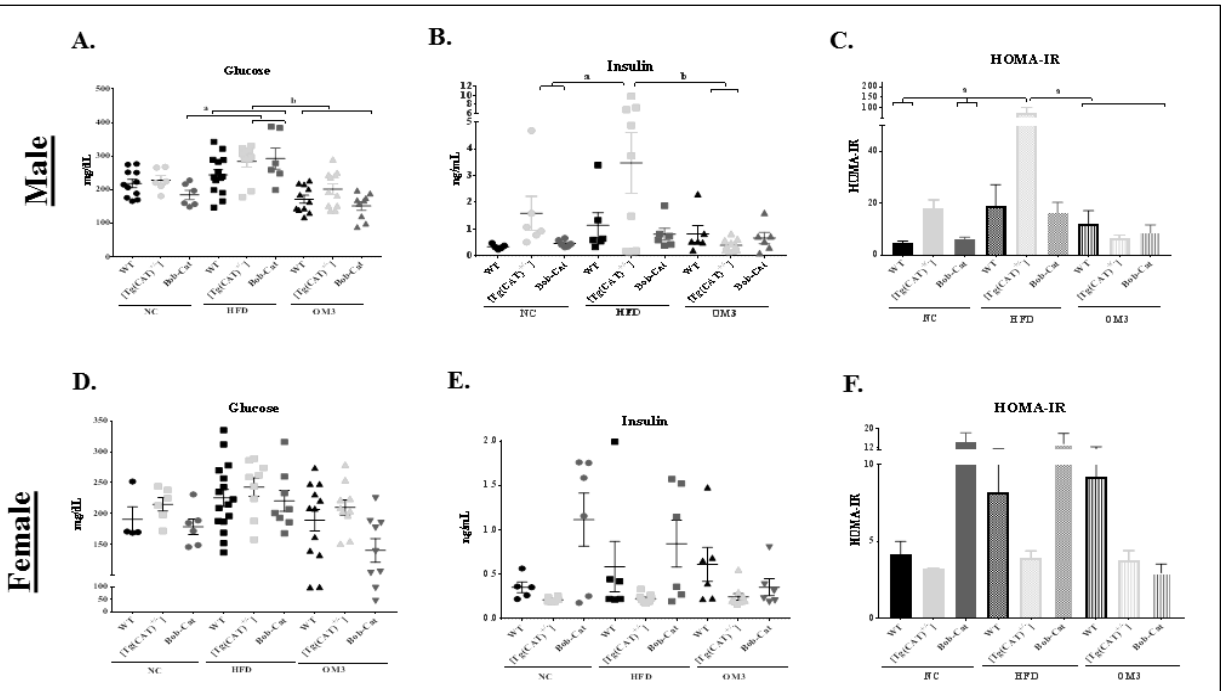

Figure 23. Insulin sensitivity in male and female mice overexpressing catalase. Quantification of fasting blood glucose (glucometer), plasma insulin (ELISA), and calculated HOMA-IR: Male, A. Glucose; B. Insulin, and; C. HOMA-IR in WT, [Tg(CAT)±], and Bob-Cat mice fed NC, HFD, and OM3 diet (n≥5/group). Graphs D-F. show data collected from female mice of each genotype and diet group (n≥4). One-way and two-way ANOVA was performed on GraphPad Prism 7. Data is represented as mean ± S.E.M. Letters indicate significant p values, a=p<0.05, b=p<0.01.

the HOMA-IR, an indirect measure of insulin sensitivity. As depicted in **Figure 23A**, a genotypic ($p<0.01$) and dietary effect ($p<0.0001$) was observed in glucose levels. There was a trend for lower glucose levels in mice fed OM3 diet compared to NC mouse groups, and significantly lower levels in mice fed OM3 vs. HFD fed groups ($p<0.01$). Bob-Cat mice on OM3 diet had the lowest glucose levels in comparison to every other group. All genotypes on HFD had increased levels of glucose compared to every other group. Similarly, a significant genotypic ($p=0.0005$) interaction was seen in circulating insulin levels (**Figure 23B**). Interestingly, in spite

of the large range within the group, the HFD fed [Tg(CAT)±] mice had the highest insulin levels compared to any other mouse group ($p<0.05$). Calculated HOMA-IR (**Figure 23C**), revealed a significant difference in genotype ($p<0.001$) and diet ($p<0.05$). As expected, due to the larger range in the insulin levels within this group, the [Tg(CAT)$^{\pm}$] mice on HFD also had the highest calculated HOMA-IR ($p<0.01$). Interestingly, ketone levels showed no significant differences in the [Tg(CAT)$^{\pm}$] male and WT mice fed NC where insulin signaling was optimal (**Table 9**). In fact, the ketone levels in the HFD fed WT male group were >2 fold higher than the levels in the [Tg(CAT)$^{\pm}$] group on HFD, thus indicating insulin is repressing ketone body production. Thus, these mice may not be classified as insulin resistant or hyperinsulinemic (Puchalska & Crawford, 2017). In contrast, [Tg(CAT)$^{\pm}$] mice on NC or OM3 had much lower insulin levels and calculated HOMA-IR.

In female mice, glucose levels showed no significant differences between groups as depicted in **Figure 23D**. However, when comparing diets, the [Tg(CAT)$^{\pm}$] mice had the highest levels of glucose within each dietary group. Also, as observed in males, there was a trend for HFD fed mice of each genotype to have an overall increase and mice provided OM3 diet to have an overall equivalent or reduced plasma glucose level compared to littermates placed on NC, though none reached significance. An overall diet interaction was observed for insulin (**Figure 23E**) among female groups ($p<0.001$). Contrary to the highest levels of insulin in the [Tg(CAT)$^{\pm}$] males, the female mice had the lowest average insulin levels of all mice provided HFD. Additionally, in contrast to males, female ketones did not significantly differ in the female HFD fed [Tg(CAT)$^{\pm}$] in comparison to any other female mouse group (**Table 9**). Bob-Cat mice within each diet group showed the highest insulin levels among the genotypes, and were significantly higher ($p<0.05$) compared to both the NC and HFD fed WT females. HOMA-IR

calculations revealed an interaction between diet and genotype ($p<0.05$) as well as a genotype interaction ($p<0.0001$). In contrast to the males, the female [$Tg(CAT)^{\pm}$] had the lowest calculated HOMA-IR and the HFD fed Bob-Cat groups had the highest, pointing to a possible sexual dimorphism in regard to insulin sensitivity within the 'stress-less' mice models.

3.3.7 Diet-Redox Stress Interaction in Adipose Tissue

3.3.7.1 Redox Status

In order to determine if differences in redox environment, due to dietary intervention, contributed to the observed metabolic changes in the 'stress-less' mouse models, we measured signatures of adipose tissue redox stress: i.e. oxidized carbonyl groups, expression of Nrf2 (a transcription factor and key regulator of redox homeostasis), and key targets reflecting the activity of Nrf2: catalase activity and HO-1 (antioxidants transcribed upon activation of Nrf2). Oxidized carbonyl groups, measured using the OxyBlot protein oxidation kit (Millipore), interestingly showed that within male groups, there was no major induction of oxidized proteins in the NC or HFD fed groups (**Figure 24A**). However, in mice fed an OM3 enriched diet, we saw higher levels of oxidized carbonyls, with the highest levels seen within the OM3 fed WT mouse group ($p<0.05$) compared to the NC and HFD groups followed by the OM3 fed Bob-Cat group (not significant). Within females (**Figure 24B**), there was a trend for the mice overexpressing catalase to have lower levels of oxidized carbonyl groups in comparison to the

WT littermates. The only exception was the Bob-Cat mice fed OM3 diet, which showed a significant increase ($p<0.05$) in oxidized carbonyl groups.

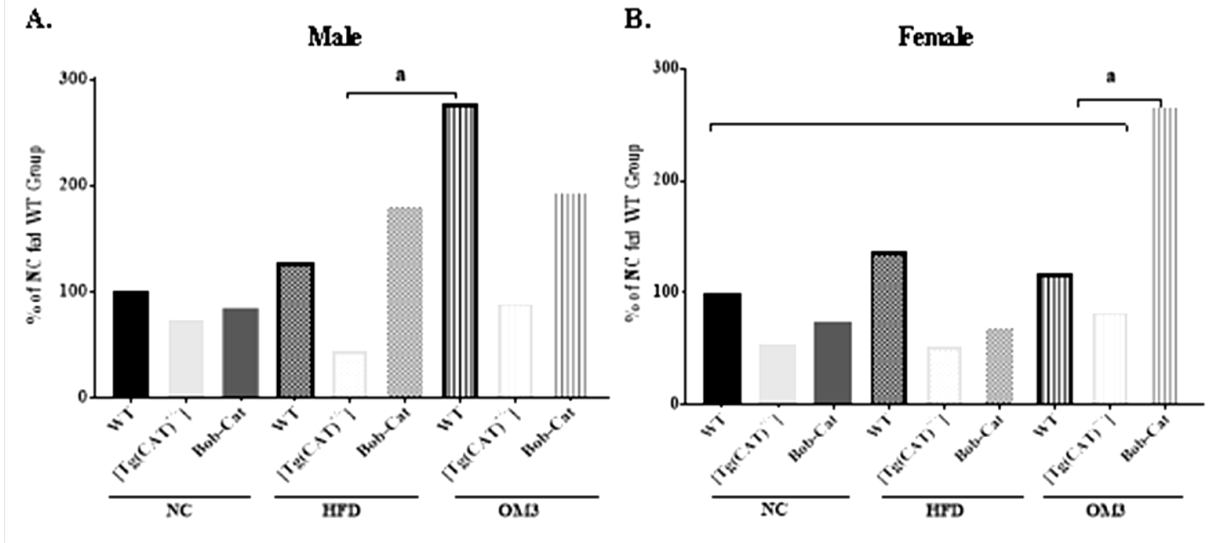

Figure 24. Adipose tissue oxidized carbonyl groups in male and female mice overexpressing catalase. Male, A. and Female, B. oxidized carbonylated proteins in perigonadal adipose tissue. Oxidized protein levels in all mouse groups are represented as % of the oxidized proteins in WT mice fed NC. One-way and two-way ANOVA was performed on GraphPad Prism 7. Letter a indicates significance at $p<0.05$.

When mRNA expression of Nrf2, a redox sensitive transcription factor was determined, the male Bob-Cat mice showed an increase in Nrf2 induction when fed HFD (>4 fold) or OM3 (>9 fold) compared to its NC fed littermates and the other genotypes fed any diet. However, none reached statistical significance (**Figure 25A**). Similar trends of Nrf2 induction were also seen in

the Bob-Cat female mice where the levels increased to >50 fold when fed HFD and >120 fold ($p<0.05$) when fed OM3 diet vs. the WT group (**Figure 25B**).

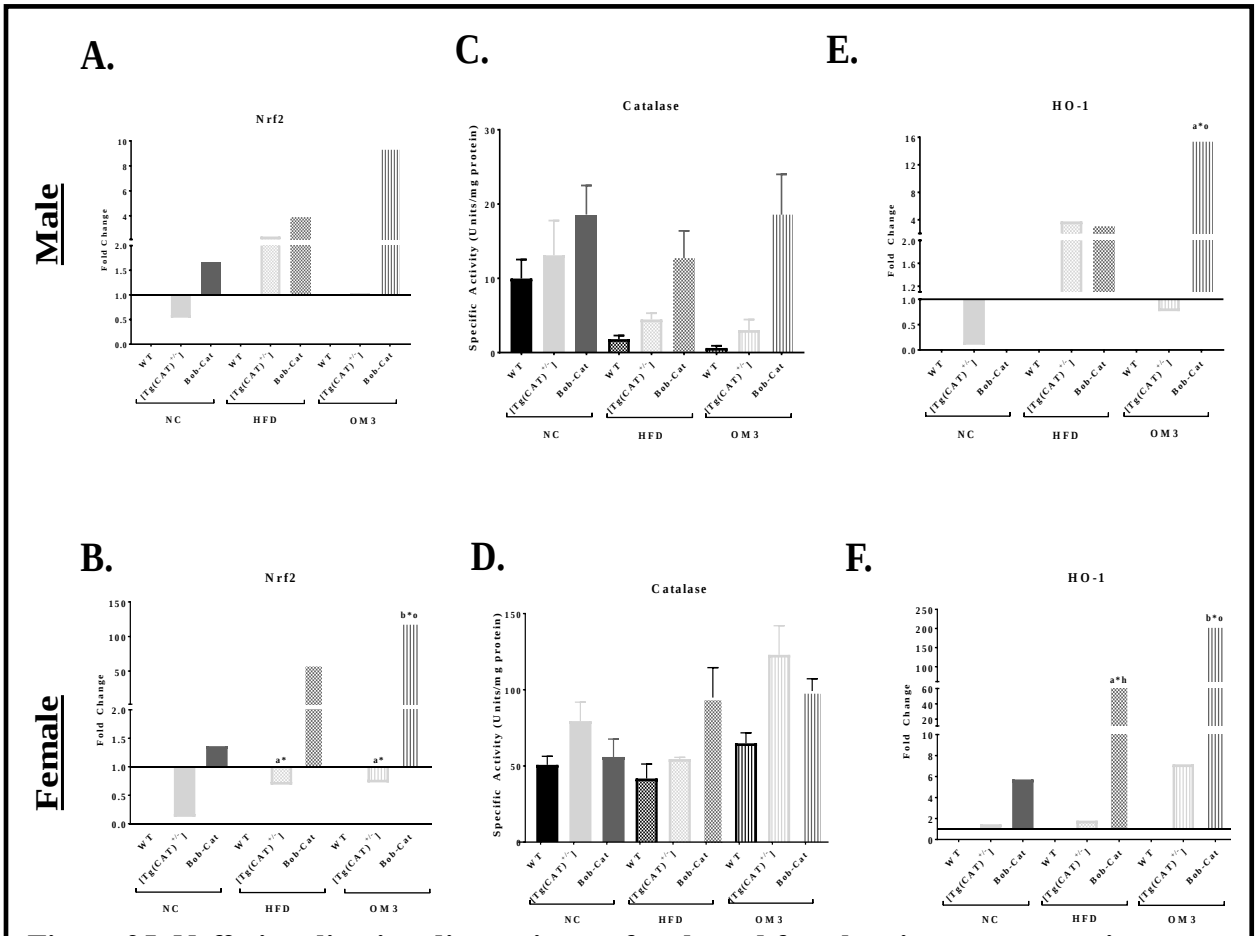

Figure 25. Nrf2 signaling in adipose tissue of male and female mice overexpressing catalase. Redox stress was evaluated in adipose tissue by measuring mRNA expression of Nrf2 (transcription factor and redox regulator), Catalase enzymatic activity and mRNA expression of HO-1 (downstream antioxidant targets of Nrf2): Male, A. and Female, B. Nrf2 mRNA expression level in the perigonadal adipose tissue measured by RT-qPCR. Male, C. and Female, D. Catalase specific activity (U/mg protein) was measured and data for Catalase activity is represented as mean ± S.E.M. of WT, [Tg(CAT)±], and Bob-Cat mice fed NC, HFD, and OM3 diet ($n\geq3$/group); Male, E. and Female F. HO-1 mRNA expression level in the perigonadal adipose tissue measured by RT-qPCR. mRNA expression is depicted as fold change compared to WT mice fed the same diet by ddCT method. One-way and two-way ANOVA was performed on GraphPad Prism 7. Letters indicate significant p values, a=$p<0.05$, b=$p<0.01$; symbols represent significant differences between genotypes * = compared to WT; an additional 'h' or 'o' represents comparison to HFD or OM3 fed WT mice respectively.

Both antioxidant catalase and HO-1 are downstream targets activated by Nrf2. Therefore, catalase activity and expression of HO-1 was measured in the adipose tissue of each mouse group (**Figure 25C-F**). Catalase activity was down-regulated in HFD and OM3 fed WT and [Tg(CAT)$^{\pm}$] male mice. However, activity levels remained 10 fold higher (not significant) in the Bob-Cat mice fed any diet, compared to the other two genotypes. Interestingly, the females expressed at least 5 fold increased catalase activity in all the genotypes compared to their male counterparts (**Figure 25C-D**). In addition, the mice overexpressing catalase trended to have higher levels of catalase activity compared to the WT mice. HO-1 mRNA expression was shown to be the highest in the male and female Bob-Cat mice groups (**Figure 25F-G**). Similar to the mRNA of its transcriptional activator, Nrf2, in males, the Bob-Cat mice showed a gradual increase in HO-1 induction when fed HFD (>3 fold) or OM3 (>15 fold, $p<0.05$) compared to the controls on the same respective diets. Similar trends were seen among the Bob-Cat female mice. An induction of HO-1 was observed in the Bob-Cat HFD group (>63 fold) and OM3 group (>208 fold) compared to WT controls fed the same diet. The induction of both catalase and HO-1 observed in the Bob-Cat male and female mice fed an OM3 diet provides evidence that Nrf2 had translocated to the nucleus and activated its downstream targets.

3.3.7.2 GPR120/FFAR4 expression

Our data thus far have shown that in general, mice overexpressing catalase fed OM3 diet in comparison to mice fed HFD or WT mice fed any of the diets, had lower body weight and fat mass, decreased energy consumption, and maintained normal glucose and insulin levels. However, sexual dimorphism was observed within some of the measured metabolic parameters. GPR120/FFAR4 is a lipid sensing, long chain fatty acid receptor highly expressed in adipose tissue and macrophages and is attributed to the beneficial anti-inflammatory and insulin

sensitizing effects of an OM3 diet (D. Y. Oh et al., 2010). Therefore, we investigated whether GPR120 was contributing to the alterations in metabolic parameters seen within the antioxidant overexpressing mice and to the observed sexual dimorphism. As shown in **Figure 26A&C**, the male [Tg(CAT)$^{\pm}$] mice had a lower expression of GPR120 at baseline (NC fed animals); however the levels increased 2-3 fold higher (not significant) than WT mice, when fed HFD or OM3 diets. In contrast, there was a gradual induction of GPR120 mRNA expression in Bob-Cat mouse groups when fed NC or HFD (>12 fold induction, $p<0.01$) and over 108 fold ($p<0.01$) when fed OM3 diet (**Figure 26A**). Western blotting of the protein expression of GPR120 showed a genotypic effect (**Figure 26B**) among the male groups ($p= 0.002$). It was intriguing that, regardless of the diet, Bob-Cat mouse groups had the highest levels of GPR120 protein expression.

In females, the [Tg(CAT)$^{\pm}$] group showed a slight decrease in GPR120 expression (**Figure 26D**) when fed HFD or OM3 ($p<0.05$), compared to the NC fed diet groups. In contrast, similar to the male mice, Bob-Cat female mice provided an OM3 diet had a significant increase ($p<0.05$) in GPR120 mRNA expression compared to WT mice. As indicated in **Figure 26 B&D**, Western blotting showed that the GPR120 protein level in the adipose tissue only had a trend towards increased expression in NC fed female mice overexpressing catalase ([Tg(CAT)$^{\pm}$] and Bob-Cat), whereas those fed HFD had a lower expression compared to their WT littermates. As

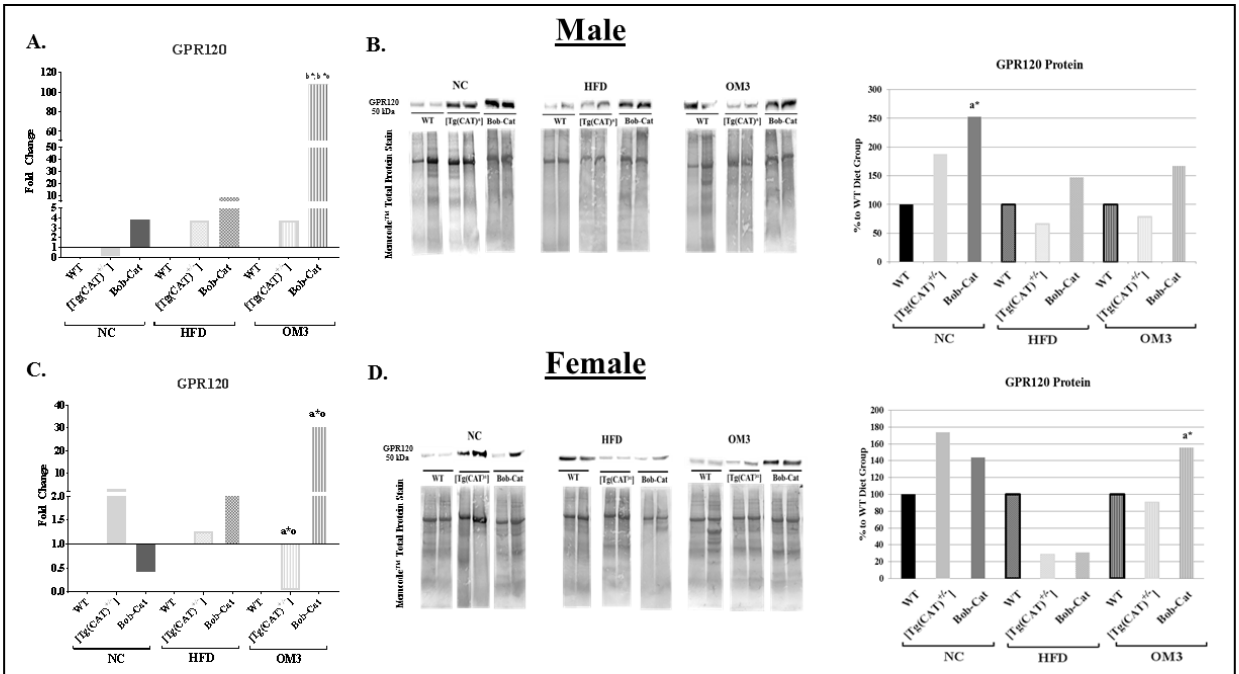

Figure 26. GPR120 mRNA and protein expression in adipose tissue of male and female mice overexpressing catalase. Male, A. and Female, C. GPR120 mRNA expression measured by RT-qPCR in the adipose tissue from WT, [Tg(CAT)±], and Bob-Cat mice fed NC, HFD, and OM3 diet depicted as fold change compared to WT mice fed the same diet by Pfaffl ΔΔCT method (n≥4 and 3/group respectively). Male, B. and Female, D. Western Blot of GPR120 protein in adipose tissue, shown as % densitometric ratio of Anti-GPR120 and total protein (memcode stain) per genotype to % ratio observed in WT mice fed similar diet (n≥4 and 3/group respectively). One-way and two-way ANOVA was performed on GraphPad Prism 7. Letters indicate significant p values: a=p<0.05, b=p<0.01; symbols represent significant differences between genotypes * = compared to WT; an additional 'o' represents comparison to OM3 fed WT.

seen in the males, OM3 fed Bob-Cat female mice also showed a significant increase ($p<0.05$) in GPR120 protein expression compared to NC fed WT mice.

3.3.7.3 Adipokine modulators of insulin sensitivity

Adipose tissue produces and secretes adipocytokines which play both an autocrine and paracrine role in metabolic pathways involving insulin sensitivity as well as in inflammation (Kern, Di Gregorio, Lu, Rassouli, & Ranganathan, 2003). Their levels can also be influenced by an OM3 rich diet (Bargut et al., 2016; Chopra, Siddhu, & Tandon, 2014) and redox status of the adipose tissue (D. L. Amos et al., 2017; Kern et al., 2003; Lawler et al., 2016; Marseglia et al.,

2014; Ruan, Zheng, Li, Wang, & Li, 2015). We first measured adiponectin, which alleviates insulin resistance by stimulating lipid oxidation and anti-inflammatory processes (Choe et al., 2016). As shown in **Figure 27A**, within male groups, we saw both a significant difference

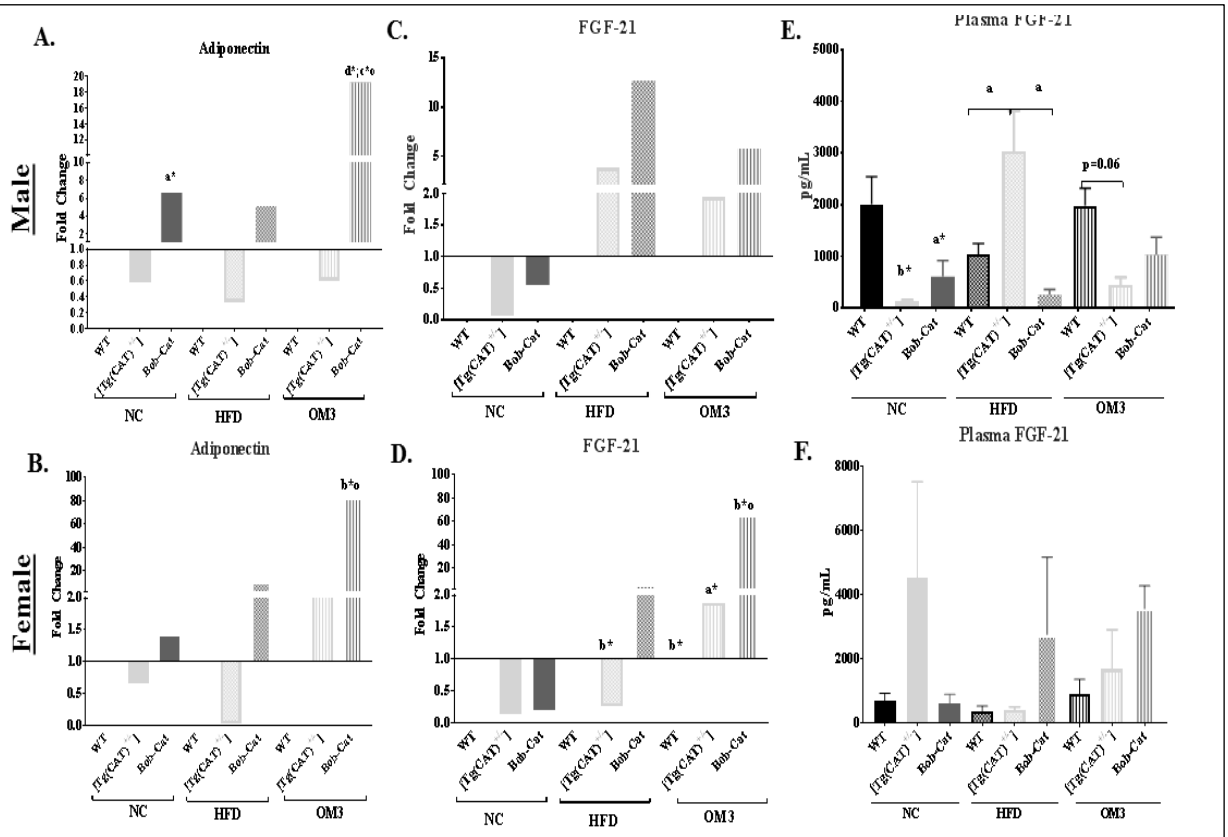

Figure 27. Adipose tissue mRNA expression and circulating levels of key adipokines determined in male and female mice overexpressing catalase. Male, A. and C. and Female, B. and D. of Adiponectin (n≥4/group) and FGF-21 (n≥4/group) respectively. Data depicted as fold change compared to WT mice fed the same respective diet using the Pfaffl ddCT method. Male, E. and Female, F. Circulating FGF-21 was measured using a mouse FGF21 ELISA kit according to manufacturer's protocol (n≥3/group). All analyses were measured in WT, [Tg(CAT)±], and Bob-Cat groups fed NC, HFD, and OM3 diet. One-way and two-way ANOVA was performed on GraphPad Prism 7. Data for serum FGF-21 levels are represented as mean ± S.E.M. Letters indicate significant p values: a=p<0.05, b=p<0.01, c=p<0.001, d=p<0.0001; symbols represent significant differences between genotypes * = compared to WT; an additional 'o' represents comparison to OM3 fed WT.

among the genotypes ($p<0.0001$) in addition to the diet ($p<0.05$). Bob-Cat mice provided a NC and OM3 rich diet had a >6 fold ($p<0.05$) and >19 fold ($p<0.001$) increase in adiponectin mRNA levels respectively, compared to the WT groups fed similar diets. All female Bob-Cat groups showed a trend to have the highest fold change (**Figure 27B**) in adiponectin expression

compared to the WT mouse groups fed the same diet, but similar to males, the most significant fold increase was within the OM3 fed Bob-Cat mouse group (>82 fold increase, $p<0.01$).

Adiponectin works in concert with Fibroblast Growth Factor 21 (FGF-21) (Hui et al., 2016), both an adipokine and hepatokine, with paracrine effects on adipose tissue (X. Lin, Liu, & Hu, 2017). It was most recently identified to be a stress response hormone (Gomez-Samano et al., 2017) in addition to its known beneficial function as a metabolic regulator of glucose and lipid homeostasis and insulin sensitivity (Z. Lin et al., 2013). Therefore, we investigated both the adipose mRNA expression and the plasma levels of FGF-21. Within the adipose tissue from male mice (**Figure 27C**), FGF-21 levels were not significantly different. However, there was a trend for mice overexpressing catalase on a NC diet to have a lower FGF-21 expression while littermates provided HFD or OM3 diet showed a >2 fold increase. The highest levels of FGF-21 within each diet group overexpressing catalase were within the HFD groups. Female mice showed similar results with the exception of the HFD fed [$Tg(CAT)^{\pm}$] group where there was a lower expression of FGF-21 in comparison to the NC ($p<0.05$) and HFD (not significant) fed WT mouse group. However, the most significant finding was that the OM3 fed Bob-Cat female mice had a >60 fold increase ($p<0.01$) compared to the WT group fed the same diet (**Figure 27D**). With FGF-21 also being secreted by liver, we used an ELISA kit to measure circulating levels of FGF-21. Within the male mouse groups, mice overexpressing catalase had significantly lower levels ($p<0.05$) than the NC WT mice as seen in **Figure 27E**. However, when provided HFD, [$Tg(CAT)^{\pm}$] had significantly higher levels ($p<0.05$) compared to every other mouse group provided HFD. Interestingly, Bob-Cat mice, regardless of the diet, showed a trend for having lower plasma FGF-21 levels than the WT mice of each respective diet group. Circulating levels of FGF-21 in female mouse groups were also measured **(Figure 27F**). Contrary to males, female

mice overexpressing catalase provided NC diet did not have significantly lower levels of circulating FGF-21 than their WT littermates. In fact, the NC fed [Tg(CAT)$^{\pm}$] had the highest levels of circulating FGF-21, which did not correlate with the mRNA expression of FGF-21 in the adipose tissue. Perhaps the liver was a major source of the circulating FGF-21. It was also surprising to find that when provided either high-fat diet (HFD or OM3) intervention, female Bob-Cat mice trended to have higher levels of plasma FGF-21 compared to their WT littermates.

3.4 DISCUSSION

Obesity and its comorbidities are characterized with increased levels of ROS that alter lipid and glucose homeostasis in key metabolic organs (Barazzoni, Gortan Cappellari, Ragni, & Nisoli, 2018; Carrier, 2017; Rani et al., 2016). This leads to increased body weight and fat mass thus increasing risk for hyperglycemia, hyperlipidemia, hyperleptinemia, systemic inflammation, and IR (Carrier, 2017). Both endogenous and exogenous antioxidant supplementation, known to mitigate the negative effects of redox stress, were shown to lower the levels of ROS in these metabolic diseases (Drummond, Selemidis, Griendling, & Sobey, 2011; Haidara et al., 2011; Park et al., 2016; B. Patel, Mann, & Chapple, 2018). Additionally, in both lean and obese rodent models, dietary interventions, such as those rich in OM3 fatty acids (including EPA and DHA) in contrast to saturated fatty acids (lard diet), also lowered body weight and fat mass, increased insulin sensitivity, and induced browning of white adipose tissue through anti-inflammatory actions (Bargut et al., 2016; Hirabara et al., 2013; Luo et al., 2016; D. Y. Oh et al., 2010). However, the mechanisms leading to these beneficial effects were not clearly defined. We recently showed that mice overexpressing catalase in a genetically obese background (Bob-Cat), in contrast to its wild-type littermates, significantly lowered redox stress (‘stress-less’ mice), improved energy metabolism, and altered the expression of key adipocytokines (D. L. Amos et al., 2017). The overexpression of catalase in this mouse model with a genetic obese background was implicated to be the key factor responsible for these effects. Therefore, these mice presented characteristics of an effective model to study the interaction between redox regulation and dietary intervention, on adipose tissue function and glucose and lipid signaling in a “diet-induced obesity” model. In the present study, eight weeks (chronic effect) of dietary intervention in the ‘stress-less’ mouse model overexpressing catalase, in comparison to their WT controls, showed

that the high-fat omega-3 enriched (OM3) diet, in contrast to the high-fat lard (HFD) diet, stabilized body weight and fat mass, maintained balanced energy metabolism and normal circadian rhythm, and sustained insulin sensitivity by regulating GPR120-Nrf2 cross-talk.

Administration of OM3 diet, in contrast to the HFD fed animals, for 8 weeks showed that mice overexpressing catalase (male and female Bob-Cats), maintained or lowered body weight and fat mass, similar to that observed in NC fed mice groups, despite a lower food intake (total g and kcal/g consumed) of chow provided ad libitum. Decreased food intake when fed HFD in comparison to a normal rodent diet has been reported in previous studies as the result of a higher caloric and satiating diet (Pendergast et al., 2013). These observations support the importance of the composition of a meal on fat accumulation and distribution during weight management/weight loss therapies in humans (Goss et al., 2013). This is of particular interest in obese subjects, where an excessive accumulation of visceral fat mass elevates the risk of numerous health conditions including coronary heart disease, IR, osteoarthritis, and hypertension (U. J. Jung & Choi, 2014), which further contributes to the 8 year reduction in life expectancy in these individuals (C. H. Jung et al., 2017; Muzumdar et al., 2008; Tzanetakou, Katsilambros, Benetos, Mikhailidis, & Perrea, 2012). In contrast, the increased life expectancy observed in studies conducted in catalase overexpressing mice (Schriner & Linford, 2006) may be attributed to the type of diet consumed.

Lean mass is representative of the muscle tissue mass equivalent of all the body parts containing water, excluding fat, bone minerals, and such substances which do not contribute to the NMR signal, such as hair, claws, etc. (ECHO-MRI (Houston, TX) user's manual). It was interesting that in the Bob-Cat male groups, we observed an increase in lean mass at 4 weeks and decrease at 8 weeks independent of diet. Other studies have shown similar fluctuations in lean

mass as the body begins to adapt to alterations in diet or food /caloric intake (V. P. Chen et al., 2016). At the 4 week time point, the body likely had not completely adjusted to the diet, however at around the 8 week time point, a complete response to the dietary intervention had occurred. In addition to lean mass, other studies have also seen similar fluctuations in bone mass and density (Weiss, Jordan, Frese, Albert, & Villareal, 2017). Nonetheless, it is unclear why only Bob-Cat male mice behaved as such compared to the other genotypes. One can only speculate that it might be a response to the differences in redox regulation in this novel mouse model.

CLAMS assessment of energy metabolism (energy intake vs. energy expenditure) showed differences between the genotypes tested on various diets. The three day CLAMS measurement of FI supported the earlier observation of lower weekly food intake by the HFD and OM3 fed groups despite the genotype (Pendergast et al., 2013). In addition, it was observed that HFD and OM3 feeding altered the eating patterns (circadian rhythm) in WT mice compared to those fed NC. This is consistent with other studies that showed HFD feeding alters the quantity, time of day, and how much chow is consumed during each visit to the food hopper (Marvyn, Bradley, Mardian, Marks, & Duncan, 2016; Sasaki, 2017; M. So, Gaidhu, Maghdoori, & Ceddia, 2011). However, this diet effect (HFD or OM3) on eating patterns was not altered in either gender of the [Tg(CAT)$^{\pm}$] and Bob-Cat mice, which followed similar circadian rhythm patterns of eating as that seen in mice provided NC diet. This observation suggested that catalase overexpression (i.e. redox balance) may be shifting the paradigm of a high-fat diet altering circadian rhythm and patterns of food intake. This speculation is further supported by our previously published observations where the secretion of key adipokines that modulate hypothalamic appetite regulation was altered in mice overexpressing catalase (D. L. Amos et al., 2017).

In addition to measurement of FI, the CLAMS analysis also provided insights into the differences in RER and EE in the various genotypes and diet interventions. We observed a significant increase in RER as well as CHO oxidation (hence lower fat oxidation) in the NC fed male mice overexpressing catalase compared to their WT groups fed NC. This might be attributed to the increased expression of human catalase gene, since other studies have shown changes in energy metabolism as a result of increased antioxidant catalase (D. L. Amos et al., 2017; Heit et al., 2017) in addition to alterations in substrate utilization as a result of differences in genetics (Albarado et al., 2004). In contrast, all groups on a high-fat diet intervention (lard or fish oil), had a lower RER and levels of CHO oxidation (higher fat oxidation) which has been reported in numerous other studies as a result of higher fat % available to be oxidized from the HFD provided to the animals (Church et al., 2009; Hatori et al., 2012; Nilsson et al., 2016). The ability of OM3 diet to lower the RER and increase fat oxidation within the male mice groups overexpressing catalase and female Bob-Cats vs the Bob-Cat mice fed NC may have contributed to the observed decrease in their body weights compared to their littermates that overexpress catalase fed NC or HFD. On the contrary, male mice overexpressing catalase provided an OM3 diet, had significantly lower fat oxidation compared to WT mice provided a NC diet. This may be a beneficial outcome from the intake of OM3 fatty acids termed “metabolic flexibility”; a newer concept describing the body’s ability to match fuel oxidation to fuel availability (Carstens et al., 2013). We believe this may have been acquired in our mouse model through intake of the OM3 diet during the 8 week study period. Another plausible reason for the lower levels of fat oxidation observed may be due to “altered metabolic partitioning” of fatty acids where there is a reduction in oxidation and increased re-esterification of particular fatty acids dependent on their structure (Forbes et al., 2006). This would also provide reasoning as to why the same effect was

not seen in the HFD fed mice overexpressing catalase. In comparison to males, fat oxidation trended to be elevated in females (kcal/h/g) even though all were provided the same type of diet and the quantity consumed by females was not higher than what was consumed by males. Even more interesting was the opposite effects of CHO vs. fat oxidation seen in male and female Bob-Cat mouse groups provided an OM3 diet. We believe this was a result of sexual dimorphism (X. Wang, Magkos, & Mittendorfer, 2011).

All HFD fed groups in our study, having significantly higher levels of EE (heat production) is consistent with previous studies (Leibel, Rosenbaum, & Hirsch, 1995), where a significant increase in EE was observed within just one week of HFD feeding (M. So et al., 2011). It is hypothesized that this phenomenon is due to the increased body mass and amount of oxygen necessary to facilitate normal cellular/tissue function in addition to higher energy required to catabolize the 45% high-fat diet vs. the 13.4% fat in the NC diet. However, the increase in EE of the HFD groups is not sufficient to create energy balance resulting in an accumulation of body weight and fat mass. Though calorically (45% fat) similar to the HFD, EE levels in OM3 fed mice remained intermediate to NC and HFD fed mice, yet EE levels were still significantly higher than the NC fed WT group. Previous studies have also shown an OM3 rich diet increases EE levels by enhancing thermogenesis via activating GPR120 (Bargut et al., 2016; Quesada-Lopez et al., 2016). Male [Tg(CAT)$^{\pm}$] and Bob-Cat mice also displayed significantly higher activity (XAMB) levels compared to WT mice fed NC or high-fat (HFD or OM3) diets. Furthermore, when provided HFD or OM3 diet, the WT mice had the lowest activity levels, not reaching above 3000 counts per two hours. These results indicate that overexpression of catalase might be increasing the activity levels within the male gender. Previous reports have suggested that in rodent models, a high caloric diet can decrease XAMB counts of physical activity by up

to 28% (M. So et al., 2011). It is also possible that the increased body weight and fat mass may have been a secondary factor in the hypo-activity. Interestingly, the effect was not as severe in groups overexpressing catalase; again, an indication of the beneficial effect of antioxidant overexpression coupled with an OM3 diet. This is of great importance since research in human obesity studies has shown that HFD promotes a more sedentary, less physically active lifestyle in addition to alterations in sleep/wake cycles (Branecky, Niswender, & Pendergast, 2015). Alterations in redox balance (as seen within the catalase overexpressing mice), such as by OM3 dietary interventions, might improve metabolic imbalance and circadian rhythm abnormalities in obese humans.

Eight weeks of dietary intervention altered the circulating metabolic profile in the catalase overexpressing mice. As seen in other studies, and expected with increased fat mass, mice fed a HFD had the highest levels of TC (L. Wu & Parhofer, 2014). The only exception was the female [Tg(CAT)$^{\pm}$] mice fed HFD which had similar TC levels to all mouse groups fed NC and OM3 diet. This female group also had significantly higher levels of activity (XAMB counts) which might have influenced the lowering of cholesterol levels (Meissner et al., 2010). In contrast to the HFD, and as previously documented (Tani et al., 2018), mice provided an OM3 diet did not alter TC and the levels remained similar to that seen in NC fed mice groups. HDL levels were highest among the groups fed HFD in both genders, but among OM3 fed mice, there was a higher ratio of HDL:TC compared to the HFD groups. Furthermore, among the OM3 fed mice groups, Bob-Cat males and females had the highest levels of HDL making their HDL:TC ratio the highest among all mice groups thus showing the significance of the regulatory interaction between overexpression of antioxidant catalase and feeding OM3 diet on lipid profile. There have been previous studies conducted in the leptin deficient Ob/Ob mice (parent group of

the Bob-Cat mouse model) showing increases in HDL level (Nishina, Lowe, Wang, & Paigen, 1994; Silver, Jiang, & Tall, 1999). It has been postulated that although typically in human obesity HDL levels are substantially lower, the decrease in functional leptin in the obese Ob/Ob mice may be playing a role in the higher HDL (being the major lipoprotein in rodents) levels (Silver et al., 1999). Since Bob-Cats are heterozygous for the Ob gene, it is plausible that leptin is playing a role in modulating HDL levels. Surprisingly, male Bob-Cats had the highest TG levels. A similar effect, although to a lower degree, was also seen in the NC and OM3 fed female Bob-Cats and the other female genotypes on similar diet. In general, the mice provided OM3 diet had lower plasma TG levels, which was expected as the result of a higher intake of OM3 fatty acids (Bargut et al., 2016; Yeop Han et al., 2010). Bob-Cat mice, compared to the other genotypes, also had increased levels of plasma ketones in all groups (except the HFD males), and those provided an OM3 diet had the highest ketone levels independent of gender. Generally, high ketone levels are classically associated with metabolic dysfunction and diabetes (Alberti, 1975; Beylot, Sautot, Laville, & Cohen, 1988; Mahendran et al., 2013; P. Yan, Cheah, Thai, & Yeo, 1983), but more recent studies have shown that lower carbohydrate diets provoking ketosis cause an inverse correlation between circulating ketones and plasma glucose levels, thus suggesting higher levels of ketones are associated with more favorable effects on glycemic control (Paoli, Rubini, Volek, & Grimaldi, 2013). Other studies have now recognized ketones as imperative signaling molecules promoting metabolic function and regulating appetite (Newman & Verdin, 2014; Puchalska & Crawford, 2017). These studies further solidify the beneficial effects of an OM3 diet coupled with antioxidant catalase overexpression on metabolic parameters.

Consistent with other studies on the metabolic effects of an OM3 enriched diet (D. Y. Oh et al., 2010; Paniagua, 2016; Sundstrom et al., 2017), irrespective of gender, the lowest glucose

levels were seen in the Bob-Cat groups fed OM3 diet. Sexual dimorphism was observed in insulin levels. The highest average levels were in the HFD fed [Tg(CAT)$^{\pm}$] males, while the HFD [Tg(CAT)$^{\pm}$] females had the overall lowest levels of plasma insulin. The same results were reflected in the HOMA-IR. Furthermore, males in general had higher levels of insulin than females regardless of diet or genotype. This could be a direct effect of the increased visceral adipose tissue and liver weights in males compared to females (Snel et al., 2012). Insulin levels are key in the metabolic function of the liver (Sheng et al., 2018), so it was interesting that the males had an increase in liver weight, but not the females, as well as NC and HFD fed [Tg(CAT)$^{\pm}$] mice groups compared to WT littermates. Despite increases in insulin, plasma ketone levels showed no significant differences in male HFD fed [Tg(CAT)$^{\pm}$] mice compared to the WT mice fed HFD. In fact, ketone levels were >2 fold in the WT vs [Tg(CAT)$^{\pm}$] HFD group indicating insulin is repressing ketone body production in the [Tg(CAT)$^{\pm}$] mice (Meidenbauer, Ta, & Seyfried, 2014; Newman & Verdin, 2014). Nevertheless, most importantly, Bob-Cat mice fed an OM3 rich diet maintained glucose and insulin homeostasis throughout the duration of the 8 week study. Mechanistically, this result was expected to occur in part by the production of OM3-derived inflammatory resolution mediators (Cipollina, 2015), the higher ketones generated, "metabolic flexibility (Carstens et al., 2013)," and potential alterations in "metabolic partitioning" (Forbes et al., 2006) (indicated by the CLAMS fat oxidation analysis) in the Bob-Cat mice. However, in addition to these effects, the major contributor to the favorable metabolic profile of the Bob-Cat mice fed OM3 diet is through the activation of its receptor, GPR120 (Ichimura, Hasegawa, Kasubuchi, & Kimura, 2014; Miyamoto et al., 2016; D. Y. Oh et al., 2010).

GPR120 (FFAR4) is a long-chain fatty acid receptor highly expressed in adipose tissue (D. Y. Oh et al., 2010) and activated by OM3 fatty acids (Imamura, 2010; D. Y. Oh et al., 2010; Oliveira et al., 2015; Quesada-Lopez et al., 2016). It plays beneficial roles in anti-inflammatory pathways in adipose tissue, food preference, glucose homeostasis, and insulin sensitivity, all of which are interrelated to regulate metabolic energy homeostasis in both physiological and pathophysiological conditions (Ichimura, Hara, & Hirasawa, 2014). Though there are contradicting reports of GPR120 not required for these beneficial effects of OM3 fatty acids (Paerregaard et al., 2016), the support for its role in OM3 mediated effects stems from genetic studies performed in humans. The human studies showed that mutations in GPR120 were associated with increased risk of obesity and IR (Ichimura, Hasegawa, et al., 2014). GPR120 is also a novel risk factor for DIO (Ichimura et al., 2012; D. Y. Oh et al., 2010). For these reasons, it was most compelling that within the OM3 fed Bob-Cat mouse group, which overexpresses antioxidant catalase within an obese parent background, we observed the highest levels of both mRNA and protein expression of GPR120 in the perigonadal adipose tissue. Based on our measurements of redox stress markers, the OM3 fed Bob-Cat mice also had an increased level of oxidized carbonyl groups within the adipose tissue. Together, this might suggest that redox regulation is playing a role in the upregulation of GPR120 expression and beneficial outcomes of the OM3 diet within the antioxidant-overexpressing mice of both genders. Redox regulation of GPR120 has not been previously shown.

Furthermore, Nuclear factor erythroid-2-related factor 2 (Nrf2) is a redox sensitive transcription factor activated by long chain fatty acids (including EPA and DHA), phenolic antioxidants, and imbalances in redox stress (Cipollina, 2015; Uruno, Yagishita, & Yamamoto, 2015). Raising levels of Nrf2 by endogenous production of electrophilic products or

pharmacological agents has been shown to prevent or act as therapy for type 2 diabetes, metabolic syndrome, obesity, and cardiovascular disease through activating anti-inflammatory pathways (Jimenez-Osorio, Gonzalez-Reyes, & Pedraza-Chaverri, 2015; Pall & Levine, 2015; Seo & Lee, 2013; Silva-Palacios, Konigsberg, & Zazueta, 2016; Tarantini et al., 2018) in addition to lowering body weight and fat mass (Valenzuela et al., 2012). Specifically, in the Bob-Cat mouse groups, when fed a diet high in OM3 fatty acids, there were higher levels of adipose tissue Nrf2 mRNA expression. We speculate this to have occurred as a result of the synergistic effect of antioxidant overexpression and consumption of an OM3 rich diet. Studies concentrated on the beneficial effects of polyunsaturated fatty acids (primarily EPA and DHA) have shown that their oxidized derivatives regulate the redox environment by covalently and reversibly reacting with nucleophilic residues on target proteins (Cipollina, 2015; Nanthirudjanar, Furumoto, Hirata, & Sugawara, 2013). These reactions trigger the activation of cytoprotective pathways, including the Nrf2 antioxidant response (Gao et al., 2007). Nrf2 activation subsequently causes an upregulation of phase II enzymes/antioxidants thus balancing oxidant: antioxidant ratios in addition to suppressing the NF-κB proinflammatory pathway (Cipollina, 2015). Both antioxidant catalase and HO-1 are two of the key antioxidants upregulated in response to induction of Nrf2 (J. Chen et al., 2014; S. E. Lee et al., 2015; Zhu et al., 2008). In our model, the Bob-Cat mouse group fed OM3 diet had the highest levels of catalase activity in addition to mRNA expression of HO-1, providing further evidence of Nrf2 induction and subsequent activation of the antioxidant and cytoprotective response.

With the administration of OM3 fatty acids, it has previously been shown that the activation of GPR120 is linked to the secretion and circulating levels of the adipokine adiponectin (Yamada et al., 2017) promoting anti-inflammation (downregulation of NF-κB) and

insulin sensitivity (Itoh et al., 2007). Interestingly, Nrf2 also decreases inflammation through the same pathway as GPR120 (Cipollina, 2015; Matzinger, Fischhuber, & Heiss, 2018), but no previous study has shown the cross-talk between GPR-120 and Nrf2. In the Bob-Cat mice fed OM3 diet, we saw a significant increase in adiponectin mRNA expression within the adipose tissue. The combined results of high expression of GPR-120, Nrf2 (and its downstream signaling-activation of catalase and HO-1) provide evidence for a potential cross-talk between activation of GPR120 and Nrf2 synergistically decreasing inflammation within the adipose tissue as well as modulating whole body metabolism in the Bob-Cat mice. Although Nrf2 has been studied in depth in the brain (Q. Liu et al., 2014; Zgorzynska et al., 2017) and heart (J. Chen et al., 2014; S. E. Lee et al., 2015), because of its cytoprotective and anti-inflammatory benefits, we provide evidence for a similar role in adipose tissue. Furthermore, as observed from our current findings from our novel mouse model fed OM3 diet, we believe there is an interaction between Nrf2, GPR120, and adiponectin which could potentially give rise to new therapies in obesity, if its induction could aid in mediating energy homeostasis through adipokine expression and secretion.

Another metabolic regulator that is induced by both GPR120 and NRf2 is FGF21 (Furusawa, Uruno, Yagishita, Higashi, & Yamamoto, 2014; Quesada-Lopez et al., 2016). In the current study, male mice overexpressing catalase trended to have increased FGF-21 mRNA expression compared to WT diet group controls, but the highest expression was in the HFD groups. Similar elevations in FGF-21 have been shown in studies investigating obese humans and rodent models (Gomez-Samano et al., 2017; Tanajak, Pongkan, Chattipakorn, & Chattipakorn, 2018; X. Zhang et al., 2008). Contrary to males, in female mice, the highest mRNA expression was within the OM3 fed groups, and mainly in Bob-Cat mice. Additionally,

we observed plasma levels in female [Tg(CAT)$^{\pm}$] and Bob-Cat mice fed HFD had opposite effects compared to males, yet, the FGF-21 levels were similarly increased when fed OM3 diet. However, there are conflicting reports on the regulation of FGF-21 by redox stress/Nrf2 activation (Chartoumpekis et al., 2011; Furusawa et al., 2014; Yu et al., 2016; L. Zhang, Dasuri, Fernandez-Kim, Bruce-Keller, & Keller, 2016) or whether increased FGF-21 is actually metabolically beneficial.

It is of special importance to discuss the sexual dimorphism observed in the results of this study within the Bob-Cat mouse groups. With gender differences in sex hormones (i.e. estrogen vs. testosterone), distribution of fat pads, and the role of epigenetics, it is essential to study both male and female genders to fully define energy–related metabolic signaling pathways (B. F. Palmer & Clegg, 2015; M. Yoon et al., 2002). Additionally, to our knowledge, no study has investigated the gender differences of supplementation of OM3 fatty acids in relation to redox homeostasis, making the findings of the sexual dimorphism in the 'stress-less' model truly novel. **Figure 28** provides a schematic overview of the sexual dimorphism observed within the Bob-Cat mice fed an OM3 enriched diet related to GPR120-Nrf2 crosstalk. As seen in humans (X. Wang et al., 2011), we also observed higher plasma TG levels in the Bob-Cat mice fed OM3 diet. Furthermore, males had significantly higher levels of plasma TG when provided an OM3 diet compared to their WT littermates provided the same diet. Female Bob-Cat mice, in contrast, trended to have lower levels compared to the female WT control group. This is of importance since clinical vintrials show that in comparison to women, men have significantly lower levels of plasma total lipids/phospholipids of α-linoleic acid (ALA) and DHA in addition to less potent metabolic effects of the OM3 fatty acids EPA and DHA in decreasing risk for IR (Abbott et al., 2016). Plasma analysis of FGF-21 showed that Bob-Cat males have lower levels compared to

WT controls and the opposite was seen within females. This is most intriguing due to recent studies showing that FGF-21 lowers TG levels within both human and rodent models (Schlein et al., 2016). Additionally, CLAMS analysis revealed that RER and CHO/fat oxidation in females trended to be higher compared to males regardless of the diet or genotype. In particular, we saw significant gender differences within the Bob-Cat mice. When fed OM3 diet, Bob-Cat males had much higher levels of RER/CHO oxidation and lower levels of fat oxidation compared to the WT mouse group. However, in females, Bob-Cats fed OM3 diet had lower RER/CHO oxidation and higher levels of fat oxidation. Previous reports have shown that males and females differ in how they process polyunsaturated fatty acids (Abbott et al., 2016) and that females retain higher levels of PUFA in circulation (Walker et al., 2014). Additionally, the differences in oxidized substrates could also potentially play a role in modulating the circulating TG and FGF-21 levels providing an explanation for why we saw differences between the genders of the Bob-Cat mice.

Therefore, overall, among the many similarities (as seen in **Figure 28**), we have shown differences in TG, FGF-21 levels, and oxidation of CHO/Fat between the Bob-Cat male and female mice. Because the same general phenotypic results occurred (body weight, fat mass, lean

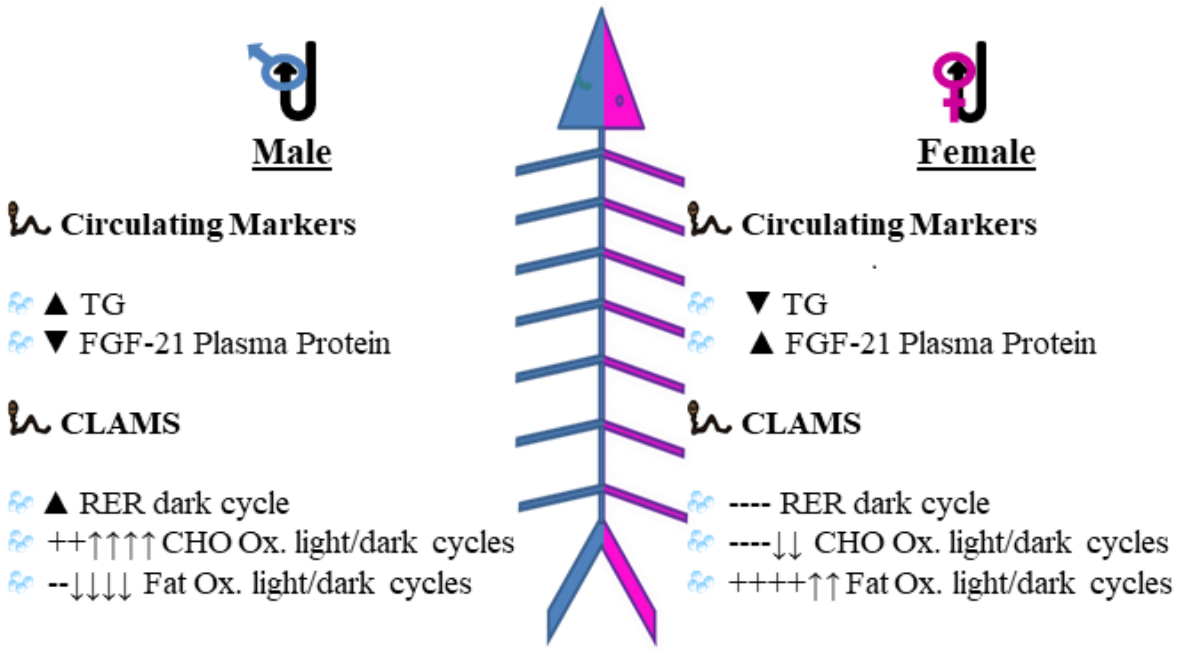

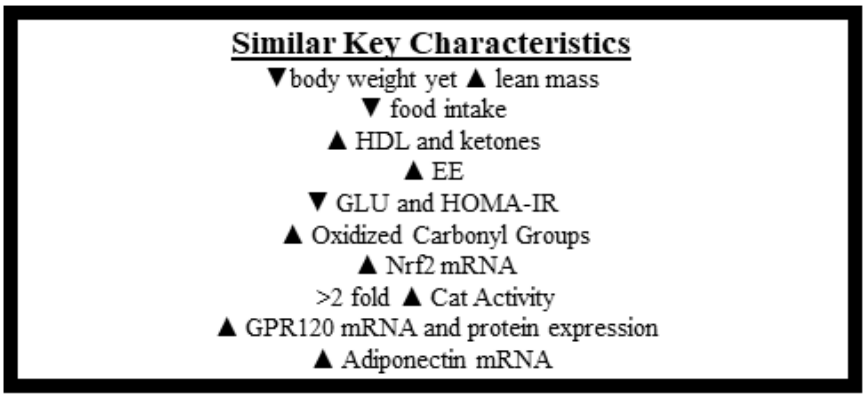

Figure 28. Sexual dimorphism observed in an OM3 fed 'stress-less' mouse model. Schematic representation of the sexual dimorphism observed in the 'stress-less' mouse model; Bob-Cat mice fed a diet enriched with OM3 fatty acids. These mice, when fed OM3 enriched diet, showed significant differences in circulating markers and CLAMS analysis of substrate oxidation. However, these differences did not impact the GPR120/Nrf2 crosstalk and downstream effects within this mouse model. Significance to WT mice fed NC and OM3 depicted as increase: +, ↑ while decrease: -, ↓ respectively. p values are represented as $p<0.01$ ++, ↑↑, $p<0.0001$ ++++, ↑↑↑↑ and likewise for a significant decrease.

mass, etc.) in both groups fed OM3 diet, we believe that the overexpression of catalase and increase in OM3 fatty acids have synergistically enhanced the Bob-Cat mouse group's ability to regulate energy metabolism in using different signaling pathways. Future studies investigating additional metabolic tissues such as the liver and skeletal muscle would help elucidate the mechanisms involved in the sexual dimorphism observed in the Bob-Cat mouse models.

3.5 CONCLUSION

Overall, this study provides compelling evidence that overexpression of catalase coupled with an enriched diet of OM3 fatty acids are metabolically beneficial. This combination was shown to increase adipose tissue expression of the GPR120/FFAR4, which by interacting with the Nrf2 pathway, resulted in decreased body weight and fat mass, enhanced or maintenance of a normal circadian rhythm, anti-inflammation and insulin sensitivity, and regulation of key adipokines compared to HFD fed mice (**Figure 15: Graphical Abstract**). In fact, to our knowledge, this is the first study to provide evidence that GPR120 expression may be modulated by redox status in addition to providing evidence of the GPR120-Nrf2 cross-talk mechanism. With the beneficial outcomes seen within the 'stress-less' Bob-Cat mouse model provided an OM3 diet, we believe that this model is an excellent tool to further study adipose tissue function, crosstalk with other metabolic tissues, and metabolic signaling pathways involving energy homeostasis in both male and female mice. Also, in addition to obesity, inflammation in adipose tissue has been linked to a number of types of carcinogenesis (Lengyel, Makowski, DiGiovanni, & Kolonin, 2018) and cardiovascular events. (Figueroa et al., 2016; Ghantous, Azrak, Hanache, Abou-Kheir, & Zeidan, 2015; Luna-Luna et al., 2015). Thus, using the 'stress-less' mice as a novel model, future studies may be conducted to look at the combination of antioxidant overexpression and other therapies for diseases of metabolic syndrome as well as lowering the risk and progression of the metabolic syndrome-associated cancers and CVD.

3.6 ACKNOWLEDGEMENTS

The authors acknowledge Dr. Jung Han Kim for her assistance with ECHO-MRI and CLAMS studies as well as Logan Efaw, Melissa Massie, Aaron Roberts, Jonique George and Sarah Marshall for their assistance with the feeding studies, quantitative PCR and Western Blotting. This study was partially supported by NIH Grant 5R01HL-074239 (NS), 5P20RR016477 (NS), 1R15AG051062-01 (NS), and WV-NASA Grant Consortium (DA).

CHAPTER IV: EXERCISE MODULATES METABOLIC TISSUE FUNCTION AND SHIFTS THE GUT MICROBIOME IN A NOVEL 'STRESS-LESS' MOUSE MODEL

A manuscript to be submitted after dissertation approval by the Committee Chair and Members.

Deborah Amos[1], Regina Lamendella[2], Justin Wright[2], Nalini Santanam[1]*

[1]Department of Biomedical Sciences, Joan C. Edwards School of Medicine, Marshall University, 1700 3rd Ave, Huntington, WV 25755-0001, United States

[2]Department of Biology, Juniata College, 601 17th Street, Huntingdon, PA 16652, United States

*Correspondence to: Nalini Santanam, PhD, MPH, FAHA, Professor, Department of Biomedical Sciences, Joan C. Edwards School of Medicine, Marshall University, 1700 3rd Ave, 435S BBSC, Huntington, WV 25755, USA. Tel: +1-(304) 696-7321; Fax: +1-(304) 696-7391, santanam@marshall.edu

ABSTRACT

Obesity, a result of excess fat accumulation, disrupted energy metabolism, and imbalance in oxidant: antioxidant ratio is now considered a chronic disease with no appropriate treatment. The need to counteract obesity is of great importance due to its contribution to the progression of cardiometabolic disease, chronic inflammation, neurological disorders, and cancer. Lifestyle modification, such as exercise, decreases risk for obesity by reducing fat mass, lowering redox stress, modifying metabolic tissue function, and regulating energy homeostasis (appetite and energy expenditure). Current studies show the gut microbiome's diversity and function play a key endocrine role in host energy metabolism, where the diversity can be altered dependent on physical activity level/intensity as well as redox stress. During prolonged exercise, Type 1 / Type 2 fiber type ratio increases and contracting skeletal muscle secretes "exercise-induced" myokines (i.e. FGF-21, PGC1-alpha). Although the current literature suggests physical activity regulates energy metabolism by altering myokine and adipokines levels, it is unknown how redox modulated changes in the gut microbiota is involved in these interactions. We tested this hypothesis by subjecting a novel stress-less obese mouse model (Bob-Cat) to eight weeks of moderate exercise. Changes in the diversity of the gut microbiome due to exercise in these mice were correlated to improvements in energy metabolism and skeletal muscle-adipose tissue-brain crosstalk. We observed that when subjected to a moderate, 8 week treadmill exercise regimen, mice overexpressing catalase ([Tg(CAT)$^{\pm}$] and Bob-Cat), had lowered body weight and fat mass (ECHO-MRI) and a healthier overall blood/lipid profile compared to sedentary controls. Additionally, we observed an increase in Type 1 / Type 2 fiber ratio in association with an induction of key myokines (FGF-21, PGC1-alpha, and FNDC5) in the exercised mice overexpressing antioxidant vs. sedentary controls. There was also a concomitant induction in

expression of adiponectin ($p<0.05$) in the adipose tissue and alterations in hypothalamic genes that regulate appetite (NPY and POMC). Our key finding was a significant shift in microbial diversity in all exercise mice groups and in particular in mice overexpressing catalase. Our results thus far suggest a synergistic effect of exercise and catalase overexpression on the diversity of the gut microbiome which results in improving overall energy metabolism via promoting skeletal muscle-adipose-brain cross-talk.

4.1 INTRODUCTION

Obesity is now a worldwide epidemic with more than 35% of adults classified as obese and rates expected to rise to 42% by 2030 (Organization, 2018). This is of great concern considering that obesity leads to other serious, life-threatening health conditions such as cardiometabolic diseases, which has the world's highest morbidity and mortality rate (Organization, 2018), responsible for more than 15.2 deaths per year (Writing Group et al., 2016). Furthermore, there are no universally effective treatments currently available for obesity.

It is well known that the expansion of visceral adipose tissue is a major risk factor for obesity and its comorbidities (Golbidi & Laher, 2014). Increased adipose mass also contributes to pro-oxidant and pro-inflammatory states by increasing free radical production (Fernandez-Sanchez et al., 2011). Reactive oxygen species (ROS) alters glucose and lipid metabolism by modulating the functions of skeletal muscle, adipose tissue, brain, and the newly classified "endocrine organ," the gut microbiome, all leading to overall changes in energy homeostasis (Alleman, Katunga, Nelson, Brown, & Anderson, 2014; Fernandez-Navarro et al., 2017; Fernandez-Sanchez et al., 2011; Gyengesi, Paxinos, & Andrews, 2012; Manna & Jain, 2015). Physical activity has been proven time and again to be the most efficacious approach and recommended therapeutic option for individuals with metabolic disorders due to its weight loss effects (Golbidi & Laher, 2014; Leal et al., 2018; Savini et al., 2013). Not only is it an effective way to lower body weight and fat mass (Fiuza-Luces et al., 2013; Golbidi et al., 2012), improve lipid profile (Sanchis-Gomar et al., 2015; Vina et al., 2012), decrease inflammation (Golbidi & Laher, 2014), boost physical performance (Vina et al., 2012), and enhance neurological function (Radak et al., 2013), it also paradoxically is beneficial by increasing redox stress which in turn induces antioxidant synthesis (Done & Traustadottir, 2016; Gomez-Cabrera, Domenech, & Vina,

2008; Ji, 2008; Savini et al., 2013; Shern-Brewer, Santanam, Wetzstein, White-Welkley, & Parthasarathy, 1998).

Research has shown that increased skeletal muscle contraction during aerobic physical activity shifts the muscle fiber-type ratio toward higher levels of Type 1 vs. Type 2 fibers (Fry et al., 2017; Y. X. Wang et al., 2004) as well as production and secretion of key myokines involved in metabolic homeostasis (Febbraio & Pedersen, 2005; Hoffmann & Weigert, 2017; Huh, 2018). Similarly, in adipose tissue, moderate exercise regulates the expression and secretion of key adipokines such as leptin and adiponectin (Golbidi & Laher, 2014; Lubkowska, Dudzinska, Bryczkowska, & Dolegowska, 2015) that are involved in regulating energy storage, energy expenditure, and appetite regulation (Bluher & Mantzoros, 2015; K. J. Oh et al., 2016).

Located within the hypothalamus of the brain are orexigenic and anorexigenic signaling pathways that primarily control satiety. The orexigenic pathway contains neurons that co-express Neuropeptide Y (NPY) and Agouti Related Peptide (AGRP), which lower satiety and energy expenditure. On the contrary, the anorexigenic pathway contains neurons that express Proopiomelanocortin (POMC) and Cocaine-Amphetamine Related Transcript (CART), which suppress appetite and increase energy expenditure (Burke et al., 2016; Wilson & Enriori, 2015). It is now known that both exercise-induced myokines, adipokines, and several secreted metabolites affect appetite regulation and energy expenditure (Benite-Ribeiro, Putt, & Santos, 2016; Delezie & Handschin, 2018; Gorgens, Eckardt, Jensen, Drevon, & Eckel, 2015; Leal et al., 2018; A. Rodriguez, Becerril, Ezquerro, Mendez-Gimenez, & Fruhbeck, 2017; A. Rodriguez et al., 2015). Although we now understand some of the underlying pathways involved in the metabolic benefits of regular physical activity, there are still gaps in knowledge in reference to

how exercise is involved in metabolic tissue crosstalk (skeletal muscle-adipose-brain) and regulation of energy metabolism.

Recent studies suggest there is a possible association between the microorganisms residing within the gut and the beneficial effects of exercise (Allen et al., 2015; Zhao et al., 2018). Although studies have shown the skeletal muscle-adipose axis (Leal et al., 2018; F. Li et al., 2017; A. Rodriguez et al., 2017), adipose-brain axis (J. Friedman, 2016; Seoane-Collazo et al., 2015; Spiegelman & Flier, 2001; Wilson & Enriori, 2015), and skeletal muscle-brain axis (Delezie & Handschin, 2018; Huh, 2018; Pedersen & Febbraio, 2012) are all involved in improving energy homeostasis, it is not yet fully investigated if gut microbes communicate with these metabolic organs, if gut-derived metabolites are involved in these interactions (Kallus & Brandt, 2012; Nehra, Allen, Mailing, Kashyap, & Woods, 2016), or how exercise and/or redox stress modulate these interactions (Allen et al., 2015; Allen et al., 2018).

We recently developed a novel obese mouse model overexpressing the antioxidant catalase (Bob-Cat) which by lowering redox stress improved overall energy metabolism (D. L. Amos et al., 2017). We additionally showed that this mouse model potentiated the beneficial effects of an omega 3 enriched fatty acid diet by inducing GPR120-Nrf2 crosstalk (D. Amos, Cook, & Santanam, 2019). Very little is known at the current time about the relationship between redox stress and the diversity and function of the microbiome, but it is evident that specific species of bacteria use ROS as defense mechanisms and others can produce antioxidants that scavenge free radicals. Additionally, some studies suggest that the gut microbiome can be altered dependent on the redox state (Borrelli et al., 2018; Staerck et al., 2017; Y. Wang et al., 2017). Therefore, in order to better understand the interplay between redox regulation and exercise intervention on the gut microbiome and its potential effects in improving energy homeostasis, we

subjected the catalase-overexpressing ‘stress-less’ mice and C57/WT mice to moderate exercise regimen and compared their outcomes on skeletal muscle-adipose-brain crosstalk. Our studies showed antioxidant overexpression in combination with exercise was beneficial in the maintenance of energy homeostasis, regulating lipid metabolism, enhancing skeletal muscle and adipose tissue function, and possibly by shifting the gut microbiome toward taxa with known metabolically beneficial effects on energy metabolism.

4.2 MATERIALS AND METHODS

4.2.1 Mouse Models and Exercise

Catalase Transgenic ([Tg(CAT)$^{\pm}$]) mice, a gift from Dr. Arlan Richardson's Laboratory (X. Chen et al., 2004), were bred and housed in Marshall University Animal Facility. "Bob-Cat" mice are a novel mouse model generated and bred in our laboratory by crossing [Tg(CAT)$^{\pm}$] mice with leptin deficient, Ob/+, heterozygous hybrids of the Ob/Ob leptin-resistant mice (heterozygous JAX 000632, B6.Cg-Lepob/J) (D. L. Amos et al., 2017). C57Bl6 (C57/WT), [Tg(CAT)$^{\pm}$], "Bob-Cat," and Ob/Ob male mice were housed in cages of 3 or 4 according to their respective genotypes. WT mice were bred at our animal facilities or bought from Hilltop Laboratories and acclimated to the mouse facilities at Marshall University. All groups were fed normal rodent chow (NC - Lab Diet 5001) ad libitum. All guidelines were followed according to IACUC rules and regulations in accordance with the approved study protocol. Each of the four mouse models were divided into exercise and sedentary groups ($n \geq 7$/group) at the age of 16 weeks which is representative of a mature adult human 20-30 yrs of age (Jackson et al., 2017). Sedentary mice remained in their respective cages in the same environment as the exercised mice. Exercised mice were subjected to a 5 day acclimation period to the treadmill (Columbus Instruments) prior to beginning the exercise protocol: 8 weeks of treadmill exercise, 5 days/week for 30 min. at a rate of 15 m/min during the light cycle. This protocol was based on physical activity level recommendations by the American Heart Association and World Health Organization (Organization, 2019) in addition to the Mayo Clinic (Laskowski, 2018). Animals were treated in compliance with Marshall University Animal Committee (Institutional Animal Care and Use Committee) regulations.

4.2.2 Body Weight and Body Composition

Body mass (g) was measured for 8 consecutive weeks to determine differences in total body weights between groups: C57/WT, [Tg(CAT)$^{\pm}$], Bob-Cat, and Ob/Ob (sedentary and exercise) throughout the study. Body composition (fat and lean mass) was determined using magnetic resonance imaging, ECHO-MRI (Houston, TX). Total water content and free water content were also calculated. Each mouse was individually placed into the MRI machine, and three or more measurements were taken per mouse. Median values of each parameter per mouse were calculated using Microsoft Excel, then averaged per genotype and intervention. Comparisons between groups were made by one or two-way ANOVA followed by Bonferonni post hoc Analysis and t-tests.

4.2.3 Comprehensive Laboratory Animal Monitoring System (CLAMS)

Metabolic parameters were determined indirectly by assessing O_2 consumption (VO_2) and CO_2 production, respiratory exchange ratio (RER), food intake (FI), Energy Expenditure (EE), as well as X-Ambulatory counts (XAMB - physical activity) using the CLAMS (Columbus Instruments, Columbus, OH, USA). Mice were supplied with ground rodent chow (Lab Diet 5001) for three days as the analysis was conducted. Computations were made on the middle 48 hours the mice were subjected to the machine, which was approximately the 0600 hour of the first day to the 0600 hour of the third day. Food intake was measured by CLAMS as chow displaced from the food hopper. RER is given as the ratio of carbon dioxide production and oxygen consumption. Carbohydrate (CHO) oxidation was calculated using the formula $((4.585*VCO_2) - (3.226*VO_2))*4$, and similarly, fat oxidation was calculated using the formula $((1.695*VO_2) - (1.701*VCO_2))*9$ (Peronnet & Massicotte, 1991). EE (heat production) was calculated as the Cal/h/lean mass (g). EE average, RER average, average FI per day, as well as

X-Ambulatory locomotor activity per day (XAMB – counts of movement across the cage) were determined for each mouse in all groups. One and two-way ANOVA were used to determine comparative changes between the various genotypes on the sedentary or exercise regimen.

4.2.4 Grip Strength Tests

The grip strength of each individual mouse was tested at the end of the 8-week study period using an apparatus consisting of a ball of tangled fine gauge metal wire and a "scale collector" (metal wire clip). At the time of the experiment, the scale collector was attached to one chain length. The number of links range from one to five (additional weights may be added). Links weighed approximately 25.7 (1 link), 34.97 (2 links), 44.24 (3 links), 53.51 (4 links), and 62.79 (5 links) grams. Mice were held by the middle/base of the tail and lowered toward the wire mesh, which they were naturally attracted to, to determine whether the mouse could grasp and hold the first weight (25.7g). The number of seconds the mouse held the weight was recorded (up to 3 sec). A hold of three seconds was the criterion for success at that weight level. If the mouse dropped the weight before 3 sec. passed, it was allowed to rest for 10 sec and retested with the same weight. If the mouse was unable to hold the weight for three consecutive trials, it was returned to the cage. If the weight was held for a minimum of 3 sec, then the mouse was tested with the next set of links. A final total score was calculated as the product of the number of links in the heaviest chain held for the full 3 sec, multiplied by the time (sec) it was held. If the heaviest weight was dropped before 3 sec, an appropriate intermediate value was calculated (Deacon, 2013).

4.2.5 Blood and Tissue Collection

After 12h fasting, mice were anesthetized using Isoflurane. Blood was obtained by cardiac puncture and placed in heparin tubes; red blood cells (RBCs) and plasma were separated

by centrifugation for 10 min. Mice were perfused intracardially with cold 1X PBS. Tissues including skeletal muscle, adipose tissue, brain, and liver were removed, weighed, and flash frozen in liquid nitrogen. All tissues were stored at -80˚C.

4.2.6 Blood Plasma Hormones and Metabolites

Whole blood was used to measure fasting glucose levels (Precision Xtra Glucometer) then centrifuged for 10 min. to separate the plasma and RBCs. Approximately 35 µL of plasma was placed on a Cholestech cassette and read on a LDX Cholestech Machine (Cholestech Corporation, Hayward, CA) to determine Glucose, High Density Lipoprotein (HDL), Low Density Lipoprotein (LDL), and Total Cholesterol (TC) levels. The remaining plasma was frozen at -80˚C.

Triglyceride (TG) levels were measured in blood plasma using the Cayman Chemical Triglyceride Colorimetric Assay Kit (Cayman, Ann Arbor, MI). Plasma insulin was analyzed using an ultrasensitive mouse Insulin ELISA Kit (Crystal Chem, Downers Grove, IL). The end point colorimetric assays were read using a BioRad Benchmark Plus microplate reader.

A Luminex 200 laser technology system was used to determine circulating leptin levels using the Milliplex Mouse Adipokine Array (Millipore) in each mouse's plasma according to manufacturer's protocol. Adipokine levels were calculated based on the known concentrations of manufacturer's standards.

Plasma irisin levels were determined using a commercially available Irisin ELISA Kit (Biovendor Laboratory Medicine, Brno, Czech Republic). All procedures performed were in accordance with the user manual. Absorbance was read using a BioRad Benchmark Plus microplate reader. Calculations were conducted in accordance with the best fit line created from the standard curve of plotted absorbance values against the known concentrations of standards.

4.2.7 RT-qPCR Adipose Tissue, Brain, and Skeletal Muscle

RNA was isolated from ≈ 100 mg of abdominal adipose tissue, the hypothalamic region of the brain, and the Gas muscle of each mouse using TRI Reagent according to the manufacturer's recommended protocol (Sigma). Concentrations of RNA were measured by use of the NanoDrop 1000 (NanoDrop Technologies Inc., Thermo Scientific, Wilmington, DE, USA). Reverse transcription of total RNA (1 μg) was performed using iScript™ cDNA Synthesis Kit (Bio-Rad, Hercules, CA, USA). RT-qPCR was conducted using iQ SYBR™ Green Supermix (Bio-Rad). The mouse specific primers for expression of leptin, adiponectin, FGF-21, and UCP-1 in adipose tissue, POMC, NPY, and LepR within the hypothalamic region of the brain, and PGC1-α, IL-6, FGF-21, and FNDC5 were used in skeletal muscle tissue. β-actin expression within each tissue type was used as the house-keeping gene. All primer accession and sequences are provided in **Table 10**. RT-qPCR was performed in the Bio-Rad MyiQ or Bio-Rad CFX Connect™ instrument. Transcription was considered nondetectable when the Cq value reached ≥40. All samples were run in duplicate or triplicate. Results were calculated using the

Pfaffl Equation ($2^{\wedge -ddCt}$) and expressed as fold change compared to either the WT control or the sedentary control within each genotype.

Primer Name	Accession Number	Forward	Reverse
Mu-Adiponectin	NM-009605	5'- gcagagatggcactcctgga -3	5'- cccttcagctcctgtcattcc -3'
Mu-FGF-21	NC_000019.10	5'- cgtctgcctcagaaggactc -3'	5'- aatcctgcttggtcttgggg -3'
Mu-UCP1	NM_009463.3	5'- tttcgtgcccgcatcaggcaa -3'	5'- ttggagggcagagaggcgtga -3'
Mu-Leptin	NM-008493	5'- ctcatgccagcactcaaaaa -3'	5'- agcaccacaaaacctgatcc -3'
Mu-POMC	NM_001278584.1	5'- gcgacggaagagaaaagaggt -3'	5'– gtcaggcctagtctctgtcg –3'
Mu-NPY	NM_023456.2	5'- cgctctgcgacactacatca –3'	5' –ttgttctgggggcgttttct –3'
Mu-LepR	NM_146146.2	5' –cttctggagcctgaacccat –3'	5' –cagggtctggtgtggtcaaa –3'
Mu-BDNF	NM_007540.4	5'- tagcttgacaaggcgaaggg–3'	5'- atttgcacgccgatcctttg–3'
Mu-PGC1-αlpha	NM_008904.2	5'- ccgagaattcatggagcaat–3'	5'- tttctgtgggtttggtgtga–3'
MU-IL-6	NM_031168	5' –catgttctctgggaaatcgtgg- 3'	5' –aacgcactaggtttgccgagta-3'
Mu-GLUT 4	NC_018928.2	5'- gattctgctgcccttctgtc -3'	5'- attggacgctctctctccaa -3'
Mu-FNDC5	NM_027402.3	5' –tgttatagctctcttctgccgc- 3'	5'- ggtttctgatgcgctcttgg- 3'
Mu-UCP-1	NM_009463.3	5' –tttcgtgcccgcatcaggcaa- 3'	5'- ttggagggcagagaggcgtga-3'
Mu-β-Actin	NM-007393	5'- ctacctcatgaagatcctcaccga -3'	5'- ttctccttaatgtcacgcacgatt -3'

Table 10. Quantitative RT-PCR primer sequences.

4.2.8 Catalase Activity

The Shimadzu UV-1800 Spectrophotometer was used to determine the enzymatic activity of catalase according to the method of Aebi (Aebi, 1984). Approximately 50 mg of tissue was homogenized and 8 µL of each sample was added to 1mL of 25mM H_2O_2 solution and analyzed for one minute in duplicate or triplicate. Change in absorbance was recorded and specific activity was calculated based on protein estimation by the Lowry Method (Lowry et al., 1951).

4.2.9 Oxidized Proteins in Adipose Tissue (OxyBlot)

Carbonylated proteins are a hallmark of redox stress (Fedorova et al., 2014). Oxidized proteins were measured in epididymal adipose tissue by determining the presence of carbonylated proteins using the Protein Oxidation Detection OxyBlot kit (Millipore, Billerica, MA) as referenced in our previous study (D. Amos et al., 2019) in accordance with the manufacturer's recommendations.

4.2.10 Preservation and Cryostat Sectioning of Skeletal Muscle

During tissue collection, the Gas skeletal muscle was removed and subsequently weighed (g) and measured (length in mm). Each individual muscle was preserved by subjecting it to cooled isopentane and frozen slowly by lowering the isopentane in liquid Nitrogen. Once fully frozen, the muscle was sliced into three segments. The middle segment was used for cryostat sectioning after being frozen in O.C.T. (Optimal Cutting Temperature) medium and kept at -80ºC until cryostat sectioning. The other two segments were frozen in separate tubes for mRNA and protein analysis. The Leica CM1900 Cryostat (Bannockburn, IL) was used to slice muscle into 5-8 µm sections. Sections were transferred to room temperature slides that were kept at -80ºC until Myosin ATPase Staining was performed.

4.2.11 Myosin ATPase Staining and Microscope Analysis

Slides were warmed from -80ºC and the Myosin ATPase Protocol (Kelly Lab-ATPase Histology Stain 2006) was followed to stain the right and left (R and L) side of each Gastrocnemius (Gas) muscle. The pH 4.3 stain protocol was used to determine the fiber type ratio of Type 1 (Oxidative) to Type 2 (Glycolytic) fibers within each mouse group. Myosin ATPase stained slides were analyzed at 10X magnification using a Nikon Eclipse Ti Inverted

Microscope (Melville, NY). Counts of muscle fiber type were determined using ImageJ Software and saved as JPEG files.

4.2.12 Microbial DNA Extraction and Quantification

Fecal samples were collected at the 8 week time point which correlated with the final analysis by MRI, and immediately frozen until shipment to Wright Labs, LLC. Nucleic acid extractions were performed on approximately 0.25 g of each sample using a Qiagen DNeasy Powersoil DNA Isolation kit following the manufacturer's instructions (Qiagen, Frederick, MD). The lysing step was performed using the Disruptor Genie cell disruptor (Scientific Industries). Genomic DNA was eluted in 50 µl of 10 mM Tris followed by quantification using a Qubit 2.0 Fluorometer (Life Technologies, Carlsbad, CA) with the double stranded DNA high sensitivity assay.

4.2.13 PCR Amplification

Illumina iTag Polymerase Chain Reactions (PCR) were performed based on the Earth Microbiome Project's 16S rRNA amplification protocol (Walters et al., 2016) where the hypervariable regions V3-V4 of bacterial 16S rRNA genes were amplified by PCR using bar-coded universal primers. The volume of each reaction was 25 µL containing the final concentration of 1X PCR buffer, 0.8 mM dNTPs 0.625 U Ex Taq DNA Polymerase (Takara), 0.2 µM 515F forward primer, 0.2 µM 806R barcoded reverse primer and approximately 10 ng of template DNA per reaction. PCR was performed using a T100 Thermal Cycler (Bio-Rad, Hercules, CA) using the following cycling conditions: 98 °C for 3 min., 35 cycles of 98 °C for 1 min., 55 °C for 40 s, 72 °C for 1 min, and the final extension was at 72 °C for 10 min. PCR products were held at 4 °C. A 2% agarose E-Gel was used with ethidium bromide (Thermo Fisher Scientific) to visualize the PCR products for bands at approximately 400 bp.

4.2.14 Library Purification, Verification, and Sequencing

PCR products were combined (pooled) in an approximate equimolar manner and run on a 2% agarose gel with Gel Star Nucleic Acid Gel Stain (Lonza) for visualization. Bands of expected product length were cut from the gel using sterile scalpels and subsequently purified using the QIAquick Gel Purification Kit (Qiagen, Frederick, MD). The pure library was then quantified using the Qubit 2.0 Fluorometer double stranded DNA high sensitivity assay (Life Technologies, Carlsbad, CA). Finally, each library on the sequencing run was combined (multiplexed) into one sequencing library. This was completed by normalizing each library's input based on the number of samples per project to ensure even sequencing and coverage. Libraries were quality checked using a 2100 Bioanalyzer high sensitivity DNA analysis kit (Agilent Technologies, Santa Clara, CA) prior to sequencing. The sequencing library was stored at -20˚C until shipment on dry ice to Laragen Inc (Culver City, CA) for sequencing.

Library pools were size verified using the Fragment Analyzer on the ABI3730 and were quantified with a KAPA Library quantification kit (Kapa Biosystem, Wilmington, MA, USA). After dilution with EBT (Illumina) to a final concentration of 2 nM, containing 15% PhiX V3 library control (Illumina, San Diego, CA, USA), the library pools were denatured for 5 min. in an equal volume of 0.2 M NaOH, then further diluted to 8 pM in HT1 buffer (Illumina) and were sequenced using an Illumina MiSeq V2 500 cycle kit cassette with 16S rRNA library sequencing primers set for 250 basepair, paired-end reads. Overall sequencing run performance was evaluated by determining if the sequencing run met the Illumina specifications for quality scores and data output. Actual run performance varied based on sample type, quality, and clusters passing filter. Specifications are based on the Illumina PhiX control library at supported cluster densities.

4.2.15 Quality Filtering and OTU Picking

Paired-end sequences were merged with a minimum overlap of 200 bases, trimmed at a length of 253 bp, and quality filtered at an expected error of less than 0.5% using USEARCH (Edgar, 2010). After quality filtering, reads were analyzed using the QIIME 1.9.0 software package (Caporaso et al., 2010; Caporaso et al., 2011). Chimeric sequences were identified using USEARCH61. Open reference operational taxonomic units (OTUs) were picked using the USEARCH61 algorithm at 97% identity (Edgar, 2013), and taxonomy assignment was performed using the Greengenes 16S rRNA gene database (13-5 release) (DeSantis et al., 2006). Taxomony was assigned to OTUs and organized into a BIOM formatted OTU table, which was summarized within QIIME 1.9.0. (Note: an OTU table contains each sample and the relative abundance of each unique bacterial taxon identified within each sample).

4.2.16 Alpha Diversity Comparisons (16S)

Alpha diversity box plots were generated within the QIIME-1.9.0 sequence analysis package using an unrarified OTU table. Samples with less than 10,000 sequences per sample were excluded from alpha diversity analyses. Multiple rarefactions were conducted on sequences across all samples to a maximum depth of 10,000 sequences, with a step size of 1,000, and 20 iterations at each step. Alpha diversities were then collated and plotted and compared using a two-sample t-test and non-parametric Monte Carlo permutations (n = 999).

4.2.17 Beta Diversity Comparisons (16S)

Principal coordinates analyses (PCoA) plots and Adonis tests for significance were generated from a weighted UniFrac distance matrix made within QIIME 1.9.0 from a CSS normalized OTU table (Paulson, Stine, Bravo, & Pop, 2013).

4.2.18 Taxonomic LEfSe Enrichment Plots

Relative abundances of bacterial taxa summarized at the genus level were multiplied by 1 million and formatted as described in Segata et al. 2011 (Segata & Huttenhower, 2011). Comparisons were made between exercised and sedentary groups within each genotype in addition to exercised groups compared to their control C57/WT sedentary and exercised mouse groups. Alpha levels of 0.05 were used for both the Kruskal–Wallis and pairwise Wilcoxon tests. Linear Discriminant Analysis (LDA) scores greater than 2.0 are displayed.

4.2.19 PICRUSt Enrichment Plots

Phylogenetic Investigation of Communities by Reconstruction of Unobserved States (PICRUSt) functional predictions were generated from a closed-reference OTU table generated within QIIME-1.9.0. Relative abundances of level 3 summarized predicted functional genes were multiplied by 1 million and formatted as described in Segata et al. (2011) (Segata & Huttenhower, 2011). Comparisons were made with "HLR_Group" as the main categorical variable ("Class"). Alpha levels of 0.05 were used for both the Kruskal–Wallis and pairwise Wilcoxon tests. LDA scores greater than 1.0 are described.

4.2.20 Statistical Analysis

Results are presented as mean ± standard error of the mean (S.E.M.). Data were evaluated by one and two-way ANOVA followed by Bonferonni's multiple comparison tests using GraphPad Prism Version 7. T-tests were also performed between pre-determined individual mouse groups in comparison to the sedentary groups. N indicates the number of animals per group. Statistical significance was accepted at $p<0.05$. RT-qPCR gene expression was determined by use of the Pfaffl equation (Pfaffl, 2001) and represented as fold change with significance denoted as differences in delta CT/genotype and intervention. Catalase activity is

represented as % of control group. Analysis of oxidized carbonyl groups are represented as the ratio of oxidized carbonyls to the total protein memcode stain. Microbial analysis statistics are defined per test used within each method subsection of that parameter.

4.3 RESULTS

4.3.1 Body Weight and Body Composition

At sixteen weeks of age, mice expressing the human catalase gene ([Tg(CAT)$^{\pm}$] and Bob-Cat) (D. L. Amos et al., 2017) in addition to the C57/WT control and Ob/Ob mice, were put on

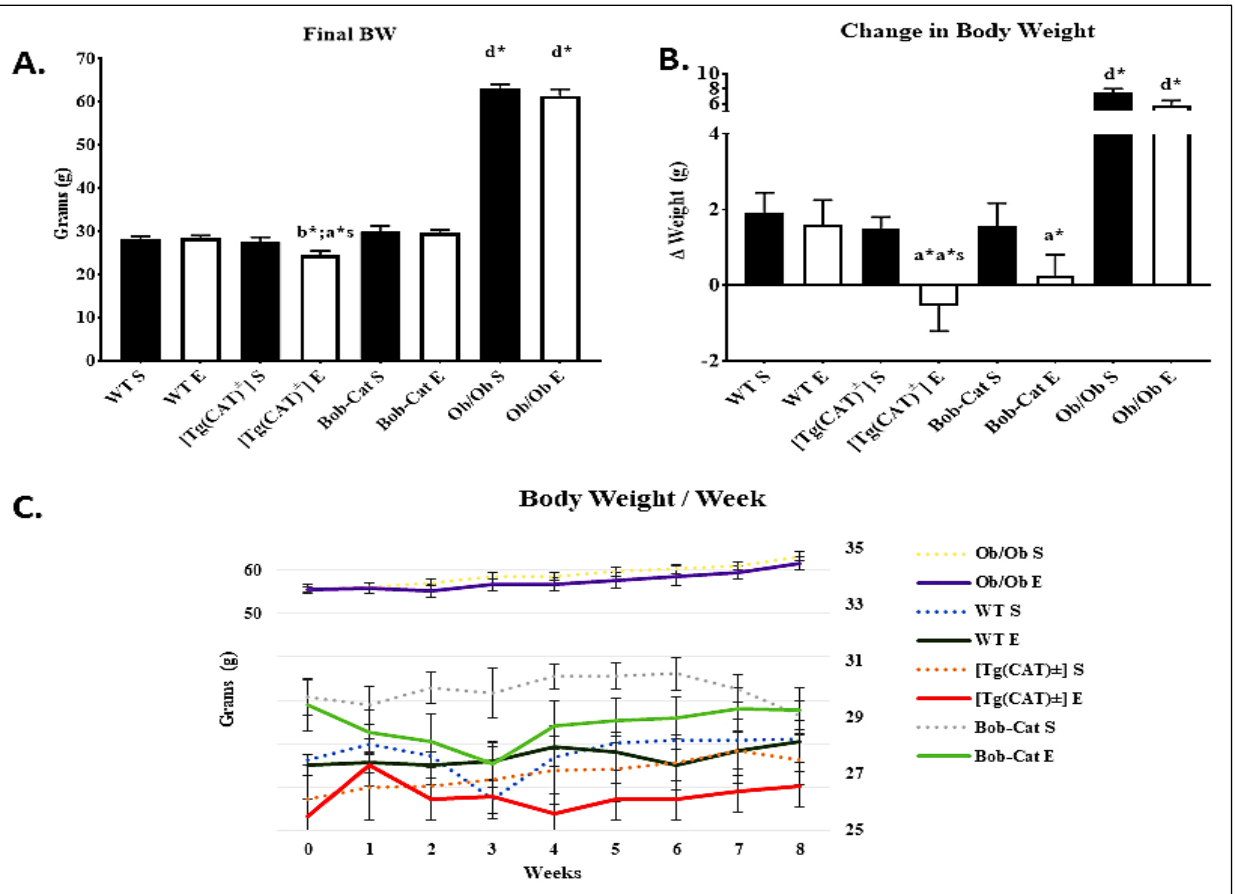

Figure 29. Weekly body weight changes. (A) Final whole-body weight (g); (B) Body weight change (initial and final body weight); (C) Overall weekly body weight measurements of WT, [Tg(CAT)$^{\pm}$], Bob-Cat and Ob/Ob mice that remained sedentary or were exercised 8 weeks (n≥7/group). The WT, [Tg(CAT)$^{\pm}$], and Bob-Cat mouse groups' data are depicted on the left vertical axis, while the Ob/Ob mice data is depicted on the right vertical axis. Mice overexpressing catalase on an exercise regimen in contrast to WT S or their sedentary cohorts showed no change or lesser gain in body weight over the eight week period. One and two-way ANOVA followed by Bonferonni post-hoc and preplanned t-tests were performed on GraphPad Prism 7. Data is represented as mean ± S.E.M. Letters indicate significant p values, a= p<0.05, b= p<0.01, d<0.0001; symbols represent significant differences between genotypes *= compared to WT S; an additional 's' represents comparison to sedentary cohorts.

an exercise regimen (30 min. of treadmill exercise, 5 days a week, at 15 m/min.) or remained sedentary in the same environment for the 8 week study period. All mouse groups were fed ad libitum normal chow diet. Changes in body weight and body composition (fat and lean mass) in the mouse groups overexpressing catalase were compared to the control WT and leptin deficient (Ob/Ob) mouse groups. Body weight (BW) was recorded each week and the final BW and change in body weight is shown in (**Figure 29A-B**). Analysis of change in BW by two-way ANOVA showed a significant interaction between genotype ($p<0.0001$). There was also a trend for lower body weight shown with exercise intervention compared to their sedentary controls, however, it did not quite reach significance ($p=0.056$). Bonferonni post hoc test did not show a significant difference between the groups, but using the t-test on preplanned groups, in comparison to the WT S and the sedentary cohorts within each genotype, the change in BW was significantly lower in exercised mouse groups, especially within the mice overexpressing catalase. Interestingly, the only group to actually lose body weight was the exercised [$Tg(CAT)^{\pm}$] mouse group. As expected, the leptin deficient Ob/Ob sedentary and exercised mouse groups gained the highest amount of BW ($p<0.0001$) with the Ob/Ob sedentary group gaining the most weight of all mouse groups. The overall changes are reflected in the plotted body weight measurements taken per week (**Figure 29C**).

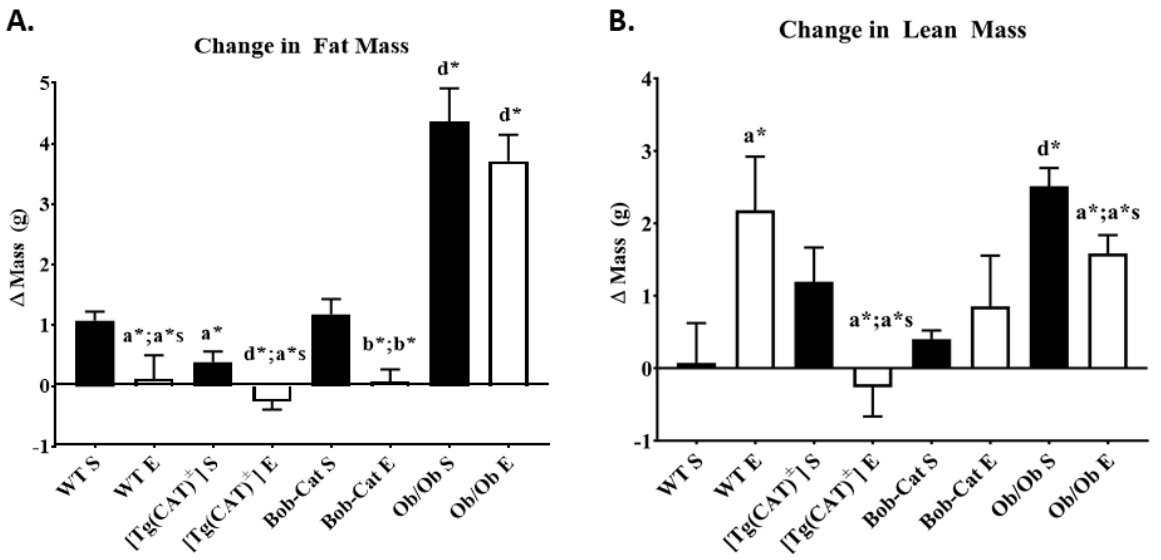

Figure 30. Fat and lean mass (ECHO-MRI). Change in (A) Fat mass and (B) lean mass (0 and 8 week time point difference calculated by ECHO-MRI average measurements) in WT, [Tg(CAT)$^{\pm}$], Bob-Cat, and Ob/Ob mouse groups that were sedentary or exercised 8 weeks. Mice overexpressing catalase on an exercise regimen in contrast to WT S or their sedentary cohorts had no change or a lower gain in fat mass. Bob-Cat E and WT E mice showed a trend for increased lean mass vs. their sedentary respective cohorts. One-way and two-way ANOVA followed by Bonferonni post hoc analysis in addition to preplanned t-tests were performed on GraphPad Prism 7. Data is represented as mean ± S.E.M. Letters indicate significant p values, a= $p<0.05$, b= $p<0.01$, d= $p<0.0001$; symbols represent significant differences between genotypes *= compared to WT S; an additional 's' represents comparison to sedentary cohorts.

Total fat and lean mass were determined for each mouse group at baseline, 4 week, and 8 week time points by ECHO-MRI. Total change in fat and lean mass between the beginning and end points of the study are shown in **Figures 30A-B**. Analysis by two-way ANOVA and Bonferonni post-hoc analysis showed a significant interaction in the change in fat mass between genotype ($p<0.0001$) in addition to exercise ($p<0.01$). Preplanned t-tests were also used to determine pair-wise differences between each exercise group and their sedentary controls. Similar to the results of body weight measurements, overexpression of catalase caused a similar change or loss in fat mass in comparison to the WT S control group. With exercise intervention, however, there was a significantly diminished gain in fat mass compared to the sedentary groups

($p<0.01$). As with body weight, the [Tg(CAT)$^{\pm}$] mice were the only group to lose fat mass which was significantly lower than the WT S control group (**Figure 30A**). Similar to the [Tg(CAT)$^{\pm}$] E mice, the Bob-Cat E group had a significantly lower change in fat mass (**Figure 30A**). Ob/Ob S and E mouse groups had the greatest increase in body fat ($p<0.0001$ and $p<0.001$ respectively). Lean mass comparisons showed an interaction ($p<0.01$) between exercise and genotype in addition to a significant difference between the genotypes ($p<0.01$). Between the genotypes, lean mass calculations showed WT E groups gained a significant amount of lean mass compared to their sedentary cohorts ($p<0.05$) and Bob-Cat groups showed a trend for increased lean mass (**Figure 30A**).

4.3.2 Adipose, Liver, and Brain Weights

Differences in subcutaneous (SubQ) and visceral adipose tissue weights and an increase in liver weight all play a key role in energy metabolism and are indicators of metabolic status (Paniagua, 2016; Sheng et al., 2018). Exercise is known to lower adipose tissue weight (J. Chen et al., 2018; Hoffmann & Weigert, 2017; Leal et al., 2018) and may play a role in maintaining the liver weight by lowering the amount of ectopic fat deposition. Therefore, as shown in **Table 11**, adipose tissue and liver weights were measured during tissue collection at the end of the study from all mouse groups. Analysis by two-way ANOVA followed by Bonferonni post hoc tests and preplanned t-tests showed a significant genotype interaction ($p<0.0001$) in both SubQ and visceral adipose tissue weight. It was interesting that in both the excised SubQ and visceral adipose tissue, the [Tg(CAT)$^{\pm}$] mouse groups had the lowest adipose tissue weight compared to the control WT S group. Exercised [Tg(CAT)$^{\pm}$] mouse had significantly lower grams of SubQ adipose tissue, while the sedentary [Tg(CAT)$^{\pm}$] had significantly lower grams of visceral adipose tissue. This result was also reflected in MRI analysis of the [Tg(CAT)$^{\pm}$] E mouse group where

the greatest amount of fat mass was lost at the end of the study (**Figure 30A**). As expected, the Ob/Ob sedentary and exercised mouse groups both had the highest levels of adipose tissue weight ($p<0.0001$) with more than 7 times the amount of fat as the WT mice and mouse groups overexpressing catalase. In addition to adipose tissue weight, analysis by two-way ANOVA followed by Bonferonni post-hoc test showed a significant interaction between the mouse groups in liver weight with regard to genotype ($p<0.0001$). Ob/Ob mice, independent of exercise intervention, had significantly higher liver weights ($p<0.0001$). It is intriguing that the Bob-Cat S and E groups showed trends for increased liver weight.

	SubQ Adipose (g)	Visceral Adipose (g)	Liver (g)	Brain (g)
WT S	0.33 ± 0.07	0.79 ± 0.07	1.19 ± 0.07	0.47 ± 0.003
WT E	0.51 ± 0.22	0.90 ± 0.20	1.15 ± 0.04	0.45 ± 0.009
[Tg(CAT)$^{\pm}$] S	0.18 ± 0.06	0.48 ± 0.07 a*	1.07 ± 0.06	0.46 ± 0.01
[Tg(CAT)$^{\pm}$] E	0.15 ± 0.04 a*	0.71 ± 0.13	1.18 ± 0.07	0.44 ± 0.01 a*s
Bob-Cat S	0.30 ± 0.04	1.02 ± 0.12	1.4 ± 0.13	0.47 ± 0.01
Bob-Cat E	0.31 ± 0.05	1.03 ± 0.07	1.31 ± 0.05	0.48 ± 0.01
Ob/Ob S	14.54 ± 0.47 d*	7.63 ± 0.17 d*	4.43 ± 0.18 d*	0.42 ± 0.003 d*
Ob/Ob E	13.93 ± 0.61 d*	8.07 ± 0.27 d*	4.16 ± 0.31 d*	0.42 ± 0.008 d*

Table 11. Tissue weights. Subcutaneous (SubQ) and visceral adipose tissue, liver, and brain weights (g) were measured during tissue collection at the end of the 8 week study ($n\geq7$/group). One and two-way ANOVA followed by Bonferonni post hoc test and preplanned t-tests were used for statistical analysis. Data are represented as mean ± S.E.M. Letters indicate significant p values, a= $p<0.05$, d= $p<0.0001$; symbols represent significant differences between genotypes *= compared to WT S; an additional 's' represents comparison to sedentary cohorts.

Decreased brain weight could be an indicator of neurodegeneration or neurological dysfunction since previous studies have found that individuals with decreased brain volume have increased cortisol levels, are at higher risk for dementia, and tend to do poorer on cognitive tests (Stern, 2012). Two-way ANOVA indicated a significant difference within genotype ($p<0001$). It was surprising to find that among the control WT and groups overexpressing catalase, the [Tg(CAT)$^{\pm}$] E group was the only group with a lower brain weight. We also observed that both sedentary and exercised Ob/Ob groups had significantly lower brain weight (10% decrease; $p<0.0001$) compared to the WT S mice in addition to every other mouse group.

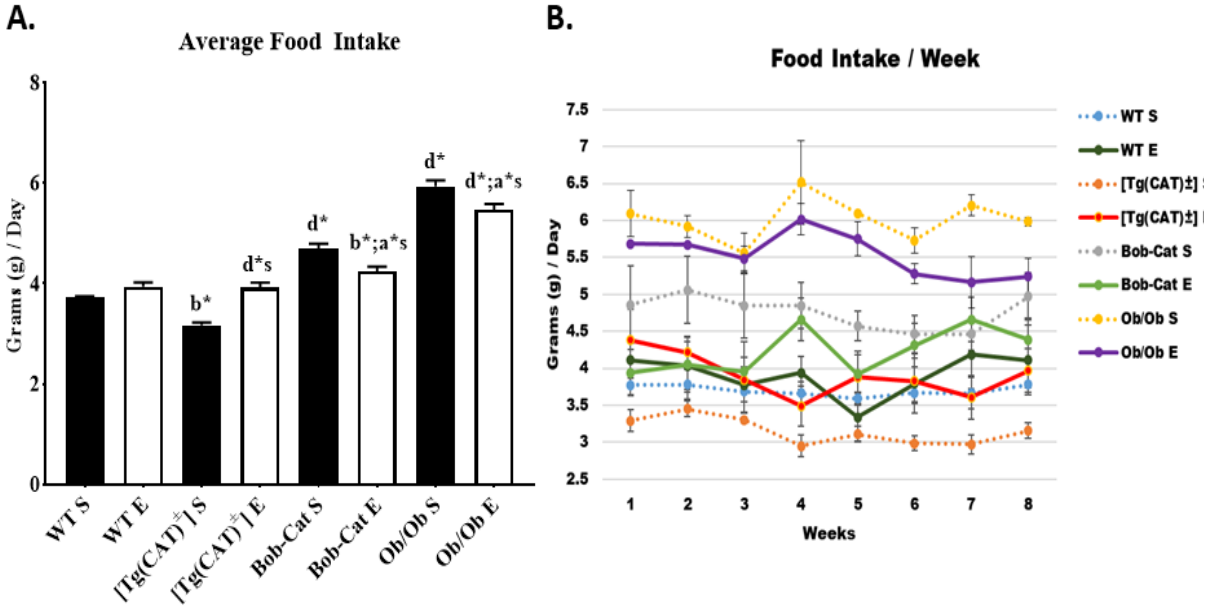

Figure 31. Weekly measurements of food consumed. (A) average weekly food consumption for 8 weeks; (B) weekly food consumption for 8 weeks per mouse group ($n\geq7$/group). WT, [Tg(CAT)$^{\pm}$], Bob-Cat, and Ob/Ob mouse groups remaining sedentary or exercised were studied. One-way and two-way ANOVA followed by Bonferonni post hoc analysis were performed on GraphPad Prism 7. Data is represented as mean ± S.E.M. Letters indicate significant p values: a= $p<0.05$, b= $p<0.01$, d= $p<0.0001$; symbols represent significant differences between genotypes * = compared to WT S; an additional 's' represents comparison to sedentary cohorts.

4.3.3 Weekly Food Consumption

Each week, the grams of food consumed were measured from each mice group. **Figure 31A** shows the average food intake of each mice group per day, and **Figure 31B** displays the food intake per mouse group each week throughout the 8 week study. In comparison to the WT S mice, the only group that consumed a significantly lower amount of chow was the [Tg(CAT)$^{\pm}$] sedentary group, which also had the lowest visceral fat mass (**Table 11**). On the other hand, although the body weight and fat mass were significantly decreased, when put on exercise intervention, it was intriguing the [Tg(CAT)$^{\pm}$] E mouse consumed a similar amount of chow compared to the WT S and WT E groups. Bob-Cat mice, independent of intervention, consumed significantly more chow than the WT mice. As expected, Ob/Ob mice consumed more chow than all other mouse groups ($p<0.0001$). However, when put on exercise regimen, the Ob/Ob mice, trended to consume less food in comparison to the sedentary group. A similar effect was seen in the Bob-Cat group ($p<0.05$). However, this opposite was observed in the other two genotypes tested (WT and [Tg(CAT)$^{\pm}$] mice).

4.3.4 Circulating Markers

Numerous studies show physical activity improves the lipid profile and insulin sensitivity in both rodents and humans (J. Chen et al., 2018; Hoffmann & Weigert, 2017; Meissner et al., 2010). Therefore, to determine the overall effect of exercise on circulating metabolic parameters, we measured plasma TC, HDL, and TG levels at the end of the 8 week study. All mice groups, with the exception of the Ob/Ob mice, had TC levels under 100 mg/dL. (This was below the detection limit of the kit, so the "<" sign was used to provide data for all groups.)

	TC (mg/dL) n=7+	HDL (mg/dL) n=7+	TG (mg/dL) n=5+	Glucose (mg/dL) n=7+	Insulin (ng/mL) n=3+
WT S	<100	46.13 ± 3.0	47.29 ± 2.8	178.4 ± 12.7	0.25 ± 0.05
WT E	<100	50.38 ± 2.65	43.27 ± 3.4	207 ± 16.7	0.26 ± 0.13
[Tg(CAT)$^{\pm}$] S	<100	52.9 ± 3.34	40.4 ± 3.4	197.1 ± 15.1	0.56 ± 0.18
[Tg(CAT)$^{\pm}$] E	<100	55.3 ± 3.14 (p=0.06)	33.2 ± 2.6 a*	198.3 ± 13.5	0.31 ± 0.05
Bob-Cat S	<100	60.6 ± 2.43 b*	46.5 ± 3.7	222.3 ± 22.2	0.80 ± 0.47
Bob-Cat E	<100	61.5 ± 2.63 b*	38.7 ± 3.0	235.5 ± 20.5 a*	1.52 ± 0.58
Ob/Ob S	142.3 ± 5.12 d*	97.9 ± 1.32 d*	90.5 ± 16.8 d*	256.2 ± 15.8 c*	7.73 ± 2.01 c*
Ob/Ob E	127.1 ± 7.36 b*	90.1 ± 5.16 d*	64.7 ± 8.7 b*	279 ± 26.2 c*	4.47 ± 1.46 b*

Table 12. Circulating levels of metabolic markers. Total Cholesterol (TC) and High Density Lipoprotein (HDL) levels were determined using the Cholestech kit, while plasma Triglyceride (TG) levels were measured using the Triglyceride Colorimetric Assay Kit. Fasting blood glucose was measured by glucometer and plasma insulin was measured by ELISA. Data were collected from WT, [Tg(CAT)$^{\pm}$], Bob-Cat, and Ob/Ob sedentary or exercised mice for 8 weeks. One and two-way ANOVA followed by Bonferonni post hoc analysis in addition to preplanned t-tests between exercise groups and sedentary controls were performed on GraphPad Prism 7. Data is represented as mean ± S.E.M. Letters indicate significant p values, a=p<0.05, b= p<0.01, c= p<0.001, d= p<0.0001; symbols represent significant differences between genotypes *= compared to WT S; an additional 's' represents significant differences between sedentary cohorts.

As shown in **Table 12**, Ob/Ob mice had significantly higher levels than all other mouse groups. However, exercise intervention showed a trend for decreasing the TC levels in the Ob/Ob E mouse group (10%). HDL levels were significantly increased in the Bob-Cat genotype

independent of exercise ($p<0.01$), although all mice overexpressing catalase had higher HDL levels (not significant) compared to the WT S group. It was also interesting that exercise increased the HDL level in every genotype on exercise with the exception of the Ob/Ob mice. Although HDL was highest among the Ob/Ob mouse groups, the TC was also very high. All mouse groups overexpressing catalase trended to have lower circulating TG levels compared to the WT S mice, with the [Tg(CAT)$^{\pm}$] mice on exercise intervention having the lowest levels ($p<0.05$). This directly correlates with their lower adipose tissue weights compared to all the other mouse groups. Exercise intervention not only lowered the TG levels ($p<0.05$), but the effect was exacerbated in the mice overexpressing catalase. On the contrary, highest TG levels were seen in the Ob/Ob sedentary mouse group ($p<0.0001$). Exercised Ob/Ob mice had significantly higher TG levels than the WT S group ($p<0.01$), but levels were not as significantly high as their sedentary cohorts.

Circulating levels of glucose and insulin were also measured and shown in Table 12 followed by one and two-way ANOVA and Bonferonni post hoc analysis. T-tests were also used between preplanned mouse groups to compare exercised mice with their sedentary cohorts. No significant differences were noted between the mouse groups regarding blood glucose levels with the exception of the Bob-Cat E mice and both Ob/Ob mouse groups. Bob-Cat exercised mice had higher ($p<0.05$) glucose levels than the WT S group, but the highest levels were observed in both the Ob/Ob mouse groups ($p<0.001$). Plasma insulin levels were significantly higher ($p<0.001$) in the Ob/Ob sedentary group of mice. The Ob/Ob mice on exercise had 8-fold higher levels compared to the WT S group ($p<0.01$), but this was much lower than the insulin levels observed in their sedentary cohorts. Therefore, exercise seemed to have a beneficial effect by lowering the insulin levels in the Ob/Ob exercised mouse group. It is also interesting that we observed the

lowest levels of circulating glucose and insulin in the WT S and [Tg(CAT)$^{\pm}$] mice on exercise intervention.

4.3.5 Comprehensive Animal Monitoring System (CLAMS) Analysis

4.3.5.1 Food Intake

At the end of the study, the Comprehensive Animal Monitoring System (CLAMS) was used to conduct a three-day assessment of food intake (FI) per mouse and averaged for each mouse group (**Figure 32A-D**). Results are displayed for two-hour time intervals for all mouse groups and between each genotype in addition to 12 h light and dark cycles per mouse group. Unlike the weekly food measures, while analyzed in the CLAMS, there were no significant

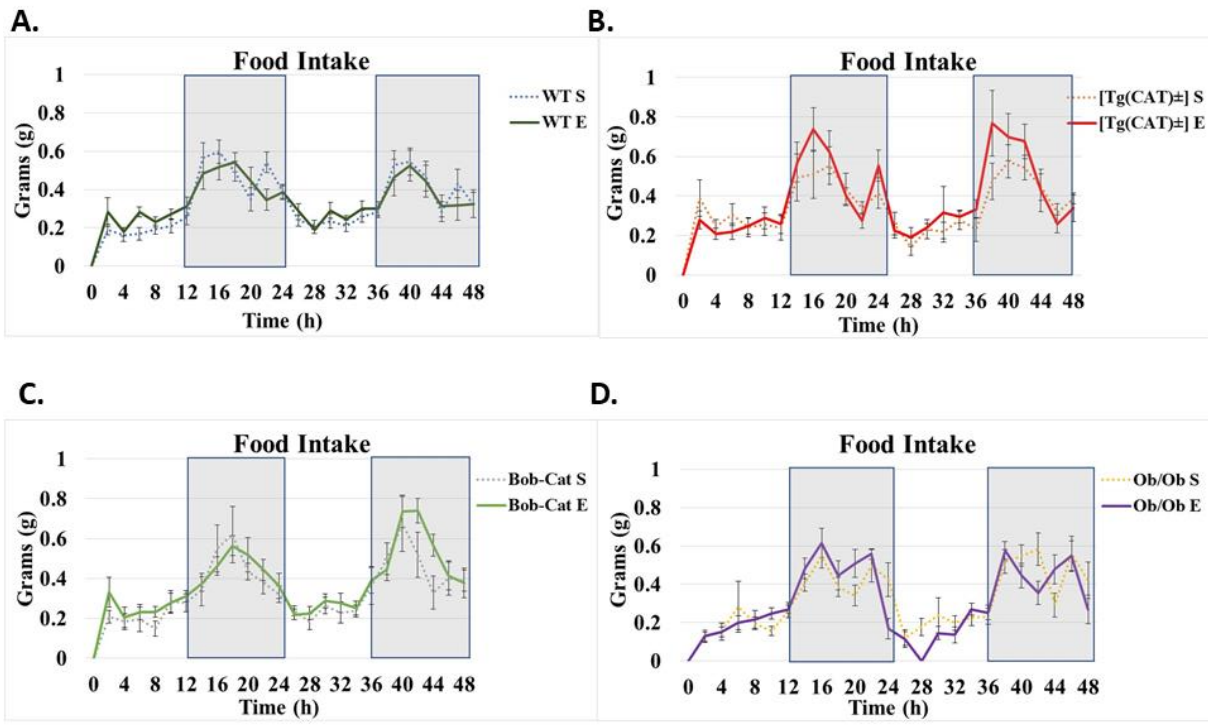

Figure 32. CLAMS analysis of food intake over a 48h time period. Light and dark cycle CLAMS measurements of (A) WT (C57/WT), (B) [Tg(CAT)$^{\pm}$], (C) Bob-Cat, and (D) Ob/Ob sedentary and exercised mice food intake as average grams/2h for 48h (n≥7/group). One-way and two-way ANOVA followed by Bonferonni post hoc analysis was performed on GraphPad Prism 7. Data is represented as mean ± S.E.M. (n≥7/group)

differences between any mouse group. However, we found that on average, mice on exercise

intervention consumed more food than their sedentary cohorts. The only exception was the Ob/Ob group. Because rodents are nocturnal, we also averaged FI during both the light and dark cycles as displayed in **Table 13**.

	FI		RER		EE		XAMB	
Group	**Light**	**Dark**	**Light**	**Dark**	**Light**	**Dark**	**Light**	**Dark**
WT S	0.20 ± 0.03	0.46 ± 0.06	0.89 ± 0.02	0.95 ± 0.02	18.39 ± 0.86	21.29 ± 0.8	593.3 ± 134	1931 ± 234
WT E	0.24 ± 0.03	0.43 ± 0.07	0.91 ± 0.01 a*	0.96 ± 0.02	17.63 ± 0.72 d*	19.88 ± 0.98	809.2 + 294.4	1763 ± 359
[Tg(CAT)$^{\pm}$] S	0.23 ± 0.05	0.46 ± 0.08	0.91 ± 0.02	0.97± 0.02	16.81 ± 1.12 d*	19.31 ± 1.32 b*	635.5 ± 177.6	2169 ± 624
[Tg(CAT)$^{\pm}$] E	0.24 ± 0.04	0.53 ± 0.09	0.93 ± 0.02 d*;b*s	0.99 ± 0.02 d*	16.64 ± 0.73 d*	20.07 ± 0.60	466.3 ± 91.8	1678 ± 1015
Bob-Cat S	0.22 ± 0.44	0.45 ± 0.27	0.86 ± 0.02 d*	0.91 ± 0.02 d*	16.63 ± 0.79 d*	19.99 ± 0.74	2064 ± 872 d*	5002 ± 1631 d*
Bob-Cat E	0.25 ± 0.04	0.50 ± 0.06	0.89 ± 0.01 d*;d*s	0.94 ± 0.01 a*s	15.54 ± 0.71 d*;a*s	18.87 ± 0.61 c*	1313.09 ± 618.1 b*;b*s	3944 ± 907 c*
Ob/Ob S	0.18 ± 0.05	0.46 ± 0.07	0.80 ± 0.04 d*	0.85 ± 0.04 d*	20.27 ± 0.81 d*	23.07 ± 0.68 a*	150.4 ± 24.45	413.4 ± 74.0 a*
Ob/Ob E	0.16 ± 0.03	0.45 ± 0.05	0.87 ± 0.01 b*;d*s	0.92 ± 0.01 d*;d*s	20.57 ± 0.83 d*	22.94 ± 0.76 a*	157.3 ± 27.71	374.23 ± 59.7 a*

Table 13. Light and dark cycles of metabolic parameters. 2h light and dark cycle averages of food intake (FI) as average grams (g) of chow consumed, average Respiratory Exchange Ratio (RER) as VCO_2/VO_2, metabolic energy expenditure (EE) as Cal/h/(g) lean mass of each mouse group, and counts of physical movement as XAMB / cycle (XAMB) of each exercised and sedentary mouse group per light (0-12, 24-36h) and dark (12-24,36-48h) cycle of the 48h analysis. One-way and two-way ANOVA followed by Bonferonni post hoc test as week as pre-planned t-tests between each genotype and sedentary control was performed using Graph-Pad Prism 7. Data are represented as mean ± S.E.M. and significant differences are displayed with letters indicating p values: a=p<0.05, b= p<0.01, c=p<0.001, d=p<0.0001; symbols represent significant differences between genotypes *= compared to WT S; an additional 's' represents significant differences between sedentary and exercise cohorts. (n≥7)

Again, although there were no significant differences, we found exercised mice trended to consume more chow than their sedentary cohorts. It was also interesting to note that the

exercised [Tg(CAT)$^{\pm}$] and Bob-Cat mice consumed among the highest levels of food overall, despite their low body weight, fat mass, and circulating levels of TG (**Figures 29-30** and **Tables 11 and 12**).

CLAMS analysis can also be indicative of normal eating patterns and circadian rhythm (can change based on the frequency of food consumption). It was surprising that the Ob/Ob mice, contrary to expectation, did not significantly differ in their frequency of food consumption.

4.3.5.2 Respiratory Exchange Ratio, CHO Oxidation, and Fat Oxidation

RER is an indication of the type of fuel (carbohydrate (CHO) vs fat) being primarily oxidized to supply energy demands. In comparison to the WT S group, shown in **Table 13**, exercised mice within each genotype showed an increase in the RER ($p<0.05$). This was also true of each exercised group compared to their sedentary cohorts. (Overall 2h time intervals are reflected in **Figure 33A-D.**)

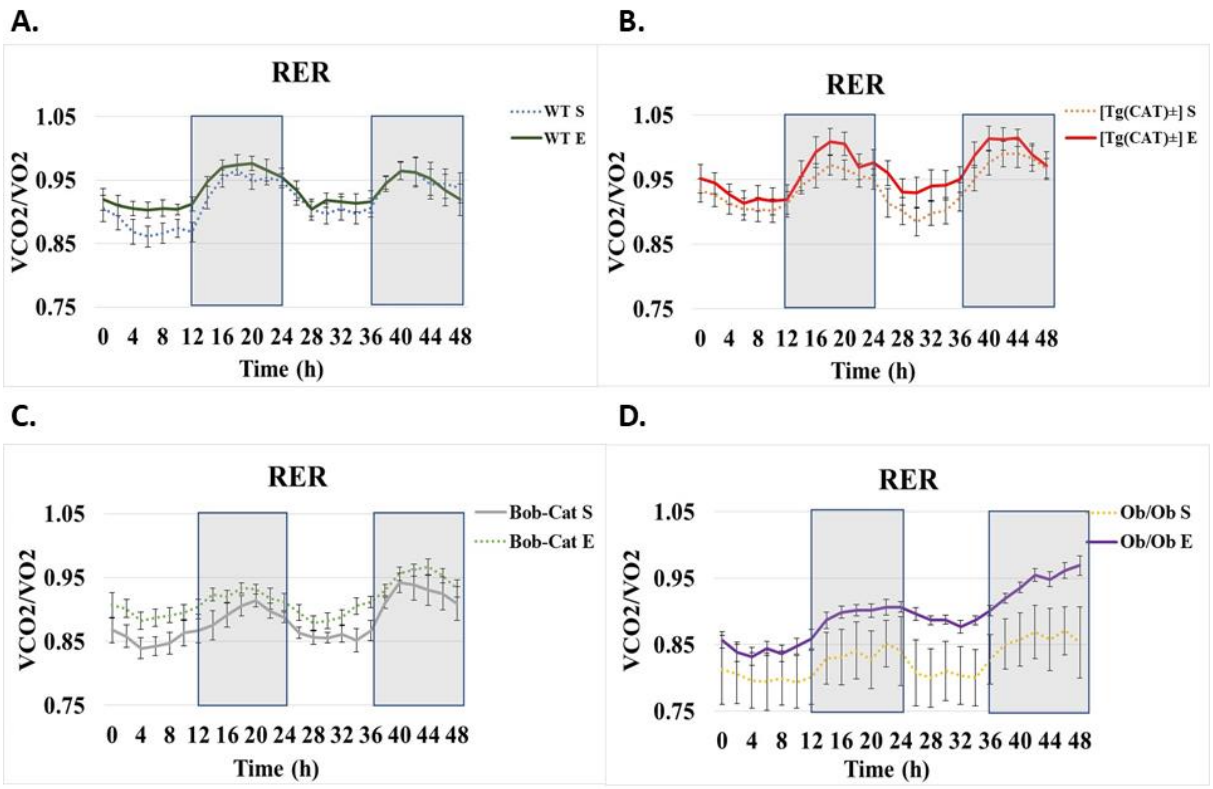

Figure 33. CLAMS analysis of respiratory exchange ratio over a 48h time period. Light and dark cycle CLAMS measurements of (A) WT (C57/WT), (B) [Tg(CAT)$^{\pm}$], (C) Bob-Cat, and (D) Ob/Ob exercised and sedentary mouse group's Respiratory Exchange Ratio (RER) is depicted as VCO_2 emission / VO_2 consumption. (n≥7/group) One and two-way ANOVA followed by Bonferonni post hoc analysis was performed on GraphPad Prism 7. Results are represented as mean ± S.E.M.

As expected, the RER of the Ob/Ob S mice was the lowest among all mouse groups, yet the Ob/Ob E group had higher levels than their sedentary cohorts (**Table 13**, $p<0.0001$). However, most interesting, was the RER measurements observed in the [Tg(CAT)$^{\pm}$] and Bob-Cat mouse groups on exercise intervention. While [Tg(CAT)$^{\pm}$] E showed the overall highest levels ($p<0.0001$) independent of the light or dark cycle, Bob-Cat E mice had increased levels compared to their sedentary cohorts yet retained similar RER levels to the WT S group (**Table 13**).

In addition to determining the RER, we further delineated the CHO and fat oxidation levels using the VO_2 and VCO_2 obtained from the CLAMS measurements (**Figure 34**).

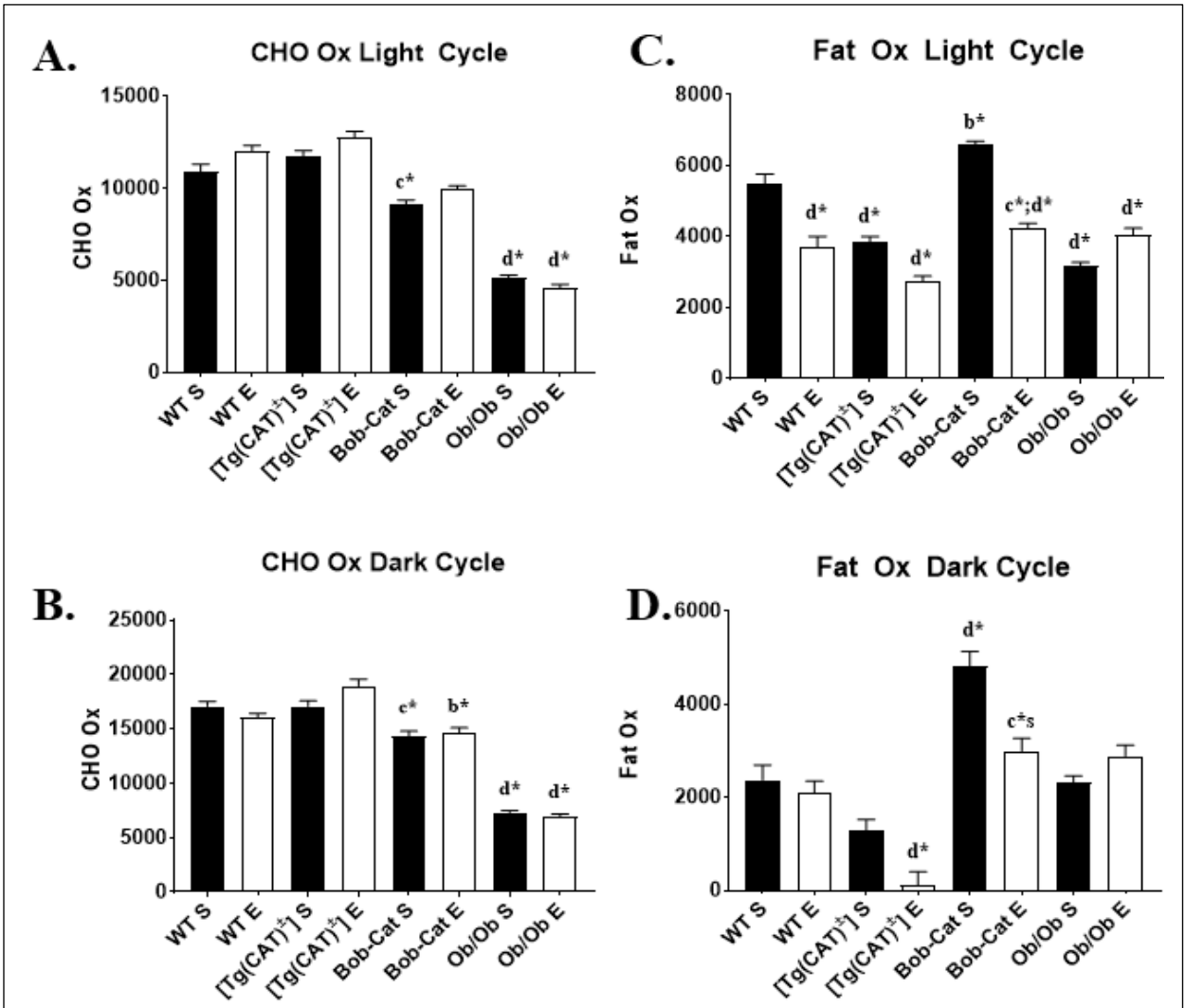

Figure 34. Substrate oxidation level over a 48h time period. Calculated oxidation levels of carbohydrate (CHO) during the (A) light and (B) dark cycles as well as the oxidation of fat during the (C) light and (D) dark cycles in WT (C57/WT), [Tg(CAT)$^{\pm}$], Bob-Cat, and Ob/Ob exercised and sedentary mice (n≥7/group). One and two-way ANOVA were performed followed by Bonferonni post hoc analysis on GraphPad Prism 7. Data is represented as mean ± S.E.M. Significant differences are displayed with letters indicating p values b= $p<0.01$, c=$p<0.001$, d=$p<0.0001$; symbols represent significant differences between genotypes *= compared to WT S; an additional 's' represents significant differences between sedentary cohorts.

In comparison to the WT S mice, exercised mouse groups showed an overall trend for higher levels of CHO oxidation and lower levels of fat oxidation independent of the light or dark

cycle. However, when comparing the two time periods, the highest levels of carbohydrate oxidation were observed during the dark (wake) cycle while the highest levels of fat oxidation were seen during the light cycle as the animals slept. Ob/Ob mice were expected to have the lowest levels of CHO oxidation and the highest levels of fat oxidation due to their obese state. However, it was unexpected that the Bob-Cat sedentary mouse group had the lowest level of CHO oxidation and the highest level of fat oxidation ($p<0.01$). In fact, their level of fat oxidation was even higher than the obese, leptin deficient Ob/Ob mouse groups.

Nonetheless, even more surprising was that the [Tg(CAT)$^{\pm}$] E group had both the overall highest levels of CHO oxidation and lowest levels of fat oxidation ($p<0.0001$) regardless of the time of day. Bob-Cat E mice, on the other hand, showed the opposite effect in the dark cycle with increased levels in fat oxidation compared to the WT S mouse group. These results indicate antioxidant catalase and/or exercise is playing a role in modulating the metabolic pathways involved in fuel oxidation within the antioxidant overexpressing mouse groups.

4.3.5.3 EE and XAMB

The CLAMS technology also provides measurements of Energy Expenditure (EE) as well as physical activity levels (XAMB). EE, indirectly calculated as Cal/h/g of lean body mass, was significantly different in each mouse group compared to the WT S mice. **Figure 35A-E** depicts the 2h time point measurements for each of the mouse groups. With the exception of the Ob/Ob mice, which had significantly higher levels ($p<0.0001$), all mouse groups overexpressing catalase or on exercise intervention had decreased levels of EE compared to the WT S group during the light cycle (**Figure 35A and Table 13**). The same trend was shown during the dark cycle, although, not all levels reached significance (**Table 13**). Exercise showed a trend for

decreasing the EE, and the exercised mouse groups overexpressing catalase (Bob-Cat and [Tg(CAT)$^{\pm}$]) had the lowest levels (**Table 13**).

XAMB, a count of beam breaks while the mice resided in the CLAMS chambers, was averaged and showed that in comparison to the WT S group, all groups overexpressing catalase showed a trend of having higher activity levels (**Table 13** and **Figure 36A-D**). The only exception was the [Tg(CAT)$^{\pm}$] E group. As shown in **Table 13** and reflected in **Figure 36**,

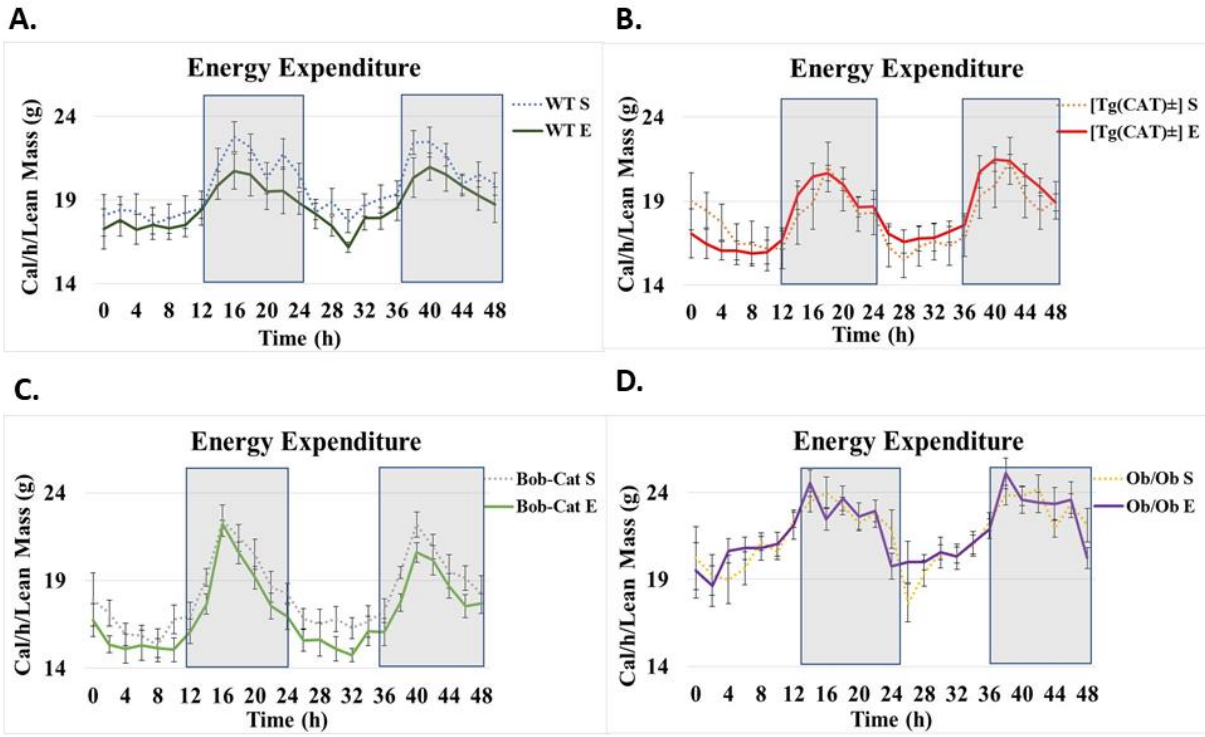

Figure 35. CLAMS analysis of energy expenditure over a 48h time period. Light and dark cycle CLAMS analysis of Energy Expenditure (EE) per 2h over a 48h time period in (A) WT (C57/WT), (B) [Tg(CAT)$^{\pm}$], (C) Bob-Cat, and (D) Ob/Ob exercised and sedentary mouse groups (n≥7/group). Metabolic EE averaged as Cal/h/Lean (g) body mass. One-way and two-way ANOVA followed by Bonferonni post hoc analysis were performed on GraphPad Prism 7. Data is represented as mean ± S.E.M.

Ob/Ob mice had the lowest levels of physical activity ($p<0.05$), independent of exercise intervention and the time of day, compared to every other mouse group. As observed in other

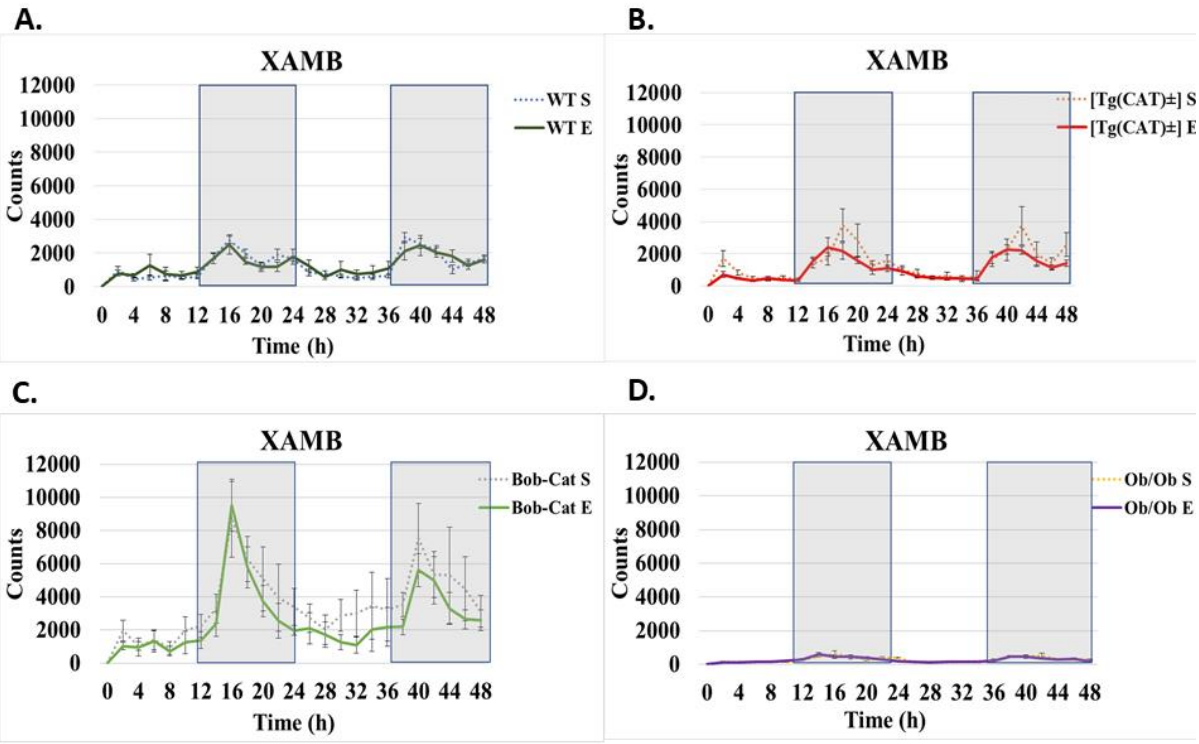

Figure 36. CLAMS analysis of total activity over a 48h time period. Light and dark cycle CLAMS analysis of X-Ambulatory movement (XAMB) per 2h over a 48h time period in (A) WT (WT/C57), (B) [Tg(CAT)±], (C) Bob-Cat, and (D) Ob/Ob exercised and sedentary mouse groups. (n≥7/group). One-way and two-way ANOVA was performed on GraphPad Prism 7. Data is represented as mean ± S.E.M.

metabolic measurements, mice overexpressing catalase continued to show intriguing results. As previously mentioned, the [Tg(CAT)$^{\pm}$] E mouse group had lower (light cycle) or similar XAMB levels (dark cycle) to the WT S mice, but Bob-Cat mice independent of intervention had significantly higher levels of activity compared to the WT S groups ($p<0.01$) (**Table 13**). This further provides evidence of an antioxidant and exercise effect on metabolic pathways in this novel mouse model.

4.3.6 Synergistic Effects of Exercise and Antioxidant Catalase on Skeletal Muscle Function

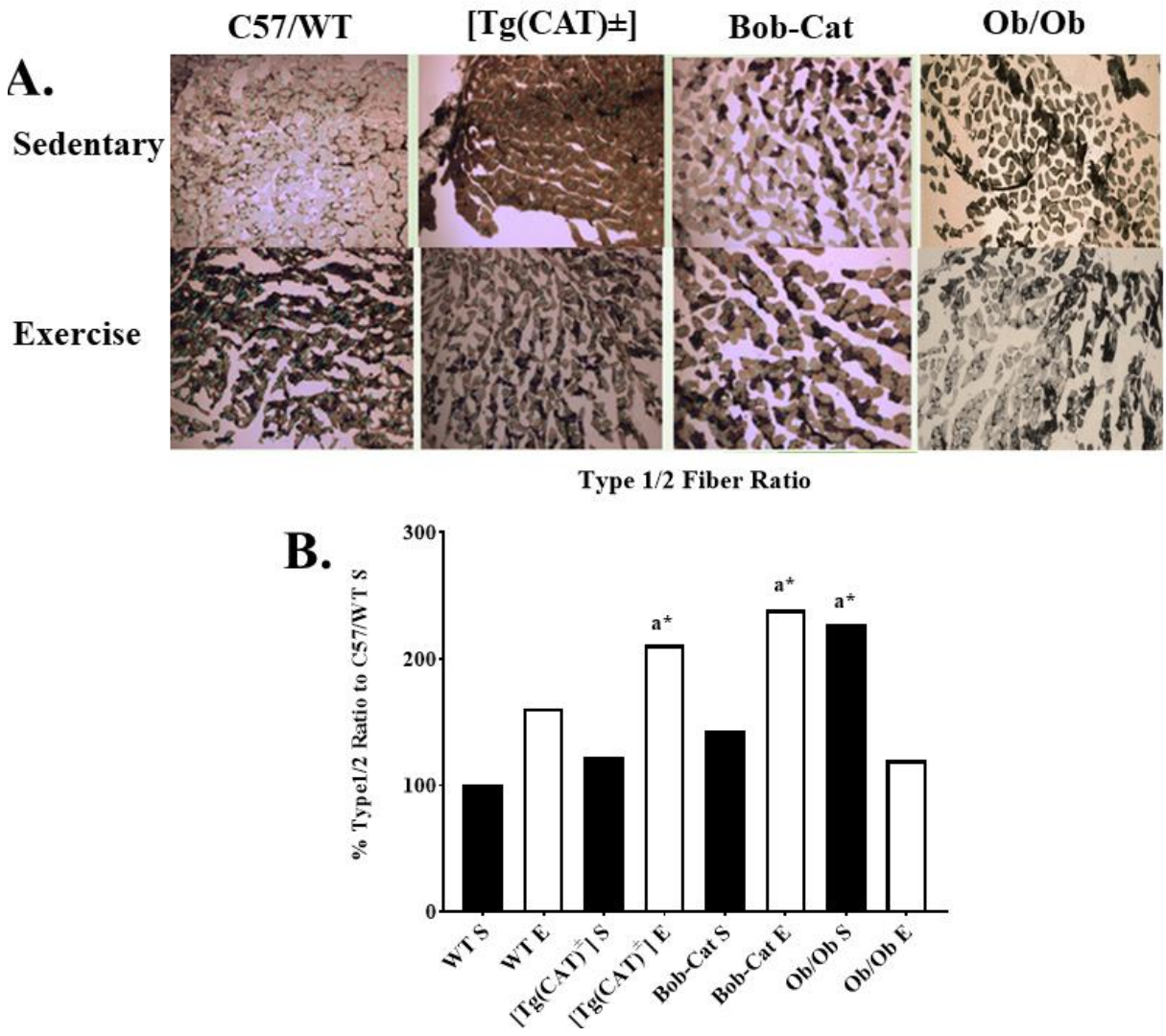

Figure 37. Type 1 / Type 2 fiber type ratio in the gastrocnemius skeletal muscle. (A) Skeletal muscle ATPase fiber type analysis (pH 4.3) images (black Type 1 vs. gray-shaded stains of Type 2 fibers) of exercised and sedentary C57/WT, [Tg(CAT)$^{\pm}$], Bob-Cat, and Ob/Ob mouse groups and (B) fiber type analysis of Type 1 / 2 ratios evidencing antioxidant and exercise intervention induced a general trend for higher Type 1 / 2 fiber ratios vs. C57/WT sedentary mice. Data shown as % of Type 1 / Type 2 fiber type ratio vs. C57/WT sedentary mice ($n \geq 6$). One-way and two-way ANOVA followed by Bonferonni post hoc tests in addition to preplanned t-tests between exercised mice and their sedentary controls were performed on GraphPad Prism 7. Significance was denoted as a*= $p<0.05$ to WT sedentary (S) group.

Exercise is known to induce morphological and physiological changes in skeletal muscles that are beneficial for metabolic health (Schnyder & Handschin, 2015; B. So et al., 2014). Therefore, we analyzed differences in muscle weight during tissue collection, grip strength (Deacon, 2013), Type 1 / Type 2 fiber type ratio, and key myokine expression and secretion. No differences were seen in average muscle weight of the Gas (0.12- 0.17g) or Soleus muscle (≤ 0.01g) within each mouse group. In addition, there were no significant differences seen within the various groups in the grip strength test. The Gas muscle is comprised of both Type 1 and Type 2 muscle fibers, while the soleus muscle is predominately comprised of Type 1 muscle fibers (Gollnick & Hodgson, 1986). Therefore, we used the Gas muscle to determine alterations in fiber type as a result of exercise intervention and antioxidant overexpression. Post staining for Myosin ATPase (pH 4.3), which provided visual evidence of Type 1 (dark) and Type 2 fibers (shades of gray) (**Figure 37**), we observed a significant increase in the Type 1 / Type 2 fiber ratio of all exercised mouse groups, except for the Ob/Ob E group ($p<0.05$). This observation within the Ob/Ob E group may have been a result of their leptin mutation since leptin is an adipokine involved in the skeletal muscle-adipose axis (A. Rodriguez et al., 2017). Most interestingly, as shown in **Figure 37**, the [Tg(CAT)$^{\pm}$] E and Bob-Cat E groups showed the highest Type 1 / Type 2 muscle fiber ratio ($p<0.05$; 211% and 239% increase respectively vs WT S). With these evidences, exercise and antioxidant overexpression had a synergistic effect on the fiber type ratio within the Gas muscle.

Increasing evidence indicates that Type 1 and Type 2 muscle fibers express and secrete different proteins which can have both autocrine and paracrine effects (Hoffmann & Weigert, 2017; S. Jung & Kim, 2014; Mizgier, Rutti, Pinget, & Bouzakri, 2018). Therefore, as a direct effect of exercise, and a synergistic effect with the combination of increased endogenous antioxidant altering the fiber type ratio, we further analyzed key myokine mRNA gene expression within the Gas skeletal muscle tissue using RT-qPCR (**Table 14**).

	mRNA Expression Fold Change to WT S Controls					**Plasma (ug/mL)**
Mouse Group	**GLUT 4**	**IL-6**	**FGF-21**	**PGC1-alpha**	**FNDC5**	**Irisin**
C57/WT S	1	1	1	1	1	2.96 ± 0.48
C57/WT E	2.5 b*	2.33	4.4	2.2	1.61 a*	2.72 ± 0.12
[Tg(CAT)±] S	1.32	1.48	1.52	0.33	0.92	3.58 ± 0.09
[Tg(CAT)±] E	2.51 b*	2.52	9.44 b*	2.35	2.37 a*a*s	2.66 ± 0.20
Bob-Cat S	1.33	1.79	2.42	1.7	1.23	3.65 ± 0.66
Bob-Cat E	1.68	1.15	3.73	2.13	1.83	2.98 ± 0.05
Ob/Ob S	0.92	0.78	6.06 a*	1.56	2.38	3.45 ± 0.14
Ob/Ob E	0.14 a*	1.66	5.54	1.12	2.36	2.40 ± 0.29

Table 14. Gastrocnemius skeletal muscle myokine expression. Skeletal muscle mRNA expression of exercise-induced myokines (GLUT 4, IL-6, FGF-21, PGC1-alpha, and FNDC5) were determined within the gastrocnemius skeletal muscle of each sedentary (S) and exercised (E) group by RT-qPCR. In addition, circulating levels of plasma irisin (ELISA) were also evaluated. ($n \geq 3$). mRNA expression is depicted as fold change to sedentary C57/WT mice by Pfaffl ddCT method. Levels of plasma irisin are represented as mean ± S.E.M. One-way and two-way ANOVA was performed followed by Bonferonni post hoc analysis in addition to preplanned t-tests between exercised mice and their sedentary controls on GraphPad Prism 7. Significant differences are displayed with letters indicating p values: a=$p<0.05$, b= $p<0.01$; symbols represent significant differences between genotypes *= compared to WT S; an additional 's' represents significant differences between sedentary cohorts.

GLUT 4 is a glucose transporter expressed in skeletal muscle tissue that aids in regulation of glucose levels and is known to be induced by exercise (Ikeda et al., 2016). With oxidative stress known to play a key role in glucose homeostasis (Grattagliano et al., 2008), we sought to determine whether GLUT 4, being an exercise-induced myokine, significantly differed among the mouse groups. As shown in **Table 14**, exercise intervention showed an increased fold change ($p<0.05$) compared to the sedentary control groups. However, it was interesting to find the plasma glucose levels were slightly elevated in all exercised mice compared to their sedentary cohorts (**Table 12**).

IL-6 is another exercise-induced myokine that is also expressed in adipose tissue and macrophages (Febbraio & Pedersen, 2005; Leal et al., 2018; Raschke & Eckel, 2013). As shown in **Table 14**, within the Gas skeletal muscle, though not significant, IL-6 showed a trend for increased expression in both mouse groups overexpressing catalase, with an exacerbated effect observed in the [Tg(CAT)$^{\pm}$] E group (>2.5 fold induction).

Another myokine increased by exercise (Leal et al., 2018), and previously shown to be induced by alterations in redox stress, is Fibroblast Growth Factor 21 (FGF-21) (Gomez-Samano et al., 2017). It plays a key role in systemic glucose homeostasis (X. Lin et al., 2017) and has been shown to modulate adipose tissue function in addition to its browning, thus inducing thermogenesis/energy expenditure (BonDurant et al., 2017; A. Rodriguez, Becerril, Ezquerro, Mendez-Gimenez, & Fruhbeck, 2016). As shown in **Table 14**, exercise intervention in each mouse group, apart from the Ob/Ob mice, caused an induction in FGF-21 levels in comparison to the WT control. Specifically, within the [Tg(CAT)$^{\pm}$] E and Bob-Cat E groups, there was > 8 fold ($p<0.01$) and 3 fold change (not significant) respectively.

With both groups expressing human antioxidant catalase, we expected oxidative stress levels within the skeletal muscle tissue played a role in the induced FGF-21 gene expression. Therefore, we also measured catalase activity using the established method of Aebi (Aebi, 1984).

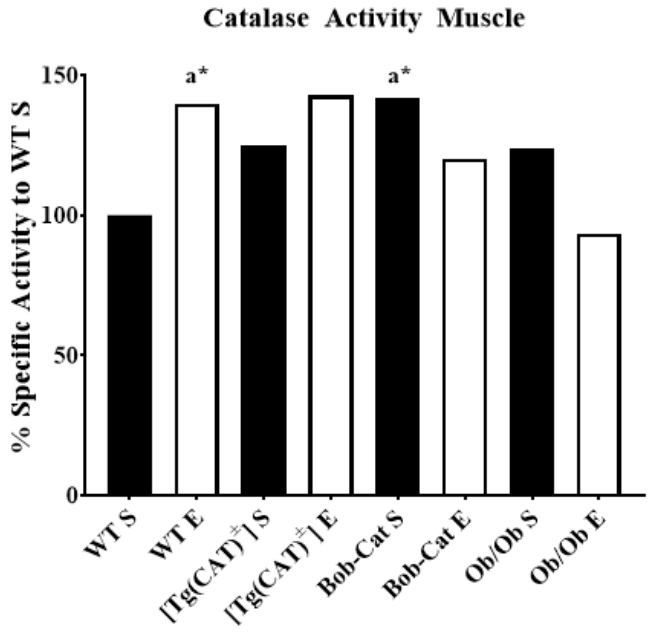

Figure 38. Skeletal muscle catalase activity level. Catalase enzymatic specific activity (U/mg protein) was calculated for each mouse using Aebi method. Data is represented as percent specific activity to the WT (C57/WT) S mouse group. One-way and two-way ANOVA followed by Bonferonni post hoc tests in addition to preplanned t-tests between each exercised group and their sedentary cohorts were performed on GraphPad Prism 7. Significance was considered as a*= $p<0.05$ to the WT sedentary (S) group.

Although not significant, specific activity calculations showed an increased level of Gas skeletal muscle catalase activity compared to the WT S group in both [Tg(CAT)$^{\pm}$] E and Bob-Cat E mice (**Figure 38**).

In recent years, one key signaling pathway that has received attention is the PGC1-alpha/FNDC5/Irisin pathway (Hoffmann & Weigert, 2017; Huh, 2018; Perakakis et al., 2017) which has been shown to be activated by exercise (Leal et al., 2018) and FGF-21 (Fisher et al., 2012; Sanchis-Gomar, Pareja-Galeano, Mayero, Perez-Quilis, & Lucia, 2014). With the induction of FGF-21 shown in the exercised mice overexpressing catalase (**Table 14**), we first

analyzed PGC1-alpha. Though not quite significant, an increased fold change in the mRNA expression of PGC1-alpha was observed in all mouse groups subjected to exercise intervention vs the WT S group and their sedentary cohorts. With this trend we further analyzed the mRNA expression of FNDC5 and saw the same effect compared to the WT S mice ($p<0.05$) (**Table 14**). Therefore, we further analyzed circulating plasma irisin levels since there has been evidence showing increased levels with chronic endurance exercise interventions (Leal et al., 2018). Surprisingly, we did not observe any significant differences within any mouse group.

4.3.7 Adipokine Expression and Adipose Tissue Redox Status

Not only does exercise play a role in skeletal muscle function, but it also decreases adipose tissue mass in addition to altering expression and secretion of key adipokines related to

	Fold Change to WT S	Protein Expression (Plasma)	Fold Change to WT S	Fold Change to WT S
Mouse Group	**Leptin mRNA**	**Leptin (pg/mL)**	**UCP-1 mRNA**	**Adiponectin mRNA**
C57/WT S	1.00	29.6 ± 13.8	1.00	1.00
C57/WT E	1.78	84.2 ± 18.8	1.08	1.55
[Tg(CAT)±] S	2.01	14.9 ± 5.3	1.69	0.49
[Tg(CAT)±] E	0.60	113 ± 46.8 b*b*s	0.58 b*	0.73
Bob-Cat S	0.51	43.61 ± 6.5	1.80	0.44
Bob-Cat E	1.66	27.5 ± 5.5	5.44	0.56
Ob/Ob S	0.60	1.34 ± 0.62	6.29 a*	0.05 b*
Ob/Ob E	0.81	0.97 ± 0.01	1.81 a*s	0.1 b*

Table 15. Adipose tissue expression level of key adipokines. mRNA expression of key adipokines (Leptin, UCP-1, and Adiponectin) involved in energy metabolism and/or inflammatory signaling were evaluated in the adipose tissue of each sedentary (S) and exercised (E) mouse group by RT-qPCR. ($n\geq3$) mRNA expression is displayed as fold change compared to C57/WT (WT) sedentary (S) mice determined by Pfaffl ddCT method. Plasma leptin levels were measured using a Mouse Adipokine Array (Millipore) on a Luminex system. One and two-way ANOVA followed by Bonferonni post hoc tests in addition to preplanned t-tests between each exercised and sedentary control were performed on GraphPad Prism 7. Significant differences are displayed with letters indicating p values: a=$p<0.05$, b= $p<0.01$; symbols represent significant differences between genotypes *= compared to WT S; an additional ‘s’ represents significant differences between sedentary cohorts.

energy metabolism (Golbidi & Laher, 2014). In recent years, evidence has indicated a crosstalk between skeletal muscle and adipose tissue (Leal et al., 2018). Some of the key factors speculated to be involved in the crosstalk include IL-6, FGF-21, irisin, and leptin (Hoffmann & Weigert, 2017; Roca-Rivada et al., 2013; A. Rodriguez et al., 2016). With our novel model showing decreased adipose tissue mass in each exercised mouse group (**Figure 30** and **Table 11**), we sought to determine if there were differences in the adipokine leptin, a 42 kD protein produced primarily in adipose tissue and a key regulator of energy homeostasis.

Leptin regulates appetite by hypothalamic signaling in the arcuate nucleus (Frago & Chowen, 2015; Wilson & Enriori, 2015). More recently it has been shown to be involved in the crosstalk between adipose tissue and secretion of myokines (A. Rodriguez et al., 2016). Compared to the WT S group, the exercised, antioxidant-overexpressing mice showed opposing effects (**Table 15**). Although not significant, the [Tg(CAT)$^{\pm}$] E group showed a slight decrease in expression while the Bob-Cat E, similar to the WT and Ob/Ob exercised groups, showed a trend for increased expression. We further analyzed plasma leptin levels using a mouse adipokine array and found that in circulation, the group with the highest leptin levels was the [Tg(CAT)$^{\pm}$] E while Bob-Cat E had similar levels in comparison to the WT S group (not significant).

On the other hand, with an upregulation of FGF-21 expression in the skeletal muscle tissue of the antioxidant overexpressing mouse groups, we analyzed the downstream modifications expected to occur in adipose tissue. FGF-21 is known to have a beneficial metabolic effect in adipose tissue by inducing browning through upregulation of UCP-1 (Fisher et al., 2012; P. Lee et al., 2014). We found this to have occurred within the Bob-Cat E mice with a 5-fold increase (trend) in UCP-1 mRNA expression compared to the WT S group. Interestingly, contrary to the Bob-Cats, [Tg(CAT)$^{\pm}$] E mice had a significant decrease in UCP-1

expression ($p<0.05$) vs the WT S group. Nonetheless, specifically within the Bob-Cat E group we observed the highest fold change of FGF-21 in adipose tissue. This may also have been a factor in the decreased body weight and fat mass at the end of the exercise study (**Figure 29 & 30, Table 11**). Additionally, a few studies have discussed the interaction between exercise-induced myokine FGF-21 and adiponectin (Manole, Ceafalan, Popescu, Dumitru, & Bastian, 2018). Therefore, we also analyzed adipose tissue adiponectin levels. Although no significant differences were noted between the genotypes, evidence was shown for an induction of adiponectin ($p<0.05$) in exercised groups providing evidence of adipose - skeletal muscle crosstalk.

As analyzed in the skeletal muscle tissue, we also evaluated the oxidative state of the adipose tissue by detecting oxidized carbonyl groups and measuring catalase activity levels (**Figure 39A-B**).

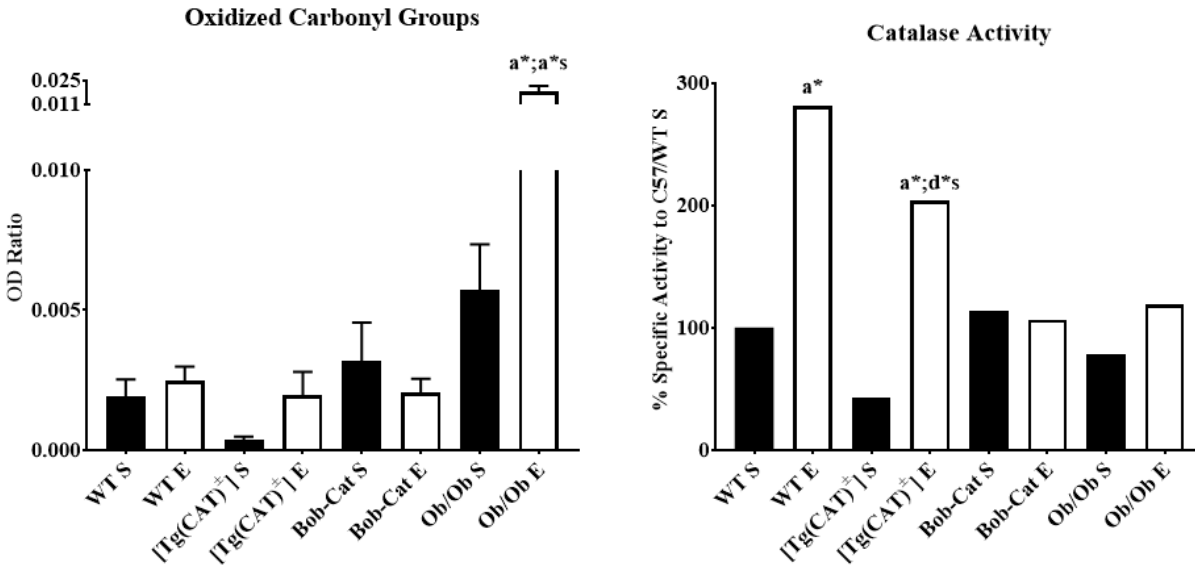

Figure 39. Oxidized carbonyl groups and catalase activity in adipose tissue. (Left) Oxyblot of oxidized carbonyl groups shown as densitometric ratios of oxidized proteins to total proteins (memcode) in adipose tissue of C57/WT (WT), [Tg(CAT)$^{\pm}$], Bob-Cat, and Ob/Ob sedentary (S) and exercised (E) mouse groups. Error is reported as mean ± S.E.M. (Right) Catalase enzymatic specific activity in adipose tissue (U/mg protein) was calculated for each mouse using the Aebi method. Data is represented as percent specific activity of each mouse group to the WT S group. One and two-way ANOVA followed by Bonferonni post hoc analysis and preplanned t-tests were performed using GraphPad Prism 7. Significance was considered as $p<0.05$, a*= $p<0.05$, d* $p<0.0001$ to the WT sedentary (S) group; an additional 's' represents significant differences between sedentary cohorts.

There were no significant differences in oxidative stress levels (oxidized carbonyl groups) between the antioxidant-overexpressing groups and WT mouse groups, but the Ob/Ob mouse groups had the highest levels of carbonylated proteins as shown in **Figure 39A**. Analysis of catalase activity showed both WT E and [Tg(CAT)$^{\pm}$] E mouse groups had significantly increased catalase activity levels (**Figure 39B**) compared to the sedentary control group. Bob-Cat E mice enzymatic activity levels were similar yet slightly increased compared to the WT S

mouse group. These results indicate that specifically, antioxidant catalase may be playing a role in adipose tissue function.

4.3.8 Hypothalamic Appetite Regulation

	mRNA expression Fold Change to C57/WT S Controls			
Mouse Group	**NPY**	**LepR**	**POMC**	**BDNF**
C57/WT S	1	1	1	1
C57/WT E	0.74	4.35 b*	5.54 a*	3.61 a*
[Tg(CAT)±] S	0.96	6.79 a*	5.89 b*	3.88
[Tg(CAT)±] E	0.76	3.09	8.29 a*	2.79
Bob-Cat S	1.2	6.7 a*	2.07	6.04
Bob-Cat E	0.94	2.83	3.52	1.34 b*
Ob/Ob S	1.65	4.15 a*	7.98 a*	2.18
Ob/Ob E	1.46	5.41 a*	12.77	3.64

Table 16. Hypothalamic mRNA gene expression. mRNA expression analysis of key genes involved in hypothalamic appetite regulation and neurogenesis (NPY, LepR, POMC, and BDNF) in the hypothalamic region of the brain by RT-qPCR. Expression levels within each sedentary (S) and exercised (E) mouse genotype are depicted as fold change to sedentary C57/WT (WT) mice by Pfaffl ddCT method. ($n \geq 3$). One-way and two-way ANOVA followed by Bonferonni post hoc test and preplanned t-tests were performed on GraphPad Prism 7. Significant differences are displayed with letters indicating p values: a=$p<0.05$, b= $p<0.01$; symbols represent significant differences between genotypes *= compared to WT S mice.

There is a well-known link between adipose tissue and hypothalamic signaling through the satiety hormone leptin (J. Friedman, 2016; Kwon, Kim, & Kim, 2016). Although we did not observe significant changes within the adipose tissue with regard to leptin mRNA expression nor plasma leptin levels (**Table 16**), we did observe changes in body weight, fat mass, and metabolic parameters which are impacted by neurons within the hypothalamus of the brain (Benite-Ribeiro et al., 2016; Funahashi et al., 2003). mRNA expression of the key orexigenic (NPY) and anorexigenic (POMC) genes were detected within each mouse group along with Brain Derived Neurotrophic Factor (BDNF). BDNF has been shown to be upregulated by exercise (Jodeiri Farshbaf et al., 2016) and plays a role in anxiety, cognition, mood, and behavior (Archer, Josefsson, & Lindwall, 2014). With regard to appetite regulation, we saw that there was a trend

for all exercised groups to have a decreased fold change in NPY mRNA expression (**Table 16**), which could cause a decrease in food intake.

On the other hand, there was an increased expression of LepR (would induce satiety) within every mouse group in comparison to the WT S mice except the [Tg(CAT)$^{\pm}$] E and Bob-Cat E groups. POMC was also analyzed. Known for its downstream effects of induced satiety and increased energy expenditure, we found POMC in both the WT E and [Tg(CAT)$^{\pm}$] S group to have >5 fold increase ($p<0.05$), and the [Tg(CAT)$^{\pm}$] E ($p<0.05$) and Ob/Ob E ($p<0.05$) mice to have the highest mRNA expression. Surprisingly, the Bob-Cat S and E groups showed only a slight fold increase, but it was not significant compared to every other mouse group vs. the WT S mice.

BDNF levels were also measured since we saw significant changes in the brain weight (**Table 11**) and its level has been shown to be increased by exercise potentially through a PGC1-alpha, FNDC5, BDNF (Jodeiri Farshbaf et al., 2016; Siamilis et al., 2009). In comparison to the WT S group, the highest levels were seen in the Bob-Cat S mouse group. However, there was also a slight increase in the Bob-Cat E group (not significant) and almost a 3-fold increase in the [Tg(CAT)$^{\pm}$] E group.

4.3.9 Impact of Exercise on Microbial Composition and Predicted Function

4.3.9.1 Alpha Diversity

Numerous studies have shown shifts in the taxa and function of the gut microbiome as a result of physical activity in both humans and mice (J. Chen et al., 2018; Denou et al., 2016; Monda et al., 2017). Exercise has been shown to increase species richness, the number of beneficial microbes, the microflora diversity, and the development of commensal bacteria (Monda et al., 2017). Nonetheless, we are not aware of any studies who have investigated the

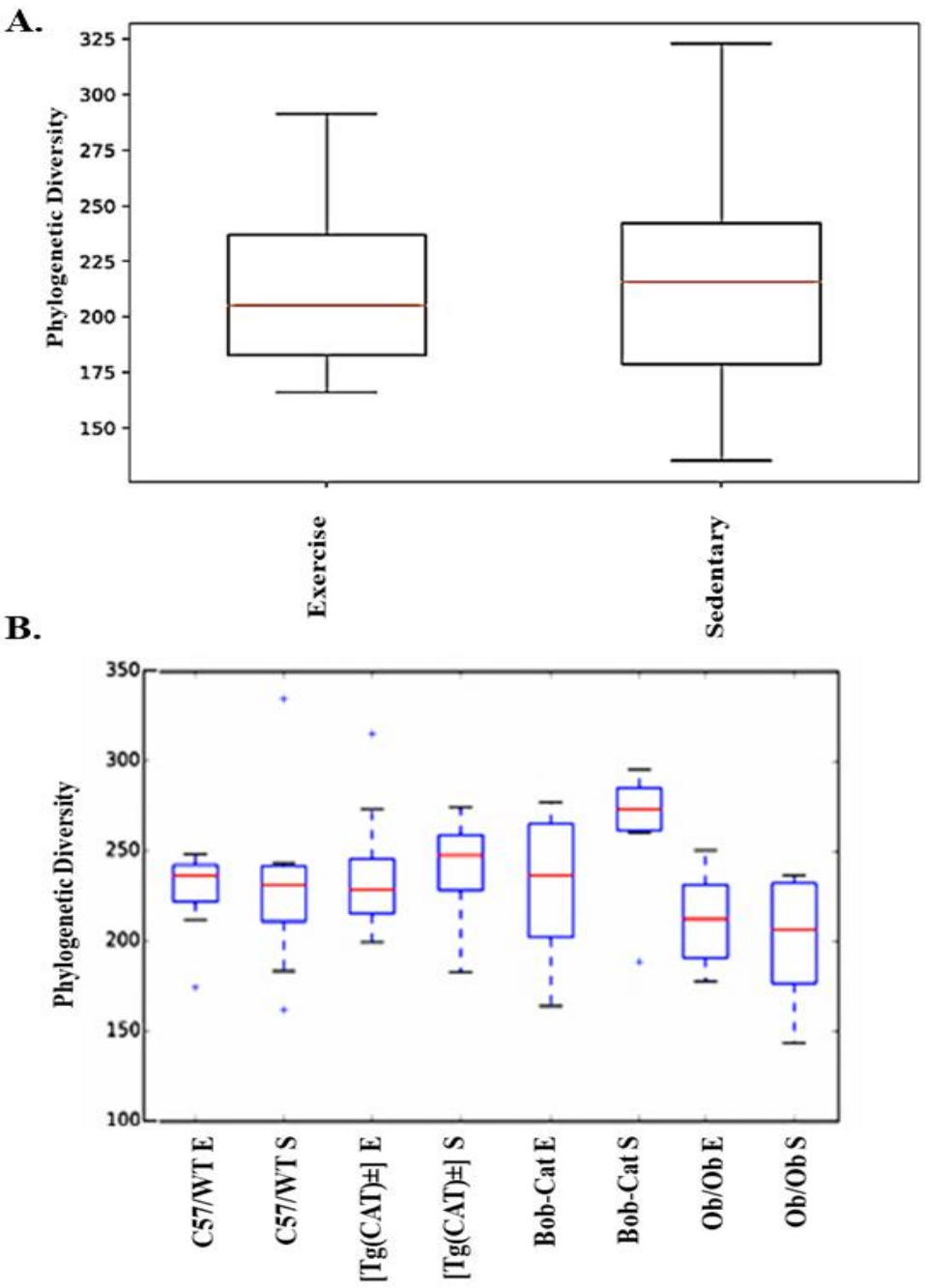

Figure 40. Boxplot of microbiome alpha diversity. A boxplot of the alpha diversity measured by Faith's phylogenetic diversity (PD) as implemented in QIIME of the (A) exercise and sedentary groups of all samples ($n \geq 27$) and (B) each intervention group per genotype ($n \geq 7$). A two-sample t-test and non-parametric Monte Carlo permutations (n = 999) were used for statistical analysis ($p < 0.05$).

synergistic effect of exercise and antioxidant overexpression on the composition and function of the gut microbiome. In our novel model, we observed changes in skeletal muscle morphology,

myokine/adipokine crosstalk, and appetite regulation with exercise which may have been a result of shifts in the gut microbiome in response to increased catalase or exercise intervention. Therefore, to further our knowledge in the field, the variable regions 3 and 4 of bacterial 16S rRNA genes were amplified by PCR and sequenced using the Illumina MiSeq platform. To determine the microbiota phylogenetic richness in each fecal sample, we analyzed the alpha diversity. No significant differences were shown between sedentary and exercised mouse groups (**Figure 40A**).

Because genotype could have played a role in the alpha diversity assessment, we chose to also analyze alpha diversity between the genotypes on sedentary or exercise regimen. When only considering the sedentary cohorts, despite differences in species richness, no statistically significant differences were observed between any pairwise cohort-to-cohort groups. This same effect was seen when only considering the exercise cohorts. Further analysis of each individual mouse group (genotype and exercise) showed slight differences in species richness, but none were statistically significant (**Figure 40B**).

4.3.9.2 β Diversity

Exercise is also known to shift the microbial species composition (Denou et al., 2016). To determine whether there were phylogenetic differences in microbial community composition (β Diversity) between the sequenced fecal samples, principal coordinate analysis (PCoA) of weighted UniFrac distances between the fecal boli samples of the various mouse groups were generated based on a CSS normalized OTU table (Paulson et al., 2013). Pairwise comparison between exercise and sedentary groups yielded significantly different clustering (anosim

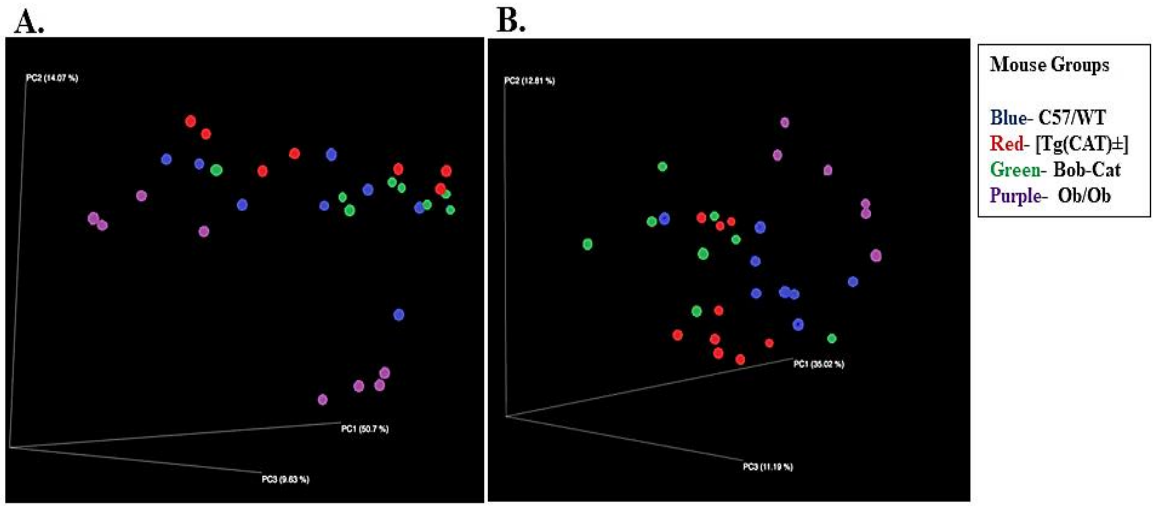

Figure 41. β-Diversity plots of sedentary and exercised mice. PCoA plots of phylogenetic differences in microbial community composition between sequenced sedentary and exercised samples. (A) C57/WT (blue), [Tg(CAT)$^{\pm}$] (red), Bob-Cat (green), and Ob/Ob (purple) sedentary mouse groups and (B) of each respective exercised cohort is displayed in the images showing a defined microbial community composition within each genotype (anosim $p < 0.05$). ($n \geq 6$)

$p<0.05$), indicating a profound shift in microbial community composition dependent on exercise. Further analysis comparing the genotypes of sedentary samples (**Figure 41A**) showed significant clustering between cohorts at an anosim $p= 0.001$, indicating a defined microbial community composition within each respective mouse group. Comparing each genotype of exercised mice (**Figure 41B**) showed the same result thus indicating a defined microbial community

composition within each respective exercised cohort. Finally, we determined if there were significantly different microbial community compositions between each genotype (**Figure 42A-D).**

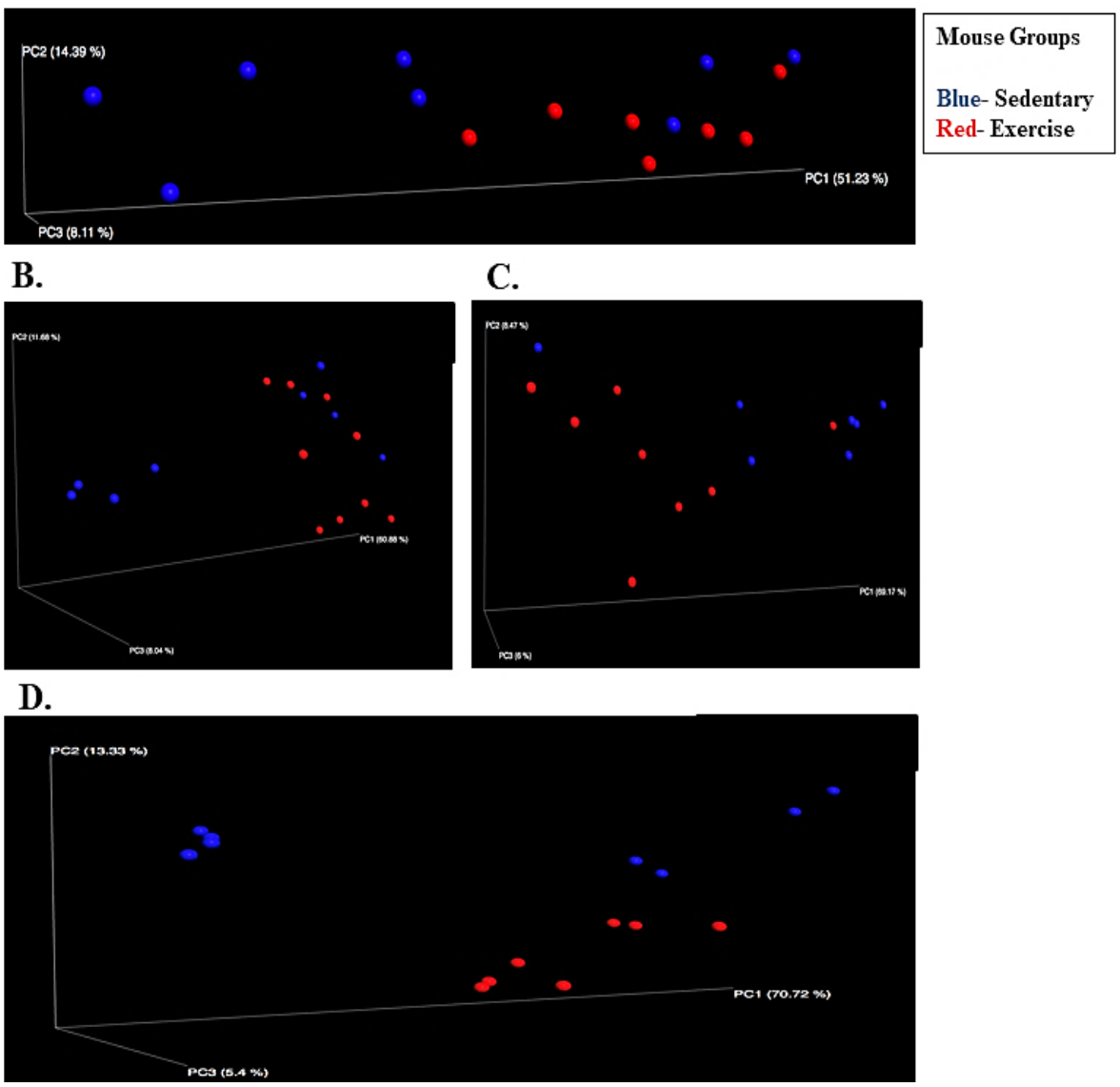

Figure 42. β-Diversity plots per genotype. PCoA plots of phylogenetic differences in microbial community composition between sequenced sedentary and exercised samples per mouse genotype. (A) C57/WT, (B) [Tg(CAT)$^{\pm}$], (C) Bob-Cat, and (D) Ob/Ob mouse groups (sedentary depicted as blue and exercise depicted as red dots) as displayed in the images show a defined microbial community composition within each E and S group of each genotype (anosim $p < 0.05$). ($n \geq 6$)

Significant clustering was observed within each genotype: C57/WT: anosim p= 0.031, [Tg(CAT)$^{\pm}$]: anosim p= 0.025, Bob-Cat: anosim p= 0.033, and Ob/Ob: anosim p= 0.021. Therefore, our data shows evidence of a defined microbial community composition within exercised and sedentary mice of each respective genotype.

4.3.9.3 Taxa LEfSE Analysis

With significant differences observed in microbial composition between sedentary and exercised groups within each genotype, we conducted LEfSE analysis to compare the microbial taxa. This allowed identification of taxonomy shifts in the microbial community composition. Comparison diagrams were created based on LEfSE results among sedentary mouse groups and separately among exercised groups of each genotype in comparison to the C57/WT mice. Between the sedentary groups it was interesting to find that the mice overexpressing catalase both were enriched with Rikenellaceae and Helicobacteraceae. Additionally, the sedentary Bob-Cat and Ob/Ob shared the taxa Weeksellaceae and Erysipelotrichaceae. Comparisons between the exercised mouse groups showed that the mouse groups overexpressing catalase were both enriched with the Helicobacteraceae while both the C57/WT and Ob/Ob mice were both enriched with Rikenellaceae. Additionally, it was interesting to find that the [Tg(CAT)$^{\pm}$] E mice were enriched with the Bifidobacteriaceae which has been shown to be increased with exercise intervention and is known to produce the SCFA butyrate (Munukka et al., 2018; Rivière, Selak, Lantin, Leroy, & De Vuyst, 2016).

We subsequently conducted an analysis to determine the impact of exercise within each specific mouse group (**Figures 43-46**). LEfSE analysis plots portrayed significantly enriched bacterial taxonomy within the sedentary and exercise cohorts of each mouse model (**Figure 43-46**).

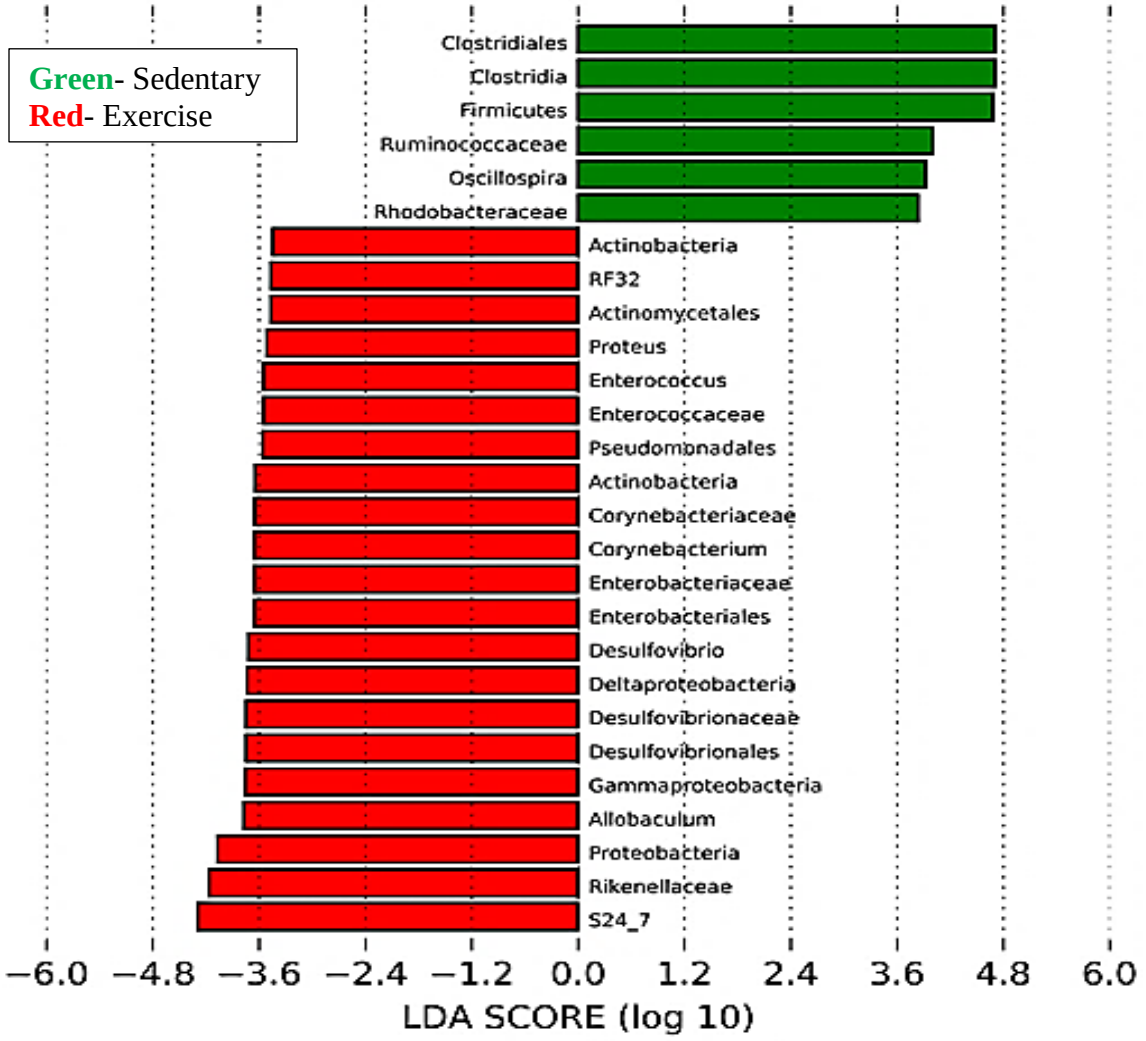

Figure 43. C57/WT taxa LEfSe analysis. Linear discriminant analysis (LDA) scores derived from LEfSe analysis showing the biomarker taxa (LDA score >2.0 and significant at $p<0.05$) of C57/WT mouse groups (green- sedentary; red-exercise) determined by Kruskal–Wallis and pairwise Wilcoxon tests. ($n\geq7$)

A total of 27 significantly differential taxa between C57/WT S and C57/WT E cohorts were observed. Of the sedentary C57/WT samples, there was an enrichment of bacteria belonging to the Firmicutes Phylum while the exercised samples showed an enrichment of the Bacteriodes S24-7**.** At the genus level, sedentary groups were significantly enriched in *Oscillospira*, while exercised groups were enriched in *Corynebacterium, Enterococcus, Desulfovibrio, and Proteus*. In comparing the [Tg(CAT)$^{\pm}$] E and S groups, LEfSE analysis only showed a total of 3 significantly different taxa, the fewest differential taxa of all experimental groups, comparing the exercise and sedentary mice (**Figure 44**).

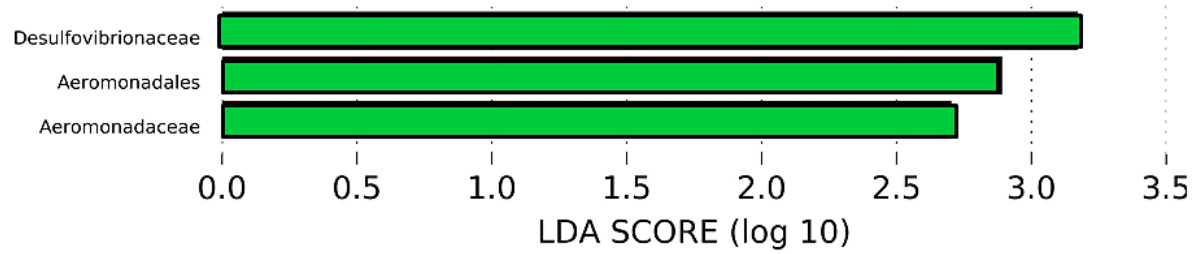

Figure 44. [Tg(CAT)±] taxa LEfSe analysis. Linear discriminant analysis (LDA) scores derived from LEfSe analysis showing the biomarker taxa (LDA score >2.0 and significant at $p<0.05$) of [Tg(CAT)$^{\pm}$] sedentary mouse groups (no significantly enriched taxa in the exercised cohort compared to the sedentary mice) determined by Kruskal–Wallis and pairwise Wilcoxon tests. ($n\geq7$)

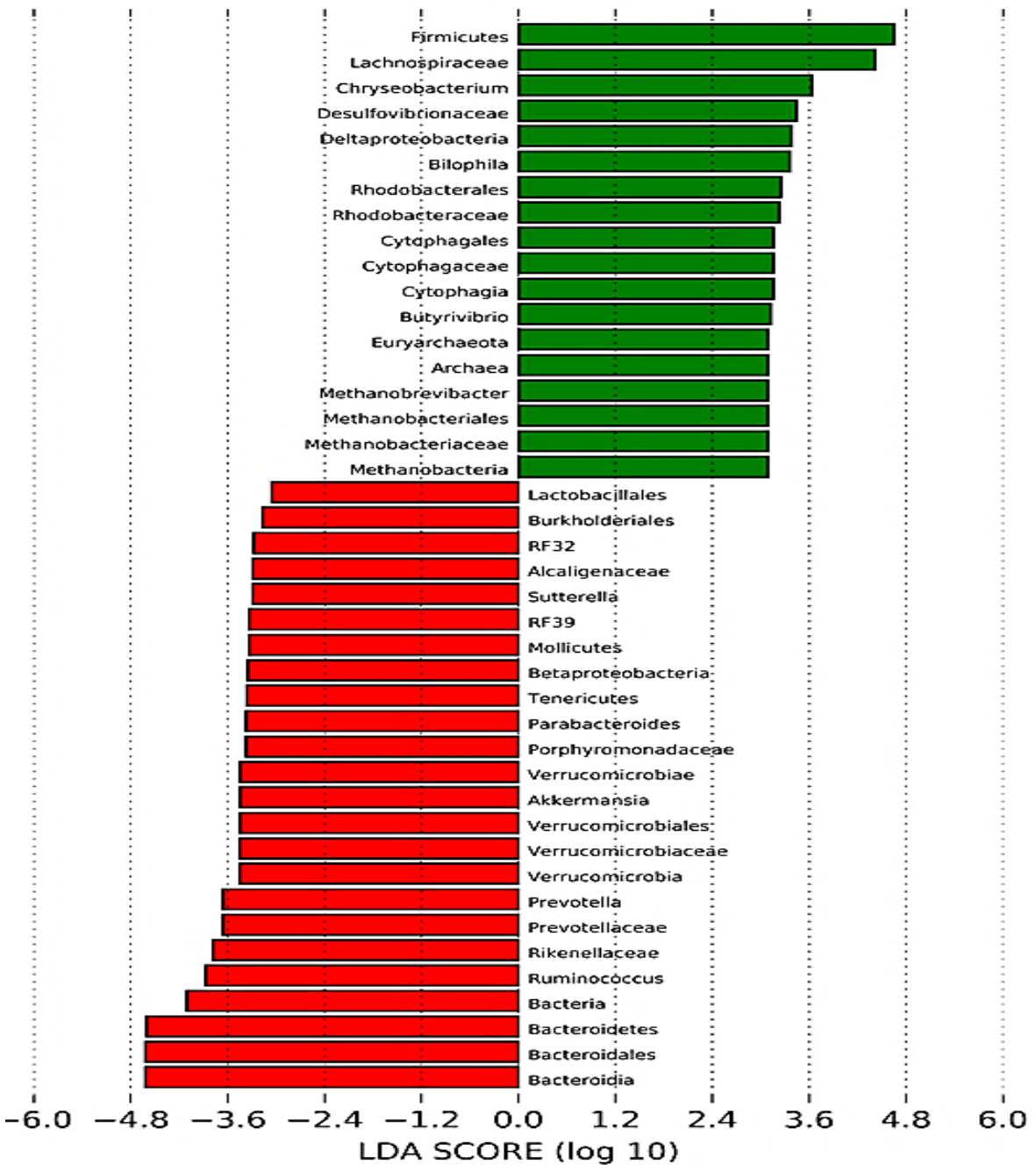

Figure 45. Bob-Cat taxa LEfSe analysis. Linear discriminant analysis (LDA) scores derived from LEfSe analysis showing the biomarker taxa (LDA score >2.0 and significant at $p<0.05$) of Bob-Cat mouse groups (green- sedentary; red-exercise) determined by Kruskal–Wallis and pairwise Wilcoxon tests. ($n\geq7$)

Also interesting was that all enriched taxa were identified within the sedentary cohort where

there was an enrichment of Desulfovibrionaceae and Aeromonadaceae at the family level. Within the Bob-Cat mouse groups, LEfSe analysis determined there was a total of 42 significantly differential taxa between the sedentary and exercise cohorts (**Figure 45**).

This was the highest number of significantly differentiating taxonomy compared to every other genotype analyzed. As with the C57/WT mice, there was also an enrichment of Firmicutes within the sedentary groups, while within the exercised Bob-Cats, the Bacteroidales was enriched. At the genus level, sedentary mice were enriched in *Methanobrevibacter, Chryseobacterium, Butyrivibrio,* and *Bilophila* in comparison to their exercised cohorts. Exercised Bob-Cat mice had significantly higher levels of *Parabacteroides, Prevotella, Ruminococcus, Sutterella,* and *Akkermansia*. Within the obese, Ob/Ob mouse groups there was a total of 26 significantly differential taxa between the exercised and sedentary cohorts (**Figure 46**).

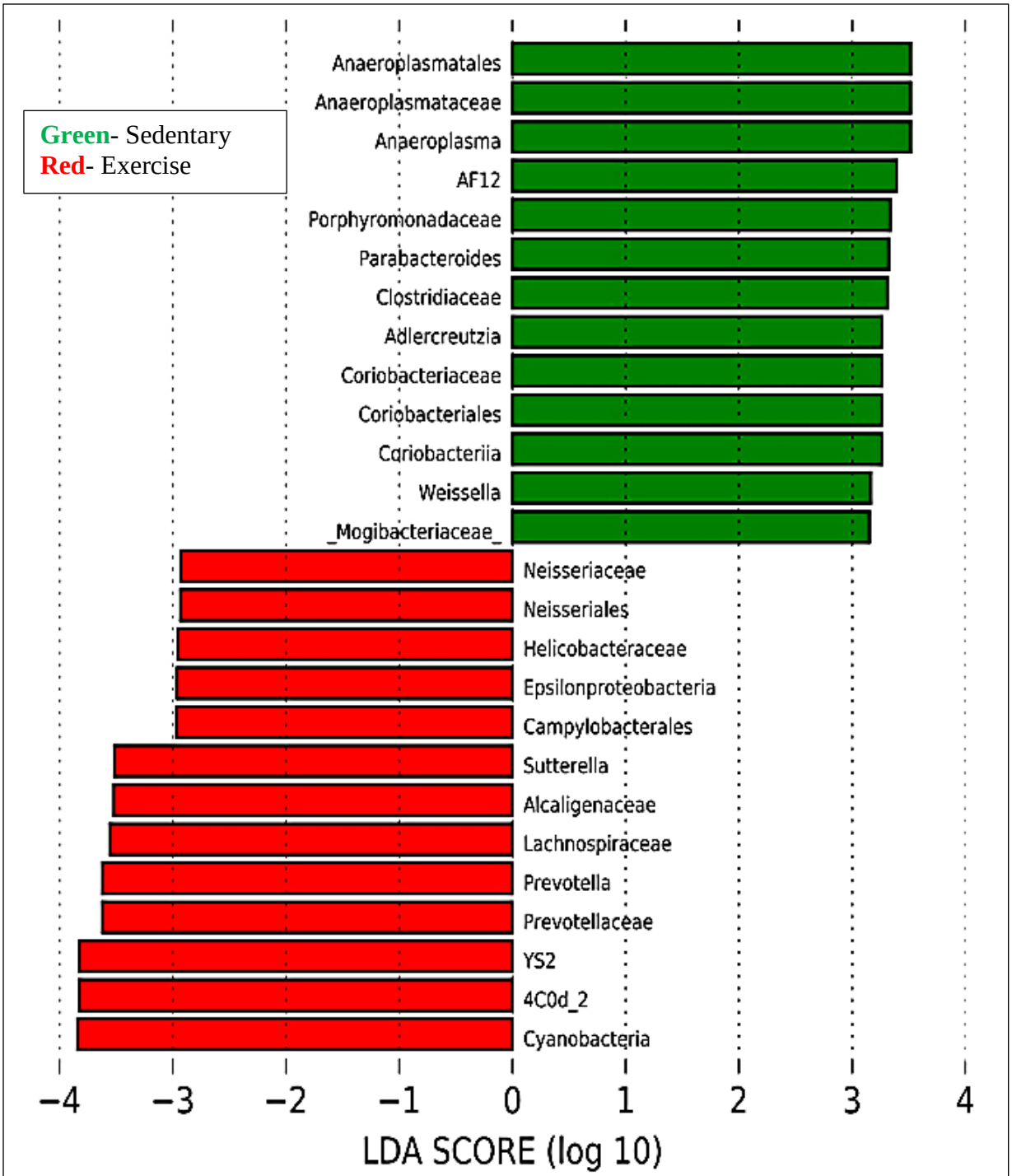

Figure 46. Ob/Ob taxa LEfSe analysis. Linear discriminant analysis (LDA) scores derived from LEfSe analysis showing the biomarker taxa (LDA score >2.0 and significant at $p<0.05$) of Ob/Ob mouse groups (green- sedentary; red-exercise) determined by Kruskal–Wallis and pairwise Wilcoxon tests. ($n\geq7$)

Specifically, the Lachnospiraceae were enriched in the exercised cohort compared to the Ob/Ob S group. Interestingly, with Ob/Ob mice being the parent group of Bob-Cat genotype, this family was also enriched in the Bob-Cat S mice yet significantly depleted in the Bob-Cat E group. Additionally, Ob/Ob S mice had significantly higher levels of *Adlercreutzia, Parabacteroides, AF12, Weissella,* and *Anaeroplasma,* while exercised groups had significantly higher levels of *Prevotella* and *Sutterella*.

4.3.9.4 PICRUSt Pairwise LEfSe Analysis

Dependent upon the microbial species present and their interaction with one another, their overall impact on the host organism changes (Heiss & Olofsson, 2018). To determine the predicted function of each mouse group's gut microbiome, PICRUSt functional predictions were generated from 16S data for each fecal sample and uploaded to the LEfSe analysis tool for functional biomarker identification between the exercise and sedentary cohort of each mouse genotype. We observed a total of 7 significantly differential functional predictions between the sedentary and exercise cohorts of the C57/WT genotype. Of all the remaining cohorts, the C57/WT genotype had the fewest number of predicted functional pathways. LEfSe analysis distinguished 29 significantly differential functional predictions between the [Tg(CAT)$^{\pm}$] S and E cohorts. Sedentary mice showed an enrichment of bacteria predicted to carry out butyrate metabolism, dioxin degradation, and xylene degradation. Within the [Tg(CAT)$^{\pm}$] E mouse group, glycan biosynthesis and metabolism as well as glycan degradation were significantly enriched. A profound number of 118 significantly differential functional predictions were found between Bob-Cat S and E cohorts by LEfSe analysis. The high number of functional predictions enriched in the exercised samples, indicates exercise contributes a strong effect on the functional potential of the microbial community. Within the Bob-Cat S group, several functional pathways involved

in cell motility were enriched including flagellar assembly, bacterial motility proteins, and bacterial chemotaxis. Bob-Cat mice in the exercised cohort showed an enrichment of glycan biosynthesis, just as was seen in the [Tg(CAT)$^{\pm}$] E group. It is also interesting that bacteria capable of LPS biosynthesis were enriched in the Bob-Cat E group. LEfSe analysis of the Ob/Ob groups showed a total of 12 significantly differential functional predictions between the sedentary and exercise cohorts. One pathway particularly enriched was fructose and mannose metabolism within the Ob/Ob exercised samples.

4.4 DISCUSSION

Cardiometabolic diseases are characterized by increased levels of ROS that alter glucose and lipid signaling pathways in key metabolic organs such as adipose tissue, skeletal muscle, and brain (Barazzoni et al., 2018; Carrier, 2017; Rani et al., 2016). These effects lead to increased visceral fat mass and risk for adipose tissue inflammation, hyperglycemia, dyslipidemia, hyperleptinemia, and IR (Carrier, 2017). Both increased endogenous antioxidant expression and exogenous antioxidant supplementation mitigate the negative effects of high redox stress and lower risk in acquiring diseases of the metabolic syndrome (Drummond et al., 2011; Haidara et al., 2011; Park et al., 2016; B. Patel et al., 2018). Additionally, in lean and obese human and rodent models, increases in moderate physical activity lowers body weight and fat mass, increases insulin sensitivity, and induces browning of white adipose tissue (Leal et al., 2018; P. Lee et al., 2014; Nunan et al., 2013; Warburton et al., 2006). Nonetheless, the mechanisms leading to exercise's beneficial effects have not been fully elucidated. Recently, we showed evidence that mice overexpressing catalase in a genetically obese background (Bob-Cat), in contrast to the C56Bl6/WT mice, significantly lowered redox stress ('stress-less' mice), improved energy metabolism, and modulated the expression of key adipocytokines (D. L. Amos et al., 2017). In the present study, the effect of an eight-week moderate exercise intervention was evaluated in the 'stress-less' Bob-Cat mice overexpressing catalase compared to WT and sedentary controls. Results showed increased antioxidant levels within the 'stress-less' mice maintained or decreased body weight and fat mass when put on exercise intervention. Additionally, these novel mice maintained balanced energy metabolism, normal circadian rhythm, and showed a trend for increased HDL and decreased plasma TG levels. Most interestingly, we saw significant differences in skeletal muscle Type 1 / Type 2 fiber ratio and

mRNA expression of key myokines which may have induced a change in adipose tissue function via the skeletal muscle-adipose tissue axis (crosstalk). This study also provided evidence for an exercise and redox-induced shift in the gut microbiome and a change in hypothalamic appetite regulation as a mechanism of the beneficial impact of exercise on metabolic homeostasis in the mice overexpressing antioxidant catalase.

Mice overexpressing catalase exercised on a mouse treadmill, in contrast to WT mice and cohorts that remained sedentary for the 8 week study period, maintained or lowered body weight and fat mass. This was to be expected due to the effects of exercise causing a deficit in energy storage from increased energy output vs. input when the mice were sedentary (Fiuza-Luces et al., 2013; Leal et al., 2018; Sanchis-Gomar et al., 2015) although other studies have not observed significant decreases in body weight post-exercise. Nonetheless, pathways modulating energy metabolism were significantly altered (Denou et al., 2016). It is also intriguing that in all groups, with the exception of the Bob-Cat mice, catalase activity in adipose tissue was increased where we also observed a loss in body weight or fat mass. Recent studies have indicated that exercise combined with another anti-obesity intervention should be studied as a therapeutic method for metabolic disease (Leal et al., 2018). Our data shows in relation to body composition, endogenous overexpression of antioxidant and exercise may be an effective means of lowering body weight and fat mass. In addition to decreases in body weight and fat mass within these groups vs. the WT S group, it was interesting that the Bob-Cat E mice showed a trend for increased lean mass compared to their sedentary cohorts and the WT S group. Increased lean mass and lowering of fat mass would be indicative of a metabolically healthier body (Kelly, Nehrenberg, Hua, Garland, & Pomp, 2011). Opposed to the beneficial effects seen in increased antioxidant and/or exercise, the Ob/Ob group showed the most significant increases in body

weight and fat mass. They also showed increases in lean mass, but this was likely only a response to the increase in body size in general. Nonetheless, it is noteworthy that the Ob/Ob E group did not have as severe obesogenic markers as their sedentary cohorts.

Because it has been found that there are different metabolic effects dependent on the levels of SubQ vs. visceral adipose tissue (Bonomini et al., 2015; Harman-Boehm et al., 2007), we also recorded the weights of each fat depot at the end of the 8 week study period during tissue collection. Bob-Cat mice had similar levels of fat mass compared to their WT controls although both sedentary and exercised [Tg(CAT)$^{\pm}$] mouse groups showed decreased levels of fat mass in comparison to the WT control groups. This was reflective of what was observed by analysis using the ECHO-MRI. As expected, both Ob/Ob mouse groups had the highest measurements of both adipose depots, but the exercised mice did not accumulate as much fat mass as their sedentary cohorts. The higher levels of fat mass likely played a role in the higher levels of oxidized carbonyl groups as was seen in the oxyblot conducted on adipose tissue. Liver weights were also measured during tissue collection. Although not significant, Bob-Cat mice, independent of exercise intervention, showed a trend for higher liver weight compared to the WT control group. This was also seen in Bob-Cat mice when analyzed in our recent Omega 3 enriched dietary intervention study (D. Amos et al., 2019). Ob/Ob mice had a significantly lower brain weight compared to every other group. In previous studies, neurodegeneration and increases in chronic stress have been associated with lower brain mass (Lupien, McEwen, Gunnar, & Heim, 2009; Stern, 2012). Therefore, it was surprising that the exercised [Tg(CAT)$^{\pm}$] mouse group had significantly lower brain weight compared to the WT S group since their sedentary cohorts had a normal brain mass and exercise has been shown to positively impact brain development, neurogenesis, and overall function (Delezie & Handschin, 2018; Jodeiri

Farshbaf et al., 2016). Nonetheless, unlike the Ob/Ob group with a very large body size, the [Tg(CAT)$^{\pm}$] E group had a lower body weight, fat mass, lean mass, and other tissue weights compared to the other mouse groups. Therefore, it is reasonable to assume that brain weight would also be lower due to decreased body size in general. Body mass and fat/lean mass is reflective of both diet and lifestyle. Food consumption over the study period showed that the only group that consumed less chow than the WT control group was the sedentary [Tg(CAT)$^{\pm}$] mouse group. As shown in previous studies, exercise caused an increase in food intake over time (M. Martin et al., 2016; Melzer, Kayser, Saris, & Pichard, 2005). Additionally, due to energy expended during the physical activity, the exercised groups (except Ob/Ob mice) did not gain as much weight or fat mass, compared to the WT S group.

In addition to body composition, another beneficial effect of exercise is improvement in the lipid profile (J. Chen et al., 2018). All mouse groups, with the exception of the leptin deficient, Ob/Ob mice, showed levels of TC lower than the detection limit of the kit (<100 mg/dL) as shown in **Table 12**. As expected, highest levels of TC were evidenced in the Ob/Ob sedentary group with exercise showing a trend for lowering these levels in the exercised cohorts. HDL and TG levels are markers of metabolic health (Coqueiro et al., 2019; Fiuza-Luces et al., 2013; Sanchis-Gomar et al., 2015), where lower levels of HDL and higher levels of plasma TG are associated with obesity and other metabolic disorders (Bonomini et al., 2015; Bryan et al., 2013). As with previous research studies analyzing the effects of exercise, HDL levels were significantly increased and plasma TG levels were lowered in the mouse groups overexpressing catalase compared to the sedentary control group. However, specifically in the Bob-Cat S and E mice, HDL was significantly higher. These groups also had significantly higher liver weights than the WT control group (**Table 11**). It was also interesting that exercise increased the HDL

level in every mouse group with the exception of the Ob/Ob mice (not significant). Although HDL was highest among the Ob/Ob mouse groups, the TC was also very high. Previous studies have shown that the ratio of HDL to TC is more indicative of metabolic health than looking strictly at the level of HDL (Association, 2017; Coqueiro et al., 2019). In this case, it is evident the Ob/Ob mice do not have a healthy lipid profile with regard to cholesterol levels. With regard to TG levels, the [Tg(CAT)$^{\pm}$] E mice displayed the lowest levels ($p<0.05$) as shown in **Table 12**. This directly correlates with their low levels of adipose tissue compared to all the other mouse groups. Exercise intervention not only lowered the TG levels ($p<0.05$), but the effect was exacerbated in the mice overexpressing catalase. In addition to the lipid profile, we surprisingly saw a trend for increased levels of plasma glucose within the exercised groups compared to their sedentary cohorts. Typically, exercise lowers glucose levels (Fryer et al., 2002; Ikeda et al., 2016). Nonetheless, with the exception of the Ob/Ob mice, all other mouse groups fell under the normal range remaining well below 250 mg/dL (Collins, Martin, Surwit, & Robidoux, 2004). Contrary to glucose levels, exercise significantly lowered plasma insulin levels. This did not come as a surprise knowing that exercise is used as a therapy for T2D as a means of regulating insulin levels (Golbidi & Laher, 2014; Phillips et al., 2015). Although levels were still high, Ob/Ob mice subjected to exercise intervention had much lower levels than their sedentary cohorts. Nonetheless, not having the parent group as an obese mouse model, the [Tg(CAT)$^{\pm}$] mice on exercise intervention had the lowest levels of plasma insulin relative to the sedentary controls. One of the mechanisms involved in glucose and insulin homeostasis is through the translocation of GLUT 4 transporters. Skeletal muscle uses this particular GLUT for maintenance of energy and muscle integrity (Ikeda et al., 2016). With trends for an increase in

skeletal muscle mRNA of this transporter in exercise groups (**Table 14**), it is plausible that GLUT 4 was involved in the insulin lowering effects.

As an additional assessment of metabolic parameters, the CLAMS technology was utilized to measure FI over a 48 h time period. In comparing the group averages, we saw a trend for all exercised groups to consume more chow than their sedentary cohorts with the exception of the Ob/Ob mouse group. Furthermore, mice overexpressing catalase had the highest levels of intake among the groups when placed on an exercise regimen. This exercise effect is not uncommon where exercised organisms typically consume more energy to provide for muscle repair and to fuel the body during exercise (Melzer et al., 2005). However, it is more interesting that there was a trend seen specifically for the mice overexpressing catalase to have the highest food intake when their body weight, fat mass, and TG levels were lower than the WT mice on an exercise or sedentary regimen indicating an increase in energy utilization (**Figures 29&30** and **Tables 11&12**). Additionally, CLAMS analysis can be indicative of normal eating patterns and circadian rhythm which can change based on the frequency of food consumption (Sasaki, 2017). It was surprising that the Ob/Ob mice did not significantly differ in the time period food was consumed as had been observed in DIO mice in our previous study (D. Amos et al., 2019).

The CLAMS technology also measured the type of fuel primarily oxidized for energy production. RER measurements showed exercised mice within each genotype had an increase in the use of carbohydrates vs. fat for energy ($p<0.05$) compared to both the WT S group and their sedentary cohorts (**Figure 34**). This was not expected, as exercise typically increases fat oxidation in low intensity and moderate exercise (Ramos-Jiménez et al., 2008). However, most interesting was the differences observed between [Tg(CAT)$^{\pm}$] and Bob-Cat mice on exercise intervention. [Tg(CAT)$^{\pm}$] E mice showed the highest RER levels ($p<0.0001$) independent of the

light or dark cycle and thus the lowest levels of fat oxidation. Bob-Cat E mice, on the other hand, had increased levels of RER and CHO oxidation compared to their sedentary cohorts yet retained similar RER levels to the WT S group on average. Another novel finding was the Bob-Cat S mice had one of the highest levels of fat oxidation compared to all other groups. Ob/Ob mice showed results consistent with the previous literature compared to leaner phenotypes of mice where their RER was significantly higher due to their increased sedentary lifestyle and/or availability of fat to be taken from storage and oxidized for energy (Hirsch et al., 2016). These combined results provide evidence for an exercise and/or antioxidant effect on fuel utilization uncommon to previous data derived from exercise studies. Mechanisms behind this result may be indicative of alternate signaling pathways utilizing increased levels of carbohydrates.

In addition to the type of fuel utilized, systemic energy expenditure also plays a role in overall energy metabolism. CLAMS technology indirectly measures the EE of mice which is then used to compare the mouse groups based on the Cal/h/g of lean body mass. Additionally, the physical activity level (XAMB) was measured which also contributes to the energy output. We observed that exercised mice, with the exception of the Ob/Ob E group, had decreased levels of EE compared to the WT S group during both light and dark cycles. It was more interesting to see that the lowest levels were among the mice overexpressing catalase on exercise regimen. This is not uncommon for organisms with lower body mass expending energy through physical exercise. If the body reaches lower levels of fuel, it will begin to decrease energy used by the body as a means of being more fuel efficient. This concept, now termed “metabolic flexibility,” may be what was observed in these exercised mouse groups (Goodpaster & Sparks, 2017). During the CLAMS analysis, all mouse groups overexpressing antioxidant showed trends of higher physical activity (XAMB) compared to WT controls with the exception of the

[Tg(CAT)$^{\pm}$] E group. This phenomenon is often observed in exercised organisms (de Carvalho, Benfato, Moretto, Barthichoto, & de Oliveira, 2016). It is expected that it is due to the body being fatigued after the increased muscle movement/contraction during the exercised regimen resulting in lower levels of movement as a result. Nonetheless, this was not the case for the Bob-Cat exercised group. Ob/Ob mice had the lowest levels of physical activity ($p<0.05$) independent of exercise intervention as well as the time of day compared to every other mouse group. This was expected as it would take much more effort for these groups to move across the cage with their high body weight. The combined data derived from the CLAMS technology, body composition, and lipid profile provides compelling evidence of an antioxidant and exercise effect on metabolic pathways in this novel mouse model.

With exercise-induced alterations in metabolic signaling pathways and energy metabolism, we investigated muscle fiber type and measured the expression levels of key myokines and adipokines involved in energy metabolism within each mouse group and found intriguing results. Exercise improves muscle function and strength (Vina et al., 2012). Although we did not observe differences in grip strength or muscle weight at tissue collection as a result of exercise intervention or antioxidant overexpression, we did observe significant differences in Type 1 / Type 2 fiber ratio and myokine levels in the gastrocnemius muscle. It is possible that the differences of the expression levels of the key myokines analyzed may be due to the higher levels of Type 1 fibers in comparison to Type 2 fibers (**Figure 37**) within the gastrocnemius muscle. Specifically, we observed increased levels of FGF-21, PGC1-alpha, and FNDC5 within the exercised mice overexpressing antioxidant catalase compared to the sedentary WT control group. It was also within these antioxidant-overexpressing mouse groups where we observed the highest levels of Type 1 / Type 2 fiber ratios (**Table 14 and Figure 37**). It is also interesting to

note that within these mouse groups there was a trend for increased catalase activity in the skeletal muscle tissue compared to the sedentary control group (**Figure 38**). We also observed an induction in GLUT 4 in the exercised mouse groups which may have played a role in the lowered insulin levels observed within the mice on exercise intervention compared to their sedentary littermates. Another myokine we investigated was IL-6. Although not significant, we observed a trend for increased expression in both mouse groups overexpressing catalase, with an exacerbated effect observed in the [Tg(CAT)$^{\pm}$] E group (>2.5 fold induction). Further exploration should be conducted to determine if this played an anti-inflammatory role in the skeletal muscle tissue.

With exercise intervention and redox playing a role in lowering fat mass, enhancing the lipid profile, and altering energy metabolism (measured by CLAMS) within the novel antioxidant mouse model, we expected one factor that might be involved in these observed changes was the induction of the redox sensitive and exercised-induced myokine, FGF-21 (Gomez-Samano et al., 2017; Raschke & Eckel, 2013). We showed FGF-21 mRNA levels in the skeletal muscle of [Tg(CAT)$^{\pm}$] E and Bob-Cat E models had a > 8 fold ($p<0.01$) and 3 fold increase (not significant) respectively. FGF-21 not only modulates skeletal muscle function, but it also crosstalks with adipose tissue (Keipert et al., 2014). Research has shown FGF-21 is able to induce browning by upregulation of UCP-1 (Fisher et al., 2012; P. Lee et al., 2014). Within adipose tissue, we observed a 5 fold increase in UCP-1 mRNA expression in the Bob-Cat E mice (not significant) yet a significant decrease in the [Tg(CAT)$^{\pm}$] E mouse group. This may have been reflective of the loss of fat mass observed in the [Tg(CAT)$^{\pm}$] E group, while the Bob-Cat E group did not actually lose any grams of fat over the 8 week intervention. Furthermore, the

induced expression of UCP-1 could have also been reflective of the increased mRNA expression of FGF-21 within the adipose and skeletal muscle tissue of the Bob-Cat E mouse group.

FGF-21's interplay with adiponectin (Manole et al., 2018), an anti-inflammatory adipokine that has been shown to be reduced in obese individuals, seems to be observed in our study as well. In exercised groups of mice, where there were increased levels of skeletal muscle FGF-21, adiponectin was also increased ($p<0.05$) providing further evidence of crosstalk between skeletal muscle and adipose tissue.

Two other key myokines, PGC1-alpha and FNDC5, may have influenced the phenotype observed in the antioxidant mouse models on exercise intervention. PGC1-alpha as well as FNDC5 ($p<0.05$), which are known to be induced by exercise showed a trend for increased fold change in mouse groups subjected to exercise intervention compared to the control WT S group and their sedentary cohorts. Previous studies have shown increased plasma irisin levels are a result of the induction of FNDC5 (Huh et al., 2012) and have a profound effect on browning of adipose tissue (Leal et al., 2018). However, we were surprised to find no significant differences in circulating plasma irisin levels between the mouse groups (**Table 14**). This could have been a result of the time the analysis took place. It is possible there was a significant increase in irisin immediately after exercise, but the blood in our study was collected after the mice had been sedentary for multiple hours since their last bout of exercise. Additionally, as described in the methods, we used an ELISA kit for human irisin. A few recent articles have noted false results in detection of irisin within these ELISA kits (Albrecht et al., 2015; Perakakis et al., 2017). Therefore, with the interesting results of UCP-1 in adipose tissue and alterations in body weight and fat mass, further studies should be done on irisin, such as measurement immediately post exercise or staining and analysis of morphology of adipose tissue. With these limitations to our

analysis of irisin, it is still possible that in addition to FGF-21, exercise-induced myokine signaling through the PGC1-alpha/FNDC5/irisin pathway modified adipose tissue function resulting in a leaner mice phenotype in the antioxidant overexpressing mice.

It is known that specific adipokines, such as leptin, influence satiety through the activation of hypothalamic appetite-regulating neurons (J. Friedman, 2016). Nonetheless, we did not observe significant differences in adipose mRNA or circulating leptin levels. We also measured expression levels of the leptin receptor (LepR), located within the appetite regulating - hypothalamic region of the brain (Abella et al., 2017). LepR was interestingly increased in every mouse group in comparison to the WT S mice except the [Tg(CAT)$^{\pm}$] E and Bob-Cat E groups. Nonetheless, with significant differences in body weight, fat mass, and metabolic parameters of exercised mouse groups overexpressing antioxidant we further evaluated expression levels of the appetite regulating genes NPY and POMC. With all exercised groups having a decreased fold change in NPY mRNA expression and increased expression of POMC (some groups did not quite reach significance), the result would be increased satiety and metabolism through dissipation of heat thus decreasing body weight/fat mass. These results provide evidence that in the [Tg(CAT)$^{\pm}$] E and Bob-Cat E mouse groups, metabolic pathways other than those regulated by leptin signaling likely contributed to the observed differences in body parameters, metabolism, and appetite regulation.

We also measured the expression levels of BDNF within the hypothalamic region, which has been shown to be induced by exercise (Walsh et al., 2018). Interestingly, one signaling mechanism involved may be through PGC1-alpha and FNDC5 signaling (Jodeiri Farshbaf et al., 2016), which is also a pathway involved in the skeletal muscle-brain axis. Additionally, in relation to obese humans and rodents, upon activation, BDNF has been associated with

cognition, neuroplasticity, glucose regulation, fat oxidation, and appetite regulation in adults (Budni, Bellettini-Santos, Mina, Garcez, & Zugno, 2015; Walsh et al., 2018). In comparison to the WT S group, the highest levels were seen in the Bob-Cat S mouse group. However, there was also a slight increase in the Bob-Cat E group (not significant) and almost a 3-fold increase in the [Tg(CAT)$^{\pm}$] E group. This warrants further study to determine whether the synergistic effects of antioxidant catalase and exercise may promote increased neuroplasticity in the novel mouse model. If so, the Bob-Cat model is potentially useful to study neurodegenerative diseases such as Alzheimer's Disease (Budni et al., 2015), or mood disorders including schizophrenia and depression (Peng, Li, Lv, Zhang, & Zhan, 2018).

Due to differing phenotypic and metabolic data in addition to appetite regulation modifications likely not related to the key satiety hormone leptin, we chose to investigate alternative pathways that may play a role in satiety in the exercised 'stress-less' mouse groups. The gut microbiome is considered an endocrine organ (G. Clarke et al., 2014) that is altered by exercise (Barton et al., 2018; Denou et al., 2016; Estaki et al., 2016; Monda et al., 2017) and has been shown to be significantly different in obese vs. lean individuals (Turnbaugh et al., 2009) and rodents (Kallus & Brandt, 2012) due to its functional roles on energy metabolism through crosstalk with other metabolic tissues. Post fecal collection, sequencing, and analysis of the gut microbes of the various mouse groups, we observed significant shifts in the microbiome. Although we only saw slight differences in the alpha diversity (species richness) between respective cohorts, highly significant differences in β diversity (microbial composition) were seen among exercise and sedentary groups, as well as mice overexpressing catalase on sedentary or exercise regimen (ANOSIM $p<0.05$). Furthermore, LEfSe analysis of the various taxa were plotted displaying significantly enriched bacterial taxa within the respective sedentary and

exercised cohorts. Analysis of microbial enrichment within the genotypes, of the sedentary and exercised groups separately, showed within the sedentary C57/WT and Bob-Cat cohorts, at the Phyla taxonomic level, there was an enrichment of Firmicutes vs. Bacteroidetes. This is consistent in the literature for both sedentary humans and animals to have an enrichment of Firmicutes vs. Bacteroidetes. This enrichment in Firmicutes is also common in DIO or overweight/obese organisms vs. the lean phenotype (Ley et al., 2005; Ley et al., 2006; Savini et al., 2013; Turnbaugh, Backhed, Fulton, & Gordon, 2008; Turnbaugh et al., 2009; Turnbaugh et al., 2006). Both sedentary mouse groups overexpressing catalase ([Tg(CAT)$^{\pm}$] and Bob-Cat) showed an enrichment of both the Rikenellaceae and Helicobacteraceae where the family of Rikenellaceae is associated with a lower BMI and healthier metabolic state compared to obese organisms (Clarke et al., 2013; Ottosson et al., 2018). The family Helicobacteraceae is classified as pathogenic (van der Mee-Marquet et al., 2017). Few studies have associated its prevalence with respect to parameters associated with obesity or its comorbidities, but Schulz et. al reported an increased abundance within mice who had been transfected with feces from cohorts fed a HFD (Schulz et al., 2014). This increase may have been associated with the increased levels of antioxidant within these mouse groups. Additionally, the sedentary Bob-Cat and Ob/Ob mouse groups were both enriched with Weeksellaceae and Erysipelotrichaceae. Weeksellaceae is pathogenic and associated with Irritable Bowel Syndrome (IBS) in humans and primates as well as rat visceral pain (Fourie et al., 2017), but no studies have specifically looked at its relevance to obesity. Additionally, there was an enrichment in the family Erysipelotrichaceae. This was of particular interest because of evidence from the literature showing a bloom of species belonging to this family in diet-induced obese animals (Turnbaugh et al., 2008). Other studies have also seen higher levels of this family in obese individuals and individuals producing higher levels of

the SCFA butyrate (Kaakoush, 2015; H. Zhang et al., 2009). With both sedentary groups having a leptin deficient background (heterozygous or homozygous for the mutation of the satiety hormone leptin) showing an enrichment, it is plausible there may be an association between this family and leptin levels. As with the sedentary groups, we also analyzed taxa enrichment between genotypes that were exercised. Exercised [Tg(CAT)$^{\pm}$] and Bob-Cat mice were both enriched with the Helicobacteraceae, while both the C57/WT and Ob/Ob mice were enriched with Rikenellaceae. Additionally, it was interesting to find that the [Tg(CAT)$^{\pm}$] E mice were enriched with the Bifidobacteriaceae which has been shown to be increased with exercise intervention and enriched in lean male mice (Munukka et al., 2018; Y. Qin et al., 2018). These results provided evidence of a synergistic effect of antioxidant and exercise on the gut microbiome as was hypothesized. It is of great interest in future studies to further explore species of the family Helicobacteraceae in relation to redox stress since there were significant differences in abundance comparing the exercise and sedentary cohorts in mice overexpressing catalase.

In addition to genotype comparisons within the sedentary and exercise groups, we also compared the enrichment of specific taxa between sedentary genotypes and their exercised cohorts individually. Within the C57/WT groups, exercise shifted the microbial taxa toward an enrichment of the *Corynebacterium, Proteus, Enterococcus,* and *Desulfovibrio*, at the genus level compared to their sedentary cohorts. At present little data has been published with the relevance of *Corynebacterium* or *Proteus* with parameters related to obesity, but many studies have shown that *Enterococcus* is associated with gut dysbiosis and depletion of commensal gut microbes which can decrease microbial diversity (Dubin & Pamer, 2014; Scotti et al., 2017). The genus *Desulfovibrio* of the family Desulfovibrionaceae has been associated with increased

voluntary exercise and may play a role in mucin function and gut permeability (T. W. Liu et al., 2015). Additionally, the family in its entirety has been found to be of higher prevalence in lean as well as healthy individuals (Million et al., 2012) in addition to the genus *Desulfovibrio* (Zietak et al., 2016). Within the [Tg(CAT)$^{\pm}$] groups, we found exercise shifted the microbiome with evidences of enriched taxa Desulfovibrionaceae and Aeromonadaceae at the family level. No taxa were defined to be significantly different between the exercised and sedentary mice of the [Tg(CAT)$^{\pm}$] genotype. As previously described, Desulfovibrionaceae has been associated with leanness (Million et al., 2012). It is of interest that the sedentary group was enriched and the exercised group was depleted of the family Aeromonadaceae which is a known human pathogen (Eid et al., 2017), has been associated with increased risk for the development of atherosclerosis, and is more abundant in T2D patients (F. Wu et al., 2019). It was of special interest that the novel Bob-Cat mice showed the largest number (42) of significantly differential taxa between the sedentary and exercise cohorts in comparison to the other genotypes. This finding indicates exercise as having a profound effect within the Bob-Cat genotype. Bob-Cat sedentary mice were enriched in *Methanobrevibacter, Chryseobacterium, Butyrivibrio,* and *Bilophila* in comparison to their exercised cohorts. Exercised Bob-Cat mice had significantly higher levels of *Parabacteroides, Prevotella, Ruminococcus, Sutterella,* and *Akkermansia*. With relevance to obesogenic characteristics, *Methanobrevibacter* has been negatively correlated with BMI (Million et al., 2012) and reduced in obese individuals (Stenman, Burcelin, & Lahtinen, 2016). *Chryseobacterium* has not been well studied, but we do know it is catalase-positive and part of the normal flora (Calderón et al., 2011). *Butyrivibrio* has been found in individuals with a healthier physical state and higher microbial diversity (Stenman et al., 2016), but contrary to the previously mentioned taxa enriched in the Bob-Cat sedentary groups, the *Bilophilia* which is

almost depleted in the exercise cohort of Bob-Cat mice is associated with increased body weight, adiposity, insulin, leptin, and inflammatory markers. Additionally, *Bilophila* are LPS-producing bacteria that theoretically could contribute to inflammation associated with obesity (Mulders et al., 2018). It was most interesting that the exercised Bob-Cat mice were enriched with taxa that did not have significant associations with increased fat mass or obesity. *Parabacteroides* were one of the five most significantly enriched taxa. *Parabateriodes* have been associated with a healthy host and gut environment (Fourie et al., 2017). The genus *Prevotella* have been positively correlated with SCFA propionate levels (Riva et al., 2017), which are typically increased with exercise and generation of enzymes found to be involved in mucin oligosaccharide degradation which protects endothelial cell wall against pathogens (Riva et al., 2017). It is also interesting that this genus was recently associated with non-westernized populations that were hunter-gatherers (healthier and characterized with a more active lifestyle than Westernized nations) (de la Cuesta-Zuluaga et al., 2018). The genus *Ruminococcus* has been negatively correlated with fasting glucose levels in humans, but as of yet, no studies have shown significant differences in other obesogenic parameters (Mulders et al., 2018). *Suterella* were enriched in a study comparing DIO to lean rodents (Clarke et al., 2013). Unlike the other taxa previously mentioned, the genus Akkermansia have been studied intensely. They are associated with a healthy gut microbiome in numerous studies. They are typically more abundant in individuals who are physically active/athletes in addition to being associated with individuals possessing a healthier metabolic profile (S. F. Clarke et al., 2014; Lai et al., 2018; Mach & Fuster-Botella, 2017). Additionally, *Akkermansia* are enriched in subjects with a low BMI and correlated with improvements in gut barrier function (G. Clarke et al., 2014). Also, a study conducted by Fourie et al. showed that epithelial inflammation, IBD, obesity, and diabetes are

decreased when there is a restoration of this genus (Fourie et al., 2017). Overall, a recent review has surmised the characteristics of *Akkermansia* to being negatively correlated with adiposity, fasting glucose, insulin, IR, leptin, inflammation, and intestinal permeability (Mulders et al., 2018). With these particular taxa being significantly enriched in the exercised Bob-Cat mouse group, this strengthens our hypothesis that the combination of exercise and overexpression of antioxidant is beneficial to the metabolic profile by positively shifting the gut microbiome.

We saw that the sedentary, obese Ob/Ob mice were enriched with taxa associated with obesogenic parameters. For example, *Anaeroplasma*, have been positively associated with DIO in mice and correlated with lower production of the SCFA butyrate which can exacerbate gut dysbiosis (Hwang et al., 2017). Additionally, there was increased abundance of the taxa *Weissella*, which have been correlated with decreased cardiovascular function and increased BW (Sherman et al., 2018). These taxa were depleted within the exercised Ob/Ob mouse group. Within the exercised cohort, we found an enrichment of the *Lachnospiraceae* family, which are butyrate producing organisms shown to be significantly depleted within diabetic mice on high fat diets (Serino, Chabo, & Burcelin, 2012). Depletion of these organisms have been associated with gut barrier disruption, metabolic endotoxemia, and low-grade inflammation leading to other debilitating diseases (Vital, Karch, & Pieper, 2017). Additionally, we found exercise caused an enrichment in the taxa *Prevotella* and *Sutterella* at the genus level. *Prevotella*, as previously mentioned, is associated with an increase in SCFA propionate, improvement in gut health, and increased in the hunter-gatherer human population (de la Cuesta-Zuluaga et al., 2018; Riva et al., 2017). Also previously mentioned, and not completely characterized, the *Sutterella* taxa, have been found to be enriched in lean vs DIO mice (Clarke et al., 2013). This is interesting where we

also saw “leaner” phenotypic characteristics in our Ob/Ob exercised mice vs. their sedentary littermates.

With regard to appetite regulation in the context of the gut microbiome, it is also interesting that previous studies have shown associations between butyrate levels and the brain. For example, acute butyrate administration decreased food intake and suppressed orexigenic neurons that express NPY within the hypothalamic region of the brain (Z. Li et al., 2018), and chronic butyrate administration prevented DIO, hyperinsulinemia, hypertriglyceridemia, as well as reduced food intake (Z. Li et al., 2018). Exercise has been shown to increase butyrate production by the gut microbiome (Lai et al., 2018; Matsumoto et al., 2008). Our findings showed that the antioxidant models overexpressing catalase put on exercise intervention had higher levels of Bifidobacteriaceae, *Suterella,* and *Akkermansia* which either produce butyrate or are associated with higher levels of the SCFA (Rivière et al., 2016; J. Ye et al., 2018). Additionally, Bob-Cat sedentary mice were enriched and exercisers were depleted of *Bilophila* and Rikenellaceae (also observed in the [Tg(CAT)$^{\pm}$] E group) which thrive in environments of low levels of butyrate (J. Ye et al., 2018). It was also particularly interesting that the lowest levels of NPY and highest levels (although not all significant) of POMC expression were found in the exercised cohorts of each genotype (**Table 16**). Also interesting is the fact that butyrate has been associated with lowering TG levels. This also correlates with our findings that the exercised mice overexpressing antioxidant catalase had lower levels of plasma TG compared to their sedentary control groups as shown in **Table 12**.

All of the described significant associations of microbes to particular mouse groups are extremely interesting; nonetheless, it is the gut microbiome as a whole and the interaction

between the various microbes that determines the impact on the host organism's metabolism (Heiss & Olofsson, 2018; Kreznar et al., 2017).

PICRUSt analysis allowed us to predict the function of the microbiome based on the species found most prevalent within each mouse group. It was interesting that the lowest number of functional differences as a result of exercise was found in the C57/WT group analysis, and the Ob/Ob group only had 12. On the contrary, mice overexpressing catalase, the [Tg(CAT)$^{\pm}$] and Bob-Cat, had 29 and 118 significantly differential functional predictions respectively. This is an indication that exercise in conjunction with catalase overexpression, is contributing a strong effect on the functional potential of the microbial community in these groups and is likely contributing to metabolic pathways related to the phenotypic changes we saw in our study. From our findings, it was most interesting to discover that within the Bob-Cat sedentary group, several functional pathways relating to cell motility were enriched including flagellar assembly, bacterial motility proteins, and bacterial chemotaxis. On the other hand, within the exercised samples, we observed an enrichment of glycan biosynthesis in addition to bacteria capable of LPS biosynthesis. Glycan biosynthesis was also enriched within the [Tg(CAT)$^{\pm}$] exercised samples in addition to bacteria capable of glycan degradation. These findings align with recent studies conducted by Hou et. al (Hou et al., 2017) where PICRUSt analysis showed, in obese individuals, there were elevated counts of bacterial chemotaxis and depletion of glycan metabolism and biosynthesis. This finding impeccably aligns with our novel Bob-Cat mice where the exercised samples showed evidence of an elevation in glycan metabolism and biosynthesis, and sedentary samples showed an enrichment in bacterial motility genes. Although in many studies lipopolysacharrides (LPS) are associated with negative health biomarkers, it is

dependent on which LPS are produced and the other microbes present (some microbes that produce LPS are beneficial to the microbial environment) (Kreznar et al., 2017).

4.5 CONCLUSION

In this study, we comprehensively compared the synergistic effects of exercise and antioxidant overexpression in a novel mouse model. We hypothesized that the combined effects of catalase overexpression and exercise may play a role in body composition and energy metabolism by altering myokine and adipokine secretion and shift the diversity and composition of the gut microbiome. As expected, exercise significantly attenuated weight gain and decreased fat mass in each mouse genotype, with an exacerbated effect in the mice overexpressing antioxidant catalase. At the tissue level, known exercised-induced myokines were upregulated and showed evidence for crosstalk between skeletal muscle and adipose tissue. Additionally, we saw changes in appetite regulating hormones which may have played a role in changes in the phenotypic and metabolic data determined in the antioxidant mouse models subjected to moderate treadmill exercise. Nonetheless, our most interesting and novel findings were discovered in our analysis of the gut microbiome. We saw shifts related to differences in the mouse groups based on exercise vs. sedentary intervention in addition to redox status. These findings mandate further studies on the role of redox stress and exercise in energy homeostasis by further correlating metadata to microbial species and conducting fecal transfer to determine if the gut microbes from our novel mouse model alter phenotypic and metabolic characteristics in other mouse models with chronic diseases (Ex. DIO, neurodegenerative models, cancer models, etc.)

4.6 FUNDING

This study was partially supported by NIH Grant 5R01HL-074239 (NS), 5P20RR016477 (NS), 1R15AG051062-01 (NS), and WV-NASA Grant Consortium (DA).

4.7 ACKNOWLEDGEMENTS

The authors acknowledge Dr. Jung Han Kim, Dr. Shekhar Mohan, Dr. Holly Cyphert, Dr. Kristeena Ray, Carla Cook, Tanner Robinson, Sarah Marshall, Alex Sommerville, Aaron Roberts, Garrett McCormick, Emily Norris, and Hugo Gutierrez for their aid in experimental procedures and animal tissue collection.

CHAPTER V: DISCUSSION AND FUTURE DIRECTIONS

DISCUSSION

At the conclusion of my research of the aforementioned studies discussed in Chapters II-IV, I am just as interested now as when I began my research regarding the complexity of energy metabolism and how it is regulated by so many extrinsic variables such as diet, exercise, genetics, and other environmental stimuli. I still desire to discover an efficient lifestyle, for myself and others, to maintain physical health among living in the most obese state (West Virginia). Obtaining knowledge to prevent or reduce the rising levels of obesity, a key risk factor for metabolic tissue dysfunction, redox stress, and thus chronic inflammatory and cardiometabolic diseases, remains important to me.

At the beginning of my research as a PhD student, I studied numerous investigations conducted in other laboratories, in addition to our own laboratory, showing evidence of redox stress impacting diseases related to metabolic tissue dysfunction and inflammatory signaling. By doing this, I saw the critical need to further explore the role of antioxidants as a therapeutic intervention. Our lab desired to determine the role of one of the key antioxidants, catalase, which is directly involved in energy metabolism. To accomplish our goal, we engineered a novel mouse model expressing the human antioxidant catalase in addition to mouse catalase with an obese parent background (D. L. Amos et al., 2017). From this point, we developed three hypotheses: I. modulating redox stress by altering endogenous antioxidant content (overexpression of catalase) alone would enhance adipose tissue function, glucose and lipid signaling, and overall energy metabolism; II. modulating redox stress by antioxidant overexpression or dietary intervention with an enriched OM3 diet (45%) vs. a HFD (45% lard) would positively regulate fatty acid signaling, glucose and lipid homeostasis, energy metabolism, and overall metabolic function; III.

antioxidant overexpression in addition to exercise would both enhance skeletal muscle and adipose tissue function, alter appetite signaling, and shift the composition and function of the gut microbiome thus improving overall energy metabolism in the 'stress-less' mice. To address our first hypothesis (Chapter II), we investigated both male and female 'stress-less' mice and found that the novel mouse model had significant differences in energy expenditure, activity levels, metabolic profile, and oxidative stress levels compared to the other genotypes studied (C57Bl6/WT, [Tg(CAT)$^{\pm}$], and Ob/Ob). Additionally, we also showed evidence of sexual dimorphism, which suggests more studies should be conducted in both male and female genders separately to better treat the population in a manner that specifically targets an individual's abnormalities. Additionally, in generating the Bob-Cat mice, being heterozygous for the Ob mutation (Ob/+) in combination with the expression of the human catalase gene, we generated a few mice that were homozygous for the Ob mutated gene and expressed the human catalase gene. This new genotype was titled "Big Bob," and its basic characteristics were also discussed in Chapter II. The intriguing characteristics of the Bob-Cat mice kindled our desire to explore the potential of coupling antioxidant catalase with other therapeutic interventions to study mechanisms involved in regulating energy metabolism.

Since redox stress plays a key role in obesity and cardiometabolic diseases, and a common treatment is dietary intervention, we tested our second hypothesis using male and female mice overexpressing endogenous antioxidant catalase to study the impact of altered redox balance and an enriched OM3 diet (D. Amos et al., 2019). As discussed in Chapter III, we discovered that after eight weeks of OM3 dietary intervention in the novel mice, compared to their littermates on HFD, the mice fed OM3 diet maintained or lowered body weight and fat mass, enhanced energy metabolism, maintained normal circadian rhythm, and sustained insulin

sensitivity. Our data showed these results were all due to the regulation of GPR120-Nrf2 cross-talk, which to our knowledge, had not been previously shown in any other studies. This study advanced the field of nutrition and in a direction showing the potential therapeutic capacity of overexpression of antioxidants. Additionally, we also saw sexual dimorphism play a role in the metabolic parameters assessed. Further investigation should be conducted on this topic to determine the mechanisms behind these differences.

With exercise being another major remedy to counteract metabolic diseases, we addressed our third hypothesis and studied the impact of a 30 min. exercise regimen, 5 days a week, for 8 weeks in the 'stress-less' mouse model. Here, we showed increased antioxidant levels in the catalase over-expressing mice maintained or decreased body weight and fat mass. Additionally, the novel mice maintained balanced energy metabolism, normal circadian rhythm, and showed a trend for increased HDL and decreased plasma TG levels. Most interestingly, we saw significant differences in skeletal muscle Type 1 / Type 2 fiber ratio and mRNA expression of key myokines which may have caused a change in adipose tissue function by a skeletal muscle-adipose tissue axis (crosstalk). This study provided additional knowledge to the field with evidence of an exercise and redox-induced shift in the gut microbiome and a change in appetite regulation as a mechanism of the beneficial impact of exercise on metabolic homeostasis in the mice overexpressing antioxidant catalase, as discussed in Chapter IV. With the results from each of the studies outlined in Chapters II-IV, it is evident our hypotheses were correct. Antioxidant catalase functions as an adjuvant to OM3 diet or exercise to enhance metabolic tissue function and improve overall energy metabolism in the novel 'stress-less' mouse. Additionally, antioxidant overexpression shifted the composition and function of the gut

microbiome, which was further shifted with exercise, showing potential for impacting the alterations seen in the body composition and metabolic measurements we collected.

In conclusion, with the newly generated Bob-Cat mice, we have successfully identified key ways this model can be used to study the impact of altered redox in the context of energy metabolism, cancer, and other chronic illnesses mandating new therapies to counter their detrimental effects on the human population. Although we have clearly shown the benefits of overexpressing catalase in mice with an obese-parent background (Bob-Cats) when provided an OM3 rich diet or put on exercise intervention, many future projects have been devised and some are already underway. By continuing our investigation, we believe that the Bob-Cat model has the potential to lead to the development of therapies that will reverse the rising levels of obesity, cardiometabolic diseases, chronic inflammatory conditions, in addition to altering signaling pathways involved in the development and progression of cancer and neurological-related disorders.

FUTURE DIRECTIONS

The Role of FGF-21 as a Hepatokine

In both our diet study and exercise study, we assessed expression levels of FGF-21, a myokine, adipokine, and hepatokine (Gomez-Samano et al., 2017) that can be induced as a result of redox imbalance, exercise intervention, cold stimulus, and starvation (Cuevas-Ramos et al., 2012; Gomez-Samano et al., 2017; Potthoff et al., 2009). With its pleotropic effects on glucose and lipid homeostasis, thermoregulation, inflammation, and energy metabolism in general, we wanted to determine if it played a role in the interventions studied in the Bob-Cat mouse. Specifically, our results showed evidence of sexual dimorphism as well as inversed levels of FGF-21 within HFD vs. NC groups overexpressing catalase as described in Chapter III and shown in **Figure 28**. Additionally, with exercise intervention, we showed an induction in skeletal muscle tissue in male mouse groups overexpressing catalase which may have contributed to an induction of adiponectin in the adipose tissue and differences in expression of UCP-1 thus stimulating thermogenesis. We have yet to assess female mice, which may show different results due to an interplay with differing hormone levels such as leptin and various sex hormones. In the current literature, research has indicated the possibility of "FGF-21-resistance" in obese individuals where FGF-21 levels are high yet FGF-21's known effects are absent. With the strong association between redox stress and obesity, and FGF-21 yet to be assessed in the context of the liver, where it is primarily secreted, further analysis of this hormone is of great interest.

Assessment of the Gut Microbiome

In our studies of the 'stress-less' mouse subjected to exercise intervention, we analyzed the gut microbiome and found that exercise significantly shifted the microbial composition and

function in the mice that overexpressed antioxidant catalase. At the current time, we have only assessed exercised male mice. However, to further the knowledge in the field of microbiology and redox homeostasis, we would like to also determine the effects of an enriched OM3 diet in both genders in addition to an assessment of exercise effects on the microbial species in female mice. Additionally, we have only began to explore the effects of redox in the novel male mouse and its relation to the gut microbiome. We plan to do further analysis using the metadata we have collected, and, if appropriate, begin deep sequencing to determine the signaling pathways causing the noted shifts in the microbial species and how that affects systemic energy homeostasis in metabolic tissues. Additionally, we plan to use the method of fecal transfer from mice overexpressing antioxidant on various mouse models to determine if the core species residing in their gut can produce the same metabolic effects (Ex. decreased body weight, fat mass, TG levels, etc.).

Aging Studies

Analysis of the generation of the original [Tg(CAT)$^{\pm}$] mice (X. Chen et al., 2003) in addition to tissue-targeted catalase transgenic mice in other studies showed that these mice displayed anti-aging effects (H.-Y. Lee et al., 2010; Linford, Schriner, & Rabinovitch, 2006). Therefore, to determine if our novel mouse which overexpresses antioxidant catalase ubiquitously (D. L. Amos et al., 2017) would confer the same effects, multiple studies have been conducted in concert with exercise intervention. Our current status is at the analysis of key signaling pathways in the context of aging and energy metabolism, since as organisms grow older there is typically a decline in metabolism, regulation of adipose storage, and dysfunction of skeletal muscle function (Shimokata & Kuzuya, 1993). We expect that by decreasing the level of free radicals through an induction of antioxidant catalase, the aging process will be allayed. If

our hypothesis is true, we would like to determine if the gut microbiome of the mice overexpressing catalase, which we have shown to be significantly shifted in our studies (Chapter IV) could potentially play a role in any anti-aging effects observed.

Behavioral Analysis

Obesity increases the risk for the development and progression of cardiometabolic diseases, diabetes, and cancer (Goossens, 2017; Manna & Jain, 2015) in addition to promoting behavior modifications (Singh, 2014). This includes excess food consumption in addition to stress, and depression which is commonly observed in individuals with high levels of adiposity (Sominsky & Spencer, 2014). Therefore, we desire to determine if lowering oxidative stress by increasing antioxidant catalase using our 'stress-less' mouse model would lower obesity-regulated behavioral stress.

REFERENCES

Aasheim, E. T., & Bohmer, T. (2008). Low preoperative vitamin levels in morbidly obese patients: a role of systemic inflammation? *Surg Obes Relat Dis, 4*(6), 779-780. doi:10.1016/j.soard.2008.09.002

Abbott, K. A., Veysey, M., Lucock, M., Niblett, S., King, K., Burrows, T., & Garg, M. L. (2016). Sex-dependent association between erythrocyte n-3 PUFA and type 2 diabetes in older overweight people. *Br J Nutr, 115*(8), 1379-1386. doi:10.1017/s0007114516000258

Abella, V., Scotece, M., Conde, J., Pino, J., Gonzalez-Gay, M. A., Gomez-Reino, J. J., . . . Gualillo, O. (2017). Leptin in the interplay of inflammation, metabolism and immune system disorders. *Nat Rev Rheumatol*. doi:10.1038/nrrheum.2016.209

Achari, A. E., & Jain, S. K. (2017). Adiponectin, a Therapeutic Target for Obesity, Diabetes, and Endothelial Dysfunction. *Int J Mol Sci, 18*(6). doi:10.3390/ijms18061321

Adlerberth, I., & Wold, A. E. (2009). Establishment of the gut microbiota in Western infants. *Acta Paediatr, 98*(2), 229-238. doi:10.1111/j.1651-2227.2008.01060.x

Aebi, H. (1984). Catalase in vitro. *Methods Enzymol, 105*, 121-126.

Agnoli, C., Grioni, S., Sieri, S., Palli, D., Masala, G., Sacerdote, C., . . . Krogh, V. (2013). Italian Mediterranean Index and risk of colorectal cancer in the Italian section of the EPIC cohort. *Int J Cancer, 132*(6), 1404-1411. doi:10.1002/ijc.27740

Albarado, D. C., McClaine, J., Stephens, J. M., Mynatt, R. L., Ye, J., Bannon, A. W., . . . Butler, A. A. (2004). Impaired Coordination of Nutrient Intake and Substrate Oxidation in Melanocortin-4 Receptor Knockout Mice. *Endocrinology, 145*(1), 243-252. doi:10.1210/en.2003-0452

Alberti, K. G. (1975). Role of glucagon and other hormones in development of diabetic ketoacidosis. *Lancet, 1*(7920), 1307-1311.

Albracht-Schulte, K., Kalupahana, N. S., Ramalingam, L., Wang, S., Rahman, S. M., Robert-McComb, J., & Moustaid-Moussa, N. (2018). Omega-3 fatty acids in obesity and metabolic syndrome: a mechanistic update. *J Nutr Biochem, 58*, 1-16. doi:10.1016/j.jnutbio.2018.02.012

Albrecht, E., Norheim, F., Thiede, B., Holen, T., Ohashi, T., Schering, L., . . . Maak, S. (2015). Irisin - a myth rather than an exercise-inducible myokine. *Sci Rep, 5*, 8889. doi:10.1038/srep08889

Alleman, R. J., Katunga, L. A., Nelson, M. A., Brown, D. A., & Anderson, E. J. (2014). The "Goldilocks Zone" from a redox perspective-Adaptive vs. deleterious responses to oxidative stress in striated muscle. *Front Physiol, 5*, 358. doi:10.3389/fphys.2014.00358

Allen, J. M., Berg Miller, M. E., Pence, B. D., Whitlock, K., Nehra, V., Gaskins, H. R., . . . Woods, J. A. (2015). Voluntary and forced exercise differentially alters the gut microbiome in C57BL/6J mice. *J Appl Physiol (1985), 118*(8), 1059-1066. doi:10.1152/japplphysiol.01077.2014

Allen, J. M., Mailing, L. J., Niemiro, G. M., Moore, R., Cook, M. D., White, B. A., . . . Woods, J. A. (2018). Exercise Alters Gut Microbiota Composition and Function in Lean and Obese Humans. *Med Sci Sports Exerc, 50*(4), 747-757. doi:10.1249/MSS.0000000000001495

Amirkhizi, F., Siassi, F., Djalali, M., & Shahraki, S. H. (2014). Impaired enzymatic antioxidant defense in erythrocytes of women with general and abdominal obesity. *Obes Res Clin Pract, 8*(1), e26-34. doi:10.1016/j.orcp.2012.07.004

Amos, D., Cook, C., & Santanam, N. (2019). Omega 3 rich diet modulates energy metabolism via GPR120-Nrf2 crosstalk in a novel antioxidant mouse model. *Biochim Biophys Acta Mol Cell Biol Lipids, 1864*(4), 466-488. doi:10.1016/j.bbalip.2019.01.002

Amos, D. L., Robinson, T., Massie, M. B., Cook, C., Hoffsted, A., Crain, C., & Santanam, N. (2017). Catalase overexpression modulates metabolic parameters in a new 'stress-less' leptin-deficient mouse model. *Biochim Biophys Acta, 1863*(9), 2293-2306. doi:10.1016/j.bbadis.2017.06.016

Andersen, L. F., Jacobs, D. R., Jr., Gross, M. D., Schreiner, P. J., Dale Williams, O., & Lee, D. H. (2006). Longitudinal associations between body mass index and serum carotenoids: the CARDIA study. *Br J Nutr, 95*(2), 358-365.

Anderson, E. J., Lustig, M. E., Boyle, K. E., Woodlief, T. L., Kane, D. A., Lin, C. T., . . . Neufer, P. D. (2009). Mitochondrial H2O2 emission and cellular redox state link excess fat intake to insulin resistance in both rodents and humans. *J Clin Invest, 119*(3), 573-581. doi:10.1172/JCI37048

Antunes, L. C., Elkfury, J. L., Jornada, M. N., Foletto, K. C., & Bertoluci, M. C. (2016). Validation of HOMA-IR in a model of insulin-resistance induced by a high-fat diet in Wistar rats. *Arch Endocrinol Metab, 60*(2), 138-142. doi:10.1590/2359-3997000000169

Archer, T., Josefsson, T., & Lindwall, M. (2014). Effects of physical exercise on depressive symptoms and biomarkers in depression. *CNS Neurol Disord Drug Targets, 13*(10), 1640-1653.

Arroyo-Johnson, C., & Mincey, K. D. (2016). Obesity Epidemiology Worldwide. *Gastroenterol Clin North Am, 45*(4), 571-579. doi:10.1016/j.gtc.2016.07.012

Asano, Y., Hiramoto, T., Nishino, R., Aiba, Y., Kimura, T., Yoshihara, K., . . . Sudo, N. (2012). Critical role of gut microbiota in the production of biologically active, free catecholamines in the gut lumen of mice. *Am J Physiol Gastrointest Liver Physiol, 303*(11), G1288-1295. doi:10.1152/ajpgi.00341.2012

Association, A. H. (2017, January 2019). What Your Cholesterol Levels Mean. Retrieved from https://www.heart.org/en/health-topics/cholesterol/about-cholesterol/what-your-cholesterol-levels-mean

Aydin, S., Kuloglu, T., Aydin, S., Kalayci, M., Yilmaz, M., Cakmak, T., . . . Ozercan, I. H. (2014). A comprehensive immunohistochemical examination of the distribution of the fat-burning protein irisin in biological tissues. *Peptides, 61*, 130-136. doi:10.1016/j.peptides.2014.09.014

Backhed, F., Ding, H., Wang, T., Hooper, L. V., Koh, G. Y., Nagy, A., . . . Gordon, J. I. (2004). The gut microbiota as an environmental factor that regulates fat storage. *Proc Natl Acad Sci U S A, 101*(44), 15718-15723. doi:10.1073/pnas.0407076101

Backhed, F., Ley, R. E., Sonnenburg, J. L., Peterson, D. A., & Gordon, J. I. (2005). Host-bacterial mutualism in the human intestine. *Science, 307*(5717), 1915-1920. doi:10.1126/science.1104816

Backhed, F., Roswall, J., Peng, Y., Feng, Q., Jia, H., Kovatcheva-Datchary, P., . . . Wang, J. (2015). Dynamics and Stabilization of the Human Gut Microbiome during the First Year of Life. *Cell Host Microbe, 17*(6), 852. doi:10.1016/j.chom.2015.05.012

Bahadoran, Z., Mirmiran, P., Hosseinpanah, F., Hedayati, M., Hosseinpour-Niazi, S., & Azizi, F. (2011). Broccoli sprouts reduce oxidative stress in type 2 diabetes: a randomized double-blind clinical trial. *Eur J Clin Nutr, 65*(8), 972-977. doi:10.1038/ejcn.2011.59

Bailey-Downs, L. C., Tucsek, Z., Toth, P., Sosnowska, D., Gautam, T., Sonntag, W. E., . . . Ungvari, Z. (2013). Aging exacerbates obesity-induced oxidative stress and inflammation in perivascular adipose tissue in mice: a paracrine mechanism contributing to vascular redox dysregulation and inflammation. *J Gerontol A Biol Sci Med Sci, 68*(7), 780-792. doi:10.1093/gerona/gls238

Balistreri, C. R., Caruso, C., & Candore, G. (2010). The Role of Adipose Tissue and Adipokines in Obesity-Related Inflammatory Diseases. *Mediators of Inflammation, 2010*, 19. doi:10.1155/2010/802078

Banerjee, R. R., & Lazar, M. A. (2003). Resistin: molecular history and prognosis. *J Mol Med (Berl), 81*(4), 218-226. doi:10.1007/s00109-003-0428-9

Barauna, V. G., Batista, M. L., Jr., Costa Rosa, L. F., Casarini, D. E., Krieger, J. E., & Oliveira, E. M. (2005). Cardiovascular adaptations in rats submitted to a resistance-training model. *Clin Exp Pharmacol Physiol, 32*(4), 249-254. doi:10.1111/j.1440-1681.2005.04180.x

Barazzoni, R., Gortan Cappellari, G., Ragni, M., & Nisoli, E. (2018). Insulin resistance in obesity: an overview of fundamental alterations. *Eat Weight Disord, 23*(2), 149-157. doi:10.1007/s40519-018-0481-6

Bargut, T. C., Silva-e-Silva, A. C., Souza-Mello, V., Mandarim-de-Lacerda, C. A., & Aguila, M. B. (2016). Mice fed fish oil diet and upregulation of brown adipose tissue thermogenic markers. *Eur J Nutr, 55*(1), 159-169. doi:10.1007/s00394-015-0834-0

Barton, W., Penney, N. C., Cronin, O., Garcia-Perez, I., Molloy, M. G., Holmes, E., . . . O'Sullivan, O. (2018). The microbiome of professional athletes differs from that of more sedentary subjects in composition and particularly at the functional metabolic level. *Gut, 67*(4), 625-633. doi:10.1136/gutjnl-2016-313627

Beltowski, J. (2012). Leptin and the regulation of endothelial function in physiological and pathological conditions. *Clin Exp Pharmacol Physiol, 39*(2), 168-178. doi:10.1111/j.1440-1681.2011.05623.x

Benite-Ribeiro, S. A., Putt, D. A., & Santos, J. M. (2016). The effect of physical exercise on orexigenic and anorexigenic peptides and its role on long-term feeding control. *Med Hypotheses, 93*, 30-33. doi:10.1016/j.mehy.2016.05.005

Beylot, M., Sautot, G., Laville, M., & Cohen, R. (1988). Metabolic studies in lipoatrophic diabetes: mechanism of hyperglycemia and evidence of resistance to insulin of lipid metabolism. *Diabete Metab, 14*(1), 20-24.

Birben, E., Sahiner, U. M., Sackesen, C., Erzurum, S., & Kalayci, O. (2012). Oxidative stress and antioxidant defense. *World Allergy Organ J, 5*(1), 9-19. doi:10.1097/WOX.0b013e3182439613

Birsoy, K., Berry, R., Wang, T., Ceyhan, O., Tavazoie, S., Friedman, J. M., & Rodeheffer, M. S. (2011). Analysis of gene networks in white adipose tissue development reveals a role for ETS2 in adipogenesis. *Development, 138*(21), 4709-4719. doi:10.1242/dev.067710

Bjelakovic, G., Nikolova, D., Gluud, L. L., Simonetti, R. G., & Gluud, C. (2012). Antioxidant supplements for prevention of mortality in healthy participants and patients with various diseases. *Cochrane Database Syst Rev*(3), Cd007176. doi:10.1002/14651858.CD007176.pub2

Bleau, C., Karelis, A. D., St-Pierre, D. H., & Lamontagne, L. (2015). Crosstalk between intestinal microbiota, adipose tissue and skeletal muscle as an early event in systemic low-grade inflammation and the development of obesity and diabetes. *Diabetes Metab Res Rev, 31*(6), 545-561. doi:10.1002/dmrr.2617

Bluher, M., & Mantzoros, C. S. (2015). From leptin to other adipokines in health and disease: facts and expectations at the beginning of the 21st century. *Metabolism, 64*(1), 131-145. doi:10.1016/j.metabol.2014.10.016

Boekholdt, S. M., Meuwese, M. C., Day, N. E., Luben, R., Welch, A., Wareham, N. J., & Khaw, K. T. (2006). Plasma concentrations of ascorbic acid and C-reactive protein, and risk of future coronary artery disease, in apparently healthy men and women: the EPIC-Norfolk prospective population study. *Br J Nutr, 96*(3), 516-522.

Bondia-Pons, I., Ryan, L., & Martinez, J. A. (2012). Oxidative stress and inflammation interactions in human obesity. *J Physiol Biochem, 68*(4), 701-711. doi:10.1007/s13105-012-0154-2

BonDurant, L. D., Ameka, M., Naber, M. C., Markan, K. R., Idiga, S. O., Acevedo, M. R., . . . Potthoff, M. J. (2017). FGF21 Regulates Metabolism Through Adipose-Dependent and -Independent Mechanisms. *Cell Metab, 25*(4), 935-944 e934. doi:10.1016/j.cmet.2017.03.005

Bonomini, F., Rodella, L. F., & Rezzani, R. (2015). Metabolic syndrome, aging and involvement of oxidative stress. *Aging Dis, 6*(2), 109-120. doi:10.14336/AD.2014.0305

Borrelli, A., Bonelli, P., Tuccillo, F. M., Goldfine, I. D., Evans, J. L., Buonaguro, F. M., & Mancini, A. (2018). Role of gut microbiota and oxidative stress in the progression of non-alcoholic fatty liver disease to hepatocarcinoma: Current and innovative therapeutic approaches. *Redox Biology, 15*, 467-479. doi:https://doi.org/10.1016/j.redox.2018.01.009

Bostrom, P., Wu, J., Jedrychowski, M. P., Korde, A., Ye, L., Lo, J. C., . . . Spiegelman, B. M. (2012). A PGC1-alpha-dependent myokine that drives brown-fat-like development of white fat and thermogenesis. *Nature, 481*(7382), 463-468. doi:10.1038/nature10777

Bouchard, G., Carrillo, M. C., Tuchweber, B., Perea, A., Ledoux, M., Poulin, D., & Yousef, I. M. (1994). Moderate long-term physical activity improves the age-related decline in bile formation and bile salt secretion in rats. *Proc Soc Exp Biol Med, 206*(4), 409-415.

Bougoulia, M., Triantos, A., & Koliakos, G. (2006). Plasma interleukin-6 levels, glutathione peroxidase and isoprostane in obese women before and after weight loss. Association with cardiovascular risk factors. *Hormones (Athens), 5*(3), 192-199.

Branecky, K. L., Niswender, K. D., & Pendergast, J. S. (2015). Disruption of Daily Rhythms by High-Fat Diet Is Reversible. *PLoS One, 10*(9), e0137970. doi:10.1371/journal.pone.0137970

Breton, J., Tennoune, N., Lucas, N., Francois, M., Legrand, R., Jacquemot, J., . . . Fetissov, S. O. (2016). Gut Commensal E. coli Proteins Activate Host Satiety Pathways following Nutrient-Induced Bacterial Growth. *Cell Metab, 23*(2), 324-334. doi:10.1016/j.cmet.2015.10.017

Brewer, A. C., Mustafi, S. B., Murray, T. V., Rajasekaran, N. S., & Benjamin, I. J. (2013). Reductive stress linked to small HSPs, G6PD, and Nrf2 pathways in heart disease. *Antioxid Redox Signal, 18*(9), 1114-1127. doi:10.1089/ars.2012.4914

Brezniceanu, M. L., Liu, F., Wei, C. C., Chenier, I., Godin, N., Zhang, S. L., . . . Chan, J. S. (2008). Attenuation of interstitial fibrosis and tubular apoptosis in db/db transgenic mice overexpressing catalase in renal proximal tubular cells. *Diabetes, 57*(2), 451-459. doi:10.2337/db07-0013

Brighton, C. A., Rievaj, J., Kuhre, R. E., Glass, L. L., Schoonjans, K., Holst, J. J., . . . Reimann, F. (2015). Bile Acids Trigger GLP-1 Release Predominantly by Accessing Basolaterally

Located G Protein-Coupled Bile Acid Receptors. *Endocrinology, 156*(11), 3961-3970. doi:10.1210/en.2015-1321

Brown, K., DeCoffe, D., Molcan, E., & Gibson, D. L. (2012). Diet-induced dysbiosis of the intestinal microbiota and the effects on immunity and disease. *Nutrients, 4*(8), 1095-1119. doi:10.3390/nu4081095

Bryan, S., Baregzay, B., Spicer, D., Singal, P. K., & Khaper, N. (2013). Redox-inflammatory synergy in the metabolic syndrome. *Can J Physiol Pharmacol, 91*(1), 22-30. doi:10.1139/cjpp-2012-0295

Buckland, G., Travier, N., Cottet, V., González, C. A., Luján-Barroso, L., Agudo, A., . . . Riboli, E. (2013). Adherence to the mediterranean diet and risk of breast cancer in the European prospective investigation into cancer and nutrition cohort study. *International Journal of Cancer, 132*(12), 2918-2927. doi:doi:10.1002/ijc.27958

Budni, J., Bellettini-Santos, T., Mina, F., Garcez, M. L., & Zugno, A. I. (2015). The involvement of BDNF, NGF and GDNF in aging and Alzheimer's disease. *Aging Dis, 6*(5), 331-341. doi:10.14336/ad.2015.0825

Burcelin, R. (2016). Gut microbiota and immune crosstalk in metabolic disease. *Mol Metab, 5*(9), 771-781. doi:10.1016/j.molmet.2016.05.016

Burke, L. K., Doslikova, B., D'Agostino, G., Greenwald-Yarnell, M., Georgescu, T., Chianese, R., . . . Heisler, L. K. (2016). Sex difference in physical activity, energy expenditure and obesity driven by a subpopulation of hypothalamic POMC neurons. *Mol Metab, 5*(3), 245-252. doi:10.1016/j.molmet.2016.01.005

Cacho, J., Sevillano, J., de Castro, J., Herrera, E., & Ramos, M. P. (2008). Validation of simple indexes to assess insulin sensitivity during pregnancy in Wistar and Sprague-Dawley rats. *Am J Physiol Endocrinol Metab, 295*(5), E1269-1276. doi:10.1152/ajpendo.90207.2008

Caesar, R., Tremaroli, V., Kovatcheva-Datchary, P., Cani, P. D., & Backhed, F. (2015). Crosstalk between Gut Microbiota and Dietary Lipids Aggravates WAT Inflammation through TLR Signaling. *Cell Metab, 22*(4), 658-668. doi:10.1016/j.cmet.2015.07.026

Calder, P. C., Ahluwalia, N., Brouns, F., Buetler, T., Clement, K., Cunningham, K., . . . Winklhofer-Roob, B. M. (2011). Dietary factors and low-grade inflammation in relation to overweight and obesity. *Br J Nutr, 106 Suppl 3*, S5-78. doi:10.1017/s0007114511005460

Calderón, G., García, E., Rojas, P., García, E., Rosso, M., & Losada, A. (2011). Chryseobacterium indologenes infection in a newborn: a case report. *Journal of Medical Case Reports, 5*(1), 10. doi:10.1186/1752-1947-5-10

Calle, E. E., Rodriguez, C., Walker-Thurmond, K., & Thun, M. J. (2003). Overweight, obesity, and mortality from cancer in a prospectively studied cohort of U.S. adults. *N Engl J Med, 348*(17), 1625-1638. doi:10.1056/NEJMoa021423

Camargos, A. C., Mendonca, V. A., Andrade, C. A., Oliveira, K. S., Tossige-Gomes, R., Rocha-Vieira, E., . . . Lacerda, A. C. (2016). Neuroendocrine Inflammatory Responses in Overweight/Obese Infants. *PLoS One, 11*(12), e0167593. doi:10.1371/journal.pone.0167593

Cani, P. D., Amar, J., Iglesias, M. A., Poggi, M., Knauf, C., Bastelica, D., . . . Burcelin, R. (2007). Metabolic endotoxemia initiates obesity and insulin resistance. *Diabetes, 56*(7), 1761-1772. doi:10.2337/db06-1491

Canoy, D., Wareham, N., Welch, A., Bingham, S., Luben, R., Day, N., & Khaw, K. T. (2005). Plasma ascorbic acid concentrations and fat distribution in 19,068 British men and women in the European Prospective Investigation into Cancer and Nutrition Norfolk cohort study. *Am J Clin Nutr, 82*(6), 1203-1209. doi:10.1093/ajcn/82.6.1203

Canto, C., & Auwerx, J. (2012). Cell biology. FGF21 takes a fat bite. *Science, 336*(6082), 675-676. doi:10.1126/science.1222646

Caporaso, J. G., Kuczynski, J., Stombaugh, J., Bittinger, K., Bushman, F. D., Costello, E. K., . . . Knight, R. (2010). QIIME allows analysis of high-throughput community sequencing data. *Nat Methods, 7*(5), 335-336. doi:10.1038/nmeth.f.303

Caporaso, J. G., Lauber, C. L., Walters, W. A., Berg-Lyons, D., Lozupone, C. A., Turnbaugh, P. J., . . . Knight, R. (2011). Global patterns of 16S rRNA diversity at a depth of millions of sequences per sample. *Proc Natl Acad Sci U S A, 108 Suppl 1*, 4516-4522. doi:10.1073/pnas.1000080107

Carlioz, A., & Touati, D. (1986). Isolation of superoxide dismutase mutants in Escherichia coli: is superoxide dismutase necessary for aerobic life? *EMBO J, 5*(3), 623-630.

Carnevale, R., Bartimoccia, S., Nocella, C., Di Santo, S., Loffredo, L., Illuminati, G., . . . Violi, F. (2014). LDL oxidation by platelets propagates platelet activation via an oxidative

stress-mediated mechanism. *Atherosclerosis, 237*(1), 108-116. doi:10.1016/j.atherosclerosis.2014.08.041

Carrier, A. (2017). Metabolic Syndrome and Oxidative Stress: A Complex Relationship. *Antioxid Redox Signal, 26*(9), 429-431. doi:10.1089/ars.2016.6929

Carstens, M. T., Goedecke, J. H., Dugas, L., Evans, J., Kroff, J., Levitt, N. S., & Lambert, E. V. (2013). Fasting substrate oxidation in relation to habitual dietary fat intake and insulin resistance in non-diabetic women: a case for metabolic flexibility? *Nutr Metab (Lond), 10*, 8. doi:10.1186/1743-7075-10-8

Ceci, R., Sabatini, S., Duranti, G., Savini, I., Avigliano, L., & Rossi, A. (2007). Acute, but not chronic, leptin treatment induces acyl-CoA oxidase in C2C12 myotubes. *Eur J Nutr, 46*(6), 364-368. doi:10.1007/s00394-007-0664-9

Cerf, M. E. (2013). Beta cell dysfunction and insulin resistance. *Front Endocrinol (Lausanne), 4*, 37. doi:10.3389/fendo.2013.00037

Chae, C. U., Albert, C. M., Moorthy, M. V., Lee, I. M., & Buring, J. E. (2012). Vitamin E supplementation and the risk of heart failure in women. *Circ Heart Fail, 5*(2), 176-182. doi:10.1161/circheartfailure.111.963793

Chartoumpekis, D. V., Ziros, P. G., Psyrogiannis, A. I., Papavassiliou, A. G., Kyriazopoulou, V. E., Sykiotis, G. P., & Habeos, I. G. (2011). Nrf2 represses FGF21 during long-term high-fat diet-induced obesity in mice. *Diabetes, 60*(10), 2465-2473. doi:10.2337/db11-0112

Chen, J., Guo, Y., Gui, Y., & Xu, D. (2018). Physical exercise, gut, gut microbiota, and atherosclerotic cardiovascular diseases. *Lipids Health Dis, 17*(1), 17. doi:10.1186/s12944-017-0653-9

Chen, J., Zhang, Z., & Cai, L. (2014). Diabetic cardiomyopathy and its prevention by nrf2: current status. *Diabetes Metab J, 38*(5), 337-345. doi:10.4093/dmj.2014.38.5.337

Chen, V. P., Gao, Y., Geng, L., Stout, M. B., Jensen, M. D., & Brimijoin, S. (2016). Butyrylcholinesterase Deficiency Promotes Adipose Tissue Growth and Hepatic Lipid Accumulation in Male Mice on High-Fat Diet. *Endocrinology, 157*(8), 3086-3095. doi:10.1210/en.2016-1166

Chen, X., Liang, H., Van Remmen, H., Vijg, J., & Richardson, A. (2004). Catalase transgenic mice: characterization and sensitivity to oxidative stress. *Arch Biochem Biophys, 422*(2), 197-210. doi:10.1016/j.abb.2003.12.023

Chen, X., Mele, J., Giese, H., Van Remmen, H., Dolle, M. E., Steinhelper, M., . . . Vijg, J. (2003). A strategy for the ubiquitous overexpression of human catalase and CuZn superoxide dismutase genes in transgenic mice. *Mech Ageing Dev, 124*(2), 219-227.

Chen, Z., Yu, R., Xiong, Y., Du, F., & Zhu, S. (2017). A vicious circle between insulin resistance and inflammation in nonalcoholic fatty liver disease. *Lipids Health Dis, 16*(1), 203. doi:10.1186/s12944-017-0572-9

Cherbut, C., Ferrier, L., Roze, C., Anini, Y., Blottiere, H., Lecannu, G., . . . Galmiche, J. (1998). Short-chain fatty acids modify colonic motility through nerves and polypeptide YY release in the rat. *American Journal of Physiology, 275*, G1415-G1422.

Chetboun, M., Abitbol, G., Rozenberg, K., Rozenfeld, H., Deutsch, A., Sampson, S. R., & Rosenzweig, T. (2012). Maintenance of redox state and pancreatic beta-cell function: role of leptin and adiponectin. *J Cell Biochem, 113*(6), 1966-1976. doi:10.1002/jcb.24065

Choe, S. S., Huh, J. Y., Hwang, I. J., Kim, J. I., & Kim, J. B. (2016). Adipose Tissue Remodeling: Its Role in Energy Metabolism and Metabolic Disorders. *Front Endocrinol (Lausanne), 7*, 30. doi:10.3389/fendo.2016.00030

Chong, A. Y., Lupsa, B. C., Cochran, E. K., & Gorden, P. (2010). Efficacy of leptin therapy in the different forms of human lipodystrophy. *Diabetologia, 53*(1), 27-35. doi:10.1007/s00125-009-1502-9

Chopra, M., Siddhu, A., & Tandon, N. (2014). Effect of Nutritional Regulation on Adipokines in Obesity: A Review. *American Journal of Food and Nutrition, 2*(4), 66-70.

Chowen, J. A., & Argente, J. (2011). Leptin and the brain. *Horm Mol Biol Clin Investig, 7*(2), 351-360. doi:10.1515/HMBCI.2011.113

Chrysohoou, C., Panagiotakos, D. B., Pitsavos, C., Skoumas, I., Papademetriou, L., Economou, M., & Stefanadis, C. (2007). The implication of obesity on total antioxidant capacity in apparently healthy men and women: the ATTICA study. *Nutr Metab Cardiovasc Dis, 17*(8), 590-597. doi:10.1016/j.numecd.2006.05.007

Chung, W. K., Belfi, K., Chua, M., Wiley, J., Mackintosh, R., Nicolson, M., . . . Leibel, R. L. (1998). Heterozygosity for Lep(ob) or Lep(rdb) affects body composition and leptin homeostasis in adult mice. *Am J Physiol, 274*(4 Pt 2), R985-990.

Church, C., Lee, S., Bagg, E. A., McTaggart, J. S., Deacon, R., Gerken, T., . . . Cox, R. D. (2009). A mouse model for the metabolic effects of the human fat mass and obesity associated FTO gene. *PLoS Genet, 5*(8), e1000599. doi:10.1371/journal.pgen.1000599

Cipollina, C. (2015). Endogenous Generation and Signaling Actions of Omega-3 Fatty Acid Electrophilic Derivatives. *Biomed Res Int, 2015*, 501792. doi:10.1155/2015/501792

Clarke, G., Stilling, R. M., Kennedy, P. J., Stanton, C., Cryan, J. F., & Dinan, T. G. (2014). Minireview: Gut microbiota: the neglected endocrine organ. *Mol Endocrinol, 28*(8), 1221-1238. doi:10.1210/me.2014-1108

Clarke, S. F., Murphy, E. F., O'Sullivan, O., Lucey, A. J., Humphreys, M., Hogan, A., . . . Cotter, P. D. (2014). Exercise and associated dietary extremes impact on gut microbial diversity. *Gut, 63*(12), 1913-1920. doi:10.1136/gutjnl-2013-306541

Clarke, S. F., Murphy, E. F., O'Sullivan, O., Ross, R. P., O'Toole, P. W., Shanahan, F., & Cotter, P. D. (2013). Targeting the microbiota to address diet-induced obesity: a time dependent challenge. *PLoS One, 8*(6), e65790. doi:10.1371/journal.pone.0065790

Clement, K., Vaisse, C., Lahlou, N., Cabrol, S., Pelloux, V., Cassuto, D., . . . Guy-Grand, B. (1998). A mutation in the human leptin receptor gene causes obesity and pituitary dysfunction. *Nature, 392*(6674), 398-401. doi:10.1038/32911

Codoner-Franch, P., Lopez-Jaen, A. B., De La Mano-Hernandez, A., Sentandreu, E., Simo-Jorda, R., & Valls-Belles, V. (2010). Oxidative markers in children with severe obesity following low-calorie diets supplemented with mandarin juice. *Acta Paediatr, 99*(12), 1841-1846. doi:10.1111/j.1651-2227.2010.01903.x

Codoner-Franch, P., Tavarez-Alonso, S., Murria-Estal, R., Tortajada-Girbes, M., Simo-Jorda, R., & Alonso-Iglesias, E. (2012). Elevated advanced oxidation protein products (AOPPs) indicate metabolic risk in severely obese children. *Nutr Metab Cardiovasc Dis, 22*(3), 237-243. doi:10.1016/j.numecd.2010.06.002

Coen, P. M., & Goodpaster, B. H. (2012). Role of intramyocelluar lipids in human health. *Trends Endocrinol Metab, 23*(8), 391-398. doi:10.1016/j.tem.2012.05.009

Collins, S., Martin, T. L., Surwit, R. S., & Robidoux, J. (2004). Genetic vulnerability to diet-induced obesity in the C57BL/6J mouse: physiological and molecular characteristics. *Physiol Behav, 81*(2), 243-248. doi:10.1016/j.physbeh.2004.02.006

Combs, T. P., & Marliss, E. B. (2014). Adiponectin signaling in the liver. *Rev Endocr Metab Disord, 15*(2), 137-147. doi:10.1007/s11154-013-9280-6

Conlon, M. A., & Bird, A. R. (2014). The impact of diet and lifestyle on gut microbiota and human health. *Nutrients, 7*(1), 17-44. doi:10.3390/nu7010017

Coqueiro, R. D. S., Soares, T. J., Pereira, R., Correia, T. M. L., Coqueiro, D. S. O., Oliveira, M. V., . . . de Magalhaes, A. C. M. (2019). Therapeutic and preventive effects of exercise on cardiometabolic parameters in aging and obese rats. *Clin Nutr ESPEN, 29*, 203-212. doi:10.1016/j.clnesp.2018.10.003

Crujeiras, A. B., Diaz-Lagares, A., Carreira, M. C., Amil, M., & Casanueva, F. F. (2013). Oxidative stress associated to dysfunctional adipose tissue: a potential link between obesity, type 2 diabetes mellitus and breast cancer. *Free Radic Res, 47*(4), 243-256. doi:10.3109/10715762.2013.772604

Crujeiras, A. B., Parra, M. D., Rodriguez, M. C., Martinez de Morentin, B. E., & Martinez, J. A. (2006). A role for fruit content in energy-restricted diets in improving antioxidant status in obese women during weight loss. *Nutrition, 22*(6), 593-599. doi:10.1016/j.nut.2006.03.008

Cuevas-Ramos, D., Almeda-Valdes, P., Meza-Arana, C. E., Brito-Cordova, G., Gomez-Perez, F. J., Mehta, R., . . . Aguilar-Salinas, C. A. (2012). Exercise increases serum fibroblast growth factor 21 (FGF21) levels. *PLoS One, 7*(5), e38022. doi:10.1371/journal.pone.0038022

Cummings, J. H., & Macfarlane, G. T. (1997). Role of intestinal bacteria in nutrient metabolism. *JPEN J Parenter Enteral Nutr, 21*(6), 357-365. doi:10.1177/0148607197021006357

Cutruzzolà, F., & Cutruzzolà, F. (2012). Nitric oxide synthesis by bacterial cytochrome cd1 nitrite reductases. *Nitric Oxide, 27*(Suppl), S10.

Cypess, A. M., Lehman, S., Williams, G., Tal, I., Rodman, D., Goldfine, A. B., . . . Kahn, C. R. (2009). Identification and importance of brown adipose tissue in adult humans. *N Engl J Med, 360*(15), 1509-1517. doi:10.1056/NEJMoa0810780

D'Archivio, M., Annuzzi, G., Vari, R., Filesi, C., Giacco, R., Scazzocchio, B., . . . Masella, R. (2012). Predominant role of obesity/insulin resistance in oxidative stress development. *Eur J Clin Invest, 42*(1), 70-78. doi:10.1111/j.1365-2362.2011.02558.x

Dandona, P., Aljada, A., Chaudhuri, A., Mohanty, P., & Garg, R. (2005). Metabolic syndrome: a comprehensive perspective based on interactions between obesity, diabetes, and inflammation. *Circulation, 111*(11), 1448-1454. doi:10.1161/01.Cir.0000158483.13093.9d

Daskalopoulou, S. S., Cooke, A. B., Gomez, Y. H., Mutter, A. F., Filippaios, A., Mesfum, E. T., & Mantzoros, C. S. (2014). Plasma irisin levels progressively increase in response to increasing exercise workloads in young, healthy, active subjects. *Eur J Endocrinol, 171*(3), 343-352. doi:10.1530/eje-14-0204

de Carvalho, F. P., Benfato, I. D., Moretto, T. L., Barthichoto, M., & de Oliveira, C. A. (2016). Voluntary running decreases nonexercise activity in lean and diet-induced obese mice. *Physiol Behav, 165*, 249-256. doi:10.1016/j.physbeh.2016.08.003

de la Cuesta-Zuluaga, J., Corrales-Agudelo, V., Velásquez-Mejía, E. P., Carmona, J. A., Abad, J. M., & Escobar, J. S. (2018). Gut microbiota is associated with obesity and cardiometabolic disease in a population in the midst of Westernization. *Scientific Reports, 8*(1), 11356. doi:10.1038/s41598-018-29687-x

Deacon, R. M. (2013). Measuring the strength of mice. *J Vis Exp*(76). doi:10.3791/2610

DeClercq, V., Enns, J. E., Yeganeh, A., Taylor, C. G., & Zahradka, P. (2013). Modulation of cardiovascular function by adipokines. *Cardiovasc Hematol Disord Drug Targets, 13*(1), 59-72.

Del Rio, D., Agnoli, C., Pellegrini, N., Krogh, V., Brighenti, F., Mazzeo, T., . . . Panico, S. (2011). Total antioxidant capacity of the diet is associated with lower risk of ischemic stroke in a large Italian cohort. *J Nutr, 141*(1), 118-123. doi:10.3945/jn.110.125120

Delezie, J., & Handschin, C. (2018). Endocrine Crosstalk Between Skeletal Muscle and the Brain. *Front Neurol, 9*, 698. doi:10.3389/fneur.2018.00698

Demarin, V., Lisak, M., & Morovic, S. (2011). Mediterranean diet in healthy lifestyle and prevention of stroke. *Acta Clin Croat, 50*(1), 67-77.

Denis, G. V., & Hamilton, J. A. (2013). Healthy obese persons: how can they be identified and do metabolic profiles stratify risk? *Curr Opin Endocrinol Diabetes Obes, 20*(5), 369-376. doi:10.1097/01.med.0000433058.78485.b3

Denou, E., Marcinko, K., Surette, M. G., Steinberg, G. R., & Schertzer, J. D. (2016). High-intensity exercise training increases the diversity and metabolic capacity of the mouse distal gut microbiota during diet-induced obesity. *Am J Physiol Endocrinol Metab, 310*(11), E982-993. doi:10.1152/ajpendo.00537.2015

DeSantis, T. Z., Hugenholtz, P., Larsen, N., Rojas, M., Brodie, E. L., Keller, K., . . . Andersen, G. L. (2006). Greengenes, a chimera-checked 16S rRNA gene database and workbench compatible with ARB. *Appl Environ Microbiol, 72*(7), 5069-5072. doi:10.1128/AEM.03006-05

Di Ciaula, A., Garruti, G., Lunardi Baccetto, R., Molina-Molina, E., Bonfrate, L., Wang, D. Q., & Portincasa, P. (2017). Bile Acid Physiology. *Ann Hepatol, 16*(Suppl. 1: s3-105.), s4-s14. doi:10.5604/01.3001.0010.5493

Diane, A., Pierce, W. D., Mangat, R., Borthwick, F., Nelson, R., Russell, J. C., . . . Proctor, S. D. (2015). Differential expression of hypothalamic, metabolic and inflammatory genes in response to short-term calorie restriction in juvenile obese- and lean-prone JCR rats. *Nutr Diabetes, 5*, e178. doi:10.1038/nutd.2015.28

Dilzer, A., & Park, Y. (2012). Implication of conjugated linoleic acid (CLA) in human health. *Crit Rev Food Sci Nutr, 52*(6), 488-513. doi:10.1080/10408398.2010.501409

Division of Nutrition, P. A., and Obesity, National Center for Chronic Disease Prevention and Health Promotion. (2018, September 14, 2018). Overweight/Obesity August 13, 2018. Retrieved from https://www.cdc.gov/obesity/data/adult.html

Dokken, B. B., Saengsirisuwan, V., Kim, J. S., Teachey, M. K., & Henriksen, E. J. (2008). Oxidative stress-induced insulin resistance in rat skeletal muscle: role of glycogen synthase kinase-3. *Am J Physiol Endocrinol Metab, 294*(3), E615-621. doi:10.1152/ajpendo.00578.2007

Done, A. J., & Traustadottir, T. (2016). Nrf2 mediates redox adaptations to exercise. *Redox Biol, 10*, 191-199. doi:10.1016/j.redox.2016.10.003

Dreger, H., Westphal, K., Weller, A., Baumann, G., Stangl, V., Meiners, S., & Stangl, K. (2009). Nrf2-dependent upregulation of antioxidative enzymes: a novel pathway for proteasome

inhibitor-mediated cardioprotection. *Cardiovasc Res, 83*(2), 354-361. doi:10.1093/cvr/cvp107

Drougard, A., Fournel, A., Valet, P., & Knauf, C. (2015). Impact of hypothalamic reactive oxygen species in the regulation of energy metabolism and food intake. *Front Neurosci, 9*, 56. doi:10.3389/fnins.2015.00056

Drummond, G. R., Selemidis, S., Griendling, K. K., & Sobey, C. G. (2011). Combating oxidative stress in vascular disease: NADPH oxidases as therapeutic targets. *Nat Rev Drug Discov, 10*(6), 453-471. doi:10.1038/nrd3403

Dubin, K., & Pamer, E. G. (2014). Enterococci and Their Interactions with the Intestinal Microbiome. *Microbiol Spectr, 5*(6). doi:10.1128/microbiolspec.BAD-0014-2016

Ebrahimi-Mamaeghani, M., Mohammadi, S., Arefhosseini, S. R., Fallah, P., & Bazi, Z. (2015). Adiponectin as a potential biomarker of vascular disease. *Vasc Health Risk Manag, 11*, 55-70. doi:10.2147/vhrm.S48753

Edgar, R. C. (2010). Search and clustering orders of magnitude faster than BLAST. *Bioinformatics, 26*(19), 2460-2461. doi:10.1093/bioinformatics/btq461

Edgar, R. C. (2013). UPARSE: highly accurate OTU sequences from microbial amplicon reads. *Nat Methods, 10*(10), 996-998. doi:10.1038/nmeth.2604

Eicher-Miller, H. A., & Boushey, C. J. (2017). How Often and How Much? Differences in Dietary Intake by Frequency and Energy Contribution Vary among U.S. Adults in NHANES 2007-2012. *Nutrients, 9*(1). doi:10.3390/nu9010086

Eid, H. M., Wright, M. L., Anil Kumar, N. V., Qawasmeh, A., Hassan, S. T. S., Mocan, A., . . . Haddad, P. S. (2017). Significance of Microbiota in Obesity and Metabolic Diseases and the Modulatory Potential by Medicinal Plant and Food Ingredients. *Front Pharmacol, 8*, 387. doi:10.3389/fphar.2017.00387

Eisenhofer, G., Aneman, A., Friberg, P., Hooper, D., Fandriks, L., Lonroth, H., . . . Mezey, E. (1997). Substantial production of dopamine in the human gastrointestinal tract. *J Clin Endocrinol Metab, 82*(11), 3864-3871. doi:10.1210/jcem.82.11.4339

Ellett, J. D., Evans, Z. P., Zhang, G., Chavin, K. D., & Spyropoulos, D. D. (2009). A rapid PCR-based method for the identification of ob mutant mice. *Obesity (Silver Spring), 17*(2), 402-404. doi:10.1038/oby.2008.443

Engin, A. (2017a). Obesity-associated Breast Cancer: Analysis of risk factors. *Adv Exp Med Biol, 960*, 571-606. doi:10.1007/978-3-319-48382-5_25

Engin, A. (2017b). The Pathogenesis of Obesity-Associated Adipose Tissue Inflammation. *Adv Exp Med Biol, 960*, 221-245. doi:10.1007/978-3-319-48382-5_9

Espinosa-Diez, C., Miguel, V., Mennerich, D., Kietzmann, T., Sanchez-Perez, P., Cadenas, S., & Lamas, S. (2015). Antioxidant responses and cellular adjustments to oxidative stress. *Redox Biol, 6*, 183-197. doi:10.1016/j.redox.2015.07.008

Estaki, M., Pither, J., Baumeister, P., Little, J. P., Gill, S. K., Ghosh, S., . . . Gibson, D. L. (2016). Cardiorespiratory fitness as a predictor of intestinal microbial diversity and distinct metagenomic functions. *Microbiome, 4*(1), 42. doi:10.1186/s40168-016-0189-7

Evans, C. C., LePard, K. J., Kwak, J. W., Stancukas, M. C., Laskowski, S., Dougherty, J., . . . Ciancio, M. J. (2014). Exercise prevents weight gain and alters the gut microbiota in a mouse model of high fat diet-induced obesity. *PLoS One, 9*(3), e92193. doi:10.1371/journal.pone.0092193

Evans, J. M., Morris, L. S., & Marchesi, J. R. (2013). The gut microbiome: the role of a virtual organ in the endocrinology of the host. *J Endocrinol, 218*(3), R37-47. doi:10.1530/JOE-13-0131

Fang, H., & Judd, R. L. (2018). Adiponectin Regulation and Function. *Compr Physiol, 8*(3), 1031-1063. doi:10.1002/cphy.c170046

Febbraio, M. A., & Pedersen, B. K. (2005). Contraction-induced myokine production and release: is skeletal muscle an endocrine organ? *Exerc Sport Sci Rev, 33*(3), 114-119.

Fedorova, M., Bollineni, R. C., & Hoffmann, R. (2014). Protein carbonylation as a major hallmark of oxidative damage: update of analytical strategies. *Mass Spectrom Rev, 33*(2), 79-97. doi:10.1002/mas.21381

Fernandez-Navarro, T., Salazar, N., Gutierrez-Diaz, I., de Los Reyes-Gavilan, C. G., Gueimonde, M., & Gonzalez, S. (2017). Different Intestinal Microbial Profile in Over-

Weight and Obese Subjects Consuming a Diet with Low Content of Fiber and Antioxidants. *Nutrients, 9*(6). doi:10.3390/nu9060551

Fernandez-Sanchez, A., Madrigal-Santillan, E., Bautista, M., Esquivel-Soto, J., Morales-Gonzalez, A., Esquivel-Chirino, C., . . . Morales-Gonzalez, J. A. (2011). Inflammation, oxidative stress, and obesity. *Int J Mol Sci, 12*(5), 3117-3132. doi:10.3390/ijms12053117

Ferretti, G., Bacchetti, T., Masciangelo, S., & Bicchiega, V. (2010). HDL-paraoxonase and membrane lipid peroxidation: a comparison between healthy and obese subjects. *Obesity (Silver Spring), 18*(6), 1079-1084. doi:10.1038/oby.2009.338

Fietta, P., & Delsante, G. (2013). Focus on adipokines. *Theor Biol Forum, 106*(1-2), 103-129.

Figueroa, A. L., Takx, R. A., MacNabb, M. H., Abdelbaky, A., Lavender, Z. R., Kaplan, R. S., . . . Tawakol, A. (2016). Relationship Between Measures of Adiposity, Arterial Inflammation, and Subsequent Cardiovascular Events. *Circ Cardiovasc Imaging, 9*(4), e004043. doi:10.1161/CIRCIMAGING.115.004043

Fisher, F. M., Kleiner, S., Douris, N., Fox, E. C., Mepani, R. J., Verdeguer, F., . . . Spiegelman, B. M. (2012). FGF21 regulates PGC-1alpha and browning of white adipose tissues in adaptive thermogenesis. *Genes Dev, 26*(3), 271-281. doi:10.1101/gad.177857.111

Fiuza-Luces, C., Garatachea, N., Berger, N. A., & Lucia, A. (2013). Exercise is the real polypill. *Physiology (Bethesda), 28*(5), 330-358. doi:10.1152/physiol.00019.2013

Flak, J. N. (2017). A role for leptin-regulated neurocircuitry in subordination stress. *Physiol Behav, 178*, 144-150. doi:10.1016/j.physbeh.2016.11.019

Flatt, P. R., & Bailey, C. J. (1981). Abnormal plasma glucose and insulin responses in heterozygous lean (ob/+) mice. *Diabetologia, 20*(5), 573-577.

Forbes, S., Robinson, S., Dungu, J., Anyaoku, V., Bannister, P., Forster, D., . . . Johnston, D. G. (2006). Sustained endogenous glucose production, diminished lipolysis and non-esterified fatty acid appearance and oxidation in non-obese women at high risk of type 2 diabetes. *Eur J Endocrinol, 155*(3), 469-476. doi:10.1530/eje.1.02240

Foundation, R. W. J. (2018). The State of Obesity (Article). Retrieved February 2, 2018, from Robert Wood Johnson Foundation https://stateofobesity.org/adult-obesity/

Fourie, N. H., Wang, D., Abey, S. K., Creekmore, A. L., Hong, S., Martin, C. G., . . . Henderson, W. A. (2017). Structural and functional alterations in the colonic microbiome of the rat in a model of stress induced irritable bowel syndrome. *Gut Microbes, 8*(1), 33-45. doi:10.1080/19490976.2016.1273999

Frago, L. M., & Chowen, J. A. (2015). Hypothalamic Leptin and Ghrelin Signaling as Targets for Improvement in Metabolic Control. *Curr Pharm Des, 21*(25), 3596-3605.

Freeman, L. R., Zhang, L., Nair, A., Dasuri, K., Francis, J., Fernandez-Kim, S. O., . . . Keller, J. N. (2013). Obesity increases cerebrocortical reactive oxygen species and impairs brain function. *Free Radic Biol Med, 56*, 226-233. doi:10.1016/j.freeradbiomed.2012.08.577

Friedman, J. (2016). The long road to leptin. *J Clin Invest, 126*(12), 4727-4734. doi:10.1172/JCI91578

Friedman, J. M., & Mantzoros, C. S. (2015). 20 years of leptin: from the discovery of the leptin gene to leptin in our therapeutic armamentarium. *Metabolism, 64*(1), 1-4. doi:10.1016/j.metabol.2014.10.023

Fry, A. C., Housh, T. J., Cramer, J. B., Weir, J. P., Beck, T. W., Schilling, B. K., . . . Nicoll, J. X. (2017). Noninvasive Assessment of Skeletal Muscle Myosin Heavy Chain Expression in Trained and Untrained Men. *J Strength Cond Res, 31*(9), 2355-2362. doi:10.1519/JSC.0000000000001645

Fryer, L. G., Foufelle, F., Barnes, K., Baldwin, S. A., Woods, A., & Carling, D. (2002). Characterization of the role of the AMP-activated protein kinase in the stimulation of glucose transport in skeletal muscle cells. *Biochem J, 363*(Pt 1), 167-174.

Fujita, K., Nishizawa, H., Funahashi, T., Shimomura, I., & Shimabukuro, M. (2006). Systemic oxidative stress is associated with visceral fat accumulation and the metabolic syndrome. *Circ J, 70*(11), 1437-1442.

Fukumoto, S., Tatewaki, M., Yamada, T., Fujimiya, M., Mantyh, C., Voss, M., . . . Takahashi, T. (2003). Short-chain fatty acids stimulate colonic transit via intraluminal 5-HT release in rats. *American Journal of Physiololgy. Regulatory, Integrative and Comparative Physiology, 284*, R1269-R1276.

Funahashi, H., Takenoya, F., Guan, J. L., Kageyama, H., Yada, T., & Shioda, S. (2003). Hypothalamic neuronal networks and feeding-related peptides involved in the regulation of feeding. *Anat Sci Int, 78*(3), 123-138. doi:10.1046/j.0022-7722.2003.00055.x

Furukawa, S., Fujita, T., Shimabukuro, M., Iwaki, M., Yamada, Y., Nakajima, Y., . . . Shimomura, I. (2004). Increased oxidative stress in obesity and its impact on metabolic syndrome. *J Clin Invest, 114*(12), 1752-1761. doi:10.1172/JCI21625

Furusawa, Y., Uruno, A., Yagishita, Y., Higashi, C., & Yamamoto, M. (2014). Nrf2 induces fibroblast growth factor 21 in diabetic mice. *Genes Cells, 19*(12), 864-878. doi:10.1111/gtc.12186

Gao, L., Wang, J., Sekhar, K. R., Yin, H., Yared, N. F., Schneider, S. N., . . . Freeman, M. L. (2007). Novel n-3 fatty acid oxidation products activate Nrf2 by destabilizing the association between Keap1 and Cullin3. *J Biol Chem, 282*(4), 2529-2537. doi:10.1074/jbc.M607622200

Garcia-Mantrana, I., Selma-Royo, M., Alcantara, C., & Collado, M. C. (2018). Shifts on Gut Microbiota Associated to Mediterranean Diet Adherence and Specific Dietary Intakes on General Adult Population. *Front Microbiol, 9*, 890. doi:10.3389/fmicb.2018.00890

Garelnabi, M., Veledar, E., White-Welkley, J., Santanam, N., Abramson, J., Weintraub, W., & Parthasarathy, S. (2012). Vitamin E differentially affects short term exercise induced changes in oxidative stress, lipids, and inflammatory markers. *Nutr Metab Cardiovasc Dis, 22*(10), 907-913. doi:10.1016/j.numecd.2011.03.002

Ge, X., Pettan-Brewer, C., Morton, J., Carter, K., Fatemi, S., Rabinovitch, P., & Ladiges, W. C. (2015). Mitochondrial catalase suppresses naturally occurring lung cancer in old mice. *Pathobiol Aging Age Relat Dis, 5*, 28776. doi:10.3402/pba.v5.28776

Ghanim, H., Sia, C. L., Upadhyay, M., Korzeniewski, K., Viswanathan, P., Abuaysheh, S., . . . Dandona, P. (2010). Orange juice neutralizes the proinflammatory effect of a high-fat, high-carbohydrate meal and prevents endotoxin increase and Toll-like receptor expression. *Am J Clin Nutr, 91*(4), 940-949. doi:10.3945/ajcn.2009.28584

Ghantous, C. M., Azrak, Z., Hanache, S., Abou-Kheir, W., & Zeidan, A. (2015). Differential Role of Leptin and Adiponectin in Cardiovascular System. *Int J Endocrinol, 2015*, 534320. doi:10.1155/2015/534320

Gill, S. R., Pop, M., Deboy, R. T., Eckburg, P. B., Turnbaugh, P. J., Samuel, B. S., . . . Nelson, K. E. (2006). Metagenomic analysis of the human distal gut microbiome. *Science, 312*(5778), 1355-1359. doi:10.1126/science.1124234

Glorieux, C., & Calderon, P. B. (2017). Catalase, a remarkable enzyme: targeting the oldest antioxidant enzyme to find a new cancer treatment approach. *Biol Chem, 398*(10), 1095-1108. doi:10.1515/hsz-2017-0131

Godin, N., Liu, F., Lau, G. J., Brezniceanu, M. L., Chenier, I., Filep, J. G., . . . Chan, J. S. (2010). Catalase overexpression prevents hypertension and tubular apoptosis in angiotensinogen transgenic mice. *Kidney Int, 77*(12), 1086-1097. doi:10.1038/ki.2010.63

Golbidi, S., & Laher, I. (2014). Exercise induced adipokine changes and the metabolic syndrome. *J Diabetes Res, 2014*, 726861. doi:10.1155/2014/726861

Golbidi, S., Mesdaghinia, A., & Laher, I. (2012). Exercise in the metabolic syndrome. *Oxid Med Cell Longev, 2012*, 349710. doi:10.1155/2012/349710

Gollnick, P. D., & Hodgson, D. R. (1986). The identification of fiber types in skeletal muscle: a continual dilemma. *Exerc Sport Sci Rev, 14*, 81-104.

Gomez-Cabrera, M. C., Domenech, E., & Vina, J. (2008). Moderate exercise is an antioxidant: upregulation of antioxidant genes by training. *Free Radic Biol Med, 44*(2), 126-131. doi:10.1016/j.freeradbiomed.2007.02.001

Gomez-Samano, M. A., Grajales-Gomez, M., Zuarth-Vazquez, J. M., Navarro-Flores, M. F., Martinez-Saavedra, M., Juarez-Leon, O. A., . . . Cuevas-Ramos, D. (2017). Fibroblast growth factor 21 and its novel association with oxidative stress. *Redox Biol, 11*, 335-341. doi:10.1016/j.redox.2016.12.024

Gonzalez-Castejon, M., & Rodriguez-Casado, A. (2011). Dietary phytochemicals and their potential effects on obesity: a review. *Pharmacol Res, 64*(5), 438-455. doi:10.1016/j.phrs.2011.07.004

Gonzalez-Muniesa, P., Martinez-Gonzalez, M. A., Hu, F. B., Despres, J. P., Matsuzawa, Y., Loos, R. J. F., . . . Martinez, J. A. (2017). Obesity. *Nat Rev Dis Primers, 3*, 17034. doi:10.1038/nrdp.2017.34

Goodpaster, B. H., & Sparks, L. M. (2017). Metabolic Flexibility in Health and Disease. *Cell Metab, 25*(5), 1027-1036. doi:10.1016/j.cmet.2017.04.015

Goossens, G. H. (2017). The Metabolic Phenotype in Obesity: Fat Mass, Body Fat Distribution, and Adipose Tissue Function. *Obes Facts, 10*(3), 207-215. doi:10.1159/000471488

Gorgens, S. W., Eckardt, K., Jensen, J., Drevon, C. A., & Eckel, J. (2015). Exercise and Regulation of Adipokine and Myokine Production. *Prog Mol Biol Transl Sci, 135*, 313-336. doi:10.1016/bs.pmbts.2015.07.002

Goss, A. M., Goree, L. L., Ellis, A. C., Chandler-Laney, P. C., Casazza, K., Lockhart, M. E., & Gower, B. A. (2013). Effects of diet macronutrient composition on body composition and fat distribution during weight maintenance and weight loss. *Obesity (Silver Spring), 21*(6), 1139-1142. doi:10.1002/oby.20191

Grattagliano, I., Palmieri, V. O., Portincasa, P., Moschetta, A., & Palasciano, G. (2008). Oxidative stress-induced risk factors associated with the metabolic syndrome: a unifying hypothesis. *J Nutr Biochem, 19*(8), 491-504. doi:10.1016/j.jnutbio.2007.06.011

Grenham, S., Clarke, G., Cryan, J. F., & Dinan, T. G. (2011). Brain-gut-microbe communication in health and disease. *Front Physiol, 2*, 94. doi:10.3389/fphys.2011.00094

Grosicki, G. J., Fielding, R. A., & Lustgarten, M. S. (2018). Gut Microbiota Contribute to Age-Related Changes in Skeletal Muscle Size, Composition, and Function: Biological Basis for a Gut-Muscle Axis. *Calcif Tissue Int, 102*(4), 433-442. doi:10.1007/s00223-017-0345-5

Guo, R., Liong, E. C., So, K. F., Fung, M. L., & Tipoe, G. L. (2015). Beneficial mechanisms of aerobic exercise on hepatic lipid metabolism in non-alcoholic fatty liver disease. *Hepatobiliary Pancreat Dis Int, 14*(2), 139-144.

Gutierrez-Lopez, L., Garcia-Sanchez, J. R., Rincon-Viquez Mde, J., Lara-Padilla, E., Sierra-Vargas, M. P., & Olivares-Corichi, I. M. (2012). Hypocaloric diet and regular moderate aerobic exercise is an effective strategy to reduce anthropometric parameters and oxidative stress in obese patients. *Obes Facts, 5*(1), 12-22. doi:10.1159/000336526

Guzik, T. J., Mangalat, D., & Korbut, R. (2006). Adipocytokines - novel link between inflammation and vascular function? *J Physiol Pharmacol, 57*(4), 505-528.

Gyengesi, E., Paxinos, G., & Andrews, Z. B. (2012). Oxidative Stress in the Hypothalamus: the Importance of Calcium Signaling and Mitochondrial ROS in Body Weight Regulation. *Curr Neuropharmacol, 10*(4), 344-353. doi:10.2174/157015912804143496

Haas, J. T., & Staels, B. (2016). An oxidative stress paradox: time for a conceptual change? *Diabetologia, 59*(12), 2514-2517. doi:10.1007/s00125-016-4117-y

Hadziabdic, M. O., Bozikov, V., Pavic, E., & Romic, Z. (2012). The antioxidative protecting role of the Mediterranean diet. *Coll Antropol, 36*(4), 1427-1434.

Haidara, M., Mikhailidis, D. P., Yassin, H. Z., Dobutovic, B., Smiljanic, K. T., Soskic, S., . . . Isenovic, E. R. (2011). Evaluation of the possible contribution of antioxidants administration in metabolic syndrome. *Curr Pharm Des, 17*(33), 3699-3712.

Harman-Boehm, I., Bluher, M., Redel, H., Sion-Vardy, N., Ovadia, S., Avinoach, E., . . . Rudich, A. (2007). Macrophage infiltration into omental versus subcutaneous fat across different populations: effect of regional adiposity and the comorbidities of obesity. *J Clin Endocrinol Metab, 92*(6), 2240-2247. doi:10.1210/jc.2006-1811

Harnroongroj, T., Jintaridhi, P., Vudhivai, N., Pongpaew, P., Tungtrongchitr, R., Phonrat, B., . . . Schelp, F. P. (2002). B vitamins, vitamin C and hematological measurements in overweight and obese Thais in Bangkok. *J Med Assoc Thai, 85*(1), 17-25.

Hatori, M., Vollmers, C., Zarrinpar, A., DiTacchio, L., Bushong, E. A., Gill, S., . . . Panda, S. (2012). Time-restricted feeding without reducing caloric intake prevents metabolic diseases in mice fed a high-fat diet. *Cell Metab, 15*(6), 848-860. doi:10.1016/j.cmet.2012.04.019

Hecksteden, A., Wegmann, M., Steffen, A., Kraushaar, J., Morsch, A., Ruppenthal, S., . . . Meyer, T. (2013). Irisin and exercise training in humans - results from a randomized controlled training trial. *BMC Med, 11*, 235. doi:10.1186/1741-7015-11-235

Heiss, C. N., & Olofsson, L. E. (2018). Gut Microbiota-Dependent Modulation of Energy Metabolism. *J Innate Immun, 10*(3), 163-171. doi:10.1159/000481519

Heit, C., Marshall, S., Singh, S., Yu, X., Charkoftaki, G., Zhao, H., . . . Vasiliou, V. (2017). Catalase deletion promotes prediabetic phenotype in mice. *Free Radic Biol Med, 103*, 48-56. doi:10.1016/j.freeradbiomed.2016.12.011

Hermsdorff, H. H., Barbosa, K. B., Volp, A. C., Puchau, B., Bressan, J., Zulet, M. A., & Martinez, J. A. (2014). Gender-specific relationships between plasma oxidized low-density lipoprotein cholesterol, total antioxidant capacity, and central adiposity indicators. *Eur J Prev Cardiol, 21*(7), 884-891. doi:10.1177/2047487312472420

Heydemann, A. (2016). An Overview of Murine High Fat Diet as a Model for Type 2 Diabetes Mellitus. *J Diabetes Res, 2016*, 14. doi:10.1155/2016/2902351

Hirabara, S. M., Folador, A., Fiamoncini, J., Lambertucci, R. H., Rodrigues, C. F., Jr., Rocha, M. S., . . . Curi, R. (2013). Fish oil supplementation for two generations increases insulin sensitivity in rats. *J Nutr Biochem, 24*(6), 1136-1145. doi:10.1016/j.jnutbio.2012.08.014

Hirsch, K. R., Smith-Ryan, A. E., Blue, M. N., Mock, M. G., Trexler, E. T., & Ondrak, K. S. (2016). Metabolic characterization of overweight and obese adults. *Phys Sportsmed, 44*(4), 362-372. doi:10.1080/00913847.2016.1248222

Hoehn, K. L., Salmon, A. B., Hohnen-Behrens, C., Turner, N., Hoy, A. J., Maghzal, G. J., . . . James, D. E. (2009). Insulin resistance is a cellular antioxidant defense mechanism. *Proc Natl Acad Sci U S A, 106*(42), 17787-17792. doi:10.1073/pnas.0902380106

Hoffmann, C., & Weigert, C. (2017). Skeletal Muscle as an Endocrine Organ: The Role of Myokines in Exercise Adaptations. *Cold Spring Harbor Perspectives in Medicine*. doi:10.1101/cshperspect.a029793

Hojman, P., Pedersen, M., Nielsen, A. R., Krogh-Madsen, R., Yfanti, C., Akerstrom, T., . . . Pedersen, B. K. (2009). Fibroblast growth factor-21 is induced in human skeletal muscles by hyperinsulinemia. *Diabetes, 58*(12), 2797-2801. doi:10.2337/db09-0713

Hokayem, M., Blond, E., Vidal, H., Lambert, K., Meugnier, E., Feillet-Coudray, C., . . . Avignon, A. (2013). Grape polyphenols prevent fructose-induced oxidative stress and insulin resistance in first-degree relatives of type 2 diabetic patients. *Diabetes Care, 36*(6), 1454-1461. doi:10.2337/dc12-1652

Holmes, B. F., Kurth-Kraczek, E. J., & Winder, W. W. (1999). Chronic activation of 5'-AMP-activated protein kinase increases GLUT-4, hexokinase, and glycogen in muscle. *J Appl Physiol (1985), 87*(5), 1990-1995. doi:10.1152/jappl.1999.87.5.1990

Hou, Y. P., He, Q. Q., Ouyang, H. M., Peng, H. S., Wang, Q., Li, J., . . . Yin, A. H. (2017). Human Gut Microbiota Associated with Obesity in Chinese Children and Adolescents. *Biomed Res Int, 2017*, 7585989. doi:10.1155/2017/7585989

Huh, J. Y. (2018). The role of exercise-induced myokines in regulating metabolism. *Arch Pharm Res, 41*(1), 14-29. doi:10.1007/s12272-017-0994-y

Huh, J. Y., Mougios, V., Kabasakalis, A., Fatouros, I., Siopi, A., Douroudos, II, . . . Mantzoros, C. S. (2014). Exercise-induced irisin secretion is independent of age or fitness level and increased irisin may directly modulate muscle metabolism through AMPK activation. *J Clin Endocrinol Metab, 99*(11), E2154-2161. doi:10.1210/jc.2014-1437

Huh, J. Y., Panagiotou, G., Mougios, V., Brinkoetter, M., Vamvini, M. T., Schneider, B. E., & Mantzoros, C. S. (2012). FNDC5 and irisin in humans: I. Predictors of circulating concentrations in serum and plasma and II. mRNA expression and circulating concentrations in response to weight loss and exercise. *Metabolism, 61*(12), 1725-1738. doi:10.1016/j.metabol.2012.09.002

Huh, J. Y., Siopi, A., Mougios, V., Park, K. H., & Mantzoros, C. S. (2015). Irisin in response to exercise in humans with and without metabolic syndrome. *J Clin Endocrinol Metab, 100*(3), E453-457. doi:10.1210/jc.2014-2416

Hui, X., Feng, T., Liu, Q., Gao, Y., & Xu, A. (2016). The FGF21-adiponectin axis in controlling energy and vascular homeostasis. *J Mol Cell Biol, 8*(2), 110-119. doi:10.1093/jmcb/mjw013

Hwang, N., Eom, T., Gupta, S. K., Jeong, S. Y., Jeong, D. Y., Kim, Y. S., . . . Unno, T. (2017). Genes and Gut Bacteria Involved in Luminal Butyrate Reduction Caused by Diet and Loperamide. *Genes (Basel), 8*(12). doi:10.3390/genes8120350

Ichimura, A., Hara, T., & Hirasawa, A. (2014). Regulation of Energy Homeostasis via GPR120. *Front Endocrinol (Lausanne), 5*, 111. doi:10.3389/fendo.2014.00111

Ichimura, A., Hasegawa, S., Kasubuchi, M., & Kimura, I. (2014). Free fatty acid receptors as therapeutic targets for the treatment of diabetes. *Front Pharmacol, 5*, 236. doi:10.3389/fphar.2014.00236

Ichimura, A., Hirasawa, A., Poulain-Godefroy, O., Bonnefond, A., Hara, T., Yengo, L., . . . Froguel, P. (2012). Dysfunction of lipid sensor GPR120 leads to obesity in both mouse and human. *Nature, 483*(7389), 350-354. doi:10.1038/nature10798

Ide, K., & Koshizaka, M. (2018). N-3 polyunsaturated fatty acids improve lipoprotein particle size and concentration in Japanese patients with type 2 diabetes and hypertriglyceridemia: a pilot study. *17*(1), 51. doi:10.1186/s12944-018-0706-8

Iizuka, K., Machida, T., & Hirafuji, M. (2014). Skeletal muscle is an endocrine organ. *J Pharmacol Sci, 125*(2), 125-131.

Ikeda, S. I., Tamura, Y., Kakehi, S., Sanada, H., Kawamori, R., & Watada, H. (2016). Exercise-induced increase in IL-6 level enhances GLUT4 expression and insulin sensitivity in mouse skeletal muscle. *Biochem Biophys Res Commun, 473*(4), 947-952. doi:10.1016/j.bbrc.2016.03.159

Imamura, T. (2010). [Ameliorative effect of n-3 fatty acid on insulin resistance through GPR120]. *Nihon Yakurigaku Zasshi, 136*(6), 359.

Imlay, J. A. (2018). Where in the world do bacteria experience oxidative stress? *Environ Microbiol*. doi:10.1111/1462-2920.14445

Ingalls, A. M., Dickie, M. M., & Snell, G. D. (1950). Obese, a new mutation in the house mouse. *J Hered, 41*(12), 317-318.

Ioffe, E., Moon, B., Connolly, E., & Friedman, J. M. (1998). Abnormal regulation of the leptin gene in the pathogenesis of obesity. *Proc Natl Acad Sci U S A, 95*(20), 11852-11857.

Itoh, M., Suganami, T., Satoh, N., Tanimoto-Koyama, K., Yuan, X., Tanaka, M., . . . Ogawa, Y. (2007). Increased adiponectin secretion by highly purified eicosapentaenoic acid in rodent models of obesity and human obese subjects. *Arterioscler Thromb Vasc Biol, 27*(9), 1918-1925. doi:10.1161/ATVBAHA.106.136853

Iwabu, M., Yamauchi, T., Okada-Iwabu, M., Sato, K., Nakagawa, T., Funata, M., . . . Kadowaki, T. (2010). Adiponectin and AdipoR1 regulate PGC-1alpha and mitochondria by Ca(2+) and AMPK/SIRT1. *Nature, 464*(7293), 1313-1319. doi:10.1038/nature08991

Izumiya, Y., Bina, H. A., Ouchi, N., Akasaki, Y., Kharitonenkov, A., & Walsh, K. (2008). FGF21 is an Akt-regulated myokine. *FEBS Lett, 582*(27), 3805-3810. doi:10.1016/j.febslet.2008.10.021

Jackson, S. J., Andrews, N., Ball, D., Bellantuono, I., Gray, J., Hachoumi, L., . . . Chapman, K. (2017). Does age matter? The impact of rodent age on study outcomes. *Laboratory Animals, 51*(2), 160-169. doi:10.1177/0023677216653984

James, P. T. (2004). Obesity: the worldwide epidemic. *Clin Dermatol, 22*(4), 276-280. doi:10.1016/j.clindermatol.2004.01.010

Ji, L. L. (2008). Modulation of skeletal muscle antioxidant defense by exercise: Role of redox signaling. *Free Radic Biol Med, 44*(2), 142-152. doi:10.1016/j.freeradbiomed.2007.02.031

Jimenez-Osorio, A. S., Gonzalez-Reyes, S., & Pedraza-Chaverri, J. (2015). Natural Nrf2 activators in diabetes. *Clin Chim Acta, 448*, 182-192. doi:10.1016/j.cca.2015.07.009

Jodeiri Farshbaf, M., Ghaedi, K., Megraw, T. L., Curtiss, J., Shirani Faradonbeh, M., Vaziri, P., & Nasr-Esfahani, M. H. (2016). Does PGC1alpha/FNDC5/BDNF Elicit the Beneficial Effects of Exercise on Neurodegenerative Disorders? *Neuromolecular Med, 18*(1), 1-15. doi:10.1007/s12017-015-8370-x

Jumpertz, R., Le, D. S., Turnbaugh, P. J., Trinidad, C., Bogardus, C., Gordon, J. I., & Krakoff, J. (2011). Energy-balance studies reveal associations between gut microbes, caloric load, and nutrient absorption in humans. *The American Journal of Clinical Nutrition, 94*(1), 58-65. doi:10.3945/ajcn.110.010132

Jung, C. H., Lee, W. J., & Song, K. H. (2017). Metabolically healthy obesity: a friend or foe? *Korean J Intern Med, 32*(4), 611-621. doi:10.3904/kjim.2016.259

Jung, S., & Kim, K. (2014). Exercise-induced PGC-1α transcriptional factors in skeletal muscle. *Integr Med Res, 3*(4), 155-160. doi:https://doi.org/10.1016/j.imr.2014.09.004

Jung, U. J., & Choi, M. S. (2014). Obesity and its metabolic complications: the role of adipokines and the relationship between obesity, inflammation, insulin resistance, dyslipidemia and nonalcoholic fatty liver disease. *Int J Mol Sci, 15*(4), 6184-6223. doi:10.3390/ijms15046184

Juraschek, S. P., Guallar, E., Appel, L. J., & Miller, E. R., 3rd. (2012). Effects of vitamin C supplementation on blood pressure: a meta-analysis of randomized controlled trials. *Am J Clin Nutr, 95*(5), 1079-1088. doi:10.3945/ajcn.111.027995

Kaakoush, N. O. (2015). Insights into the Role of Erysipelotrichaceae in the Human Host. *Front Cell Infect Microbiol, 5*, 84. doi:10.3389/fcimb.2015.00084

Kaidar-Person, O., Person, B., Szomstein, S., & Rosenthal, R. J. (2008a). Nutritional deficiencies in morbidly obese patients: a new form of malnutrition? Part A: vitamins. *Obes Surg, 18*(7), 870-876. doi:10.1007/s11695-007-9349-y

Kaidar-Person, O., Person, B., Szomstein, S., & Rosenthal, R. J. (2008b). Nutritional deficiencies in morbidly obese patients: a new form of malnutrition? Part B: minerals. *Obes Surg, 18*(8), 1028-1034. doi:10.1007/s11695-007-9350-5

Kajimura, S., Spiegelman, B. M., & Seale, P. (2015). Brown and Beige Fat: Physiological Roles beyond Heat Generation. *Cell Metab, 22*(4), 546-559. doi:10.1016/j.cmet.2015.09.007

Kallus, S. J., & Brandt, L. J. (2012). The intestinal microbiota and obesity. *J Clin Gastroenterol, 46*(1), 16-24. doi:10.1097/MCG.0b013e31823711fd

Kanda, H., Tateya, S., Tamori, Y., Kotani, K., Hiasa, K., Kitazawa, R., . . . Kasuga, M. (2006). MCP-1 contributes to macrophage infiltration into adipose tissue, insulin resistance, and hepatic steatosis in obesity. *J Clin Invest, 116*(6), 1494-1505. doi:10.1172/jci26498

Karaouzene, N., Merzouk, H., Aribi, M., Merzouk, S. A., Yahia Berrouiguet, A., Tessier, C., & Narce, M. (2011). Effects of the association of aging and obesity on lipids, lipoproteins and oxidative stress biomarkers: A comparison of older with young men. *Nutrition, Metabolism and Cardiovascular Diseases, 21*(10), 792-799. doi:10.1016/j.numecd.2010.02.007

Karastergiou, K., Smith, S. R., Greenberg, A. S., & Fried, S. K. (2012). Sex differences in human adipose tissues - the biology of pear shape. *Biology of sex differences, 3*(1), 13-13. doi:10.1186/2042-6410-3-13

Keaney, J. F., Jr., Larson, M. G., Vasan, R. S., Wilson, P. W., Lipinska, I., Corey, D., . . . Framingham, S. (2003). Obesity and systemic oxidative stress: clinical correlates of oxidative stress in the Framingham Study. *Arterioscler Thromb Vasc Biol, 23*(3), 434-439. doi:10.1161/01.ATV.0000058402.34138.11

Keipert, S., Ost, M., Johann, K., Imber, F., Jastroch, M., Schothorst, E. M. V., . . . Klaus, S. (2014). Skeletal muscle mitochondrial uncoupling drives endocrine cross-talk through the induction of FGF21 as a myokine. *American Journal of Physiology-Endocrinology and Metabolism, 306*(5), E469-E482. doi:10.1152/ajpendo.00330.2013

Kelly, S. A., Nehrenberg, D. L., Hua, K., Garland, T., Jr., & Pomp, D. (2011). Exercise, weight loss, and changes in body composition in mice: phenotypic relationships and genetic architecture. *Physiol Genomics, 43*(4), 199-212. doi:10.1152/physiolgenomics.00217.2010

Kensler, T. W., Wakabayashi, N., & Biswal, S. (2007). Cell survival responses to environmental stresses via the Keap1-Nrf2-ARE pathway. *Annu Rev Pharmacol Toxicol, 47*, 89-116. doi:10.1146/annurev.pharmtox.46.120604.141046

Kern, P. A., Di Gregorio, G. B., Lu, T., Rassouli, N., & Ranganathan, G. (2003). Adiponectin expression from human adipose tissue: relation to obesity, insulin resistance, and tumor necrosis factor-alpha expression. *Diabetes, 52*(7), 1779-1785.

Kern, P. A., Ranganathan, S., Li, C., Wood, L., & Ranganathan, G. (2001). Adipose tissue tumor necrosis factor and interleukin-6 expression in human obesity and insulin resistance. *Am J Physiol Endocrinol Metab, 280*(5), E745-751. doi:10.1152/ajpendo.2001.280.5.E745

Kershaw, E. E., & Flier, J. S. (2004). Adipose tissue as an endocrine organ. *J Clin Endocrinol Metab, 89*(6), 2548-2556. doi:10.1210/jc.2004-0395

Kharitonenkov, A., Shiyanova, T. L., Koester, A., Ford, A. M., Micanovic, R., Galbreath, E. J., . . . Shanafelt, A. B. (2005). FGF-21 as a novel metabolic regulator. *J Clin Invest, 115*(6), 1627-1635. doi:10.1172/jci23606

Kim, H. J., So, B., Choi, M., Kang, D., & Song, W. (2015). Resistance exercise training increases the expression of irisin concomitant with improvement of muscle function in aging mice and humans. *Exp Gerontol, 70*, 11-17. doi:10.1016/j.exger.2015.07.006

Kim, J., Paik, H. D., Shin, M. J., & Park, E. (2012). Eight weeks of conjugated linoleic acid supplementation has no effect on antioxidant status in healthy overweight/obese Korean individuals. *Eur J Nutr, 51*(2), 135-141. doi:10.1007/s00394-011-0199-y

Kim, K. H., Kim, S. H., Min, Y. K., Yang, H. M., Lee, J. B., & Lee, M. S. (2013). Acute exercise induces FGF21 expression in mice and in healthy humans. *PLoS One, 8*(5), e63517. doi:10.1371/journal.pone.0063517

Kim, S. H., & Plutzky, J. (2016). Brown Fat and Browning for the Treatment of Obesity and Related Metabolic Disorders. *Diabetes Metab J, 40*(1), 12-21. doi:10.4093/dmj.2016.40.1.12

Korge, P., Calmettes, G., & Weiss, J. N. (2015). Increased reactive oxygen species production during reductive stress: The roles of mitochondrial glutathione and thioredoxin reductases. *Biochim Biophys Acta, 1847*(6-7), 514-525. doi:10.1016/j.bbabio.2015.02.012

Kreznar, J. H., Keller, M. P., Traeger, L. L., Rabaglia, M. E., Schueler, K. L., Stapleton, D. S., . . . Rey, F. E. (2017). Host Genotype and Gut Microbiome Modulate Insulin Secretion and Diet-Induced Metabolic Phenotypes. *Cell Rep, 18*(7), 1739-1750. doi:10.1016/j.celrep.2017.01.062

Krueger, P. M., Coleman-Minahan, K., & Rooks, R. N. (2014). Race/ethnicity, nativity and trends in BMI among U.S. adults. *Obesity (Silver Spring), 22*(7), 1739-1746. doi:10.1002/oby.20744

Krzystek-Korpacka, M., Patryn, E., Boehm, D., Berdowska, I., Zielinski, B., & Noczynska, A. (2008). Advanced oxidation protein products (AOPPs) in juvenile overweight and obesity prior to and following weight reduction. *Clin Biochem, 41*(12), 943-949. doi:10.1016/j.clinbiochem.2008.04.024

Kuryszko, J., Slawuta, P., & Sapikowski, G. (2016). Secretory function of adipose tissue. *Pol J Vet Sci, 19*(2), 441-446. doi:10.1515/pjvs-2016-0056

Kusminski, C. M., Bickel, P. E., & Scherer, P. E. (2016). Targeting adipose tissue in the treatment of obesity-associated diabetes. *Nat Rev Drug Discov, 15*(9), 639-660. doi:10.1038/nrd.2016.75

Kusunoki, C., Yang, L., Yoshizaki, T., Nakagawa, F., Ishikado, A., Kondo, M., . . . Maegawa, H. (2013). Omega-3 polyunsaturated fatty acid has an anti-oxidant effect via the Nrf-2/HO-1 pathway in 3T3-L1 adipocytes. *Biochem Biophys Res Commun, 430*(1), 225-230. doi:10.1016/j.bbrc.2012.10.115

Kwon, O., Kim, K. W., & Kim, M. S. (2016). Leptin signalling pathways in hypothalamic neurons. *Cell Mol Life Sci, 73*(7), 1457-1477. doi:10.1007/s00018-016-2133-1

Lai, Z. L., Tseng, C. H., Ho, H. J., Cheung, C. K. Y., Lin, J. Y., Chen, Y. J., . . . Wu, C. Y. (2018). Fecal microbiota transplantation confers beneficial metabolic effects of diet and exercise on diet-induced obese mice. *Sci Rep, 8*(1), 15625. doi:10.1038/s41598-018-33893-y

Laskowski, E. R. (2018). How much should the average adult exercise every day (Article). Retrieved 12/12/18, from The Mayo Clinic https://www.mayoclinic.org/healthy-lifestyle/fitness/expert-answers/exercise/faq-20057916

Laterza, M. C., de Matos, L. D., Trombetta, I. C., Braga, A. M., Roveda, F., Alves, M. J., . . . Rondon, M. U. (2007). Exercise training restores baroreflex sensitivity in never-treated hypertensive patients. *Hypertension, 49*(6), 1298-1306. doi:10.1161/hypertensionaha.106.085548

Lau, G. J., Godin, N., Maachi, H., Lo, C. S., Wu, S. J., Zhu, J. X., . . . Chan, J. S. (2012). Bcl-2-modifying factor induces renal proximal tubular cell apoptosis in diabetic mice. *Diabetes, 61*(2), 474-484. doi:10.2337/db11-0141

Lawler, H. M., Underkofler, C. M., Kern, P. A., Erickson, C., Bredbeck, B., & Rasouli, N. (2016). Adipose Tissue Hypoxia, Inflammation, and Fibrosis in Obese Insulin-Sensitive

and Obese Insulin-Resistant Subjects. *J Clin Endocrinol Metab, 101*(4), 1422-1428. doi:10.1210/jc.2015-4125

Le Chatelier, E., Nielsen, T., Qin, J., Prifti, E., Hildebrand, F., Falony, G., . . . Pedersen, O. (2013). Richness of human gut microbiome correlates with metabolic markers. *Nature, 500*(7464), 541-546. doi:10.1038/nature12506

Leal, L. G., Lopes, M. A., & Batista, M. L., Jr. (2018). Physical Exercise-Induced Myokines and Muscle-Adipose Tissue Crosstalk: A Review of Current Knowledge and the Implications for Health and Metabolic Diseases. *Front Physiol, 9*, 1307. doi:10.3389/fphys.2018.01307

Lee, H.-Y., Choi, C. S., Birkenfeld, A. L., Alves, T. C., Jornayvaz, F. R., Jurczak, M. J., . . . Shulman, G. I. (2010). Targeted Expression of Catalase to Mitochondria Prevents Age-Associated Reductions in Mitochondrial Function and Insulin Resistance. *Cell Metabolism, 12*(6), 668-674. doi:10.1016/j.cmet.2010.11.004

Lee, M. C. (2013). Assessment of oxidative stress and antioxidant property using electron spin resonance (ESR) spectroscopy. *J Clin Biochem Nutr, 52*(1), 1-8. doi:10.3164/jcbn.12-58

Lee, M. Y., Koh, J. H., Nam, S. M., Jung, P. M., Sung, J. K., Kim, S. Y., . . . Chung, C. H. (2008). Short insulin tolerance test can determine the effects of thiazolidinediones treatment in type 2 diabetes. *Yonsei Med J, 49*(6), 901-908. doi:10.3349/ymj.2008.49.6.901

Lee, P., Linderman, J. D., Smith, S., Brychta, R. J., Wang, J., Idelson, C., . . . Celi, F. S. (2014). Irisin and FGF21 are cold-induced endocrine activators of brown fat function in humans. *Cell Metab, 19*(2), 302-309. doi:10.1016/j.cmet.2013.12.017

Lee, S. E., Kim, G. D., Yang, H., Son, G. W., Park, H. R., Cho, J. J., . . . Park, Y. S. (2015). Effects of Eicosapentaenoic Acid on the Cytoprotection Through Nrf2-Mediated Heme Oxygenase-1 in Human Endothelial Cells. *J Cardiovasc Pharmacol, 66*(1), 108-117. doi:10.1097/FJC.0000000000000251

Lei, X. G., & Cheng, W. H. (2005). New roles for an old selenoenzyme: evidence from glutathione peroxidase-1 null and overexpressing mice. *J Nutr, 135*(10), 2295-2298.

Leibel, R. L., Rosenbaum, M., & Hirsch, J. (1995). Changes in Energy Expenditure Resulting from Altered Body Weight. *New England Journal of Medicine, 332*(10), 621-628. doi:10.1056/nejm199503093321001

Leiherer, A., Mundlein, A., & Drexel, H. (2013). Phytochemicals and their impact on adipose tissue inflammation and diabetes. *Vascul Pharmacol, 58*(1-2), 3-20. doi:10.1016/j.vph.2012.09.002

Lengyel, E., Makowski, L., DiGiovanni, J., & Kolonin, M. G. (2018). Cancer as a Matter of Fat: The Crosstalk between Adipose Tissue and Tumors. *Trends Cancer, 4*(5), 374-384. doi:10.1016/j.trecan.2018.03.004

Lewis, K. H., Edwards-Hampton, S. A., & Ard, J. D. (2016). Disparities in Treatment Uptake and Outcomes of Patients with Obesity in the USA. *Curr Obes Rep, 5*(2), 282-290. doi:10.1007/s13679-016-0211-1

Ley, R. E., Backhed, F., Turnbaugh, P., Lozupone, C. A., Knight, R. D., & Gordon, J. I. (2005). Obesity alters gut microbial ecology. *Proc Natl Acad Sci U S A, 102*(31), 11070-11075. doi:10.1073/pnas.0504978102

Ley, R. E., Peterson, D. A., & Gordon, J. I. (2006). Ecological and evolutionary forces shaping microbial diversity in the human intestine. *Cell, 124*(4), 837-848. doi:10.1016/j.cell.2006.02.017

Li, F., Li, Y., Duan, Y., Hu, C. A., Tang, Y., & Yin, Y. (2017). Myokines and adipokines: Involvement in the crosstalk between skeletal muscle and adipose tissue. *Cytokine Growth Factor Rev, 33*, 73-82. doi:10.1016/j.cytogfr.2016.10.003

Li, Z., Yi, C. X., Katiraei, S., Kooijman, S., Zhou, E., Chung, C. K., . . . Wang, Y. (2018). Butyrate reduces appetite and activates brown adipose tissue via the gut-brain neural circuit. *Gut, 67*(7), 1269-1279. doi:10.1136/gutjnl-2017-314050

Lin, X., Liu, Y. B., & Hu, H. (2017). Metabolic role of fibroblast growth factor 21 in liver, adipose and nervous system tissues. *Biomed Rep, 6*(5), 495-502. doi:10.3892/br.2017.890

Lin, Z., Tian, H., Lam, K. S., Lin, S., Hoo, R. C., Konishi, M., . . . Li, X. (2013). Adiponectin mediates the metabolic effects of FGF21 on glucose homeostasis and insulin sensitivity in mice. *Cell Metab, 17*(5), 779-789. doi:10.1016/j.cmet.2013.04.005

Linford, N. J., Schriner, S. E., & Rabinovitch, P. S. (2006). Oxidative damage and aging: spotlight on mitochondria. *Cancer Res, 66*(5), 2497-2499. doi:10.1158/0008-5472.CAN-05-3163

Lipinski, B. (2002). Evidence in support of a concept of reductive stress. *Br J Nutr, 87*(1), 93-94; discussion 94. doi:10.1079/BJN2001435

Liu, J., Marino, M. W., Wong, G., Grail, D., Dunn, A., Bettadapura, J., . . . Bernard, C. C. (1998). TNF is a potent anti-inflammatory cytokine in autoimmune-mediated demyelination. *Nat Med, 4*(1), 78-83.

Liu, Q., Wu, D., Ni, N., Ren, H., Luo, C., He, C., . . . Su, H. (2014). Omega-3 polyunsaturated fatty acids protect neural progenitor cells against oxidative injury. *Mar Drugs, 12*(5), 2341-2356. doi:10.3390/md12052341

Liu, T. W., Park, Y. M., Holscher, H. D., Padilla, J., Scroggins, R. J., Welly, R., . . . Swanson, K. S. (2015). Physical Activity Differentially Affects the Cecal Microbiota of Ovariectomized Female Rats Selectively Bred for High and Low Aerobic Capacity. *PLoS One, 10*(8), e0136150. doi:10.1371/journal.pone.0136150

Liu, Y., Qi, W., Richardson, A., Van Remmen, H., Ikeno, Y., & Salmon, A. B. (2013). Oxidative damage associated with obesity is prevented by overexpression of CuZn- or Mn-superoxide dismutase. *Biochem Biophys Res Commun, 438*(1), 78-83. doi:10.1016/j.bbrc.2013.07.029

Liu, Y., Turdi, S., Park, T., Morris, N. J., Deshaies, Y., Xu, A., & Sweeney, G. (2013). Adiponectin corrects high-fat diet-induced disturbances in muscle metabolomic profile and whole-body glucose homeostasis. *Diabetes, 62*(3), 743-752. doi:10.2337/db12-0687

Lloret, A., Fuchsberger, T., Giraldo, E., & Vina, J. (2016). Reductive Stress: A New Concept in Alzheimer's Disease. *Curr Alzheimer Res, 13*(2), 206-211.

Lord, G. M., Matarese, G., Howard, J. K., Baker, R. J., Bloom, S. R., & Lechler, R. I. (1998). Leptin modulates the T-cell immune response and reverses starvation-induced immunosuppression. *Nature, 394*(6696), 897-901. doi:10.1038/29795

Lowry, O. H., Rosebrough, N. J., Farr, A. L., & Randall, R. J. (1951). Protein measurement with the Folin phenol reagent. *J Biol Chem, 193*(1), 265-275.

Lubkowska, A., Dudzinska, W., Bryczkowska, I., & Dolegowska, B. (2015). Body Composition, Lipid Profile, Adipokine Concentration, and Antioxidant Capacity Changes during Interventions to Treat Overweight with Exercise Programme and Whole-Body Cryostimulation. *Oxid Med Cell Longev, 2015*, 803197. doi:10.1155/2015/803197

Luna-Luna, M., Medina-Urrutia, A., Vargas-Alarcon, G., Coss-Rovirosa, F., Vargas-Barron, J., & Perez-Mendez, O. (2015). Adipose Tissue in Metabolic Syndrome: Onset and Progression of Atherosclerosis. *Arch Med Res, 46*(5), 392-407. doi:10.1016/j.arcmed.2015.05.007

Luo, X., Jia, R., Yao, Q., Xu, Y., Luo, Z., Luo, X., & Wang, N. (2016). Docosahexaenoic acid attenuates adipose tissue angiogenesis and insulin resistance in high fat diet-fed middle-aged mice via a sirt1-dependent mechanism. *Mol Nutr Food Res, 60*(4), 871-885. doi:10.1002/mnfr.201500714

Lupien, S. J., McEwen, B. S., Gunnar, M. R., & Heim, C. (2009). Effects of stress throughout the lifespan on the brain, behaviour and cognition. *Nature Reviews Neuroscience, 10*, 434. doi:10.1038/nrn2639

Ma, W., Yuan, L., Yu, H., Xi, Y., & Xiao, R. (2014). Mitochondrial dysfunction and oxidative damage in the brain of diet-induced obese rats but not in diet-resistant rats. *Life Sci, 110*(2), 53-60. doi:10.1016/j.lfs.2014.07.018

MacDonald, C., Wojtaszewski, J. F., Pedersen, B. K., Kiens, B., & Richter, E. A. (2003). Interleukin-6 release from human skeletal muscle during exercise: relation to AMPK activity. *J Appl Physiol (1985), 95*(6), 2273-2277. doi:10.1152/japplphysiol.00242.2003

Mach, N., & Fuster-Botella, D. (2017). Endurance exercise and gut microbiota: A review. *J Sport Health Sci, 6*(2), 179-197. doi:10.1016/j.jshs.2016.05.001

Mackie, R. I., Sghir, A., & Gaskins, H. R. (1999). Developmental microbial ecology of the neonatal gastrointestinal tract. *Am J Clin Nutr, 69*(5), 1035s-1045s. doi:10.1093/ajcn/69.5.1035s

Macpherson, R. E., Huber, J. S., Frendo-Cumbo, S., Simpson, J. A., & Wright, D. C. (2015). Adipose Tissue Insulin Action and IL-6 Signaling after Exercise in Obese Mice. *Med Sci Sports Exerc, 47*(10), 2034-2042. doi:10.1249/mss.0000000000000660

Mahendran, Y., Vangipurapu, J., Cederberg, H., Stancakova, A., Pihlajamaki, J., Soininen, P., . . . Laakso, M. (2013). Association of ketone body levels with hyperglycemia and type 2 diabetes in 9,398 Finnish men. *Diabetes, 62*(10), 3618-3626. doi:10.2337/db12-1363

Mahgoub, M. O., D'Souza, C., Al Darmaki, R., Baniyas, M., & Adeghate, E. (2018). An update on the role of irisin in the regulation of endocrine and metabolic functions. *Peptides, 104*, 15-23. doi:10.1016/j.peptides.2018.03.018

Mandar, R., & Mikelsaar, M. (1996). Transmission of mother's microflora to the newborn at birth. *Biol Neonate, 69*(1), 30-35. doi:10.1159/000244275

Manna, P., & Jain, S. K. (2015). Obesity, Oxidative Stress, Adipose Tissue Dysfunction, and the Associated Health Risks: Causes and Therapeutic Strategies. *Metab Syndr Relat Disord, 13*(10), 423-444. doi:10.1089/met.2015.0095

Manole, E., Ceafalan, L. C., Popescu, B. O., Dumitru, C., & Bastian, A. E. (2018). Myokines as Possible Therapeutic Targets in Cancer Cachexia. *Journal of Immunology Research, 2018*, 9. doi:10.1155/2018/8260742

Margaritelis, N. V., Kyparos, A., Paschalis, V., Theodorou, A. A., Panayiotou, G., Zafeiridis, A., . . . Vrabas, I. S. (2014). Reductive stress after exercise: The issue of redox individuality. *Redox Biol, 2*, 520-528. doi:10.1016/j.redox.2014.02.003

Marseglia, L., Manti, S., D'Angelo, G., Nicotera, A., Parisi, E., Di Rosa, G., . . . Arrigo, T. (2014). Oxidative stress in obesity: a critical component in human diseases. *Int J Mol Sci, 16*(1), 378-400. doi:10.3390/ijms16010378

Martin, M., Krystof, S., Jiri, R., Martina, D., Renata, V., Ondrej, M., . . . Vladimir, T. (2016). Modulation of Energy Intake and Expenditure Due to Habitual Physical Exercise. *Curr Pharm Des, 22*(24), 3681-3699.

Martin, R. L., Perez, E., He, Y. J., Dawson, R., Jr., & Millard, W. J. (2000). Leptin resistance is associated with hypothalamic leptin receptor mRNA and protein downregulation. *Metabolism, 49*(11), 1479-1484. doi:10.1053/meta.2000.17695

Martinez-Useros, J., & Garcia-Foncillas, J. (2016). Obesity and colorectal cancer: molecular features of adipose tissue. *J Transl Med, 14*, 21. doi:10.1186/s12967-016-0772-5

Marvyn, P. M., Bradley, R. M., Mardian, E. B., Marks, K. A., & Duncan, R. E. (2016). Data on oxygen consumption rate, respiratory exchange ratio, and movement in C57BL/6J female mice on the third day of consuming a high-fat diet. *Data in Brief, 7*, 472-475. doi:https://doi.org/10.1016/j.dib.2016.02.066

Matsumoto, M., Inoue, R., Tsukahara, T., Ushida, K., Chiji, H., Matsubara, N., & Hara, H. (2008). Voluntary running exercise alters microbiota composition and increases n-butyrate concentration in the rat cecum. *Biosci Biotechnol Biochem, 72*(2), 572-576. doi:10.1271/bbb.70474

Matzinger, M., Fischhuber, K., & Heiss, E. H. (2018). Activation of Nrf2 signaling by natural products-can it alleviate diabetes? *Biotechnology Advances, 36*(6), 1738-1767. doi:https://doi.org/10.1016/j.biotechadv.2017.12.015

McArdle, M. A., Finucane, O. M., Connaughton, R. M., McMorrow, A. M., & Roche, H. M. (2013). Mechanisms of obesity-induced inflammation and insulin resistance: insights into the emerging role of nutritional strategies. *Front Endocrinol (Lausanne), 4*, 52. doi:10.3389/fendo.2013.00052

McClung, J. P., Roneker, C. A., Mu, W., Lisk, D. J., Langlais, P., Liu, F., & Lei, X. G. (2004). Development of insulin resistance and obesity in mice overexpressing cellular glutathione peroxidase. *Proc Natl Acad Sci U S A, 101*(24), 8852-8857. doi:10.1073/pnas.0308096101

McDonald, D. M., O'Kane, F., McConville, M., Devine, A. B., & McVeigh, G. E. (2013). Platelet redox balance in diabetic patients with hypertension improved by n-3 fatty acids. *Diabetes Care, 36*(4), 998-1005. doi:10.2337/dc12-0304

McMurray, F., Patten, D. A., & Harper, M. E. (2016). Reactive Oxygen Species and Oxidative Stress in Obesity-Recent Findings and Empirical Approaches. *Obesity (Silver Spring), 24*(11), 2301-2310. doi:10.1002/oby.21654

Meidenbauer, J. J., Ta, N., & Seyfried, T. N. (2014). Influence of a ketogenic diet, fish-oil, and calorie restriction on plasma metabolites and lipids in C57BL/6J mice. *Nutr Metab (Lond), 11*, 23. doi:10.1186/1743-7075-11-23

Meilhac, O., Ramachandran, S., Chiang, K., Santanam, N., & Parthasarathy, S. (2001). Role of arterial wall antioxidant defense in beneficial effects of exercise on atherosclerosis in mice. *Arterioscler Thromb Vasc Biol, 21*(10), 1681-1688.

Meilhac, O., Zhou, M., Santanam, N., & Parthasarathy, S. (2000). Lipid peroxides induce expression of catalase in cultured vascular cells. *J Lipid Res, 41*(8), 1205-1213.

Meissner, M., Havinga, R., Boverhof, R., Kema, I., Groen, A. K., & Kuipers, F. (2010). Exercise enhances whole-body cholesterol turnover in mice. *Med Sci Sports Exerc, 42*(8), 1460-1468. doi:10.1249/MSS.0b013e3181cfcb02

Melzer, K., Kayser, B., Saris, W. H., & Pichard, C. (2005). Effects of physical activity on food intake. *Clin Nutr, 24*(6), 885-895. doi:10.1016/j.clnu.2005.06.003

Mentor, S., & Fisher, D. (2017). Aggressive Antioxidant Reductive Stress Impairs Brain Endothelial Cell Angiogenesis and Blood Brain Barrier Function. *Curr Neurovasc Res, 14*(1), 71-81. doi:10.2174/1567202613666161129113950

Miana, V. V., & González, E. A. P. (2018). Adipose tissue stem cells in regenerative medicine. *Ecancermedicalscience, 12*, 822. doi:10.3332/ecancer.2018.822

Million, M., Maraninchi, M., Henry, M., Armougom, F., Richet, H., Carrieri, P., . . . Raoult, D. (2012). Obesity-associated gut microbiota is enriched in Lactobacillus reuteri and depleted in Bifidobacterium animalis and Methanobrevibacter smithii. *Int J Obes (Lond), 36*(6), 817-825. doi:10.1038/ijo.2011.153

Mittal, P. C., & Kant, R. (2009). Correlation of increased oxidative stress to body weight in disease-free post menopausal women. *Clin Biochem, 42*(10-11), 1007-1011. doi:10.1016/j.clinbiochem.2009.03.019

Miyamoto, J., Hasegawa, S., Kasubuchi, M., Ichimura, A., Nakajima, A., & Kimura, I. (2016). Nutritional Signaling via Free Fatty Acid Receptors. *Int J Mol Sci, 17*(4), 450. doi:10.3390/ijms17040450

Mizgier, M. L., Rutti, S., Pinget, M., & Bouzakri, K. (2018). Beta-Cell Function and Survival Are Modulated Differentially by Type I or Type II Muscle through Specific Myokines. *Diabetes, 67*(Supplement 1), 266-LB. doi:10.2337/db18-266-LB

Molina-Molina, E., Lunardi Baccetto, R., Wang, D. Q., de Bari, O., Krawczyk, M., & Portincasa, P. (2018). Exercising the hepatobiliary-gut axis. The impact of physical activity performance. *Eur J Clin Invest, 48*(8), e12958. doi:10.1111/eci.12958

Monda, V., Villano, I., Messina, A., Valenzano, A., Esposito, T., Moscatelli, F., . . . Messina, G. (2017). Exercise Modifies the Gut Microbiota with Positive Health Effects. *Oxid Med Cell Longev, 2017*, 3831972. doi:10.1155/2017/3831972

Mulders, R. J., de Git, K. C. G., Schéle, E., Dickson, S. L., Sanz, Y., & Adan, R. A. H. (2018). Microbiota in obesity: interactions with enteroendocrine, immune and central nervous systems. *Obesity Reviews, 19*(4), 435-451. doi:doi:10.1111/obr.12661

Munukka, E., Ahtiainen, J. P., Puigbó, P., Jalkanen, S., Pahkala, K., Keskitalo, A., . . . Pekkala, S. (2018). Six-Week Endurance Exercise Alters Gut Metagenome That Is not Reflected in Systemic Metabolism in Over-weight Women. *Front Microbiol, 9*(2323). doi:10.3389/fmicb.2018.02323

Muzumdar, R., Allison, D. B., Huffman, D. M., Ma, X., Atzmon, G., Einstein, F. H., . . . Barzilai, N. (2008). Visceral adipose tissue modulates mammalian longevity. *Aging Cell, 7*(3), 438-440. doi:10.1111/j.1474-9726.2008.00391.x

Nanthirudjanar, T., Furumoto, H., Hirata, T., & Sugawara, T. (2013). Oxidized eicosapentaenoic acids more potently reduce LXRalpha-induced cellular triacylglycerol via suppression of SREBP-1c, PGC-1beta and GPA than its intact form. *Lipids Health Dis, 12*, 73. doi:10.1186/1476-511X-12-73

Nehra, V., Allen, J. M., Mailing, L. J., Kashyap, P. C., & Woods, J. A. (2016). Gut Microbiota: Modulation of Host Physiology in Obesity. *Physiology (Bethesda), 31*(5), 327-335. doi:10.1152/physiol.00005.2016

Newman, J. C., & Verdin, E. (2014). Ketone bodies as signaling metabolites. *Trends in Endocrinology & Metabolism, 25*(1), 42-52. doi:https://doi.org/10.1016/j.tem.2013.09.002

Nicholson, J. K., Holmes, E., Kinross, J., Burcelin, R., Gibson, G., Jia, W., & Pettersson, S. (2012). Host-gut microbiota metabolic interactions. *Science, 336*(6086), 1262-1267. doi:10.1126/science.1223813

Nigro, E., Scudiero, O., Monaco, M. L., Palmieri, A., Mazzarella, G., Costagliola, C., . . . Daniele, A. (2014). New insight into adiponectin role in obesity and obesity-related diseases. *Biomed Res Int, 2014*, 658913. doi:10.1155/2014/658913

Nikolaidis, M. G., Kerksick, C. M., Lamprecht, M., & McAnulty, S. R. (2012). Redox biology of exercise. *Oxid Med Cell Longev, 2012*, 407978. doi:10.1155/2012/407978

Nilsson, J., Ericsson, M., Joibari, M. M., Anderson, F., Carlsson, L., Nilsson, S. K., . . . Burén, J. (2016). A low-carbohydrate high-fat diet decreases lean mass and impairs cardiac function in pair-fed female C57BL/6J mice. *Nutrition & Metabolism, 13*(1), 79. doi:10.1186/s12986-016-0132-8

Nishina, P. M., Lowe, S., Wang, J., & Paigen, B. (1994). Characterization of plasma lipids in genetically obese mice: the mutants obese, diabetes, fat, tubby, and lethal yellow. *Metabolism, 43*(5), 549-553.

Nunan, D., Mahtani, K. R., Roberts, N., & Heneghan, C. (2013). Physical activity for the prevention and treatment of major chronic disease: an overview of systematic reviews. *Syst Rev, 2*, 56. doi:10.1186/2046-4053-2-56

O'Neil, C. E., Nicklas, T. A., Rampersaud, G. C., & Fulgoni, V. L., 3rd. (2012). 100% orange juice consumption is associated with better diet quality, improved nutrient adequacy, decreased risk for obesity, and improved biomarkers of health in adults: National Health and Nutrition Examination Survey, 2003-2006. *Nutr J, 11*, 107. doi:10.1186/1475-2891-11-107

Oh, D. Y., & Olefsky, J. M. (2012). Omega 3 fatty acids and GPR120. *Cell Metab, 15*(5), 564-565. doi:10.1016/j.cmet.2012.04.009

Oh, D. Y., Talukdar, S., Bae, E. J., Imamura, T., Morinaga, H., Fan, W., . . . Olefsky, J. M. (2010). GPR120 is an omega-3 fatty acid receptor mediating potent anti-inflammatory and insulin-sensitizing effects. *Cell, 142*(5), 687-698. doi:10.1016/j.cell.2010.07.041

Oh, D. Y., Walenta, E., Akiyama, T. E., Lagakos, W. S., Lackey, D., Pessentheiner, A. R., . . . Olefsky, J. M. (2014). A Gpr120-selective agonist improves insulin resistance and chronic inflammation in obese mice. *Nat Med, 20*(8), 942-947. doi:10.1038/nm.3614

Oh, K. J., Lee, D. S., Kim, W. K., Han, B. S., Lee, S. C., & Bae, K. H. (2016). Metabolic Adaptation in Obesity and Type II Diabetes: Myokines, Adipokines and Hepatokines. *Int J Mol Sci, 18*(1). doi:10.3390/ijms18010008

Olivares-Corichi, I. M., Viquez, M. J., Gutierrez-Lopez, L., Ceballos-Reyes, G. M., & Garcia-Sanchez, J. R. (2011). Oxidative stress present in the blood from obese patients modifies the structure and function of insulin. *Horm Metab Res, 43*(11), 748-753. doi:10.1055/s-0031-1286305

Oliveira, V., Marinho, R., Vitorino, D., Santos, G. A., Moraes, J. C., Dragano, N., . . . Cintra, D. E. (2015). Diets Containing alpha-Linolenic (omega3) or Oleic (omega9) Fatty Acids Rescues Obese Mice From Insulin Resistance. *Endocrinology, 156*(11), 4033-4046. doi:10.1210/en.2014-1880

Organization, W. H. (2018). Overweight and Obesity (Article). Retrieved December 12, 2018, from World Health Organization https://www.who.int/news-room/fact-sheets/detail/obesity-and-overweight

Organization, W. H. (2019). Global Strategy on Diet, Physical Activity and Health (Article). Retrieved 12/14/18, from World Health Organization https://www.who.int/dietphysicalactivity/factsheet_adults/en/

Orihata, M., Sarna, S., Orihata, M., & Sarna, S. (1994). Inhibition of nitric oxide synthase delays gastric emptying of solid meals. *Journal of Pharmacology and Experimental Therapeutics, 271*, 660-670.

Ortega, R. M., Rodriguez-Rodriguez, E., Aparicio, A., Jimenez-Ortega, A. I., Palmeros, C., Perea, J. M., . . . Lopez-Sobaler, A. M. (2012). Young children with excess of weight show an impaired selenium status. *Int J Vitam Nutr Res, 82*(2), 121-129. doi:10.1024/0300-9831/a000101

Ottosson, F., Brunkwall, L., Ericson, U., Nilsson, P. M., Almgren, P., Fernandez, C., . . . Orho-Melander, M. (2018). Connection Between BMI-Related Plasma Metabolite Profile and Gut Microbiota. *The Journal of Clinical Endocrinology & Metabolism, 103*(4), 1491-1501. doi:10.1210/jc.2017-02114

Paerregaard, S. I., Agerholm, M., Serup, A. K., Ma, T., Kiens, B., Madsen, L., . . . Jensen, B. A. (2016). FFAR4 (GPR120) Signaling Is Not Required for Anti-Inflammatory and Insulin-Sensitizing Effects of Omega-3 Fatty Acids. *Mediators Inflamm, 2016*, 1536047. doi:10.1155/2016/1536047

Paglialunga, S., Ludzki, A., Root-McCaig, J., & Holloway, G. P. (2015). In adipose tissue, increased mitochondrial emission of reactive oxygen species is important for short-term high-fat diet-induced insulin resistance in mice. *Diabetologia, 58*(5), 1071-1080. doi:10.1007/s00125-015-3531-x

Pall, M. L., & Levine, S. (2015). Nrf2, a master regulator of detoxification and also antioxidant, anti-inflammatory and other cytoprotective mechanisms, is raised by health promoting factors. *Sheng Li Xue Bao, 67*(1), 1-18.

Palmer, B. F., & Clegg, D. J. (2015). The sexual dimorphism of obesity. *Mol Cell Endocrinol, 402*, 113-119. doi:10.1016/j.mce.2014.11.029

Palmer, C., Bik, E. M., DiGiulio, D. B., Relman, D. A., & Brown, P. O. (2007). Development of the human infant intestinal microbiota. *PLoS Biol, 5*(7), e177. doi:10.1371/journal.pbio.0050177

Paniagua, J. A. (2016). Nutrition, insulin resistance and dysfunctional adipose tissue determine the different components of metabolic syndrome. *World J Diabetes, 7*(19), 483-514. doi:10.4239/wjd.v7.i19.483

Paoli, A., Rubini, A., Volek, J. S., & Grimaldi, K. A. (2013). Beyond weight loss: a review of the therapeutic uses of very-low-carbohydrate (ketogenic) diets. *European Journal Of Clinical Nutrition, 67,* 789. doi:10.1038/ejcn.2013.116

Parastatidis, I., Weiss, D., Joseph, G., & Taylor, W. R. (2013). Overexpression of catalase in vascular smooth muscle cells prevents the formation of abdominal aortic aneurysms. *Arterioscler Thromb Vasc Biol, 33*(10), 2389-2396. doi:10.1161/ATVBAHA.113.302175

Park, Y. S., Uddin, M. J., Piao, L., Hwang, I., Lee, J. H., & Ha, H. (2016). Novel Role of Endogenous Catalase in Macrophage Polarization in Adipose Tissue. *Mediators Inflamm, 2016,* 8675905. doi:10.1155/2016/8675905

Parthasarathy, S., & Santanam, N. (1994). Mechanisms of oxidation, antioxidants, and atherosclerosis. *Curr Opin Lipidol, 5*(5), 371-375.

Patel, B., Mann, G. E., & Chapple, S. J. (2018). Concerted redox modulation by sulforaphane alleviates diabetes and cardiometabolic syndrome. *Free Radic Biol Med, 122*, 150-160. doi:10.1016/j.freeradbiomed.2018.02.004

Patel, C., Ghanim, H., Ravishankar, S., Sia, C. L., Viswanathan, P., Mohanty, P., & Dandona, P. (2007). Prolonged reactive oxygen species generation and nuclear factor-kappaB activation after a high-fat, high-carbohydrate meal in the obese. *J Clin Endocrinol Metab, 92*(11), 4476-4479. doi:10.1210/jc.2007-0778

Paulson, J. N., Stine, O. C., Bravo, H. C., & Pop, M. (2013). Differential abundance analysis for microbial marker-gene surveys. *Nat Methods, 10*(12), 1200-1202. doi:10.1038/nmeth.2658

Paz-Filho, G., Mastronardi, C., Wong, M. L., & Licinio, J. (2012). Leptin therapy, insulin sensitivity, and glucose homeostasis. *Indian J Endocrinol Metab, 16*(Suppl 3), S549-555. doi:10.4103/2230-8210.105571

Pedersen, B. K. (2013). Muscle as a secretory organ. *Compr Physiol, 3*(3), 1337-1362. doi:10.1002/cphy.c120033

Pedersen, B. K., & Febbraio, M. A. (2012). Muscles, exercise and obesity: skeletal muscle as a secretory organ. *Nat Rev Endocrinol, 8*(8), 457-465. doi:10.1038/nrendo.2012.49

Pekkala, S., Wiklund, P. K., Hulmi, J. J., Ahtiainen, J. P., Horttanainen, M., Pollanen, E., . . . Cheng, S. (2013). Are skeletal muscle FNDC5 gene expression and irisin release regulated by exercise and related to health? *J Physiol, 591*(21), 5393-5400. doi:10.1113/jphysiol.2013.263707

Pendergast, J. S., Branecky, K. L., Yang, W., Ellacott, K. L., Niswender, K. D., & Yamazaki, S. (2013). High-fat diet acutely affects circadian organisation and eating behavior. *Eur J Neurosci, 37*(8), 1350-1356. doi:10.1111/ejn.12133

Peng, S., Li, W., Lv, L., Zhang, Z., & Zhan, X. (2018). BDNF as a biomarker in diagnosis and evaluation of treatment for schizophrenia and depression. *Discov Med, 26*(143), 127-136.

Perakakis, N., Triantafyllou, G. A., Fernandez-Real, J. M., Huh, J. Y., Park, K. H., Seufert, J., & Mantzoros, C. S. (2017). Physiology and role of irisin in glucose homeostasis. *Nat Rev Endocrinol, 13*(6), 324-337. doi:10.1038/nrendo.2016.221

Peronnet, F., & Massicotte, D. (1991). Table of nonprotein respiratory quotient: an update. *Can J Sport Sci, 16*(1), 23-29.

Petersen, A. M., & Pedersen, B. K. (2005). The anti-inflammatory effect of exercise. *J Appl Physiol (1985), 98*(4), 1154-1162. doi:10.1152/japplphysiol.00164.2004

Pfaffl, M. W. (2001). A new mathematical model for relative quantification in real-time RT–PCR. *Nucleic Acids Research, 29*(9), e45-e45.

Pfister, R., Sharp, S. J., Luben, R., Wareham, N. J., & Khaw, K. T. (2011). Plasma vitamin C predicts incident heart failure in men and women in European Prospective Investigation into Cancer and Nutrition-Norfolk prospective study. *Am Heart J, 162*(2), 246-253. doi:10.1016/j.ahj.2011.05.007

Phillips, S. A., Mahmoud, A. M., Brown, M. D., & Haus, J. M. (2015). Exercise interventions and peripheral arterial function: implications for cardio-metabolic disease. *Prog Cardiovasc Dis, 57*(5), 521-534. doi:10.1016/j.pcad.2014.12.005

Pigeyre, M., Yazdi, F. T., Kaur, Y., & Meyre, D. (2016). Recent progress in genetics, epigenetics and metagenomics unveils the pathophysiology of human obesity. *Clin Sci (Lond), 130*(12), 943-986. doi:10.1042/CS20160136

Pil-Byung, C., Shin-Hwan, Y., Il-Gyu, K., Gwang-Suk, H., Jae-Hyun, Y., Han-Joon, L., . . . Yong-Seok, J. (2011). Effects of exercise program on appetite-regulating hormones, inflammatory mediators, lipid profiles, and body composition in healthy men. *J Sports Med Phys Fitness, 51*(4), 654-663.

Pinchuk, I., Shoval, H., Dotan, Y., & Lichtenberg, D. (2012). Evaluation of antioxidants: scope, limitations and relevance of assays. *Chem Phys Lipids, 165*(6), 638-647. doi:10.1016/j.chemphyslip.2012.05.003

Potter, A. S., Foroudi, S., Stamatikos, A., Patil, B. S., & Deyhim, F. (2011). Drinking carrot juice increases total antioxidant status and decreases lipid peroxidation in adults. *Nutr J, 10*, 96. doi:10.1186/1475-2891-10-96

Potthoff, M. J., Inagaki, T., Satapati, S., Ding, X., He, T., Goetz, R., . . . Burgess, S. C. (2009). FGF21 induces PGC-1alpha and regulates carbohydrate and fatty acid metabolism during the adaptive starvation response. *Proc Natl Acad Sci U S A, 106*(26), 10853-10858. doi:10.1073/pnas.0904187106

Pou, K. M., Massaro, J. M., Hoffmann, U., Vasan, R. S., Maurovich-Horvat, P., Larson, M. G., . . . Fox, C. S. (2007). Visceral and subcutaneous adipose tissue volumes are cross-sectionally related to markers of inflammation and oxidative stress: the Framingham Heart Study. *Circulation, 116*(11), 1234-1241. doi:10.1161/circulationaha.107.710509

Pratesi, A., Tarantini, F., & Di Bari, M. (2013). Skeletal muscle: an endocrine organ. *Clin Cases Miner Bone Metab, 10*(1), 11-14. doi:10.11138/ccmbm/2013.10.1.011

Puchalska, P., & Crawford, P. A. (2017). Multi-dimensional Roles of Ketone Bodies in Fuel Metabolism, Signaling, and Therapeutics. *Cell Metabolism, 25*(2), 262-284. doi:https://doi.org/10.1016/j.cmet.2016.12.022

Qin, J., Li, R., Raes, J., Arumugam, M., Burgdorf, K. S., Manichanh, C., . . . Wang, J. (2010). A human gut microbial gene catalogue established by metagenomic sequencing. *Nature, 464*(7285), 59-65. doi:10.1038/nature08821

Qin, Y., Roberts, J. D., Grimm, S. A., Lih, F. B., Deterding, L. J., Li, R., . . . Wade, P. A. (2018). An obesity-associated gut microbiome reprograms the intestinal epigenome and leads to altered colonic gene expression. *Genome Biol, 19*(1), 7. doi:10.1186/s13059-018-1389-1

Quesada-Lopez, T., Cereijo, R., Turatsinze, J. V., Planavila, A., Cairo, M., Gavalda-Navarro, A., . . . Villarroya, F. (2016). The lipid sensor GPR120 promotes brown fat activation and FGF21 release from adipocytes. *Nat Commun, 7*, 13479. doi:10.1038/ncomms13479

Quinn, L. S., Strait-Bodey, L., Anderson, B. G., Argiles, J. M., & Havel, P. J. (2005). Interleukin-15 stimulates adiponectin secretion by 3T3-L1 adipocytes: evidence for a skeletal muscle-to-fat signaling pathway. *Cell Biol Int, 29*(6), 449-457. doi:10.1016/j.cellbi.2005.02.005

Radak, Z., Marton, O., Nagy, E., Koltai, E., & Goto, S. (2013). The complex role of physical exercise and reactive oxygen species on brain. *Journal of Sport and Health Science, 2*(2), 87-93. doi:http://dx.doi.org/10.1016/j.jshs.2013.04.001

Ramos-Jiménez, A., Hernández-Torres, R. P., Torres-Durán, P. V., Romero-Gonzalez, J., Mascher, D., Posadas-Romero, C., & Juárez-Oropeza, M. A. (2008). The Respiratory Exchange Ratio is Associated with Fitness Indicators Both in Trained and Untrained Men: A Possible Application for People with Reduced Exercise Tolerance. *Clin Med Circ Respirat Pulm Med, 2*, 1-9.

Rani, V., Deep, G., Singh, R. K., Palle, K., & Yadav, U. C. (2016). Oxidative stress and metabolic disorders: Pathogenesis and therapeutic strategies. *Life Sci, 148*, 183-193. doi:10.1016/j.lfs.2016.02.002

Raschke, S., & Eckel, J. (2013). Adipo-myokines: two sides of the same coin--mediators of inflammation and mediators of exercise. *Mediators Inflamm, 2013*, 320724. doi:10.1155/2013/320724

Reitman, A., Friedrich, I., Ben-Amotz, A., & Levy, Y. (2002). Low plasma antioxidants and normal plasma B vitamins and homocysteine in patients with severe obesity. *Isr Med Assoc J, 4*(8), 590-593.

Ren, Y., Li, Y., Yan, J., Ma, M., Zhou, D., Xue, Z., . . . Da, Y. (2017). Adiponectin modulates oxidative stress-induced mitophagy and protects C2C12 myoblasts against apoptosis. *Sci Rep, 7*(1), 3209. doi:10.1038/s41598-017-03319-2

Rindler, P. M., Plafker, S. M., Szweda, L. I., & Kinter, M. (2013). High dietary fat selectively increases catalase expression within cardiac mitochondria. *J Biol Chem, 288*(3), 1979-1990. doi:10.1074/jbc.M112.412890

Riva, A., Borgo, F., Lassandro, C., Verduci, E., Morace, G., Borghi, E., & Berry, D. (2017). Pediatric obesity is associated with an altered gut microbiota and discordant shifts in Firmicutes populations. *Environ Microbiol, 19*(1), 95-105. doi:doi:10.1111/1462-2920.13463

Rivière, A., Selak, M., Lantin, D., Leroy, F., & De Vuyst, L. (2016). Bifidobacteria and Butyrate-Producing Colon Bacteria: Importance and Strategies for Their Stimulation in the Human Gut. *Front Microbiol, 7*, 979. doi:10.3389/fmicb.2016.00979

Roca-Rivada, A., Castelao, C., Senin, L. L., Landrove, M. O., Baltar, J., Belen Crujeiras, A., . . . Pardo, M. (2013). FNDC5/irisin is not only a myokine but also an adipokine. *PLoS One, 8*(4), e60563. doi:10.1371/journal.pone.0060563

Rochette, L., Zeller, M., Cottin, Y., & Vergely, C. (2014). Diabetes, oxidative stress and therapeutic strategies. *Biochim Biophys Acta, 1840*(9), 2709-2729. doi:10.1016/j.bbagen.2014.05.017

Rodriguez, A., Becerril, S., Ezquerro, S., Mendez-Gimenez, L., & Fruhbeck, G. (2016). Cross-talk between adipokines and myokines in fat browning. *Acta Physiol (Oxf)*. doi:10.1111/apha.12686

Rodriguez, A., Becerril, S., Ezquerro, S., Mendez-Gimenez, L., & Fruhbeck, G. (2017). Crosstalk between adipokines and myokines in fat browning. *Acta Physiol (Oxf), 219*(2), 362-381. doi:10.1111/apha.12686

Rodriguez, A., Ezquerro, S., Mendez-Gimenez, L., Becerril, S., & Fruhbeck, G. (2015). Revisiting the adipocyte: a model for integration of cytokine signaling in the regulation of energy metabolism. *Am J Physiol Endocrinol Metab, 309*(8), E691-714. doi:10.1152/ajpendo.00297.2015

Rodriguez, E., Peiroten, A., Landete, J. M., Medina, M., & Arques, J. L. (2015). Gut Catalase-Positive Bacteria Cross-Protect Adjacent Bifidobacteria from Oxidative Stress. *Microbes Environ, 30*(3), 270-272. doi:10.1264/jsme2.ME15025

Rosen, Evan D., & Spiegelman, Bruce M. (2014). What We Talk About When We Talk About Fat. *Cell, 156*(1–2), 20-44. doi:http://doi.org/10.1016/j.cell.2013.12.012

Ruan, Y., Zheng, F.-p., Li, L., Wang, Z., & Li, H. (2015). Reactive oxygen species up-regulates SOCS-3 in 3T3-L1 adipocytes. *International Journal of Diabetes in Developing Countries, 35*(3), 471-476. doi:10.1007/s13410-014-0201-3

Sacks, H., & Symonds, M. E. (2013). Anatomical locations of human brown adipose tissue: functional relevance and implications in obesity and type 2 diabetes. *Diabetes, 62*(6), 1783-1790. doi:10.2337/db12-1430

Saini, R. K., & Keum, Y. S. (2018). Omega-3 and omega-6 polyunsaturated fatty acids: Dietary sources, metabolism, and significance - A review. *Life Sci, 203*, 255-267. doi:10.1016/j.lfs.2018.04.049

Samieri, C., Okereke, O. I., E, E. D., & Grodstein, F. (2013). Long-term adherence to the Mediterranean diet is associated with overall cognitive status, but not cognitive decline, in women. *J Nutr, 143*(4), 493-499. doi:10.3945/jn.112.169896

Samuel, B. S., Shaito, A., Motoike, T., Rey, F. E., Backhed, F., Manchester, J. K., . . . Gordon, J. I. (2008). Effects of the gut microbiota on host adiposity are modulated by the short-chain fatty-acid binding G protein-coupled receptor, Gpr41. *Proceedings of the National Academy of Sciences, 105*(43), 16767. doi:10.1073/pnas.0808567105

Sanchis-Gomar, F., Fiuza-Luces, C., & Lucia, A. (2015). Exercise as the master polypill of the 21st century for the prevention of cardiovascular disease. *Int J Cardiol, 181*, 360-361. doi:10.1016/j.ijcard.2014.12.048

Sanchis-Gomar, F., Pareja-Galeano, H., Mayero, S., Perez-Quilis, C., & Lucia, A. (2014). New molecular targets and lifestyle interventions to delay aging sarcopenia. *Front Aging Neurosci, 6*, 156. doi:10.3389/fnagi.2014.00156

Santanam, N., Auge, N., Zhou, M., Keshava, C., & Parthasarathy, S. (1999). Overexpression of human catalase gene decreases oxidized lipid-induced cytotoxicity in vascular smooth muscle cells. *Arterioscler Thromb Vasc Biol, 19*(8), 1912-1917.

Santilli, F., Guagnano, M. T., Vazzana, N., La Barba, S., & Davi, G. (2015). Oxidative stress drivers and modulators in obesity and cardiovascular disease: from biomarkers to therapeutic approach. *Curr Med Chem, 22*(5), 582-595.

Sartipy, P., & Loskutoff, D. J. (2003). Monocyte chemoattractant protein 1 in obesity and insulin resistance. *Proc Natl Acad Sci U S A, 100*(12), 7265-7270. doi:10.1073/pnas.1133870100

Sasaki, T. (2017). Neural and Molecular Mechanisms Involved in Controlling the Quality of Feeding Behavior: Diet Selection and Feeding Patterns. *Nutrients, 9*(10). doi:10.3390/nu9101151

Savini, I., Catani, M. V., Evangelista, D., Gasperi, V., & Avigliano, L. (2013). Obesity-associated oxidative stress: strategies finalized to improve redox state. *Int J Mol Sci, 14*(5), 10497-10538. doi:10.3390/ijms140510497

Scherer, P. E. (2006). Adipose tissue: from lipid storage compartment to endocrine organ. *Diabetes, 55*(6), 1537-1545. doi:10.2337/db06-0263

Schleicher, R. L., Carroll, M. D., Ford, E. S., & Lacher, D. A. (2009). Serum vitamin C and the prevalence of vitamin C deficiency in the United States: 2003-2004 National Health and Nutrition Examination Survey (NHANES). *Am J Clin Nutr, 90*(5), 1252-1263. doi:10.3945/ajcn.2008.27016

Schlein, C., Talukdar, S., Heine, M., Fischer, A. W., Krott, L. M., Nilsson, S. K., . . . Scheja, L. (2016). FGF21 Lowers Plasma Triglycerides by Accelerating Lipoprotein Catabolism in White and Brown Adipose Tissues. *Cell Metab, 23*(3), 441-453. doi:10.1016/j.cmet.2016.01.006

Schnyder, S., & Handschin, C. (2015). Skeletal muscle as an endocrine organ: PGC-1alpha, myokines and exercise. *Bone, 80*, 115-125. doi:10.1016/j.bone.2015.02.008

Schriner, S. E., & Linford, N. J. (2006). Extension of mouse lifespan by overexpression of catalase. *Age (Dordr), 28*(2), 209-218. doi:10.1007/s11357-006-9010-z

Schulz, M. D., Atay, C., Heringer, J., Romrig, F. K., Schwitalla, S., Aydin, B., . . . Arkan, M. C. (2014). High-fat-diet-mediated dysbiosis promotes intestinal carcinogenesis independently of obesity. *Nature, 514*(7523), 508-512. doi:10.1038/nature13398

Scotti, E., Boué, S., Sasso, G. L., Zanetti, F., Belcastro, V., Poussin, C., . . . Hoeng, J. (2017). Exploring the microbiome in health and disease:Implications for toxicology. *Toxicology Research and Application, 1*, 2397847317741884. doi:10.1177/2397847317741884

Seaver, L. C., & Imlay, J. A. (2001). Hydrogen peroxide fluxes and compartmentalization inside growing Escherichia coli. *J Bacteriol, 183*(24), 7182-7189. doi:10.1128/JB.183.24.7182-7189.2001

Segata, N., & Huttenhower, C. (2011). Toward an efficient method of identifying core genes for evolutionary and functional microbial phylogenies. *PLoS One, 6*(9), e24704. doi:10.1371/journal.pone.0024704

Seo, H. A., & Lee, I. K. (2013). The role of Nrf2: adipocyte differentiation, obesity, and insulin resistance. *Oxid Med Cell Longev, 2013*, 184598. doi:10.1155/2013/184598

Seoane-Collazo, P., Ferno, J., Gonzalez, F., Dieguez, C., Leis, R., Nogueiras, R., & Lopez, M. (2015). Hypothalamic-autonomic control of energy homeostasis. *Endocrine, 50*(2), 276-291. doi:10.1007/s12020-015-0658-y

Serino, M., Chabo, C., & Burcelin, R. (2012). Intestinal MicrobiOMICS to define health and disease in human and mice. *Curr Pharm Biotechnol, 13*(5), 746-758.

Serra, D., Mera, P., Malandrino, M. I., Mir, J. F., & Herrero, L. (2013). Mitochondrial fatty acid oxidation in obesity. *Antioxid Redox Signal, 19*(3), 269-284. doi:10.1089/ars.2012.4875

Shahidi, F., & Ambigaipalan, P. (2018). Omega-3 Polyunsaturated Fatty Acids and Their Health Benefits. *Annu Rev Food Sci Technol, 9*, 345-381. doi:10.1146/annurev-food-111317-095850

Sharma, N., Lee, J., Youssef, I., Salifu, M. O., & McFarlane, S. I. (2017). Obesity, Cardiovascular Disease and Sleep Disorders: Insights into the Rising Epidemic. *J Sleep Disord Ther, 6*(1). doi:10.4172/2167-0277.1000260

Sheehan, M. T., & Jensen, M. D. (2000). Metabolic complications of obesity. Pathophysiologic considerations. *Med Clin North Am, 84*(2), 363-385, vi.

Sheehan, S. M., Tatsumi, R., Temm-Grove, C. J., & Allen, R. E. (2000). HGF is an autocrine growth factor for skeletal muscle satellite cells in vitro. *Muscle Nerve, 23*(2), 239-245.

Sheng, X., Che, H., Ji, Q., Yang, F., Lv, J., Wang, Y., . . . Wang, L. (2018). The Relationship Between Liver Enzymes and Insulin Resistance in Type 2 Diabetes Patients with Nonalcoholic Fatty Liver Disease. *Horm Metab Res, 50*(5), 397-402. doi:10.1055/a-0603-7899

Sherman, S. B., Sarsour, N., Salehi, M., Schroering, A., Mell, B., Joe, B., & Hill, J. W. (2018). Prenatal androgen exposure causes hypertension and gut microbiota dysbiosis. *Gut Microbes, 9*(5), 400-421. doi:10.1080/19490976.2018.1441664

Shern-Brewer, R., Santanam, N., Wetzstein, C., White-Welkley, J., & Parthasarathy, S. (1998). Exercise and cardiovascular disease: a new perspective. *Arterioscler Thromb Vasc Biol, 18*(7), 1181-1187.

Shill, D. D., Southern, W. M., Willingham, T. B., Lansford, K. A., McCully, K. K., & Jenkins, N. T. (2016). Mitochondria-specific antioxidant supplementation does not influence endurance exercise training-induced adaptations in circulating angiogenic cells, skeletal muscle oxidative capacity or maximal oxygen uptake. *J Physiol, 594*(23), 7005-7014. doi:10.1113/JP272491

Shimasaki, H., Maeba, R., Tachibana, R., & Ueta, N. (1995). Lipid peroxidation and ceroid accumulation in macrophages cultured with oxidized low density lipoprotein. *Gerontology, 41 Suppl 2*, 39-51. doi:10.1159/000213724

Shimokata, H., & Kuzuya, F. (1993). [Aging, basal metabolic rate, and nutrition]. *Nihon Ronen Igakkai Zasshi, 30*(7), 572-576.

Siamilis, S., Jakus, J., Nyakas, C., Costa, A., Mihalik, B., Falus, A., & Radak, Z. (2009). The effect of exercise and oxidant-antioxidant intervention on the levels of neurotrophins and free radicals in spinal cord of rats. *Spinal Cord, 47*(6), 453-457. doi:10.1038/sc.2008.125

Sies, H., Stahl, W., & Sevanian, A. (2005). Nutritional, dietary and postprandial oxidative stress. *J Nutr, 135*(5), 969-972. doi:10.1093/jn/135.5.969

Silva-Palacios, A., Konigsberg, M., & Zazueta, C. (2016). Nrf2 signaling and redox homeostasis in the aging heart: A potential target to prevent cardiovascular diseases? *Ageing Res Rev, 26*, 81-95. doi:10.1016/j.arr.2015.12.005

Silventoinen, K., Jelenkovic, A., Sund, R., Hur, Y. M., Yokoyama, Y., Honda, C., . . . Kaprio, J. (2016). Genetic and environmental effects on body mass index from infancy to the onset of adulthood: an individual-based pooled analysis of 45 twin cohorts participating in the COllaborative project of Development of Anthropometrical measures in Twins (CODATwins) study. *Am J Clin Nutr, 104*(2), 371-379. doi:10.3945/ajcn.116.130252

Silver, D. L., Jiang, X. C., & Tall, A. R. (1999). Increased high density lipoprotein (HDL), defective hepatic catabolism of ApoA-I and ApoA-II, and decreased ApoA-I mRNA in ob/ob mice. Possible role of leptin in stimulation of HDL turnover. *J Biol Chem, 274*(7), 4140-4146.

Singh, M. (2014). Mood, food, and obesity. *Front Psychol, 5*, 925. doi:10.3389/fpsyg.2014.00925

Small, C. J., & Bloom, S. R. (2004). Gut hormones as peripheral anti obesity targets. *Curr Drug Targets CNS Neurol Disord, 3*(5), 379-388.

Smith, K. B., & Smith, M. S. (2016). Obesity Statistics. *Prim Care, 43*(1), 121-135, ix. doi:10.1016/j.pop.2015.10.001

Snel, M., Jonker, J. T., Schoones, J., Lamb, H., de Roos, A., Pijl, H., . . . Jazet, I. M. (2012). Ectopic fat and insulin resistance: pathophysiology and effect of diet and lifestyle interventions. *Int J Endocrinol, 2012*, 983814. doi:10.1155/2012/983814

So, B., Kim, H. J., Kim, J., & Song, W. (2014). Exercise-induced myokines in health and metabolic diseases. *Integr Med Res, 3*(4), 172-179. doi:10.1016/j.imr.2014.09.007

So, M., Gaidhu, M. P., Maghdoori, B., & Ceddia, R. B. (2011). Analysis of time-dependent adaptations in whole-body energy balance in obesity induced by high-fat diet in rats. *Lipids Health Dis, 10*, 99. doi:10.1186/1476-511X-10-99

Sobko, T., Reinders, C., Jansson, E., Norin, E., Midtvedt, T., Lundberg, J., . . . Lundberg, J. (2005). Gastrointestinal bacteria generate nitric oxide from nitrate and nitrite. *Nitric Oxide, 13*, 272-278.

Sofi, F., Abbate, R., Gensini, G. F., & Casini, A. (2010). Accruing evidence on benefits of adherence to the Mediterranean diet on health: an updated systematic review and meta-analysis. *Am J Clin Nutr, 92*(5), 1189-1196. doi:10.3945/ajcn.2010.29673

Sominsky, L., & Spencer, S. J. (2014). Eating behavior and stress: a pathway to obesity. *Front Psychol, 5*, 434. doi:10.3389/fpsyg.2014.00434

Spahis, S., Borys, J. M., & Levy, E. (2017). Metabolic Syndrome as a Multifaceted Risk Factor for Oxidative Stress. *Antioxid Redox Signal, 26*(9), 445-461. doi:10.1089/ars.2016.6756

Spiegelman, B. M., & Flier, J. S. (2001). Obesity and the regulation of energy balance. *Cell, 104*(4), 531-543.

Spychalowicz, A., Wilk, G., Sliwa, T., Ludew, D., & Guzik, T. J. (2012). Novel therapeutic approaches in limiting oxidative stress and inflammation. *Curr Pharm Biotechnol, 13*(13), 2456-2466.

Staerck, C., Gastebois, A., Vandeputte, P., Calenda, A., Larcher, G., Gillmann, L., . . . Fleury, M. J. J. (2017). Microbial antioxidant defense enzymes. *Microb Pathog, 110*, 56-65. doi:10.1016/j.micpath.2017.06.015

Standl, E. (2012). Dysglycemia and abdominal obesity. *Curr Vasc Pharmacol, 10*(6), 678-679.

Stenman, L. K., Burcelin, R., & Lahtinen, S. (2016). Establishing a causal link between gut microbes, body weight gain and glucose metabolism in humans – towards treatment with probiotics. *Beneficial Microbes, 7*(1), 11-22. doi:10.3920/bm2015.0069

Stern, Y. (2012). Cognitive reserve in ageing and Alzheimer's disease. *Lancet Neurol, 11*(11), 1006-1012. doi:10.1016/S1474-4422(12)70191-6

Strauss, R. S. (1999). Comparison of serum concentrations of alpha-tocopherol and beta-carotene in a cross-sectional sample of obese and nonobese children (NHANES III). National Health and Nutrition Examination Survey. *J Pediatr, 134*(2), 160-165.

Styskal, J., Van Remmen, H., Richardson, A., & Salmon, A. B. (2012). Oxidative stress and diabetes: what can we learn about insulin resistance from antioxidant mutant mouse models? *Free Radic Biol Med, 52*(1), 46-58. doi:10.1016/j.freeradbiomed.2011.10.441

Sundstrom, L., Myhre, S., Sundqvist, M., Ahnmark, A., McCoull, W., Raubo, P., . . . Winzell, M. S. (2017). The acute glucose lowering effect of specific GPR120 activation in mice is mainly driven by glucagon-like peptide 1. *12*(12), e0189060. doi:10.1371/journal.pone.0189060

Surmi, B. K., & Hasty, A. H. (2010). The role of chemokines in recruitment of immune cells to the artery wall and adipose tissue. *Vascul Pharmacol, 52*(1-2), 27-36. doi:10.1016/j.vph.2009.12.004

Suzuki, K., Inoue, T., Hioki, R., Ochiai, J., Kusuhara, Y., Ichino, N., . . . Ito, Y. (2006). Association of abdominal obesity with decreased serum levels of carotenoids in a healthy Japanese population. *Clin Nutr, 25*(5), 780-789. doi:10.1016/j.clnu.2006.01.025

Tan, S., Du, P., Zhao, W., Pang, J., & Wang, J. (2018). Exercise Training at Maximal Fat Oxidation Intensity for Older Women with Type 2 Diabetes. *Int J Sports Med, 39*(5), 374-381. doi:10.1055/a-0573-1509

Tanajak, P., Pongkan, W., Chattipakorn, S. C., & Chattipakorn, N. (2018). Increased plasma FGF21 level as an early biomarker for insulin resistance and metabolic disturbance in obese insulin-resistant rats. *Diabetes and Vascular Disease Research, 15*(3), 263-269. doi:10.1177/1479164118757152

Tani, S., Matsuo, R., & Matsumoto, N. (2018). A longitudinal study of the association of the eicosapentaenoic acid/arachidonic acid ratio derived from fish consumption with the serum lipid levels: a pilot study. *Heart Vessels*. doi:10.1007/s00380-018-1226-1

Tannock, G. W. (2007). What immunologists should know about bacterial communities of the human bowel. *Semin Immunol, 19*(2), 94-105. doi:10.1016/j.smim.2006.09.001

Tarantini, S., Valcarcel-Ares, M. N., Yabluchanskiy, A., Tucsek, Z., Hertelendy, P., Kiss, T., . . . Csiszar, A. (2018). Nrf2 Deficiency Exacerbates Obesity-Induced Oxidative Stress, Neurovascular Dysfunction, Blood-Brain Barrier Disruption, Neuroinflammation, Amyloidogenic Gene Expression, and Cognitive Decline in Mice, Mimicking the Aging Phenotype. *J Gerontol A Biol Sci Med Sci, 73*(7), 853-863. doi:10.1093/gerona/glx177

Teodoro, J. S., Rolo, A. P., & Palmeira, C. M. (2013). The NAD ratio redox paradox: why does too much reductive power cause oxidative stress? *Toxicol Mech Methods, 23*(5), 297-302. doi:10.3109/15376516.2012.759305

Tilg, H., & Moschen, A. R. (2006). Adipocytokines: mediators linking adipose tissue, inflammation and immunity. *Nat Rev Immunol, 6*(10), 772-783. doi:10.1038/nri1937

Tran, B., Oliver, S., Rosa, J., & Galassetti, P. (2012). Aspects of inflammation and oxidative stress in pediatric obesity and type 1 diabetes: an overview of ten years of studies. *Exp Diabetes Res, 2012*, 683680. doi:10.1155/2012/683680

Trayhurn, P., Bing, C., & Wood, I. S. (2006). Adipose tissue and adipokines--energy regulation from the human perspective. *J Nutr, 136*(7 Suppl), 1935S-1939S. doi:10.1093/jn/136.7.1935S

Trostchansky, A., Quijano, C., Yadav, H., Kelley, E. E., & Cassina, A. M. (2016). Interplay between Oxidative Stress and Metabolism in Signalling and Disease. *Oxid Med Cell Longev, 2016*, 3274296. doi:10.1155/2016/3274296

Tsoli, M., Moore, M., Burg, D., Painter, A., Taylor, R., Lockie, S. H., . . . Robertson, G. (2012). Activation of thermogenesis in brown adipose tissue and dysregulated lipid metabolism associated with cancer cachexia in mice. *Cancer Res, 72*(17), 4372-4382. doi:10.1158/0008-5472.CAN-11-3536

Tsuchiya, Y., Ando, D., Goto, K., Kiuchi, M., Yamakita, M., & Koyama, K. (2014). High-intensity exercise causes greater irisin response compared with low-intensity exercise under similar energy consumption. *Tohoku J Exp Med, 233*(2), 135-140.

Turnbaugh, P. J., Backhed, F., Fulton, L., & Gordon, J. I. (2008). Diet-induced obesity is linked to marked but reversible alterations in the mouse distal gut microbiome. *Cell Host Microbe, 3*(4), 213-223. doi:10.1016/j.chom.2008.02.015

Turnbaugh, P. J., Hamady, M., Yatsunenko, T., Cantarel, B. L., Duncan, A., Ley, R. E., . . . Gordon, J. I. (2009). A core gut microbiome in obese and lean twins. *Nature, 457*(7228), 480-484. doi:10.1038/nature07540

Turnbaugh, P. J., Ley, R. E., Mahowald, M. A., Magrini, V., Mardis, E. R., & Gordon, J. I. (2006). An obesity-associated gut microbiome with increased capacity for energy harvest. *Nature, 444*(7122), 1027-1031. doi:10.1038/nature05414

Tzanetakou, I. P., Katsilambros, N. L., Benetos, A., Mikhailidis, D. P., & Perrea, D. N. (2012). "Is obesity linked to aging?": adipose tissue and the role of telomeres. *Ageing Res Rev, 11*(2), 220-229. doi:10.1016/j.arr.2011.12.003

Umanskaya, A., Santulli, G., Xie, W., Andersson, D. C., Reiken, S. R., & Marks, A. R. (2014). Genetically enhancing mitochondrial antioxidant activity improves muscle function in aging. *Proceedings of the National Academy of Sciences, 111*(42), 15250-15255. doi:10.1073/pnas.1412754111

Uruno, A., Yagishita, Y., & Yamamoto, M. (2015). The Keap1-Nrf2 system and diabetes mellitus. *Arch Biochem Biophys, 566*, 76-84. doi:10.1016/j.abb.2014.12.012

Valenzuela, R., Espinosa, A., González-Mañán, D., D'Espessailles, A., Fernández, V., Videla, L. A., & Tapia, G. (2012). N-3 Long-Chain Polyunsaturated Fatty Acid Supplementation Significantly Reduces Liver Oxidative Stress in High Fat Induced Steatosis. *PLoS One, 7*(10), e46400. doi:10.1371/journal.pone.0046400

van der Mee-Marquet, N. L., Bénéjat, L., Diene, S. M., Lemaignen, A., Gaïa, N., Smet, A., . . . François, P. (2017). A Potential New Human Pathogen Belonging to Helicobacter Genus, Identified in a Bloodstream Infection. *Front Microbiol, 8*, 2533. doi:10.3389/fmicb.2017.02533

van Dijk, S. J., Feskens, E. J., Bos, M. B., de Groot, L. C., de Vries, J. H., Muller, M., & Afman, L. A. (2012). Consumption of a high monounsaturated fat diet reduces oxidative phosphorylation gene expression in peripheral blood mononuclear cells of abdominally overweight men and women. *J Nutr, 142*(7), 1219-1225. doi:10.3945/jn.111.155283

Via, M. (2012). The malnutrition of obesity: micronutrient deficiencies that promote diabetes. *ISRN Endocrinol, 2012*, 103472. doi:10.5402/2012/103472

Villaret, A., Galitzky, J., Decaunes, P., Estève, D., Marques, M. A., Sengenès, C., . . . Bouloumié, A. (2010). Adipose tissue endothelial cells from obese human subjects: differences among depots in angiogenic, metabolic, and inflammatory gene expression and cellular senescence. *Diabetes, 59*(11), 2755-2763. doi:10.2337/db10-0398

Villarreal-Molina, M. T., & Antuna-Puente, B. (2012). Adiponectin: anti-inflammatory and cardioprotective effects. *Biochimie, 94*(10), 2143-2149. doi:10.1016/j.biochi.2012.06.030

Vina, J., Sanchis-Gomar, F., Martinez-Bello, V., & Gomez-Cabrera, M. C. (2012). Exercise acts as a drug; the pharmacological benefits of exercise. *Br J Pharmacol, 167*(1), 1-12. doi:10.1111/j.1476-5381.2012.01970.x

Viroonudomphol, D., Pongpaew, P., Tungtrongchitr, R., Phonrat, B., Supawan, V., Vudhivai, N., & Schelp, F. P. (2000). Erythrocyte antioxidant enzymes and blood pressure in relation to overweight and obese Thai in Bangkok. *Southeast Asian J Trop Med Public Health, 31*(2), 325-334.

Visioli, F., Grande, S., Bogani, P., & Galli, C. (2004). The role of antioxidants in the mediterranean diets: focus on cancer. *Eur J Cancer Prev, 13*(4), 337-343.

Vital, M., Karch, A., & Pieper, D. H. (2017). Colonic Butyrate-Producing Communities in Humans: an Overview Using Omics Data. *mSystems, 2*(6). doi:10.1128/mSystems.00130-17

Vucenik, I., & Stains, J. P. (2012). Obesity and cancer risk: evidence, mechanisms, and recommendations. *Ann N Y Acad Sci, 1271*, 37-43. doi:10.1111/j.1749-6632.2012.06750.x

Walker, C. G., Browning, L. M., Mander, A. P., Madden, J., West, A. L., Calder, P. C., & Jebb, S. A. (2014). Age and sex differences in the incorporation of EPA and DHA into plasma fractions, cells and adipose tissue in humans. *Br J Nutr, 111*(4), 679-689. doi:10.1017/S0007114513002985

Walsh, J. J., D'Angiulli, A., Cameron, J. D., Sigal, R. J., Kenny, G. P., Holcik, M., . . . Goldfield, G. S. (2018). Changes in the Brain-Derived Neurotrophic Factor Are Associated with Improvements in Diabetes Risk Factors after Exercise Training in Adolescents with

Obesity: The HEARTY Randomized Controlled Trial. *Neural Plast, 2018*, 7169583. doi:10.1155/2018/7169583

Walters, W., Hyde, E. R., Berg-Lyons, D., Ackermann, G., Humphrey, G., Parada, A., . . . Knight, R. (2016). Improved Bacterial 16S rRNA Gene (V4 and V4-5) and Fungal Internal Transcribed Spacer Marker Gene Primers for Microbial Community Surveys. *mSystems, 1*(1). doi:10.1128/mSystems.00009-15

Wang, N., Tabas, I., Winchester, R., Ravalli, S., Rabbani, L. E., & Tall, A. (1996). Interleukin 8 is induced by cholesterol loading of macrophages and expressed by macrophage foam cells in human atheroma. *J Biol Chem, 271*(15), 8837-8842.

Wang, S., & Kaufman, R. J. (2012). The impact of the unfolded protein response on human disease. *J Cell Biol, 197*(7), 857-867. doi:10.1083/jcb.201110131

Wang, X., & Hai, C. (2015). Redox modulation of adipocyte differentiation: hypothesis of "Redox Chain" and novel insights into intervention of adipogenesis and obesity. *Free Radic Biol Med, 89*, 99-125. doi:10.1016/j.freeradbiomed.2015.07.012

Wang, X., Magkos, F., & Mittendorfer, B. (2011). Sex differences in lipid and lipoprotein metabolism: it's not just about sex hormones. *J Clin Endocrinol Metab, 96*(4), 885-893. doi:10.1210/jc.2010-2061

Wang, Y., Wu, Y., Wang, Y., Xu, H., Mei, X., Yu, D., . . . Li, W. (2017). Antioxidant Properties of Probiotic Bacteria. *Nutrients, 9*(5), 521. doi:10.3390/nu9050521

Wang, Y. X., Zhang, C. L., Yu, R. T., Cho, H. K., Nelson, M. C., Bayuga-Ocampo, C. R., . . . Evans, R. M. (2004). Regulation of muscle fiber type and running endurance by PPARdelta. *PLoS Biol, 2*(10), e294. doi:10.1371/journal.pbio.0020294

Wang, Z. V., & Scherer, P. E. (2016). Adiponectin, the past two decades. *J Mol Cell Biol, 8*(2), 93-100. doi:10.1093/jmcb/mjw011

Warburton, D. E., Nicol, C. W., & Bredin, S. S. (2006). Health benefits of physical activity: the evidence. *CMAJ, 174*(6), 801-809. doi:10.1503/cmaj.051351

Watkins, J. B., 3rd, Crawford, S. T., & Sanders, R. A. (1994). Chronic voluntary exercise may alter hepatobiliary clearance of endogenous and exogenous chemicals in rats. *Drug Metab Dispos, 22*(4), 537-543.

Weiss, E. P., Jordan, R. C., Frese, E. M., Albert, S. G., & Villareal, D. T. (2017). Effects of Weight Loss on Lean Mass, Strength, Bone, and Aerobic Capacity. *Med Sci Sports Exerc, 49*(1), 206-217. doi:10.1249/mss.0000000000001074

Whaley-Connell, A., & Sowers, J. R. (2012). Oxidative stress in the cardiorenal metabolic syndrome. *Curr Hypertens Rep, 14*(4), 360-365. doi:10.1007/s11906-012-0279-2

Williamson, J. R., Kilo, C., & Ido, Y. (1999). The role of cytosolic reductive stress in oxidant formation and diabetic complications. *Diabetes Res Clin Pract, 45*(2-3), 81-82.

Wilson, J. L., & Enriori, P. J. (2015). A talk between fat tissue, gut, pancreas and brain to control body weight. *Mol Cell Endocrinol, 418 Pt 2*, 108-119. doi:10.1016/j.mce.2015.08.022

Wong, J. M., de Souza, R., Kendall, C. W., Emam, A., & Jenkins, D. J. (2006). Colonic health: fermentation and short chain fatty acids. *J Clin Gastroenterol, 40*(3), 235-243.

Writing Group, M., Mozaffarian, D., Benjamin, E. J., Go, A. S., Arnett, D. K., Blaha, M. J., . . . Stroke Statistics, S. (2016). Heart Disease and Stroke Statistics-2016 Update: A Report From the American Heart Association. *Circulation, 133*(4), e38-360. doi:10.1161/CIR.0000000000000350

Wu, F., Yang, L., Islam, M. T., Jasmine, F., Kibriya, M. G., Nahar, J., . . . Chen, Y. (2019). The role of gut microbiome and its interaction with arsenic exposure in carotid intima-media thickness in a Bangladesh population. *Environment International, 123*, 104-113. doi:https://doi.org/10.1016/j.envint.2018.11.049

Wu, J., Cohen, P., & Spiegelman, B. M. (2013). Adaptive thermogenesis in adipocytes: is beige the new brown? *Genes Dev, 27*(3), 234-250. doi:10.1101/gad.211649.112

Wu, J., Jin, Z., Zheng, H., & Yan, L. J. (2016). Sources and implications of NADH/NAD(+) redox imbalance in diabetes and its complications. *Diabetes Metab Syndr Obes, 9*, 145-153. doi:10.2147/dmso.S106087

Wu, L., & Parhofer, K. G. (2014). Diabetic dyslipidemia. *Metabolism, 63*(12), 1469-1479. doi:10.1016/j.metabol.2014.08.010

Xiong, Y., Miyamoto, N., Shibata, K., Valasek, M., Motoike, T., Kedzierski, R., . . . Yanagisawa, M. (2004). Short-chain fatty acids stimulate leptin production in adipocytes through the G protein-coupled receptor GPR41. *PNAS, 101*, 1045-1050.

Xue, P., Hou, Y., Chen, Y., Yang, B., Fu, J., Zheng, H., . . . Pi, J. (2013). Adipose deficiency of Nrf2 in ob/ob mice results in severe metabolic syndrome. *Diabetes, 62*(3), 845-854. doi:10.2337/db12-0584

Yamada, H., Umemoto, T., Kakei, M., Momomura, S. I., Kawakami, M., Ishikawa, S. E., & Hara, K. (2017). Eicosapentaenoic acid shows anti-inflammatory effect via GPR120 in 3T3-L1 adipocytes and attenuates adipose tissue inflammation in diet-induced obese mice. *Nutr Metab (Lond), 14*, 33. doi:10.1186/s12986-017-0188-0

Yamamoto, M., Kensler, T. W., & Motohashi, H. (2018). The KEAP1-NRF2 System: a Thiol-Based Sensor-Effector Apparatus for Maintaining Redox Homeostasis. *Physiol Rev, 98*(3), 1169-1203. doi:10.1152/physrev.00023.2017

Yamauchi, T., Kamon, J., Waki, H., Terauchi, Y., Kubota, N., Hara, K., . . . Kadowaki, T. (2001). The fat-derived hormone adiponectin reverses insulin resistance associated with both lipoatrophy and obesity. *Nat Med, 7*(8), 941-946. doi:10.1038/90984

Yan, L. J. (2014). Pathogenesis of chronic hyperglycemia: from reductive stress to oxidative stress. *J Diabetes Res, 2014*, 137919. doi:10.1155/2014/137919

Yan, P., Cheah, J. S., Thai, A. C., & Yeo, P. P. (1983). Current concepts of the pathogenesis and management of diabetic ketoacidosis (DKA). *Ann Acad Med Singapore, 12*(4), 596-605.

Yao, C., Behring, J. B., Shao, D., Sverdlov, A. L., Whelan, S. A., Elezaby, A., . . . Bachschmid, M. M. (2015). Overexpression of Catalase Diminishes Oxidative Cysteine Modifications of Cardiac Proteins. *PLoS One, 10*(12), e0144025. doi:10.1371/journal.pone.0144025

Ye, J., Lv, L., Wu, W., Li, Y., Shi, D., Fang, D., . . . Li, L. (2018). Butyrate Protects Mice Against Methionine–Choline-Deficient Diet-Induced Non-alcoholic Steatohepatitis by Improving Gut Barrier Function, Attenuating Inflammation and Reducing Endotoxin Levels. *Front Microbiol, 9*(1967). doi:10.3389/fmicb.2018.01967

Ye, L., Wu, J., Cohen, P., Kazak, L., Khandekar, M. J., Jedrychowski, M. P., . . . Spiegelman, B. M. (2013). Fat cells directly sense temperature to activate thermogenesis. *Proc Natl Acad Sci U S A, 110*(30), 12480-12485. doi:10.1073/pnas.1310261110

Yeop Han, C., Kargi, A. Y., Omer, M., Chan, C. K., Wabitsch, M., O'Brien, K. D., . . . Chait, A. (2010). Differential effect of saturated and unsaturated free fatty acids on the generation of monocyte adhesion and chemotactic factors by adipocytes: dissociation of adipocyte hypertrophy from inflammation. *Diabetes, 59*(2), 386-396. doi:10.2337/db09-0925

Yiamouyiannis, C. A., Martin, B. J., & Watkins, J. B., 3rd. (1993). Chronic physical activity alters hepatobiliary excretory function in rats. *J Pharmacol Exp Ther, 265*(1), 321-327.

Yonekura, S., Senoo, T., Kobayashi, Y., Yonezawa, T., Katoh, K., & Obara, Y. (2003). Effects of acetate and butyrate on the expression of leptin and short-form leptin receptor in bovine and rat anterior pituitary cells. *Gen Comp Endocrinol, 133*(2), 165-172.

Yoon, M., Jeong, S., Nicol, C. J., Lee, H., Han, M., Kim, J. J., . . . Oh, G. T. (2002). Fenofibrate regulates obesity and lipid metabolism with sexual dimorphism. *Exp Mol Med, 34*(6), 481-488. doi:10.1038/emm.2002.67

Yoon, M. Y., Min, K. B., Lee, K. M., Yoon, Y., Kim, Y., Oh, Y. T., . . . Yoon, S. S. (2016). A single gene of a commensal microbe affects host susceptibility to enteric infection. *Nat Commun, 7*, 11606. doi:10.1038/ncomms11606

Yu, Y., He, J., Li, S., Song, L., Guo, X., Yao, W., . . . Li, D. (2016). Fibroblast growth factor 21 (FGF21) inhibits macrophage-mediated inflammation by activating Nrf2 and suppressing the NF-kappaB signaling pathway. *Int Immunopharmacol, 38*, 144-152. doi:10.1016/j.intimp.2016.05.026

Yuzefovych, L. V., Musiyenko, S. I., Wilson, G. L., & Rachek, L. I. (2013). Mitochondrial DNA damage and dysfunction, and oxidative stress are associated with endoplasmic reticulum stress, protein degradation and apoptosis in high fat diet-induced insulin resistance mice. *PLoS One, 8*(1), e54059. doi:10.1371/journal.pone.0054059

Zgorzynska, E., Dziedzic, B., Gorzkiewicz, A., Stulczewski, D., Bielawska, K., Su, K. P., & Walczewska, A. (2017). Omega-3 polyunsaturated fatty acids improve the antioxidative defense in rat astrocytes via an Nrf2-dependent mechanism. *Pharmacol Rep, 69*(5), 935-942. doi:10.1016/j.pharep.2017.04.009

Zhang, H., DiBaise, J. K., Zuccolo, A., Kudrna, D., Braidotti, M., Yu, Y., . . . Krajmalnik-Brown, R. (2009). Human gut microbiota in obesity and after gastric bypass. *Proc Natl Acad Sci U S A, 106*(7), 2365-2370. doi:10.1073/pnas.0812600106

Zhang, L., Dasuri, K., Fernandez-Kim, S. O., Bruce-Keller, A. J., & Keller, J. N. (2016). Adipose-specific ablation of Nrf2 transiently delayed high-fat diet-induced obesity by altering glucose, lipid and energy metabolism of male mice. *Am J Transl Res, 8*(12), 5309-5319.

Zhang, R., Gao, Y., Zhao, X., Gao, M., Wu, Y., Han, Y., . . . Ge, G. (2018). FSP1-positive fibroblasts are adipogenic niche and regulate adipose homeostasis. *PLoS Biol, 16*(8), e2001493. doi:10.1371/journal.pbio.2001493

Zhang, X., Yeung, D. C., Karpisek, M., Stejskal, D., Zhou, Z. G., Liu, F., . . . Xu, A. (2008). Serum FGF21 levels are increased in obesity and are independently associated with the metabolic syndrome in humans. *Diabetes, 57*(5), 1246-1253. doi:10.2337/db07-1476

Zhao, X., Zhang, Z., Hu, B., Huang, W., Yuan, C., & Zou, L. (2018). Response of Gut Microbiota to Metabolite Changes Induced by Endurance Exercise. *Front Microbiol, 9*, 765. doi:10.3389/fmicb.2018.00765

Zheng, M., Wang, X., Templeton, L. J., Smulski, D. R., LaRossa, R. A., & Storz, G. (2001). DNA microarray-mediated transcriptional profiling of the Escherichia coli response to hydrogen peroxide. *J Bacteriol, 183*(15), 4562-4570. doi:10.1128/JB.183.15.4562-4570.2001

Zhu, H., Jia, Z., Zhang, L., Yamamoto, M., Misra, H. P., Trush, M. A., & Li, Y. (2008). Antioxidants and phase 2 enzymes in macrophages: regulation by Nrf2 signaling and protection against oxidative and electrophilic stress. *Exp Biol Med (Maywood), 233*(4), 463-474. doi:10.3181/0711-RM-304

Zietak, M., Kovatcheva-Datchary, P., Markiewicz, L. H., Stahlman, M., Kozak, L. P., & Backhed, F. (2016). Altered Microbiota Contributes to Reduced Diet-Induced Obesity upon Cold Exposure. *Cell Metab, 23*(6), 1216-1223. doi:10.1016/j.cmet.2016.05.001

APPENDIX A: INSTITUTIONAL REVIEW BOARD APPROVAL

MARSHALL UNIVERSITY.
www.marshall.edu

Office of Research Integrity

February 11, 2019

Debbie Amos
2026 Blennerhassett Heights
Parkersburg, WV 26101

Dear Ms. Amos:

This letter is in response to the submitted thesis abstract entitled *"Endogenous Antioxidant Overexpression as an Adjuvant to Diet or Exercise Intervention as Therapy to Counteract Obesity and Beneficially Shift the Gut Microbiome."* After assessing the abstract it has been deemed not to be human subject research and therefore exempt from oversight of the Marshall University Institutional Review Board (IRB). The Institutional Animal Care and Use Committee (IACUC) has reviewed and approved the study under protocol #585. The applicable human and animal federal regulations have set forth the criteria utilized in making this determination. If there are any changes to the abstract you provided then you would need to resubmit that information to the Office of Research Integrity for review and a determination.

I appreciate your willingness to submit the abstract for determination. Please feel free to contact the Office of Research Integrity if you have any questions regarding future protocols that may require IRB review.

Sincerely,

Bruce F. Day, ThD, CIP
Director

APPENDIX B: LIST OF ABBREVIATIONS

IR	Insulin Resistance
T2D	Type 2 diabetes
NAFLD	Non-alcoholic fatty liver disease
BMI	Body mass index
CVD	Cardiovascular disease
POMC	Proopiomelanocortin
NPY	Neuropeptide Y
WAT	White adipose tissue
BAT	Brown adipose tissue
UCP-1	Uncoupling protein 1
TNF-alpha (α)	Tumor necrosis factor alpha
IL-6	Interleukin 6
MCP-1/JE	Monocyte chemotactic protein 1
LepR	Leptin receptor
ARC	Arcuate nucleus
IL	Interleukin
H_2O_2	Hydrogen peroxide
NADPH	Nicotinamide adenine dinucleotide phosphate hydrogen
ESR	Electron spin resonance
O.S.	Oxidative Stress
Ox-LDL	Oxidatively modified low density lipoprotein
AAOP	Arachidonic acid oxidation product

TBARS	Thiobarbituric acid reactive molecules
Nrf2	Nuclear factor erythroid 2-related factor 2
Keap1	Kelch like ECH associated protein 1
SOD	Superoxide dismutase
GPX	Glutathione peroxidase
TAC	Total antioxidant capacity
LDL	Low-density lipoproteins
ROS	Reactive oxygen species
RNS	Reactive nitrogen species
TG	Triglyceride
ATP	Adenosine triphosphate
TCA	Tricarboxylic acid
NADH	Nicotinamide adenine dinucleotide
FADH	Flavin adenine dinucleotide
ER	Endoplasmic Reticulum
MetS	Metabolic syndrome
HDL	High-density lipoproteins
PI3k	Phosphatidylinositol 3-kinase
Akt	Protein kinase B
NO/NOX	Nitric oxide
mTOR	Rapamycin
SFA	Saturated fatty acids
DIO	Diet induced obesity

FFA	Free fatty acids
HFD	High fat diet
OM6 PUFA	Omega 6 polyunsaturated fatty acids
CLA	Conjugated linoleic acids
MUFA	Monounsaturated fatty acids
OM3 PUFA	Omega 3 polyunsaturated fatty acids
GPR120	G-protein coupled receptor 120
FFAR4	Free fatty acid receptor 4
GLUT-4	Glucose transporter 4
HO-1	Heme oxygenase 1
FGF	Fibroblast growth factor
FGF-21	Fibroblast growth factor 21
PGC1-alpha	Peroxisome proliferator-activated receptor -y coactivator -1 alpha
FNDC5	Fibronectin type III domain-containing protein 5
AMPK	AMP- activated protein kinase
OM3	Omega 3-enriched diet
AMP	Adenosine monophosphate
IBD	Inflammatory bowel disease
HOMA-IR	Homeostasis model assessment for insulin resistance
GPBAR-1	G protein-coupled bile acid receptor 1
FXR	Farnesoid X receptor
PYY	Peptide YY
SCFA	Short chain fatty acid

5-HT	5-hydroxytryptamine
NF-κB	Nuclear factor kappa-light-chain-enhancer of activated B cells
LPS	Lipopolysaccharides
ClpB	Caseinolytic protease B
CNS	Central nervous system
[Tg(CAT)$^{\pm}$]	Catalase transgenic mice
U.S.A.	United States of America
hCAT	Human catalase
EtOH	Ethanol
TE	Tris – EDTA
WT	Wild type
EtBr	Ethidium bromide
ECHO-MRI	ECHO magnetic resonance imaging
CLAMS	Comprehensive lab animal monitoring system
VO_2	Volume of O_2 consumption
VCO_2	Volume of CO_2 production
RER	Respiratory Exchange Ratio/Rate
XAMB/X-AMB	X Ambulatory
EE	Energy Expenditure
FI	Food Intake
RBCs	Red blood cells
IM	Intestinal mucosa
TC	Total Cholesterol

mCAT	Mouse catalase
RIPA buffer	Radioimmunoprecipitation assay buffer
1X TBST	1X Tris buffered saline
SDS	Sodium dodecyl sulfate
DNP	Dinitrophenylhydrazone
DNPH	Dinitrophenylhydrazine
1X PBST	Phosphate buffered saline and Tween 20
BSA	Bovine serum albumin
S.E.M.	Standard Error of the Mean
PUFA	Polyunsaturated fatty acids
C57Bl6	C57/WT
NC	Normal Chow
CHO	Carbohydrate (CHO) Oxidation
ALA	α-linoleic acid
AGRP	Agouti Related Peptide
CART	Cocaine-Amphetamine Related Transcript
Gas	Gastrocnemius
OCT	Optimal Cutting Temperature
OTU	Operational Taxonomic Units
PCoA	Principal coordinates analyses
LDA	Linear Discriminant Analysis
BW	Body Weight
SubQ	Subcutaneous

E	Exercise
S	Sedentary
PICRUSt	Phylogenetic Investigation of Communities by Reconstruction of Unobserved States
BDNF	Brain Derived Neurotrophic Factor
IBS	Irritable Bowel Syndrome

APPENDIX C: CURRICULUM VITAE

Deborah L. Amos
amos23@marshall.edu
2026 Blennerhassett Heights, Parkersburg, WV 26101
(304)-991-5932

EDUCATION

Ph.D. Candidate in Biomedical Sciences, Marshall University, Huntington, WV
Emphasis Cardiovascular Disease, Diabetes, and Obesity
B.S. in Biology, Biology Education, and General Science Education, Spring 2013, University of Charleston, Charleston, WV
Minor in Chemistry, Spring 2013, University of Charleston, Charleston, WV

RESEARCH EXPERIENCE

Graduate Student, Fall 2013 to present
Marshall University, Dr. Nalini Santanam
Assessing the effects of exercise on appetite regulation and the microbiome using an antioxidant mouse model with the following techniques and reagents:

- Breeding of Mice and Genotyping (Tail DNA)
- Mouse Grip Strength Tests as a measure of muscle function
- Mouse Treadmill Operation according to developed protocol (Columbus Instruments; Columbus, OH)
- Mouse MRI (Magnetic Resonance Imaging) use and analysis
- Mouse CLAMS (Comprehensive Animal Monitoring System) use and analysis
- Animal Anesthetization, Blood Draw, and Tissue Collection
- Muscle Sectioning via Cryostat
- Muscle Fiber Typing (myosin ATPase Staining) and H&E staining
- Microscope Analysis of Muscle Fiber Types
- Agarose Gel Electrophoresis
- RNA isolation and reverse transcription
- Real-time Polymerase Chain Reaction (PCR) to determine presence and expression of adipokines, cytokines, myokines, and oxidative stress markers in collected tissues
- Protein quantification by Lowry method
- SDS-Page and Western blotting
- OxyBlot for detection of oxidized proteins in collected tissues
- Enzymatic Activity of Catalase (use of Kinetics Programing on a Spectrophotometer)
- Simple Protein “Wes” Training
- iLab Training Software
- Basic Cell Culture
- GraphPad Prism 7 Software (Statistical Analysis)
- SPSS Software (Statistical Analysis)

Capstone Student Mentor, Summer and Fall 2016 and 2017; Spring 2016, 2017, and 2018 at Marshall University

- Trained undergraduate students to work on an exercise/redox regulation project

Summer Undergraduate Research Student Mentor, Summer 2015, Summer 2016

- Assisted in developing and overseeing projects of students in the NIH-funded WV-INBRE program and SRIMS program

Summer Medical Student Research Student Mentor, Summer 2018

- Assisted in developing and advising medical students in conducting biomedical research funded by the Joan C. Edwards School of Medicine.

PUBLICATIONS

Omega 3 diet modulates energy metabolism via GPR120-Nrf2 crosstalk in a novel antioxidant mouse model. Amos DL, Cook C, Hoffsted A, Crain C, Santanam N.
Biochim Biophys Acta Mol Cell Biol Lipids. January 2019; doi: 10.1016/j.bbalip.2019.01.002

Catalase overexpression modulates metabolic parameters in a new 'stress-less' leptin-deficient mouse model. Amos DL, Robinson T, Massie MB, Cook C, Hoffsted A, Crain C, Santanam N.
Biochim Biophys Acta. June 2017; 1863(9):2293-2306. doi: 10.1016/j.bbadis.2017.06.016.

Mitochondrial redox status as a target for cardiovascular disease.
James Walters, Deborah Amos, Kristeena Ray, Nalini Santanam. *Current Opinion in Pharmacology* April 2016; 27:50-55. doi: 10.1016/j.coph.2016.01.006.

SCHOLARSHIPS and GRANTS

2017-2018 WV State NASA Space Grant Consortium: Graduate Student Fellowship ($12,000 Grant); "Exercise Regulates the Gut Microbiome through Skeletal Muscle Myokine Secretion"
2016-2017 WV State NASA Space Grant Consortium: Graduate Student Fellowship ($12,000 Grant); "Exercise Regulates Brain-adipose Tissue Crosstalk in the Stress less Mouse Model"
2015-2016 WV State NASA Space Grant Consortium: Graduate Student Fellowship ($12,000 Grant); "Exercise Improves Skeletal Muscle Function in the 'Stress-less' Mouse"
Graduate Student Organization Master's Student Scholarship August 2014
Marshall University Cross Country and Track/Field Scholarship 2013-2014
Kanawha City Lion's Club Grant: Safety Goggles at Capitol High School Spring 2013

HONORS and AWARDS

- World Congress Targeting Microbiota 2018 Director's Selection Poster Presentation Award – "Synergistic effects of exercise and antioxidant-overexpression on myokines and gut microbiome" October 2018
- Kappa Delta Pi Member of the Month (October 2018)
- Kappa Delta Pi Excellence Award: for outstanding service and contributions in education April 27, 2018; December 8, 2018

- Marshall University "Spirit of Excellence Award" Recipient: Given to a student with exceptional contributions to student life. The award formally honors students who excel in campus involvement and service to the University, their peers, and the broader community April 19, 2018
- 2nd Year in a Row Awarded "Who's Who Among Students in American Universities and Colleges"- Recognizing outstanding members of the Marshall University student community for their contributions of leadership and service. April 16, 2018
- Recognized as both Kappa Delta Pi Education Honorary Outstanding Member Award (service and contributions) and Most Active Member December 8, 2017
- Marshall University's Most Outstanding Graduate School Student 2016-2017 (Biomedical Sciences) August 18, 2017
- Awarded "Who's Who Among Students in American Universities and Colleges"- Recognizing outstanding members of the Marshall University student community for their contributions of leadership and service. April 14, 2017
- Second Place Poster Presentation Obesity and Diabetes 2016 Appalachian Regional Cell Conference October 1, 2016.
- 2016 Young WV Award (recognition for leadership in West Virginia)
- Honorarium: Research Seminar at Juniata College: "Exercise, Redox, Microbiome?" June 2016
- First Prize Graduate Poster Presentation Competition NASA S.P.A.C.E. Day April 2016
- ASBMB (American Society for Biochemistry and Molecular Biology) Graduate Travel Award April 2016
- Marshall Campus Rec Fitness Award: Fall 2014, Spring 2015, Spring 2016
- Kanawha City Lions Club Community Service Award November 2015
- Run, Run, Rudolph (5K Road Race) Fall 2014
- Track and Field Conference Champion 5K Spring 2013
- WVIAC Scholar-Athlete Award (one female chosen per institution) Spring 2013
- First Team Capital One Academic All-District selections Spring 2013
- Academic All-American (Cross Country) Fall 2011, Fall 2012
- University of Charleston Outstanding Student in Science Research April 2012

ABSTRACTS, CONFERENCES, and PRESENTATIONS

- Marshall University Joan C. Edwards School of Medicine Research Day "Redox regulation of behavior changes in diet-induced 'stress-less' obese mouse model," 2019 Huntington, WV
- World Congress Targeting Microbiota 2018: "Synergistic effects of exercise and antioxidant-overexpression on myokines and gut microbiome" 2018 Director's Selection Poster Presentation Award, October 30, 2018, Porto, Portugal

- Marshall University Joan C. Edwards School of Medicine Research Day "Redox Balance Regulates FGF21 in the Novel "Stress-less" Mouse Model" March 2018; Huntington, WV
- 2017 Appalachian Regional Cell Conference, Oral Presentation "Exercise Improves Energy Metabolism in a Novel Obese "Stress-Less" Mouse Model" December 2, 2017, Athens, OH

- Biomedical Science Lecture on Research Topic: "Adipose Tissue: What is the Storage Depot We Call Fat Tissue?" September 1, 2017
- Graduate School Lecture on Research Topic: "Obesity: What is the storage molecule we call fat?" April 26, 2017 Marshall University Huntington, WV
- CCTS Spring Conference "Exercise Modulates Energy Metabolism in an Obese 'Stress-Less' Mouse Model" March 30, 2017, Lexington, Kentucky
- Marshall University Joan C. Edwards School of Medicine Research Day "Exercise Modulates Energy Metabolism in an Obese 'Stress-Less' Mouse Model" March 24, 2017; Huntington, WV
- Lay Talk to Marshall University Undergraduates on Current Research Progress: "Exercise, Redox Regulation, and Appetite" February 21, 2017; Huntington, WV
- 2016 Appalachian Regional Cell Conference, November 2016; Huntington, WV * 2nd Place Poster Presentation
- Research Seminar "Exercise, Redox, Microbiome?" Juniata College June 8, 2016; Huntingdon, PA
- CCTS (Center for Clinical and Translational Science) Spring Conference, April 2016; Lexington, Kentucky
- 2nd Annual NASA S.P.A.C.E. Day, April 2016; Fairmont, WV *1st Prize Poster Presentation
- Experimental Biology Conference, April 2016; San Diego, CA * ASBMB Travel Award Recipient
- Biomedical Science State of the Art Seminar "Exercise and its myriad of benefits: A mechanistic update." at Marshall University March 2016; Huntington, WV
- Marshall University School of Medicine Research Day, March 2016; Huntington, WV
- 2015 Appalachian Regional Cell Conference, November 2015; Huntington, WV
- Marshall University School of Medicine Research Day, March 2015; Huntington, WV
- Biomedical Science Research Retreat, August 2015; Huntington, WV
- 2014 Appalachian Regional Cell Conference, November 2014; Huntington, WV
- Biomedical Science Research Retreat, August 2014; Huntington, WV

WORK EXPERIENCE

Marshall University School of Medicine Live Patient for Examination- Fall 2013 -Spring 2015

- Served as a "dummy" for medical and pharmacy student examinations.

Mountaineer Family Restaurant- Parkersburg, WV- May 2009 – Summer 2015

- Hostess/Waitress- provided assistance as a server, cashier, and food prep personnel.

Resident Assistant- University of Charleston- Charleston, WV -June 2010 – May 2013

- Directed a minimum of five service projects per year, attended weekly meetings to organize events and work hours, served as secretary of the Residence Hall Association,

attended regional meetings to develop further skills in communication and conflict resolution.

AmeriCorps Energy Express- Martin Elementary School- Parkersburg, WV -June–Aug 2010 - 2013

- Served as a mentor for children K-3rd Grade. Provided instruction in reading, writing, art, and drama. Taught table manners and directed two community service projects each summer.

TEACHING EXPERIENCE

Ohio Valley University: Parkersburg, WV (Spring 2019)

- Instructed undergraduates in Microbiology and Human Anatomy and Physiology

Teaching Practicum: Huntington, WV (Spring 2017)

- Taught undergraduates in Cell Metabolism in the Marshall University Biomedical Science Program

Covenant School 9th Grade Biology Teacher: Huntington, WV (2014-2015)

- Solely instructed the high school biology course for Covenant School

Capitol High School: Charleston, WV (Fall 2012)

- Student Teaching
- Semester long: 9-12th grade Biology, Advanced Biology, AP Biology

DuPont Middle School (Spring 2012)

- Semester long: 6th grade science : focus on the cell and metabolism

AFFILIATIONS

Marshall University Summer Biomedical Science Writing Group Summer 2018

American Heart Association, Student Member 2017-Present

Graduate Women in Science, Student Member 2017-Present

Student Government Association, Senator and Finance Representative 2016-2017, 2017-2018

Gamma Beta Phi – National Honor Society, Member September 2016-Present

Golden Key International Honor Society, Member September 2016-Present

Kappa Delta Pi (KDP) – Education Honorary, Member September 2016-Present

American Nutrition Society (ASN), Member 2015-Present

American Association for the Advancement of Science (AAAS) Program for Excellence in Science, Member 2015-Present

Graduate Student Organization, Secretary (2014-2015) Vice President (2015-2016), Marshall University BMS program

- Scheduled and led monthly meetings and overseeing activities

- Aided in organization of student opportunities such as tutoring for first year students and various fundraising initiatives (International Food Festival, 50/50 raffle)
- Served as BMS graduate program liaison for communication between directors, faculty, and students within the Biomedical Sciences program
- Attended presentations by peers and potential faculty
- Volunteered as a Tutor for Graduate Level Entrance Courses
- Volunteered for BMS Open House and Ph.D. interview events

Marshall University Lions Club, President, (2015-2016) (2016-2017) (2017-2018) Marshall University

- Responsible for scheduling and leading bimonthly meetings and overseeing activities
- Communication between Regional Lion's Clubs and coordinating service events between the region
- Organized Bake Sales and Other Fundraising Events (all monetary funds go toward giving back to the community)
- Providing Marshall University Students with opportunities to serve the community through novel events (Trick or Treat for TP, the "Jared Box," Cabell Huntington's Children's Hospital Valentine's Day, Wingate Care Facility Easter Baskets, etc.)
- Served weekly to provide basic necessities to Huntington's Homeless

Marshall University "Unraveled" (Knitting/Crochet Club) Treasurer, **(2015-2016) (2016-2017) (2017-2018)** Marshall University

- Communicated with Marshall University Student Organization Office to acquire funding and report budget status.
- Kept records of money spent and housing club materials

COMMUNITY INVOLVEMENT and PHILANTHROPY

26th Street church of Christ – Summer 2013 –current

- Attended biweekly services and participated in community dinners, seminars, and sings
- Contributed to organizations providing aid in third world countries and local disaster relief
- Made cheer baskets for the elderly of the Huntington Community

Herd 4 Christ, 26th Street church of Christ– Summer 2013-current

- Habitat for Humanity- roofing and basic building maintenance
- Mid-Western Children's Home Retreat- providing assistance in lawn/building maintenance for orphans
- Biannual Senior Dinners – serving to cook and waitress for the elderly in the congregation
- Kids for Christ Conference – creating activities for elementary and middle school age children

Marshall Medical Outreach (MMO) / Saturday Street Ministry- Spring 2014 -current

- Organizing hygiene products and snack packs for those in need
- Clothing Donations (ie. Coat drive, knitting hats/scarves)

- Knitting for the Homeless (various hats, scarves, blankets)
- Volunteer Recruitment

Biological Dissections Spring 2018
- Teaching 5th Grade Cabell County "Talented and Gifted" students how to dissect earthworms, crayfish, grasshoppers, frogs, and fetal pigs

Brain Expo- Fall 2015, Fall 2016, Spring 2017, Spring 2018
- Teaching Elementary Age Students about "Brain Health"

Science "Blitz" Day Spring 2018
- Teaching Elementary – High School students how to properly conduct science projects in their home

Jared Box Fall 2013, 2014, 2015, 2016, 2017, 2018
- Organized, collected, wrapped, and delivered toys, donated by the community, for children in Cabell Huntington Hospital

Medical Mission Trips to Managua, Nicarauga (2010, 2011)
- Aided in collection of toiletry products
- Assisted doctors and nurses with blood pressure, pulse, etc.

Director of Covenant School First Annual Science Fair
- Volunteer recruiter/organizer
- Reservation coordinator
- Presenter of Awards

ADDITIONAL SKILLS/CERTIFICATIONS
Laboratory: CITI Certification for Handling of Mice, Handling of Rats, and Surgical Procedures; Marshall University Biosafety and Chemical Safety; Flinn Scientific Laboratory/Chemical Safety Certification

Languages: Conversational Spanish